ORNL/Sub--91-SG913/1

DE93 005858

RECOMMENDED ENGINEERING PRACTICE TO ENHANCE THE EMI/EMP IMMUNITY OF ELECTRIC POWER SYSTEMS

Charles L. Wagner
William E. Feero
Electric Research and Management, Inc.
P.O. Box 165
State College, PA 16801

December 1992

Prepared Under Subcontract 15X-SG913V

for

Oak Ridge National Laboratory
Oak Ridge, Tennessee 37831
Managed by
Martin Marietta Energy Systems, Inc.
for the
U.S. Department of Energy
Under Contract DE-AC05-840R21400

MASTER

DISTRIBUTION OF THIS DOCUMENT IS UNLIMITED

TABLE OF CONTENTS

Page

EXECUTIVE SUMMARY xvii

1.0 INTRODUCTION 1

2.0 ELECTROMAGNETIC PULSE ENVIRONMENT 2

3.0 E_1 WAVES 10

3.1 Overhead Lines 10
3.2 Power Cables 19
3.3 Transmission and Distribution Equipment 23
3.3.1 Surge Arresters 23
3.3.2 Power Transformers 29
3.3.3 Distribution Transformers 31
3.3.4 Apparatus Bushings 36
3.3.5 Reclosers 37
3.4 Power Plants 37
3.5 Protective Relaying 40
3.6 Communication and Control Equipment 57
3.6.1 Building Shielding 59
3.6.2 Building Penetrations 69
3.6.3 Protective Devices 74
3.7 Summary 86

4.0 E_3 WAVES 88

4.1 Geomagnetically Induced Current Characteristics ... 88
4.2 Effect of Geomagnetically Induced Current on Power Systems 91
4.2.1 Power Transformers 91
4.2.2 Instrument Transformers 101
4.2.3 Protective Relaying 103
4.2.4 Communications 104
4.2.5 Other System Effects 105
4.3 Geomagnetically Induced Current Mitigation Measures 106
4.3.1 Polarizing Cells 106
4.3.2 Linear Resistor 106
4.3.3 Non-Linear Resistor (MOV) 106
4.3.4 Active Direct Current Device 107
4.3.5 Neutral Capacitors 107
4.3.6 Series Capacitors 109
4.4 E_3 Characteristics 109
4.5 Effect of E_3 on Power Systems 115
4.6 E_3 System Study 127
4.7 E_3 Mitigation Measures 133

4.8 Summary 133

5.0 HIGH ALTITUDE ELECTROMAGNETIC PULSE MITIGATION MEASURES 136

5.1 E_1 Surges 136
5.2 E_3 Surges 138

6.0 STANDARDS 140

6.1 Protective Device Standards 140
6.2 Cable and Shielding Standards 145
6.3 Equipment Withstand Standards 150
6.4 Standards Modifications 153
6.4.1 Protective Device Standards 153
6.4.2 Relay Standards 153
6.4.3 Grounding and Shielding Standards.. 155
6.4.4 E_3 Standards 155

7.0 CONCLUSIONS 156

ACKNOWLEGEMENTS 160

APPENDIX A 161

LIST OF FIGURES

Figure		Page
2-1	Transient E_1 Waveforms to the West of Ground Zero	3
2-2	An Example of Variations in High Altitude Electromagnetic Pulse Peak Electric Field on Surface of Continental United States	5
2-3	Electromagnetic Pulse Ground Coverage (Tangent Radius) and Total Area of Coverage as Functions of Height of Burst	5
2-4	Radiated Electromagnetic Pulse Field Propagates Locally as a Plane Wave	6
2-5	Illustration of (A) Non Corona and (B) Corona Distortion with Distance Along a Line	8
2-6	Test Data from Tidd Project for a Single Conductor	8
2-7	Example of Normalized Magnetohydrodynamic-Electromagnetic Pulse F(t) Function	9
3.1-1	High Altitude Electromagnetic Pulse Field Magnitudes in kilovolts/meter within the Area of Illumination	12
3.1-2	Plot of High Altitude Electromagnetic Pulse-Induced Voltages for Phase Number 3 of 12-kV Line	12
3.1-3	Coordinates Defining Azimuth and Elevation Angles of Incidence	13
3.1-4	Cumulative Distribution of High Altitude Electromagnetic Pulse-Induced Voltage on the 12-kV Line (Probability of Exceeding a Voltage)	13
3.1-5	High Altitude Electromagnetic Pulse-Induced Flashover Vulnerability for Phase Number 3 of the 12-kV Line	16
3.1-6	Probability of the Peak Transformer Voltage Exceeding the Abscissa Value	18

Figure		Page

3.1-7	Probability of the Peak Transformer Voltage Exceeding the Abscissa Value for Line in a 500-km Square Region Centered Over the Position of Maximum Line Response	18
3.2-1	Normalized Current Waveform for Various Values of Depth (d) for Incident Exponential Pulse $E(t) = E_0 e^{-t/r}$	20
3.2-2	Relative Transfer Impedance as a Function of Frequency for Different Cables	21
3.3.1-1	Arrester Peak Voltage vs. Peak Steep-front Short-duration Current. Series A: 10-kV Metal Oxide Varistor, 24 In. Lead; Series B: 10-kV Gapped Silicon Carbide, 45 In. Lead; Series C: 10-kV Gapped Silicon Carbide, 24 In. Lead	25
3.3.1-2	Current Waveshapes for the 9-kV Metal Oxide Varistor Arrester at Approximately 5- and 20-kA Peak	26
3.3.1-3	Metal Oxide Varistor Arrester Voltages During the 5-kA and 20-kA Current Pulses Shown in Fig. 3.3.1-2	26
3.3.1-4	Voltage Across the Aluminum Tube During a 10-kA Current Pulse	27
3.3.1-5	Aluminum Tube Voltage (Fig. 3.3.1-4, Extrapolated to 5-kA Equivalent Peak Current) Subtracted from the 5-kA Metal Oxide Varistor Voltage Pulse in Fig. 3.3.1-3	28
3.3.1-6	Residual Voltage versus Peak Arrester Current for Two 9-kV Metal Oxide Varistor Arresters and One 9-kV Silicon Carbide Arrester. The 8/20 μs Voltages for a Typical 9-kV Metal Oxide Varistor Arrester Are Also Shown	28
3.3.3-1	Impulse Voltage Distribution for 50-kVA Core Form Transformer at Specific Times	32
3.3.3-2	Idealized Single Phase Power Distribution Line	33
3.3.3-3	Contour Plot of Peak Value of High Altitude Electromagnetic Pulse Electric Field on Earth's Surface (Contours in kilovolts/meter)	33

Figure		Page

Figure	Title	Page
3.3.3-4	Open-Circuit Voltage (a) and Loaded Voltage (b) Across Transformer for Line at Position P (-1130, 0.0) km. Guy Wire is Absent.	34
3.3.3-5	Probability of the Peak Transformer Voltage Exceeding the Abscissa Value	35
3.3.3-6	Probability of the Peak Transformer Voltage Exceeding the Abscissa Value for Line at Position of Maximum Positive Response	35
3.3.3-7	Probability of the Peak Transformer Voltage Exceeding the Abscissa Value for Line in a 500 km Square Region Centered Over the Position of Maximum Line Response	36
3.4-1	Envelope of Voltages Following Closure of Switch	38
3.4-2	Machine Impulse Voltage Withstand Envelope	38
3.5-1	Protection Scheme for Relay Output Circuits	41
3.5-2	Protection Scheme for Relay Input Circuits	42
3.5-3	Induced Voltage Along Pilot Wire by Line Fault	43
3.5-4	Recommended Protection Schemes for Pilot Wire Circuits	44
3.5-5	Relay Surge Withstand Capability Fast Transient Test Waveform Specified by IEEE/ANSI C37.90.1-1989	45
3.5-6	Test Setup for Radiated Susceptibility	46
3.5-7	Pulse Generator Waveforms into a 50 Ohm Load	48
3.5-8	Time Domain Waveforms for Horizontal Component of Short-Range Thin) and Long-Range (Bold) High Altitude Electromagnetic Pulse Fields	50
3.5-9	Time Domain Waveforms for Vertical Component of Short-Range (Thin) and Long-Range (Bold) High Altitude Electromagnetic Pulse Fields	51
3.6-1	Examples of First Level Barriers	60

Figure | Page

3.6.1-1 Shielding Integrity Near Interference-Carrying External Conductors 61

3.6.1-2 Electromagnetic Penetration of Small Apertures 63

3.6.1-3 Use of Single Entry Panel tc Minimize External Excitation of Electromagnetic Pulse Shield 64

3.6.1-4 Example of Zoned Protection 66

3.6.1-5 Estimates of Shielding by Substation Structures Based on Rod Antenna Measurements 67

3.6.1-6 Field Measurement Locations. The Outline of the Computer Room Encloses Locations 1 and 2 68

3.6.2-1 Entry Panel 70

3.6.2-2 Treatment of Power and Ground 72

3.6.3-1 Related Voltage Spike in the Residual Voltage Waveshape of Arrester Blocks and a Complete Arrester (U_{MCOV} = 136 kV) 76

3.6.3-2 Use of Spark Gaps, Filters, Varistors, and Zenor Diodes to Limit Surges from Electromagnetic Pulses on Electronic Equipment 77

3.6.3-3 Use of Two- and Three-Electrode Spark Gaps with Current Limiting Non-Linear Resistance 78

3.6.3-4 Common-Mode Interference and Some Remedies 79

3.6.3-5 Reasons for Nonideality of Real Capacitors (a) Equivalent Circuit of Shunting Capacitor, Not Constructed as Feed Through. (b) Feed-Through Configuration 80

3.6.3-6 Attenuation of So-Called Capacitors 82

3.6.3-7 Transformer-Coupled Input 83

3.6.3-8 Optoelectronic Coupler Circuit 83

3.6.3-9 Block Diagram of the Experimental Setup to Perform the Filter Tests 84

Figure		Page
4.1-1	General Areas of Igneous Rock Geology in the United States and Canada	89
4.1-2	Induced Earth-Surface-Potential Producing Geomagnetically Induced Currents in Power Systems	89
4.1-3	Magnetogram from Poste-de-la-Baleine Magnetic Observatory, James Bay, Quebec, Canada	90
4.1-4	Typical Geomagnetic Storm Electric Field	91
4.2.1-1	Flux and Magnetising Current Waveforms for a Transformer in Partial Saturation	92
4.2.1-2	Direct Current Flux Path for Several Core Arrangements	93
4.2.1-3	Typical Transformer Alternating Current Saturation Curve	96
4.2.1-4	Short Time Overexcitation Limits of Power Transformers	96
4.2.1-5	Alternating Current Magnetization Characteristic for Public Service Electric and Gas Salem Generator Stepup Unit Transformer	98
4.2.1-6	Magnetization Characteristic for Public Service Electric and Gas Salem Generator Stepup Unit Transformer with 60 Amps Direct Current in the High Voltage Winding	99
4.2.1-7	Phase Exciting-Currents of 5-leg, Core-form Transformer with .1 Per Unit Geomagnetically Induced Current	99
4.2.1-8	Model Calculations of the Effects of Geomagnetically Induced Current on Transformer T4 at Williston Showing the Relation Between: (1) Total Magnetising Current, (2) 60-Hz Harmonic Current, (3) 120-Hz Harmonic Current, (4) 180-Hz Harmonic Current, (5) Reactive Power Demand, and the Magnitude of Geomagnetically Induced Current	100
4.2.2-1	Calculated Current Transformer Secondary Current with and without Geomagnetically Induced Current	101

Figure		Page

4.2.2-2	Current Transformer Secondary Saturation Characteristic	102
4.3.5-1	Schematic for Neutral Blocking/Bypass Device	108
4.4-1	Normalized Composite Magnetohydrodynamic Electromagnetic Pulse Electric Field	110
4.4-2	Magnetohydrodynamic Electromagnetic Pulse-Induced Current for Transmission Lines (Case 1)	110
4.4-3	Magnetohydrodynamic Electromagnetic Pulse-Induced Current for Subtransmission and Distribution Lines (Case 2 - Substation Grounding)	111
4.4-4	Magnetohydrodynamic Electromagnetic Pulse-Induced Current for Subtransmission and Distribution Lines (Case 3 - Stake Grounding at One End and Substation Grounding at the Other)	111
4.4-5a	Normalized Worst-Case Magnetohydrodynamic Electromagnetic Pulse Electric Field	112
4.4-5b	Typical Geomagnetic Storm Electric Field	113
4.4-6	Comparison of the Spectra of the Magnetohydrodynamic Electromagnetic Pulse Field and the Geomagnetic Storm Electric Field	113
4.4-7	Computed Electric Field Components for October 28, 1991	114
4.4-8	Comparison of Magnetohydrodynamic Electromagnetic Pulse with Geomagnetic Storm Electric Field Waveforms	114
4.5-1	Forbes Direct Current Injection Test - T8, June 24, 1991.	116
4.5-2	Time to Saturation as a Function of Transformer Loading for an 1100 MVA 115/500 kV Three-Phase Delta/Grounded-Wye Connected Power Transformer Consisting of 115/288 kV Single Phase Transformers	116

Figure | Page

Figure	Title	Page
4.5-3	Geomagnetically Induced Current in Neutral of Autotransformer	118
4.5-4	Normalized Composite Magnetohydrodynamic Electromagnetic Pulse Electric Field	118
4.5-5a	The Maximum Magnetization Current for the Early Time Magnetohydrodynamic Electromagnetic Pulse Waveform and p=100 Ω-m - Shield Wire Connected to Tower with Span of 0.16 km	120
4.5-5b	The Maximum Magnetization Current for the Early-Time Magnetohydrodynamic Electromagnetic Pulse Waveform and p=100 Ω-m - Shield Wire Connected to Tower with Span of 0.40 km	120
4.5-5c	The Maximum Magnetization Current for the Early-Time Magnetohydrodynamic Electromagnetic Pulse Waveform and p=100 Ω-m. Shield Wire Insulated from Tower	121
4.5-6a	The Maximum Magnetization Current for the Late-Time Magnetohydrodynamic Electromagnetic Pulse Waveform and p=100 Ω-m. Shield Wire Connected to Tower with Span of 0.16 km	121
4.5-6b	The Maximum Magnetization Current for the Late-Time Magnetohydrodynamic Electromagnetic Pulse Waveform and p=100 Ω-m. Shield Wire Connected to Tower with Span of 0.40 km	122
4.5-6c	The Maximum Magnetization Current for the Late-Time Magnetohydrodynamic Electromagnetic Pulse Waveform and p=100 Ω-m. Shield Wire Insulated from Tower	122
4.5-7a	Time Delay to Transformer Saturation for the Late-Time Magnetohydrodynamic Electromagnetic Pulse Waveform and p=100 Ω-m. Shield Wire Connected to Tower with Span of 0.16 km	123
4.5-7b	Time Delay to Transformer Saturation for the Late-Time Magnetohydrodynamic Electromagnetic Pulse Waveform and p=100 Ω-m. Shield Wire Connected to Tower with Span of 0.40 km	124
4.5-7c	Time Delay to Transformer Saturation for the Late-Time Magnetohydrodynamic Electromagnetic Pulse Waveform and p=100 Ω-m. Shield Wire Insulated from Tower	125

Figure		Page
4.6-1	Example of Magnetohydrodynamic Electromagnetic Disturbance f(t) Function	128
4.6-2	Non-scaled Magnitude Contours of Magnetohydrodynamic Electromagnetic Pulse	128
4.6-3	Direction of Magnetohydrodynamic Electromagnetic Pulse Gradients	129
4.6-4	Typical Voltage Responses	131
4.6-5	Typical Swing Curves	131
4.7-1	Long-Pulse Treatment--Overall Arrangement of Power Service	134
4.7-2	Long-Pulse Treatment--Distribution Transformer in Configuration to Serve as the Long-Pulse Barrier	135
6.1-1	Graph Illustrating Voltage Overshoot, Response Time, and Overshoot Duration	148
6.3-1	Typical Oscillatory Surge Withstand Capability Test Wave (Open Circuit)	151
6.3-2	Typical Fast Transient Surge Withstand Capability Test Wave (Open Circuit)	151
6.3-3	Waveshape of a Single Pulse into a 50 Ω Load	154

LIST OF TABLES

Table		Page
2-1	Characteristics of Steep-front Short-duration Impulse Sources	7
2-2	Lightning Stroke Current Data	7
3.1-1	Steep-front Short-duration Impulse Test Results	11
3.1-2	Estimated High Altitude Electromagnetic Pulse Line-Insulation Strength by Operating Voltage	14
3.1-3	Comparison of High Altitude Electromagnetic Pulse-Induced Voltage to Estimated High Altitude Electromagnetic Pulse-Insulation Strength	14
3.1-4	Sensitivity of High Altitude Electromagnetic Pulse-Flashover Vulnerability to Various High Altitude Electromagnetic Pulse Field Strengths for the Area of Illumination	17
3.1-5	Sensitivity of High Altitude Electromagnetic Pulse-Induced, 12-kV Line Flashover Vulnerability to Various High Altitude Electromagnetic Pulse Field Strengths for 400 by 400 km Maximum-Voltage Region	17
3.2-1	Comparison of Cable Shielding Materials	22
3.3.1-1	Results of Tests on 96-kV Silicon Carbide Station-Class Arresters	23
3.3.1-2	Results of Tests on 96-kV Metal Oxide Varistor Station-Class Arresters	24
3.3.1-3	Results of Tests on 30-kV Silicon Carbide Distribution-Class Arresters	24
3.3.2-1	Zinc Oxide Arrester Discharge Voltage (Per Unit of 8x20 Microsecond Wave)	29
3.3.2-2	Fast-Front-Wave Insulation Levels (per unit of Basic Insulation Level)	29

Table		Page
3.3.2-3	Protective Margins (258-kV Zinc Oxide Arrester)	30
3.3.4-1	Impulse Testing on Power-Apparatus Bushings	37
3.4-1	Probabilities of Generation Loss Based on 480-Volt Motor Damage	39
3.5-1	Characteristics of Oscillatory and Fast Transient Surge Withstand Capability Tests	45
3.5-2	Relay Test Summary	49
3.5-3	Norms for Transient Bus Currents and Voltages	52
3.5-4	Norms for Incident Electric and Magnetic Fields at Ground	52
3.5-5	Norms for Induced Shield Currents	53
3.5-6	Zero-Peak Amplitudes for Transient Control-Wire Currents and Voltages for 150 Ω, Current Transformer, and Direct Current Battery Impedances (Summed for All Coupling Modes)	53
3.5-7	Load Currents and Voltages for Sum Over All Coupling Modes	55
3.5-8	Open-Circuit Voltages and Short-Circuit Currents for Sum Over All Coupling Modes	55
3.5-9	Effect of Filter Capacitance on Load/Filter Stress Levels for 2 Per Unit Disconnect Switching Interference Coupling to Current Transformer Control Cables (150-Ohm Load)	56
3.5-10	Effect of Filter Capacitance on Load/Filter Stress Levels for Surge Withstand Capability Fast Transient and Oscillatory Test Levels (Same for Unshielded and Shielded Cables) (150-Ohm Load)	58
3.6.1-1	Peak Transient Electric Field Amplitudes Generated by Line Disconnects as a Function of Location and Construction Stage	68

Table		Page
3.6.3-1	Performance Summary of Power Line Filter C with and without a Transient Voltage Suppressor Installed at the Filter's Input Terminal	85
4.2.1-1	Relative Sensitivity to Geomagnetically Induced Current Damage as Measured by Per Unit Core Area Available for Direct Current Flux Return	95
4.2.1-2	Per Unit Harmonic Composition of Magnetizing Current for Geomagnetically Induced Current Equal to 4.8% of Rated Load Current in the High Voltage Winding	100
4.2.2-1	Percent Current Transformer Remanent Flux vs. Geomagnetically Induced Current. Current Transformer Ratio 400:1. Standard Burden 1.0 + j1.73 Ohms	102
4.2.5-1	Examples of Estimated Voltage Droop Due to Geomagnetically Induced Current Based on Summer 1980 Load Flow	105
4.5-1	System Upsets Caused by the October 28 Geomagnetic Storms	117
4.5-2	Peak Magnetohydrodynamic Electromagnetic Pulse Electric Fields Used in Parametric Study	119
4.5-3	Line and Ground Constants Used in Parametric Study	119
4.5-4	Saturation Time Constant for Loaded Transformer	127
4.6-1	Magnetohydrodynamic Maximum Direct Current Values	130
4.6-2	Summary of Area Interchange without the Presence of Magnetohydrodynamic Electromagnetic Pulse	132
4.6-3	Summary of Area Interchange During a Magnetohydrodynamic Electromagnetic Pulse Event	132

Table		Page

6.1-1	Protective Characteristics of Gapped Silicon-Carbide Station Arresters	142
6.1-2	Protective Characteristics of Gapped Silicon-Carbide Intermediate Valve Arresters	143
6.1-3	Protective Characteristics of Gapped Silicon-Carbide Distribution Arresters	144
6.1-4	Protective Characteristics of Gapped Silicon-Carbide Secondary Arresters	144
6.1-5	Westinghouse Type SMX Station Surge Arrester Characteristics	146
6.1-6	Westinghouse Type IMX Surge Arrester Characteristics	147
6.1-7	Performance Characteristics: Type RMX Riser Pole Arresters	147
6.1-8	Impulse Breakdown in Volts	148

EXECUTIVE SUMMARY

Many papers and reports have been written on studies conducted by the Oak Ridge National Laboratory and investigations by others on the effect of high-altitude electromagnetic pulses (HEMP) on electric power systems. More than 100 of the published unclassified documents were reviewed with the objectives of:

1. summarizing the mitigation methods suggested in the documents and providing a subjective evaluation of each;

2. discussing various standards that presently apply to the effects of HEMP on utility systems and suggesting additions or modifications or new standards where deficiencies appear to exist; and

3. recommending future studies or actions to improve the utility response to HEMP.

While all three components of HEMP were mentioned, only the early-time short-duration E_1 pulse and the late-time long-duration E_3 pulse were considered in detail; the E_2 intermediate component was not considered to affect the power system significantly.

E_1 Surges

Since the characteristics of the E_1 surges are very similar to those of certain lightning and switching impulses, the mitigation measures recommended for the latter apply also to the E_1 pulses.

- The major protection for transmission and distribution lines and equipment is surge arresters applied directly on the equipment terminals. For E_1 protection, it is especially important to keep down leads as short as possible to minimize the inductance (rate of change of current with respect to time) voltage drop.

- When modern relay system practice using various limiters and/or filters on the relay terminals and shielded cable for the control wiring is installed, protection against E_1 as well as other transient surges is provided.

- If an electromagnetic barrier is installed around the essential parts of communication and control equipment, the communication and control systems can be protected. An effective electromagnetic barrier consists of an essentially closed conductive surface (shield) around the equipment--around the complete building or control house, individual rooms, control cabinets, or even individual control elements. Special care must be taken to divert the disturbing signals from entering the shield on power, signal, and ground wires that penetrate the shield. Various protective devices, such as arresters, filters, and optoelectronic couplers, are available and must be applied at the building or equipment barriers.

If these mitigation practices and procedures and those others specified in standards and utility guides are followed (e.g., short arrester down leads, proper cable grounding and shielding), the E_1 components of HEMP should cause only relatively minor problems.

A number of ANSI (American National Standards Institute) and IEC International Electrotechnical Commission) standards written for lightning and switching surges also apply for E_1 surges. Standards C37, C57, and other equipment standards specify the rated values and test methods for the equipment insulation and operation. The C62 standards specify similar requirements for the protective devices. Several standards pertaining to cable and shielding practices, while ostensively covering both low- and high-frequency noise, are devoted primarily to low (audio and power) frequencies. There is a danger, therefore, that the user of these standards will miss the high-frequency nuances and use only the low-frequency recommendations and feel (falsely) that he has E_1 and lightning protection. Since the rapidly increasing practice of employing direct digital transfer of control data requires consideration of frequency effects orders of magnitude above the audio range, pressure should be mounting for specific standards covering high-frequency effects. There is a real need, therefore, for a separate standard on grounding and shielding cables for digital equipment applications.

While most of the requirements of these standards apply to E_1 surges, certain changes should be made to the existing standards and several new standards should be developed to cover the more extreme characteristics of these types of surges more completely. Some suggested modifications and a suggested new standard are as follows:

- Increase the rates of rise of the applied test voltages and currents for lower voltage (34.5 kV and below) surge arresters.
- Develop E_1-type test waves and protective levels for low-voltage surge protective devices used on ac systems of 1000 V root-mean-square (rms) or less or dc systems of 1200 V or less.
- Modify C37.90.1 to require the application of the surge withstand capability test waves to each relay terminal separately.
- The working group considering modifications to C37.90.2 and the new working group of the Power System Relaying Committee considering equipment installed in the switchyard (as opposed to equipment in the control house)

should consider the magnitude and wave shape of the fields encountered because of lightning and switching surges as well as HEMP.

- A new standard or guide for the protection of electronic communication, control and protection, and digital processing equipment against high-frequency transient interference should be developed by a joint group from the Power Engineering Society, Electromagnetic Compatibility Society and Industrial Applications Society.

E_3 Surges

The circuit shielding and filters used for the mitigation of E_1 pulses in control and communication facilities are relatively ineffective for the E_3 pulses. For these longer pulses, transformers, capacitors, or fiber optics must be used to interrupt the currents. Delta-wye transformers, for example, could be used on the power supply inputs to ensure that remote ground currents go to earth rather than into the facility ground.

Since the characteristics of the E_3 surges are similar to the geomagnetic induced current (GIC) wave that accompanies the geomagnetic storm, the following mitigation methods suggested for GIC have been considered for protection of the *system* against E_3 surges. None of these is considered practical for general use for the reasons cited:

- <u>Polarizing cells:</u> Too many blocking cells required with resulting excessive costs.

- <u>Linear resistors:</u> Transformer neutral voltage (and thus insulation) and resistor losses are too high.

- <u>Nonlinear resistors:</u> Too many units required for fault energy dissipation with resulting excessive cost.

- <u>Active DC devices:</u> Require broken delta tertiary in transformer (not usually available); does not block E_3 from system (just in neutral); scheme is more complex than neutral capacitor.

- <u>Neutral capacitors:</u> Probably the most effective and economical device. Its problems are: (1) It can block neutral currents but not series winding currents in autotransformers, (2) A complex system study is required to find the correct neutrals to block, (3) It must be bypassed during faults, (4) It can cause ferroresonance problems so requires a high speed bypass device, (5) There are possible relay problems caused by the capacitor's effect on impedance to the fault, and induced transients caused by shorting the capacitor influencing the relay, (6) The fault contribution from the far end of the line can also be affected, and (7) It is expensive.

- Series capacitors: The installation of series capacitors in the transmission lines overcomes the objection that the neutral capacitors do not block the currents in the series windings of the autotransformers. Series capacitors also improve the power transmission capabilities of the system in addition to their quasi-dc blocking ability. Unfortunately, their cost is prohibitive unless they are required for reasons other than dc blocking.

As previously stated, all of these methods are considered impractical for general use as E_3 mitigation devices. Neither are they considered practical for GIC mitigation. Joint investigations for new methods to solve both problems, therefore, are indicated.

Currently, no standards specifically address the equipment capabilities or protective characteristics for E_3 type waves, including GIC. Until more is known about these capabilities or characteristics and practical mitigation measures are developed, standards or guides are not possible. It is hoped that joint studies between the GIC and HEMP communities will soon develop this data. At that time, new standards will be developed or existing standards will be modified accordingly.

Future Activities

Suggestions for modifications to the existing standards or new standards were given previously. In addition, the following studies or activities are suggested:

- The effect of HEMP on distribution automation deserves further study. How will the E_1 surges affect the communication equipment, the meter packages, the house units, etc? A momentary disruption will not hurt them, but equipment damage might be of concern. Can equipment be designed to withstand these surges? What protective devices are available? Is the potential damage level sufficiently low that just maintaining an adequate supply of spares will be satisfactory?

- Since the E_3 effects are so similar to the effects of GIC, work on the detection and mitigation devices or equipment should be coordinated and perhaps cosponsored. For example:

  a) Practical mitigation measures for both GIC and E_3 surges should be developed.

  b) Equipment and protection standards for both GIC and E_3 surges will be required.

c) While GIC can definitely damage transformers, it is felt that the duration of the E_3 surges is too short to cause damage. Further studies should validate or disprove this opinion.

d) Existing studies claim that distribution systems are not damaged by E_3 pulses, but indications are that certain consumer electronic devices could be affected. This area should be examined.

- While equipment failures may be minimal, there will be system outages due to both the E_1 and E_3 waves. Proper restoration procedures should be developed and adopted for such a contingency.

- Articles should be written in the various utility journals warning of the potential hazards of not adhering to proper design, installation, and operating procedures. These articles should also stress that while lines and substations may be relatively immune to HEMP and other system transients, communication facilities, including any telephone company facilities, must be protected similarly. More and more electronics and communication equipment will be used in the future. Utilities should design *now* for electromagnetic compatibility against switching, lightning, and fault transients; then HEMP transients, should they ever occur, will be taken care of. If protection is not designed now, it might not be possible to design it later.

1.0 INTRODUCTION

A number of excellent studies and investigations have been conducted or sponsored by the Oak Ridge National Laboratory (ORNL) and others on the effect of high-altitude electromagnetic pulses (HEMP) on electric power systems. The results of these studies have been reported in various classified and unclassified documents. More than 100 of the unclassified documents have been reviewed and abstracts of one or more pages prepared on each. A listing of the documents reviewed (but not the abstracts) is given in Appendix A of this report.

This report will summarize the conclusions reached from this review. Specifically, it will summarize the mitigation methods suggested and give a subjective evaluation of each. It will discuss the various standards that presently apply to the effects of these HEMP environments on utility equipment and suggest additions or modifications to these standards, or suggest new standards where it is felt that existing standards are deficient. Finally, it will recommend future studies or actions that might be undertaken to improve the utility system response to HEMP.

In the documents that were reviewed, various terms were used to describe the HEMP environment. There are three components to HEMP: the initial early-time, steep-front short-duration (SFSD) E_1 component; the intermediate-time, moderate-duration E_2 component; and the later-time, long-duration E_3 component. Some investigators use "HEMP" when they are really discussing the E_1 wave; others use the correct term "E_1." Some investigators use the term magnetohydrodynamic electromagnetic pulse (MHD-EMP) for the E_3 wave; others use the term "E_3." In this report the authors will try to use the term "HEMP" when discussing the overall environment and "E_1," "E_2," and "E_3" when discussing the individual components. When the authors of the specific documents are quoted directly, however, (such as in the tables and figures), the other terms may appear.

The various investigators also use the acronym "SFSD" different ways. Most define it as "steep-front short-duration", but others define it as "short-front short-duration". Still others call these waves "fast-front short-duration" surges. In this report, the authors will use "steep-front short-duration".

In the report, all the tables and figures were taken directly from the documents that were reviewed. Changes were not made for clarity or otherwise. Credit to and the numbers of the specific figures and tables referenced are given for each, using the document numbering system of Appendix A. A complete explanation of these tables and figures is not given in the text. Only comments pertinent to the subject of the report will be made. Also, the authors are not responsible for any errors contained in these figures or tables. Any errors known to the authors, however, will be indicated in the text.

2.0 ELECTROMAGNETIC PULSE ENVIRONMENT

A nuclear electromagnetic pulse (NEMP or EMP) is often classified according to the height of burst: surface, air, or high-altitude. The surface detonation occurs on or near the ground (0 to 2km in altitude) and produces what is referred to as a source region EMP (SREMP). Within the source region producing this environment, the SREMP disturbance is characterized by a large pulse having an electric field (E-field) amplitude of up to several hundred kilovolts per meter (kV/m) and a rise time of 30 to 50 ns. Electrical power systems within this region will probably be damaged or destroyed by the blast and shock environments arising from the detonation. Outside the source region, the SREMP field propagates away from the burst point, decreasing in amplitude at a rate slightly faster than 1/R, where R is the distance from the burst. This decrease in the radiated fields implies that the potentially damaging effects of SREMP will be localized to a region near to the detonation. Nearby power lines, however, can couple strongly to this environment, and the resulting induced current surges on the lines can propagate for many kilometers to affect distant equipment.

The air burst occurs between 2 and 20 km above ground. While it covers a larger area, it is relatively weak, being at least one order of magnitude lower than air bursts created by the surface blast.

The high-altitude burst takes place 40 km or more above the ground and has been of primary concern to utility systems. While the effects of SREMP are localized to a region near the detonation, a high-altitude burst can cover a significant portion of the continental United States with an intense electromagnetic (EM) field. This environment is referred to as a HEMP. Such widespread and virtually simultaneous coverage of the country by this *global* transient pulse poses problems for the power system that are different from those arising from *local* disturbances such as lightning strikes and switching events.

HEMP is defined in terms of E_1, SFSD waves having magnitudes of tens of kilovolts/meter, fronts of approximately 5 to 10 ns, and durations of less than 1 μs; E_2, intermediate waves having magnitudes of hundreds of volts/meter and durations of 1 μs to 0.1 s; and E_3, waves having magnitudes on the order of tens of V/kilometer and durations of a few seconds to many tens of seconds. The E_1 and E_3 waves are considered significant, but preliminary studies suggest that the E_2 fields should not pose serious problems.

The early-time E_1 component of HEMP is known to have an amplitude, waveshape, and polarization that depend on the observer's location relative to the burst point. Early investigations into the possible effects of E_1 on electrical systems used a worst-case, bounding waveform [I-1] for the environment. This so-called "Bell Laboratory waveform" has a magnitude of 50 kV/m, a 10 to 90% rise time of 4.6 ns, and a 90 to 10% fall time of 550 ns. Although the E_1 environment is known to be predominantly horizontally polarized in the region illuminated by the burst, the Bell Laboratory waveform was usually used with the worst-case polarization of the incident field on a system. This provided an upper bound on the system response. As such, the main use of this pulse was to design a hardened system for military purposes.

For the purpose of assessing the E_1 effects on the power system (as opposed to designing a hardened system), an alternate E_1 environmental description has been developed which takes into account the details of the waveform variations in the illuminated region [I-5]. This is frequently called the "Longmire environment". As a result, the calculated current and voltage levels in power system components for this environment are significantly smaller than for the Bell Laboratory waveform. As an example of the early-time E-fields produced by a E_1 pulse, Fig. 2-1 shows typical incident field waveforms calculated for an idealized 1 MT detonation at an altitude of 400 km, plotted for several ground ranges to the west of ground zero. For this particular detonation, the maximum E_1 amplitude is slightly over 39 kV/m, but the wave duration is quite a bit shorter than that of the Bell Laboratory waveform.

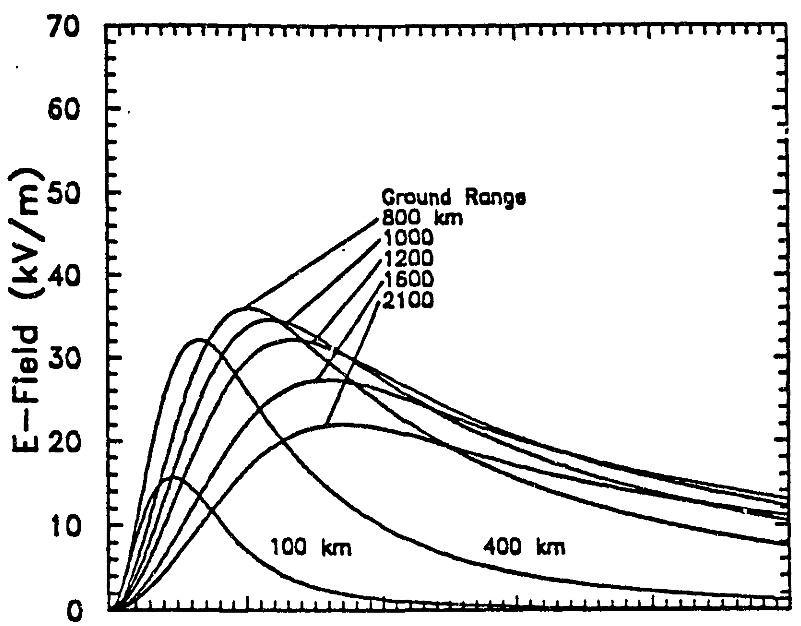

Fig. 2-1. Transient E_1 waveforms to the west of ground zero.
Source: Fig. 2-1 of Document I-5.

The specific choice of burst altitude, yield, and device characteristics will affect this peak E-field; a higher peak field strength frequently used for assessment purposes is 50 kV/m. The maximum value of this environment occurs just south of ground zero. Fig. 2-2 shows that the field strengths at other locations on the earth vary as a function of position in the illuminated region. The actual size of this illuminated region is a function of the height of burst (HOB), as shown in Fig. 2-3. Note that with a 300-km burst, the tangent point defining the outer radius of the illuminated region is about 2000 km. This indicates that practically the entire United States would be illuminated by a burst over the center part of the country.

The E_1 field propagates as a plane EM wave having mutually perpendicular electric (E) and magnetic (H) fields, as shown in Fig. 2-4. For a peak E-field of 50 kV/m, the corresponding H-field is 130 A/m. The total energy contained in the E_1 pulse may be evaluated as:

$$W = \frac{1}{Z_c} \int_{-\infty}^{\infty} |E(t)|^2 \, dt$$

where Z_c = 377 Ω is the impedance of free space. For the Bell Laboratory waveform, the waveform energy is $W \approx 0.96 \text{ J/m}^2$, and for the slightly lower magnitude but shorter duration Longmire waveform, this energy is $W \approx 0.08 \text{ J/m}^2$.

These E_1 values may seem extreme, but comparable values already exist on utility systems. While lightning and switching surges are normally thought of as having much longer wave fronts and durations than E_1 (μseconds instead of nanoseconds), Tables 2-1 and 2-2 show that in many cases they are comparable. The lightning strokes considered are the second and later components of multiple lightning strokes. Tower backflashes also cause these steep front surges. The fronts of these surges are quickly attenuated, however, as they travel away from the stroke location.

For example, Fig. 2-5 shows calculated curves of how corona (curves B) and normal line loss without corona (curves A) attenuate and slope off the front of a typical lightning wave as it travels along the line. Fig. 2-6 shows test data for different conductors of the increase in front time of the wave per thousand feet of travel due to the corona effect. The E_1-induced effects, however, may be continually reinforced by the inducing wave propagating along the conductor and thus suffer no attenuation. Note also that the field strengths, while very localized (such as directly under the switched line or near to the lightning strike), are also comparable: 10 and 40 kV/m versus 50 kV/m.

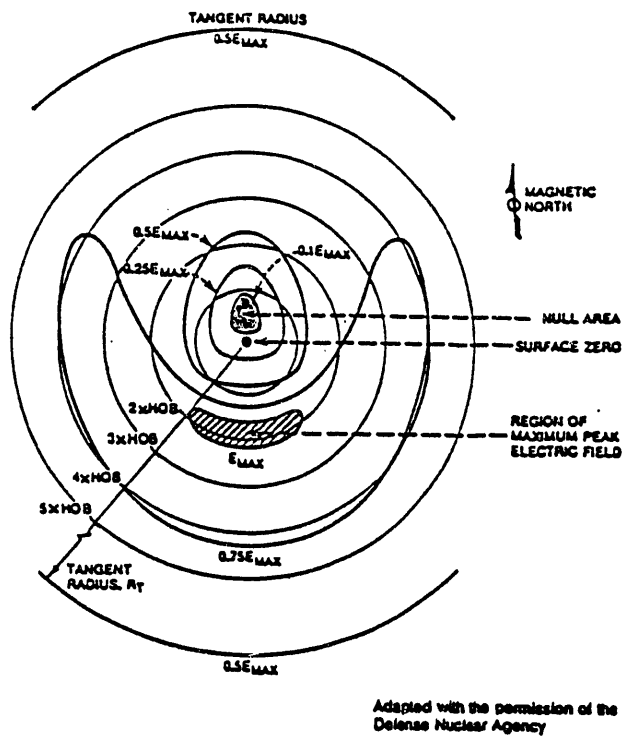

Fig. 2-2. An example of variations in high altitude electromagnetic pulse peak electric field on surface of continental United States.
Source: Document I-1.

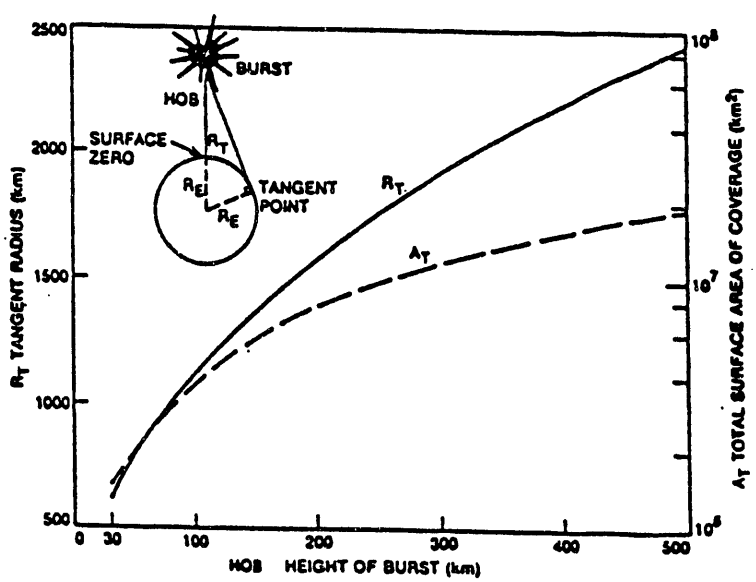

Fig. 2-3. Electromagnetic pulse ground coverage (tangent radius) and total area of coverage as functions of height of burst.
Source: Document I-1.

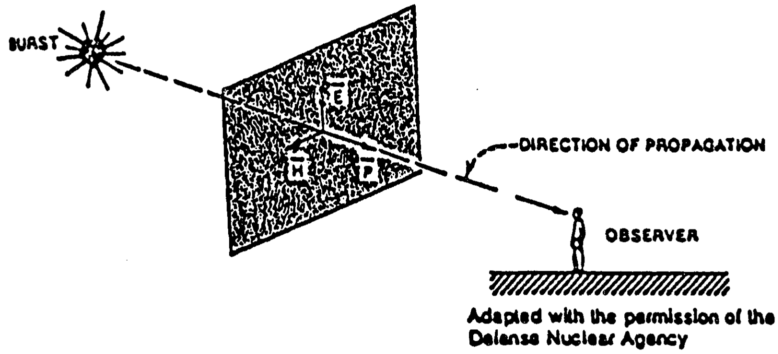

Fig. 2-4. Radiated electromagnetic pulse field propagates locally as a plane wave.
Source: Document I-1.

Table 2-1. Characteristics of steep-front short-duration impulse sources.
Source: Document V-6.

CHARACTERISTIC		SFSD IMPULSE TYPE		
		LIGHTNING	EMP PLANE WAVEFORM (TYPICAL WAVEFORM)	SYSTEM-GENERATED
FIELD STRENGTH (FREE SPACE)	Electric (E)	† 40 kV/m	50 kV/m	10 kV/m
	Magnetic(M)	300 A/m	†† ~~2000 A/m~~	300 A/m
IMPULSE SHAPE	Rise time	20-500 ns	10 ns	10 ns
	Time to half value	5-20 µs	††† ~~10-200 µs~~	1-5 µs
PEAK CURRENT		200 kA	10 kA*	—
PEAK VOLTAGE		—	2000 kV*	2-3X system voltage
PULSE DURATION		10-1000 µs	1 µs	1-10 µs

*Peak induced values.

† About 25 m in distance from a nearby strike.

†† This value is suspect since for electromagnetic pulses it should be related to the electric field by the impedance of free space (377 ohms).

††† These times are inconsistent with all other reports on the time duration of E_1. Possibly the originating authors mistakenly listed the times for E_2 waves.

Table 2-2. Lightning stroke current data.
Source: Document XI-6.

	First Stroke					Subsequent Strokes				
	% Exceeding the Value					% Exceeding the Value				
Parameter	95%	50% (M)	5%	β	ρ	95%	50% (M)	5%	β	ρ
Crest Current, kA	14	31.1	69	0.48	0.38	5	12.3	29	0.53	0.56
Maximum Steepness, kA/µs	9	24.3	65	0.60	0.38	10	39.9	162	0.85	0.56
Minimum Linear Front, µs	0.5	1.28	3.5	0.61	--	0.1	0.31	1.0	0.71	--
Time-to-Half Value, µs	30	77.5	200	0.58	--	7	30.2	140	0.93	--

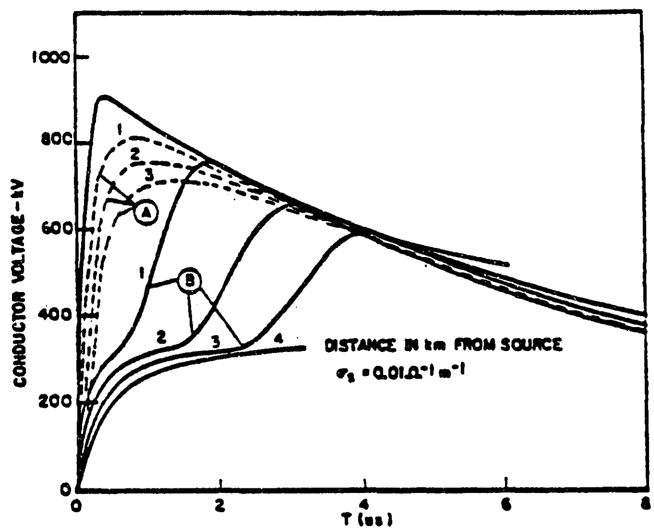

Fig. 2-5. Illustration of (A) non corona and (B) corona distortion with distance along a line.
Source: Document V-1.

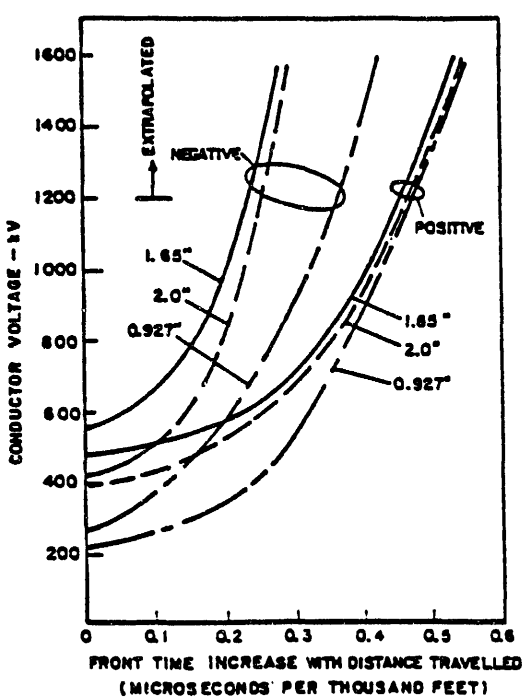

Fig. 2-6. Test data from Tidd Project for a single conductor.
Source: Document V-1.

Document X-1 shows that the E and H field strengths for air-insulated disconnect switch operations in 115- and 500-kV stations are on the same order of magnitude as the E_1 fields. It also shows that a phase-to-ground fault in the 500-kV station also produces equivalent fields. A direct lightning stroke to the station produces an even higher field strength. While this is an extreme condition, it demonstrates that higher values than E_1 can occur from natural causes.

It should be noted (see Document I-14), that although lightning, faults, and switching can cause equivalent fields, they represent local events and disturbances; as mentioned previously, E_1 fields can exist system-wide. As will be discussed in later sections, this can affect the overall system effects of these fields.

In addition to this extremely fast E_1 transient, the E_3 component, perceived at much later times (seconds to hundreds of seconds after the burst), has a much lower magnitude and a much longer duration. This component is sometimes called the MHD-EMP transient. Fig. 2-7 shows an example of the time plot of such a pulse. The effects of the E_3 pulse are often compared with solar disturbances (solar storms) that produce geomagnetically induced current (GIC) effects in power transmission systems. The E_3 pulse has a greater intensity and time rate-of-change than the storm effects but has a shorter duration, lasting a few hundred seconds compared with tens of minutes to hours for the storm [II-22]. Their equivalent frequencies are both less than 1 Hz (in effect dc currents). Despite their differences, there is sufficient similarity that their effects on the power system can be analyzed similarly.

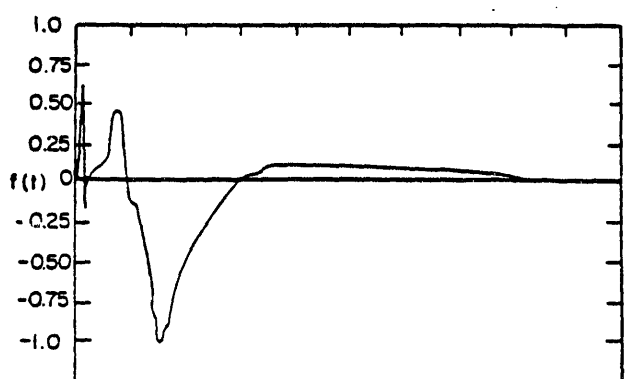

Fig. 2-7. Example of normalized magnetohydrodynamic electromagnetic pulse F(t) function.
Source: Document II-15.

3.0 E_1 WAVES

The literature describes tests and analytical investigations on the effect of SFSD waves on various elements of the power system. These elements are overhead lines, power cables, transmission and distribution (T & D) equipment, power plants, protective relaying, and communication and control equipment. These elements will be discussed in the following sections, together with the presently used protective devices and measures used to mitigate the effects of these SFSD waves.

3.1 Overhead Lines

The E and H fields of Fig. 2-4 induce voltages and/or currents on lines, cables, apparatuses and structures in their path. Document III-1 develops formulas for this coupling, and computer programs are available for calculating the open circuit voltages and induced currents.

All of these voltages have the SFSD wave shapes of the EMP fields themselves. Thus before the effect of these waves on the T & D lines can be determined, one must determine the insulation strength of the lines for these wave shapes. Documents III-2, 3, 7, 8, and V-6 describe tests run on various types of line and bus insulators. Table 3.1-1, for example, shows the critical flashover (CFO) values for SFSD waves, as well as for the standard 1.2 x 50 μs waves, for different pin and suspension insulators including the effect of different lengths of wood crossarms. These data, as well the other test results, indicate that the CFO for the SFSD waves is 1.5 to 2.0 times the CFO for the standard 1.2 x 50 μs waves. Since the latter is published for all major air insulation paths, the 1.5 to 2.0 value can be used to estimate the SFSD strength of these same insulation paths.

Document III-5 describes a study to determine the vulnerability of T & D lines to HEMP. Using the nominal 39 kV/m maximum E_1 field at the surface of the earth, the field strengths throughout the United States were calculated (see Fig. 3.1-1). Using these field strengths, the open-circuit induced voltages were then calculated for the worst line orientation (that giving the maximum voltage) for each of four typical transmission and distribution lines: 500 kV, 230 kV, 69 kV and 12 kV. Fig. 3.1-2 shows the results for the 12-kV line case.

The area of illumination was then divided into 100 equally spaced locations and since the induced voltage depends on the orientation of the line with respect to the direction of propagation of the surge (see Fig. 3.1-3), at each of these locations the line orientation was varied from 0 to 360° in 10° increments. The magnitude of induced voltage for each exposure was then calculated. The total results of these 3600 calculations were combined into a cumulative probability distribution. Fig. 3.1-4 shows the results for the 12-kV line.

Table 3.1-1. Steep-front short-duration impulse test results.
Source: Table 1 of Document III-8.

Insulator	Type	Rated* CFO(kV)	SFSD Waveform	SFSD CFO(kV)	CFO Ratio	Comments
pin	55-4	105	65X5000ns	220	2.1	1
pin	55-5	130	65X5000ns	245	1.88	1
pin	55-6	150	65X5000ns	320	2.13	1
pin	55-6	150	35X325ns	312	2.08	2,sd=2.7
pin	55-3	90	-------	---	---	6
pin +wood	55-4	N/A	N/A	N/A	N/A	3,5
pin	55-2	70	--------	----	---	6
one SI	52-3	142**	40X500ns	295	2.08	2,sd=3.3
two SI	52-3	323**	40X500ns	423	1.31	2
two SI	52-3	323**	40X500ns	492	1.52	2,4
two SI	52-3	323**	30X350ns	625	1.93	2
two SI	4-in	188**	65X5000ns	400	2.13	1
two SI	4-in	238**	65X5000ns	465	1.95	1,5

* CFO Rated by ANSI Class (type) Sec. 4.7, ANSI C29.1,1982.
** tested value
N/A-not available
SI-Suspension Insulator
sd-standard deviation in percent.
1. MSU test results @ 400-500ns time to flashover.
2. CPS test results-average values.
3. MSU retest results.
4. with 8 in. of wood.
5. with 6 in. of wood.
6. not tested.

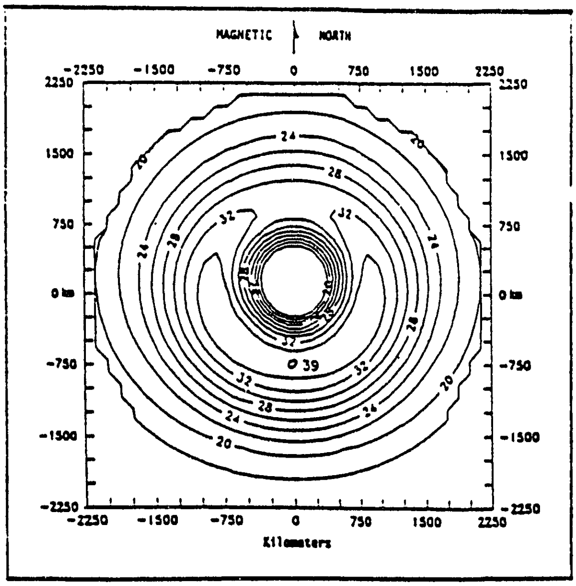

Fig. 3.1-1. High altitude electromagnetic pulse field magnitudes in kV/m within the area of illumination.
Source: Fig. 1 of Document III-5.

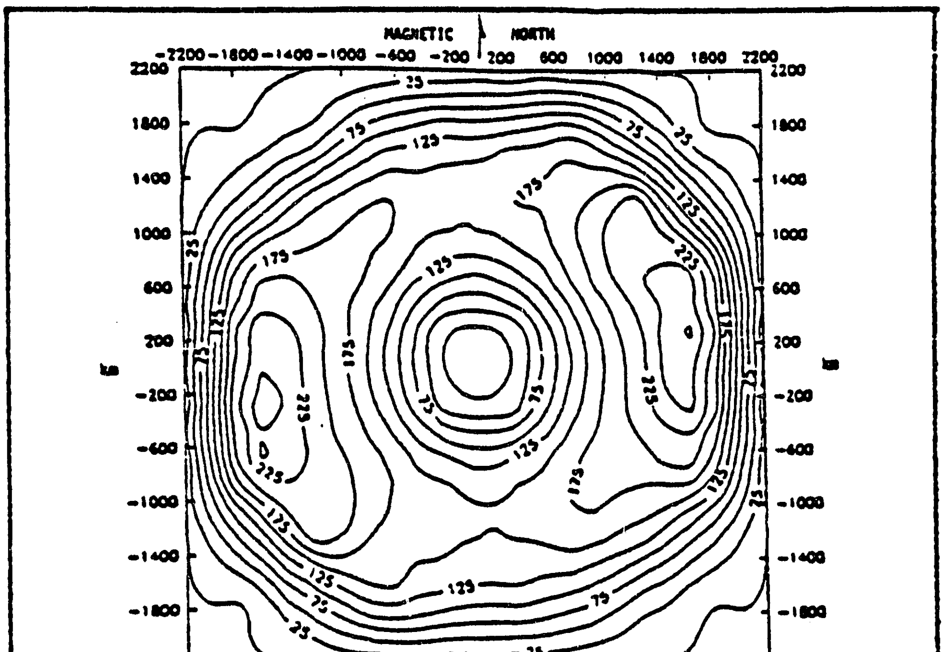

Fig. 3.1-2. Plot of high altitude electromagnetic pulse-induced voltages for phase number 3 of 12-kV line.
Source: Fig. 7 of Document III-5.

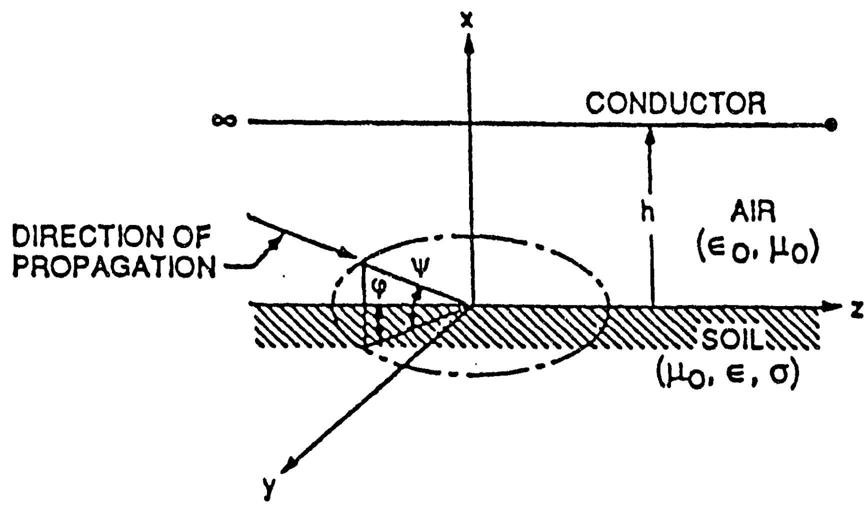

Fig. 3.1-3. Coordinates defining azimuth and elevation angles of incidence.
Source: Fig. 1-3 of Document VIII-2.

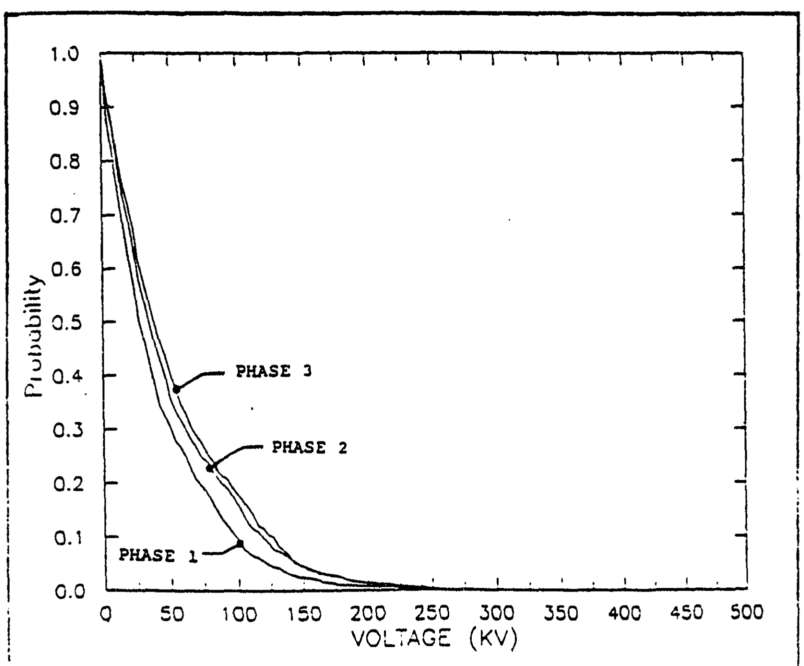

Fig. 3.1-4. Cumulative distribution of high altitude electromagnetic pulse-induced voltage on the 12 kV-line (probability of exceeding a voltage).
Source: Fig. 8 of Document III-5.

As mentioned, insulation test results have shown that the line insulation level for SFSD waves similar to the E_1 waves is 1.5 to 2 times the 1.2 x 50 wave value. Using the 1.5 factor, Table 3.1-2 shows the range of insulation levels used for the four typical lines. Table 3.1-3 shows that the maximum induced voltages for the 69-, 230-, and 500-kV lines are less than their CFOs so they should not be subject to insulation flashovers. The 12-kV circuits, however, are vulnerable.

Table 3.1-2. Estimated high-altitude electromagnetic pulse line insulation strength by operating voltage.
Source: Document III-5.

LINE OPERATING VOLTAGE kV	RANGE BASED ON CURRENT PRACTICE ESTIMATED HEMP LINE-INSULATION STRENGTH 1.5x Min. kV	1.5x Max. kV
500	2445	3900
230	1467	2445
69	488	975
12	140	165

Table 3.1-3. Comparison of high-altitude electromagnetic pulse-induced voltage to estimated high-altitude electromagnetic pulse-insulation strength.
Source: Document III-5.

LINE OPERATING VOLTAGE kV	ESTIMATED HEMP LINE-INSULATION STRENGTH 1.5x Min. kV	1.5x Max. kV	MAXIMUM INDUCED VOLTAGE kV	
500	2445	3900	800	INVULNERABLE
230	1467	2445	725	INVULNERABLE
69	488	975	450	INVULNERABLE
12	140	165	275	VULNERABLE

Fig. 3.1-5 shows the probability curves and the CFO ranges and demonstrates the vulnerability of the 12-kV line. For a 140-kV CFO, the probability of flashover is 6%. For a 165-kV CFO, the probability is 3.1%. Table 3.1-4 shows these probabilities plus the zero probabilities for the higher voltage lines. The table also shows the results if lower (25 kV/m) and higher (50 kV/m) maximum E_1 field strengths were assumed.

These probabilities are for the complete illumination area. In other words, they are essentially the average results for all the lines of all the utilities in the United States. Table 3.1-5 shows the results in just a 400 x 400 km area that was subjected to the maximum field strengths. These results are several times higher than the average.

The values in Tables 3.1-4 and 3.1-5 assume a single high-altitude burst. Multiple bursts would increase these probability values. For multiple bursts, the assumption is that the occurrence is sequential, occurring at least 1s apart. Since the E_1 surge is only microseconds in duration, the effects of multiple E_1 events appear as sequential events, each event ending before the next occurs. It would appear that the probabilities would therefore be a product function: $P_n = (1-P^n)$. This is not strictly so; the effects are more complicated. For example, once a fuse is blown, it cannot be blown again. Once a recloser trips, it may or may not have reclosed before the second burst occurs. Thus while the probabilities increase, the amount of increase is difficult to establish.

Figs. 3.1-6 and 3.1-7 show the results of a similar study [III-6] made for a 12.47-kV distribution circuit. While the study was primarily interested in the effects of E_1 on transformers connected to this circuit, the open circuit curves can be compared with the line results of the other study. Note that Fig. 3.1-6 refers to the average U.S. results and compares favorably with the 39 kV/meter-values of Table 3.1-4. Fig. 3.1-7 is similar to Table 3.1-5.

Figs. 3.1-6 and 3.1-7 show that transformers reduce the magnitude of the induced voltages, at least at the transformer terminals. If surge arresters were used on the transformers, these voltages would be further reduced.

The conclusion to be drawn from these studies is that transmission and subtransmission lines will be unaffected by E_1 pulses. Distribution lines of 15 kV and below may encounter some flashovers. The trend of increased use of higher voltages for distribution will reduce this effect. The use of surge arresters at every two or three poles (perhaps metal oxide varistors either used as or built into the line insulators) would alleviate this problem.

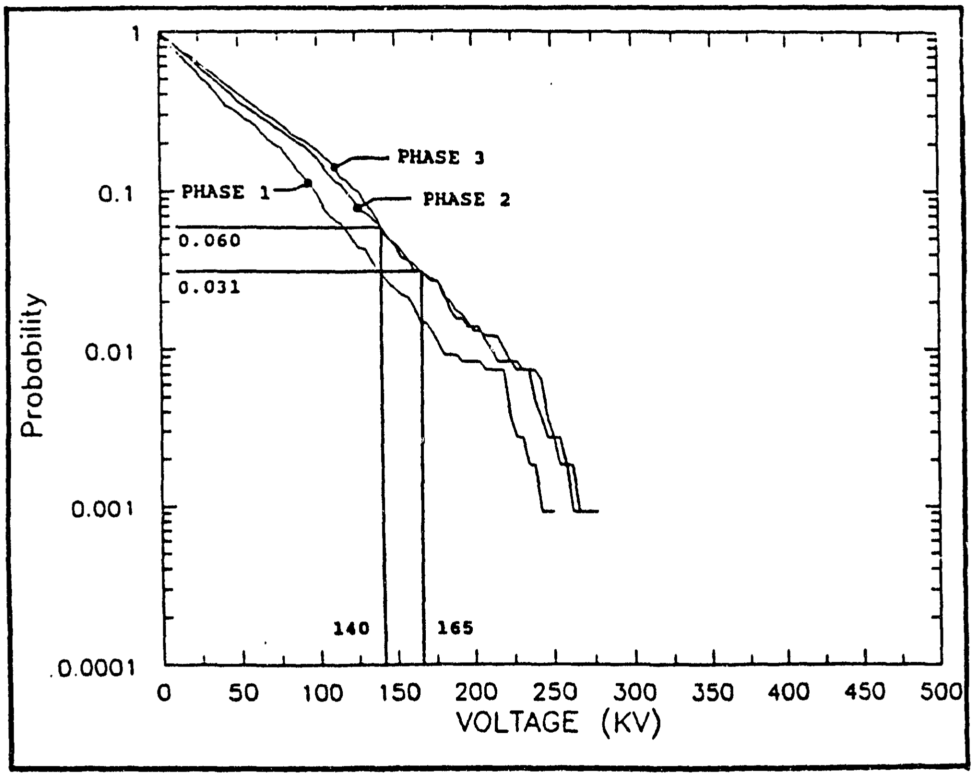

Fig. 3.1-5. High altitude electromagnetic pulse-induced flashover vulnerability for phase number 3 of the 12 kV-line.
Source: Document III-5.

Table 3.1-4. Sensitivity of high altitude electromagnetic pulse-flashover vulnerability to various high altitude electromagnetic pulse field strengths for the area of illumination.
Source: Document III-5.

OPERATING VOLTAGE kV	25 kV/m FIELD PERCENT		39 kV/m FIELD PERCENT		50 kV/m FIELD PERCENT	
	Min.	Max.	Min.	Max.	Min.	Max.
12	3.0	5.8	9.0	11.	12.	18.

Table 3.1-5. Sensitivity of high altitude electromagnetic pulse-induced, 12-kV line flashover vulnerability to various high altitude electromagnetic pulse-field strengths for 400 by 400 km maximum-voltage region.
Source: Document III-5.

OPERATING VOLTAGE kV	25 kV/m FIELD PERCENT		39 kV/m FIELD PERCENT		50 kV/m FIELD PERCENT	
	Min.	Max.	Min.	Max.	Min.	Max.
500	0.0	0.0	0.0	0.0	0.0	0.0
230	0.0	0.0	0.0	0.0	0.0	0.0
69	0.0	0.0	0.0	0.0	0.0	1.7
12	0.2	1.0	3.1	6.0	9.0	15.

The above studies assumed straight line distribution circuits with directional orientations uniformly distributed from 0 to 360°. They also assumed a maximum E_1 field of 39 kV/m. A recent unpublished study--using a maximum field strength of approximately twice this value and assuming that every distribution circuit had at least a portion of its length in the direction of the maximum field strength and unprotected by transformers or arresters--showed that essentially every circuit 12 kV and below over an area of approximately 1600 by 1600 km (1000 by 1000 miles) would flash over.

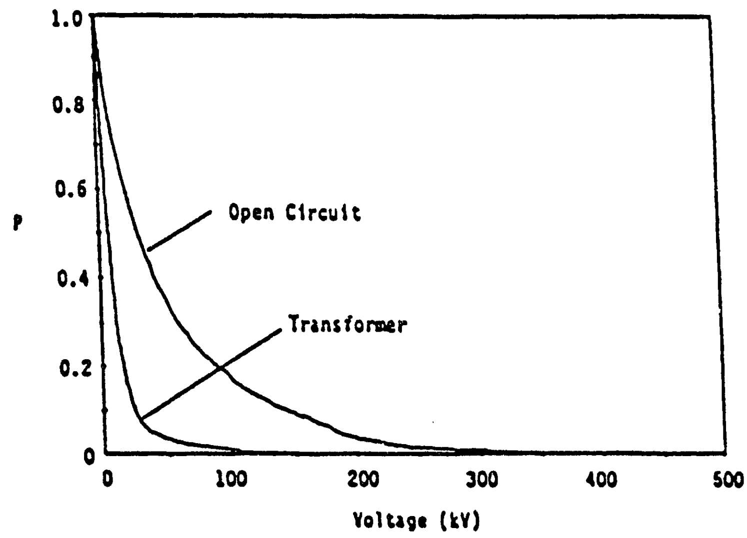

Fig. 3.1-6. Probability of the peak transformer voltage exceeding the abscissa value.
Source: Document III-6.

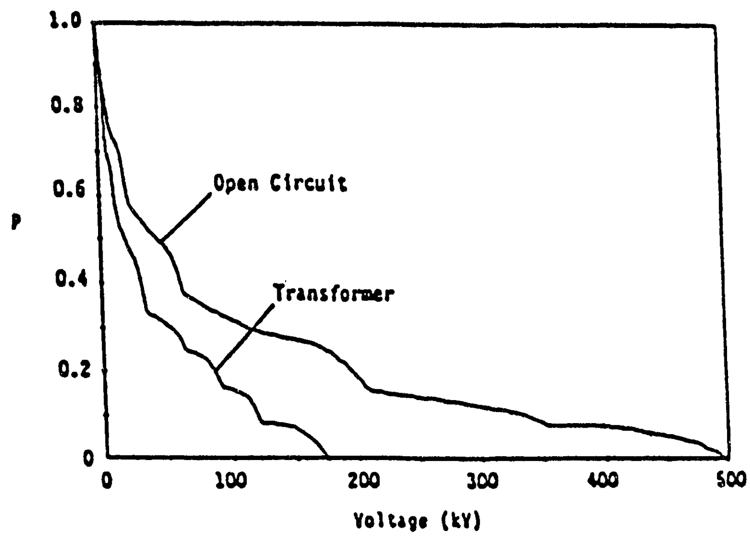

Fig. 3.1-7. Probability of the peak transformer voltage exceeding the abscissa value for line in a 500-km square region centered over the position of maximum line response.
Source: Document III-6.

Should these assumptions prove correct, a whole system or several neighboring systems could have all their overhead distribution circuits lost. With multiple bursts judiciously spaced over the continental United States, all utilities could be similarly affected.

The consequences of such a scenario depend on the amount of load represented by the overhead 12 kV and below distribution circuits (as opposed to underground circuits and commercial and industrial loads). For some utilities, this load represents a small percentage of the system load; they would be relatively unaffected. Others with higher percentages could encounter generator tripouts or system splitups due to instability considerations.

This same study also showed a possibility of high induced voltages on the 220-volt secondaries from the transformer to the residence. This could cause residential outages if the secondary protectors cannot handle this duty.

3.2 Power Cables

Voltages and/or currents are induced in power cables in the same manner as in overhead lines. The only difference is that cables are usually buried underground, so the depth of burial affects the induced quantities (Fig. 3.2-1).

The cables are usually shielded so that the voltage on the conductor is $V(\omega) = I(\omega) x Z_T$, where Z_T, the transfer impedance, depends on the type of shield. Document III-1 also develops formulas for overhead and buried cable and shows how to calculate Z_T for the various types of shielded cables. Fig. 3.2-2 shows some transfer impedances for coaxial and other types of cables, including power cables. These are expressed in multiples of R_0, the dc resistance of the sheath. Table 3.2-1 compares the shielding effectiveness, weight, and cost of different cable shielding methods.

There is little data on the insulation strength of power cables to E_1 type impulses, but what there is indicates that flashovers or failures should not be a problem. Document III-7 gives data on 15- and 25-kV terminators (potheads) which indicate the SFSD strength is 2 to 3 times the standard 1.2 x 50 μs values. If surge arresters are properly applied on the potheads, there should be no problems. There could be problems if the arresters are installed too far from the pothead or with too long a down lead. This effect is discussed in Section 3.3.1. (Note that the failure mode, should a failure ever occur, would always be a destructive puncture as opposed to a recoverable flashover that usually occurs on air bushings. So any failure from an E_1 pulse would lead to a permanent outage and not one cleared by a recloser operation.)

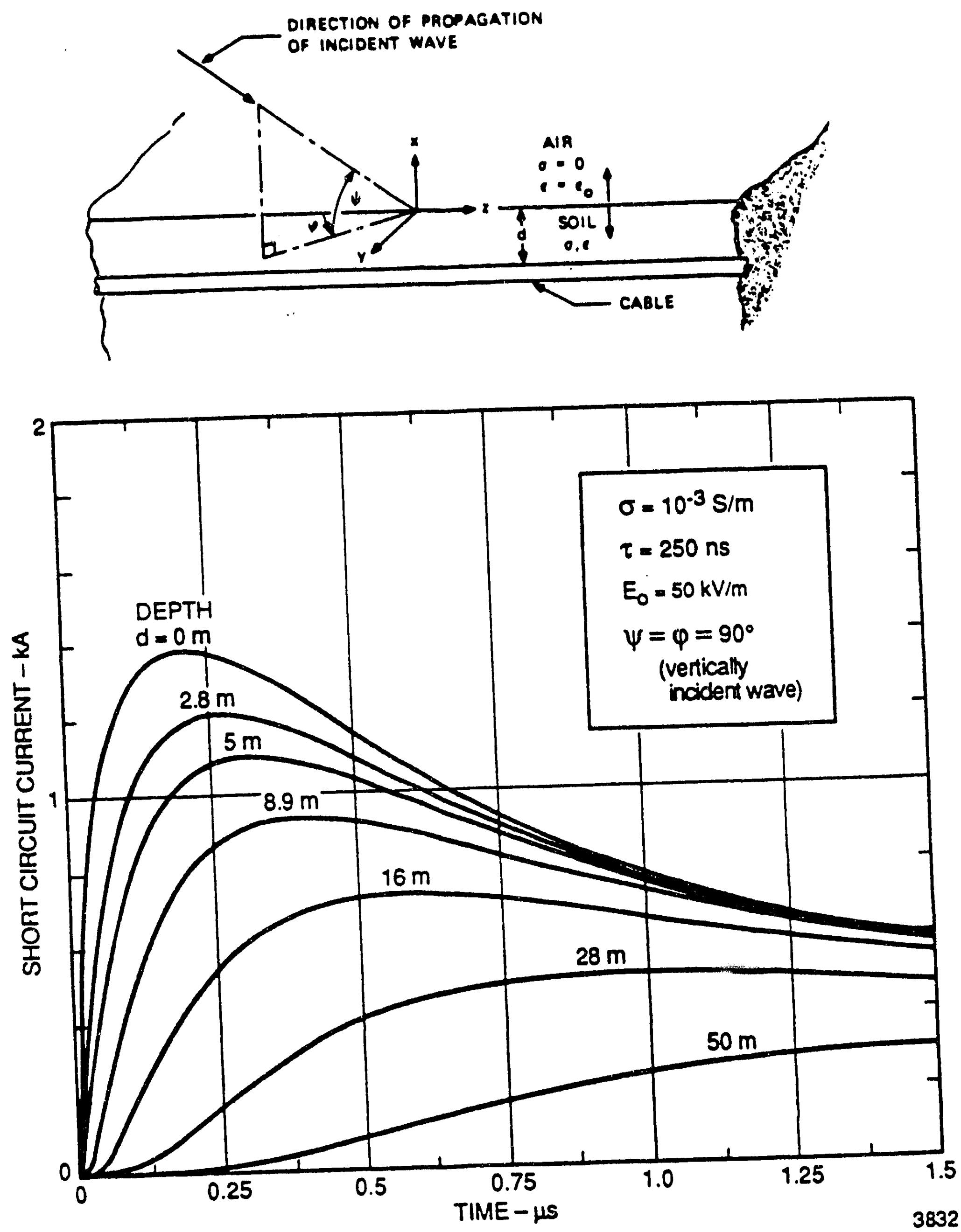

Fig. 3.2-1. Normalized current waveform for various values of depth d for incident exponential pulse $E(t)=E_0e^{-t/\tau}$.
Source: Document VIII-2.

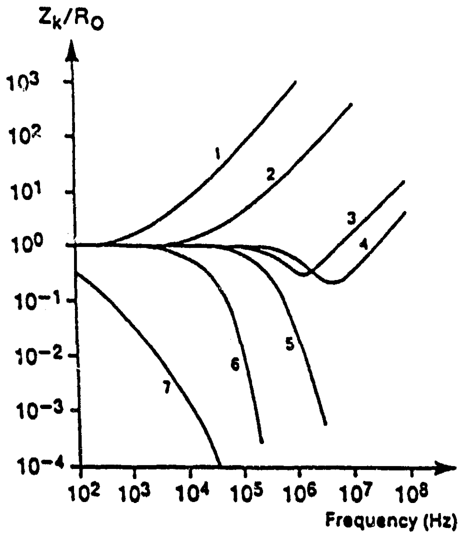

Relative transfer impedance as a function of frequency for different cables. The d.c. resistance of the sheath, R_{e}, is often 1–10 mohm/m

1 Aluminium tape wound with a helix angle of 25°
2 Power cable EKFR (10 x 1.5)
3 Braided coaxial cable RG 11
4 Mains cables (EKLR or FKLR)
5 1.4 mm thick homogeneous lead pipe
6 1 mm thick homogeneous aluminium pipe
7 Steel tape between two homogeneous aluminium pipes

Fig. 3.2-2. Relative transfer impedance as a function of frequency for different cables.
Source: Document I-10.

Table 3.2-1. Comparison of cable shielding materials.
Source: Document VIII-2.

	Shielding Effectiveness (dB)	Relative Weight	Relative Cost
Solid Shields	> 110	--	--
Ferromagnetic			
Permalloy, Hipernom	Excellent	Thin/light	High
Steel	Excellent	Thin/light	Low
Nonmagnetic			
Aluminum	Excellent	Light	Low
Copper	Excellent	Heavy	Moderate
Brass	Excellent	Heavy	Moderate
Braid Shields (Single layer)	20 to 50	-- --	
Tinned copper	Excellent	Moderate	Low
Nickel-plated copper	Excellent	Moderate	Low
Monel	Good	Moderate	Moderate
Nickel	Good	Moderate	Moderate
Stainless steel	Good	Moderate	Moderate
Multilayer Braid Shields			
Double-braid	70 to 100	Heavy	Moderate
Triple-braid	90 to 120	Very heavy	High

Document IV-1 found that repeated surges (40- and 70-kV square waves and 120-kV ringing waves) and 25-kV thumper tests did not appear to affect the ac or impulse strength of the cables being tested but did affect the cable life. It was interesting that failures did not occur at the time of the applied impulse but occurred later under power frequency conditions. This might explain why more cable failures occur *after* thunderstorms.

Based on the above, it can be concluded that power cable systems (cables and potheads) with properly applied surge arresters should not present a problem during a nuclear detonation. The degradation phenomenon should not be a factor here, since there will be few (and hopefully no) exposures to impulses due to this cause.

3.3 Transmission & Distribution Equipment

3.3.1 Surge Arresters

The characteristics of surge arresters to SFSD waves are discussed in three of the documents. Tables 3.3.1-1 and 3.3.1-2 from Document V-6 show the critical impulse sparkover (CISO) and front-of-wave (FOW) sparkover of 96-kV silicon carbide (SiC) and metal oxide varistor (MOV) station class arresters for the following three test waves:

- 1.2 x 50 μs lightning impulse
- 10 x 150 ns HEMP impulse
- 100 x 500 ns slower EMP impulse

Table 3.3.1-1. Results of tests on 96-kV silicon carbide station-class arresters.
Source: Document V-6.

WAVEFORM	INITIAL CISO[a] (kV)	FOW SPARK-OVER (kV)	1.2 × 50 μs CISO AFTER SFSD[b] (kV)	RATIOS	
				CISO(SFSD) / CISO(1.2×50)	FOW(SFSD) / FOW(1.2×50)
1.2 × 50 μs	190	219	N/A	N/A	N/A
100 × 500 ns	294	333	184	1.6	1.5
10 × 150 ns	314	918	191	1.6	4.2

Table 3.3.1-2. Results of tests on 96-kV metal oxide varistor, station-class arresters.
Source: Document V-6.

WAVEFORM	INITIAL CISO[a] (kV)	FOW SPARKOVER (kV)	1.2 × 50 μs CISO AFTER SFSD[b] (kV)	RATIOS	
				CISO(SFSD) / CISO(1.2×50)	FOW(SFSD) / FOW(1.2×50)
1.2 × 50 μs	170	208	N/A	N/A	N/A
100 × 500 ns	202	---	172	1.2	---
10 × 150 ns	248	685	162	1.5	3.3

The ratio of the CISO for the SFSD waves to the CISO of the 1.2 x 50 μs wave is 1.2:1.6.

Table 3.3.1-3 shows similar data for the 30-kV SiC distribution-class arrester. Here the ratios are 1.1:2.0. Reference V-6 shows only front-of-wave data on the 30 kV distribution class MOV arrester. Therefore, no meaningful conclusions can be drawn from these data.

Table 3.3.1-3. Results of tests on 30-kV silicon carbide distribution-class arresters.
Source: Document V-6.

WAVEFORM	INITIAL CISO[a] (kV)	FOW SPARKOVER (kV)	1.2 × 50 μs CISO AFTER SFSD[b] (kV)	RATIOS	
				CISO(SFSD) / CISO(1.2×50)	FOW(SFSD) / FOW(1.2×50)
1.2 × 50 μs	75	81	N/A	N/A	N/A
100 × 500 ns	85	187	76	1.1	---
10 × 150 ns	148	483	76	2.0	6.0

Note that the ratios of FOW sparkover for the SFSD waves to the 1.2 x 50 μs wave are much higher (3.3:6.0). This ratio is probably due to the inductive voltage drop (di/dt) of the leads as discussed in Documents III-7 and IX-1.

Document III-7 shows test results on 10-kV MOV and SiC arresters for 60 x 300 ns waves. Fig. 3.3.1-1 shows the arrester peak voltages as a function of the surge current.

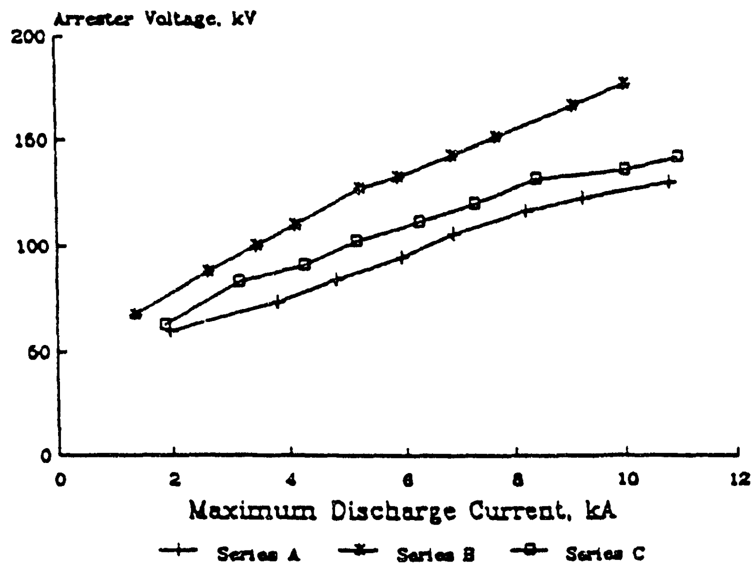

Fig. 3.3.1-1. Arrester peak voltage vs. peak steep-front short-duration current. Series A: 10-kV metal oxide varistor, 24 in. lead; Series B: 10-kV gapped silicon carbide, 45 in. lead; Series C: 10-kV gapped silicon carbide, 24 in. lead.
Source: Fig. 6 of Document III-7.

Comparable values for the 10 kA 8 x 20 test current wave are 27 kV for the SiC arrester and 33 kV for the MOV arrester. This big difference is probably due to the inductance of the arresters and the leads (which were approximately 24 in. for the test). The steep slope of Fig. 3.3.1-1 is indicative of the L di/dt of the leads and arresters.

In Document IX-1 pulser tests were run on two 9-kV MOV arresters and one SiC arrester. Current and voltage wave shapes for 5-kA and 20-kA surges on one of the MOV arresters are shown on Figs. 3.3.1-2 and 3.3.1-3. The voltage rise time is approximately 50 ns.

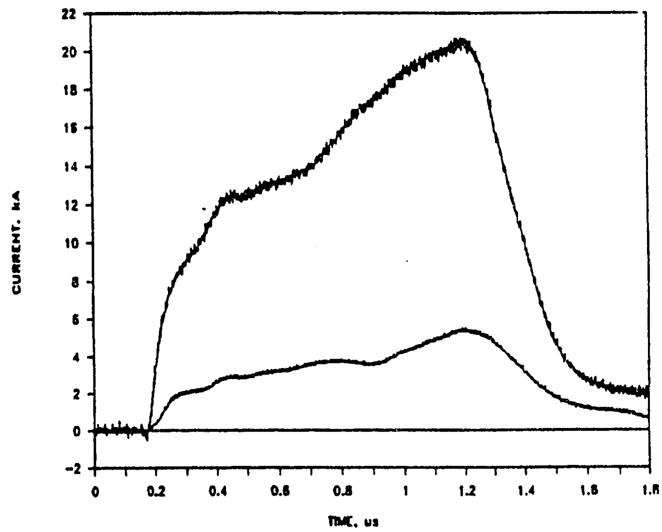

Fig. 3.3.1-2. Current waveshapes for the 9-kV metal oxide varistor arrester at approximately 5- and 20-kA peak.
Source: Document IX-1.

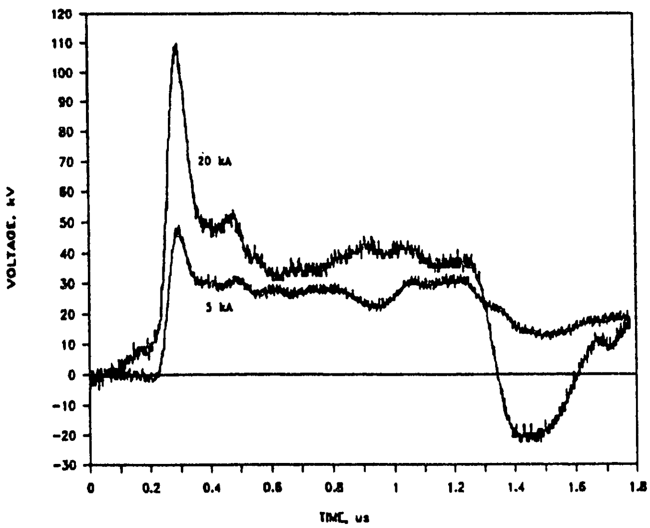

Fig. 3.3.1-3. Metal oxide varistor arrester voltages during the 5-kA and 20-kA current pulses shown in Fig. 3.3.1-2.
Source: Document IX-1.

The "overshoot" on the voltage wave is due to the inductance of the arrester. This was proved by inserting an aluminum tube of the same dimensions as the arrester in the circuit instead of the arrester. Fig. 3.3.1-4 shows the same shape as the "overshoot", with the "residual" voltage essentially zero. The inductance was calculated to be about 0.03 μhenries/cm. (This is 0.914 μhenries/ft., which seems too high--0.4 μhenries/ft. is the normally assumed value for a length of lead having a return circuit at an infinite distance. As the paper suggests, further testing should verify this value.)

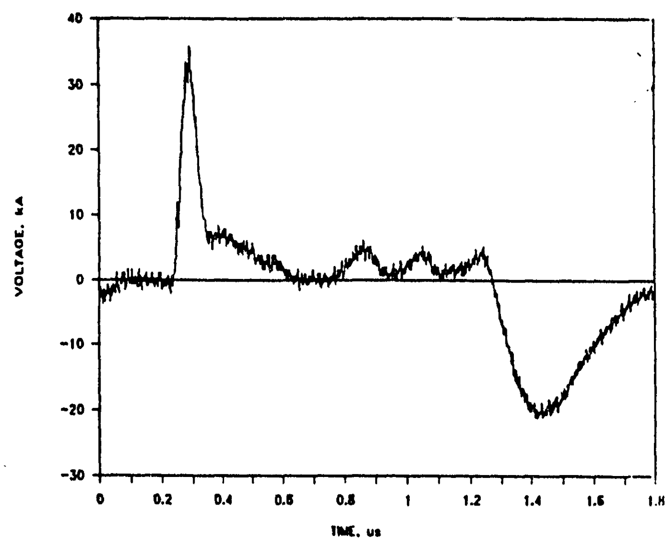

Fig. 3.3.1-4. Voltage across the aluminum tube during a 10-kA current pulse.
Source: Document IX-1.

By subtracting the inductive drop shown on Fig. 3.3.1-4 from the 5-kA MOV voltage wave, Fig. 3.3.1-5 shows the rapid turn-on characteristic of the arrester.

The "residual" voltage (the total arrester voltage minus the inductive drop) for the SiC arrester is higher than the MOV values by a factor of 1.5 to 1. A plot of the "residual" voltages as a function of discharge current is shown on Fig. 3.3.1-6. Comparing Figs. 3.3.1-1 and 3.3.1-6 (modified by the 10% difference in arrester ratings), the effect of the lead and arrester inductance is apparent.

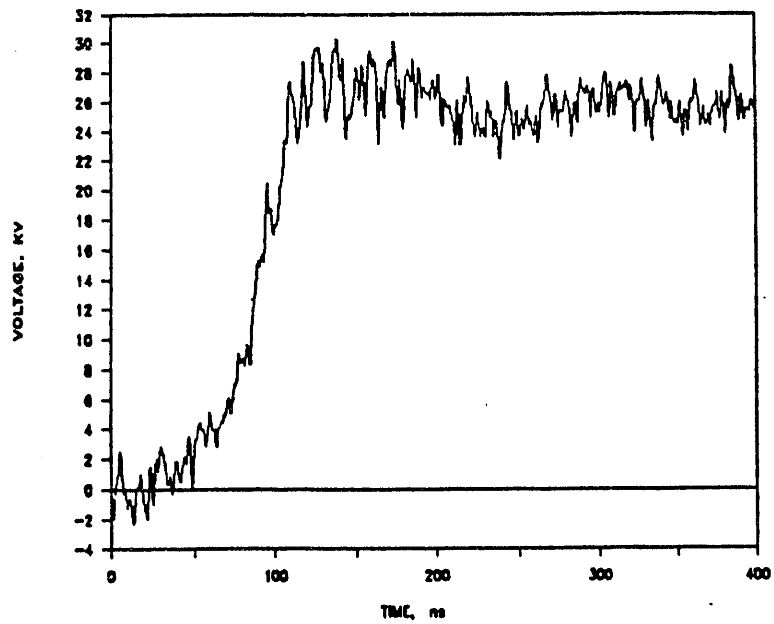

Fig. 3.3.1-5. Aluminum tube voltage (Fig. 3.3.1-4, extrapolated to 5-kA equivalent peak current) subtracted from the 5-kA metal oxide varistor voltage pulse in Fig. 3.3.1-3.
<u>Source</u>: Document IX-1.

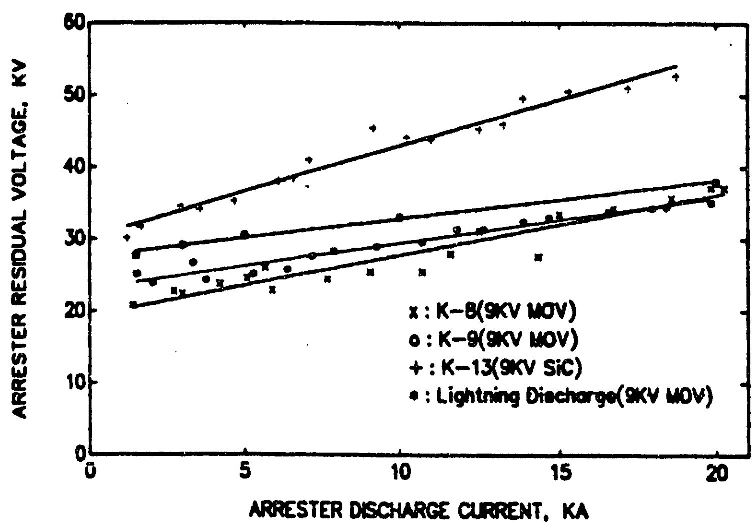

Fig. 3.3.1-6. Residual voltage versus peak arrester current for two 9-kV metal oxide varistor arresters and one 9-kV silicon carbide arrester. The 8/20 μs voltages for a typical 9-kV metal oxide varistor arrester are also shown.
<u>Source</u>: Document IX-1.

Based on these data, one might conclude that the protective levels of surge arresters, neglecting lead lengths, for E_1 type surges are at most 1.2 to 1.6 times the protective level of lightning-type surges. Because of the steep fronts of E_1 waves, however, the lead lengths should be kept as short as possible.

3.3.2 Power Transformers

The authors of Document V-1 equate the E_1 waves to the second or later components of lightning strokes (see Sect. 3.1 of this report). To examine the effect of these steep front lightning surges on power transformers, they assumed the arrester volt-time turn-up characteristics of Table 3.3.2-1 and the transformer insulation volt-time turn-up characteristics of Table 3.3.2-2. (In these tables, "mcsec" is an abbreviation of microsecond.) They then took a 900-kV basic insulation level (BIL) transformer protected by a 258 kV ZnO arrester and varied the lead lengths (from 0 to 20 ft.) and the stroke current (10, 20, & 40 kA) with a di/dt of 100 kA/μs. Using normal chopped wave and fast front insulation levels, the protective margins in one standard deviation of voltage were determined. Table 3.3.2-3 shows that protection is difficult and arrester lead lengths must be kept short.

Table 3.3.2-1. Zinc Oxide arrester discharge voltage (per unit of 8x20 microsecond wave)
Source: Document V-1.

Front time (mcsec)	.1	.2	.4
Multiplier	1.3	1.23	1.17

Table 3.3.2-2. Fast-front-wave insulation levels (per unit of basic insulation level).
Source: Document V-1.

Front Time (mcsec)	.1	.2	.4
Multiplier	1.5	1.3	1.2

Table 3.3.2-3. Protective margins (258-kV zinc oxide arrester).
Source: Document V-1.

Case	Figure	Lead Length (Feet)	Stroke Current (kA)	Overvoltage MAG (kV)	Overvoltage Front Time (mcsec)	CWW* (kV)	Protective Margins Margin (%)	FFW* (kV)	Margin (%)
1	-	0	10	750	.15	990	32	1242	66
2	-	0	20	806	.15	990	23	1242	54
3	-	0	40	881	.15	990	12	1242	41
4	7	5	10	1041	.15	990	- 5	1242	19
5	-	5	20	1191	.2	990	-17	1170	- 2
6	-	5	40	—	—	-	-	—	-
7	-	10	10	1196	.25	990	-17	1134	- 5
8	-	10	20	1290	.25	990	-23	1134	-12
9	-	10	40	—	—	-	-	—	-
10	-	15	10	1206	.25	990	-18	1134	- 6
11	-	15	20	1296	.25	990	-24	1134	-12
12	-	15	40	1353	.25	990	-27	1134	-16
13	-	20	10	1201	.30	990	-18	1102	- 8
14	-	20	20	1259	.30	990	-21	1102	-12
15	-	20	40	1324	.30	990	-25	1102	-17

*CWW - Chopped-Wave
FFW - Fast-Front-Wave

It should be noted that the 100 kA/μs used in the study for the di/dt is quite high. A comparison with Table 2-2 shows that very few strokes have these characteristics. Also, since the stroke current flows in two directions from the point of stroke, the current through the arrester is less than the total lightning stroke current. However, it is still good practice to keep the arrester leads as short as possible.

The authors of Document V-6 also attempted the testing of a power transformer. The first 16 pancake segments (representing 20% of the primary winding) of a 16.4 MVA, 230-kV core-form transformer were tested. Problems were encountered when testing with the two fast waves (the 10 x 165 ns wave and the 110 x 500 ns wave). The breakdowns encountered were thought to be due to the connection of the test leads. The failures occurred, however, at turn-to-turn voltage stresses 4 to 8 times those normally encountered in routine testing of the transformers.

While no hard and fast test failure data on transformers exist for E_1 type surges, the conclusions from the above data seem to indicate that, provided that arrester leads are kept short, power transformers will be relatively immune to these surges.

3.3.3 Distribution Transformers

A number of tests were performed on distribution transformers with and without surge arresters. In Document V-6, tests were run on 75 kVA, 14.4/24.9 kV, 125-kV BIL shell-form and core-form transformers using 10 * 150 and 100 * 500 ns waves. No failures occurred with tank-mounted and direct-connected arresters for any of the SFSD test waves. No failures occurred with an arrester with an external gap using the 100 * 500 ns wave, but a failure occurred at 205 kV on the tenth shot of the 10 * 150 ns wave. A failure also occurred on the fourth shot at 229 kV when no arrester was present.

In Document V-2, 19 25 kVA, 7200/12470 volt, 95-kV BIL distribution transformers were tested to determine their vulnerability to SFSD surges. Open circuit pulser tests of 400, 500, 800, and 1000 kV having rise times of 60 ns and times to half value of 2000 ns were applied. No insulation failures occurred with units protected by surge arresters mounted on the tank. Bushing failures and internal failures occurred on unprotected units. When the bushings flashed over, they did not necessarily protect the internal insulation. Failures occurred at a 250- to 300-kV peak. When the arrester was mounted remotely (1.2 to 1.8 m from the transformer), a failure occurred during an 800-kV test.

Tests described in Document V-3 were performed on a 50-kVA, 14.4-kV, 125-kV BIL core form distribution transformer and a 75-kVA, 14.4 kV, 125-kV BIL shell form unit. The voltages were measured at various taps throughout the winding to determine the turn-to-turn stresses in the windings. The units were pulsed with the following waves:

10 * 175 ± 75 ns
100 * 500 ± 100 ns
500 * 1000 ± 200 ns
1.2 * 50 μs (standard)

Fig. 3.3.3-1 shows the voltage distribution in the windings at the indicated times (which were the time the response wave peaked). Note that for the fast front, ≈ 70% of the applied surge appears across the first 10% of the winding. This produces high turn-to-turn and layer-to-layer stresses.

To determine the overall vulnerability of distribution transformers to E_1 pulses, a study similar to the one described in Sect. 3.1 of this document was performed. This study is described in Document III-6.

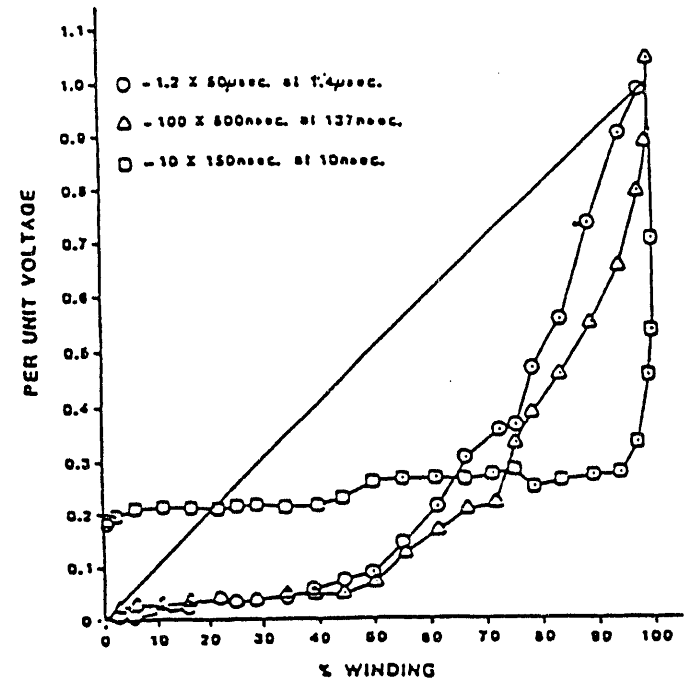

Fig. 3.3.3-1. Impulse voltage distribution for 50-kVA core form transformer at specific times.
<u>Source</u>: Document V-3.

Impulse measurements were first made on a 25-kVA, 12470/7200 volt distribution transformer to obtain the input impedance to SFSD E_1 impulses. Using this impedance characteristic, calculations were made of the circuit of Fig. 3.3.3-2, using the field strengths shown on Fig. 3.3.3-3 for the complete illumination field (the United States). The voltages were calculated across the transformer and for an open circuit (no transformer) for line incidence angles of from 0 to 360° in 10° steps. Fig. 3.3.3-4 shows typical values.

Probability values are shown on Fig. 3.3.3-5 for the whole illumination area, Fig. 3.3.3-6 for a line at the maximum field strength location, and Fig. 3.3.3-7 for a 500-km^2 area around the point of maximum field strength.

From the above, it appears that there is a very small probability of transformer failure even without surge arresters. Document I-7 has estimated that less than 2% of the unprotected transformers would be damaged for the nominal E_1 pulse burst of 39 kV/m and less than 4% for the 50 kV/m E_1 burst. Using the 1.5 turn-up value of Document V-1, the 95-kV BIL of the transformer of Document III-6 would appear as 142.5 kV to E_1 waves. Using this value in Fig. 3.3.3-5, even the 2 and 4% values appear high.

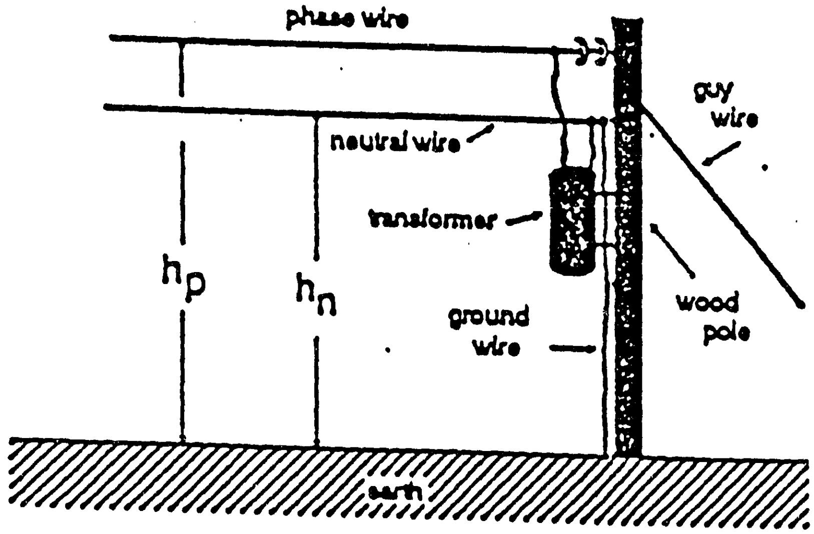

Fig. 3.3.3-2. Idealized single phase power distribution line.
Source: Document III-6.

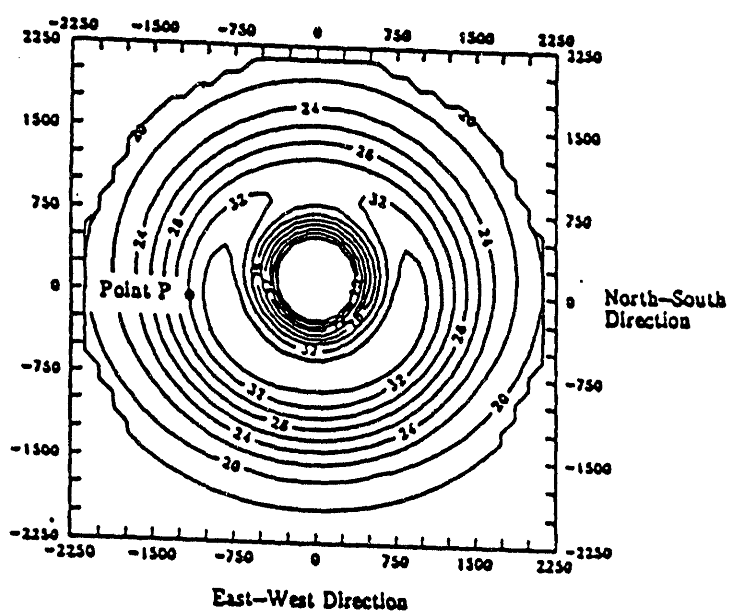

Fig. 3.3.3-3. Contour plot of peak value of high altitude electromagnetic pulse electric field on earth's surface (contours in kilovolts/meter).
Source: Document III-6.

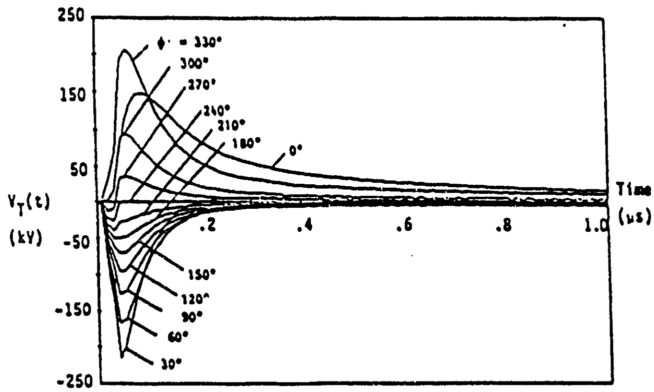

a. open–circuit

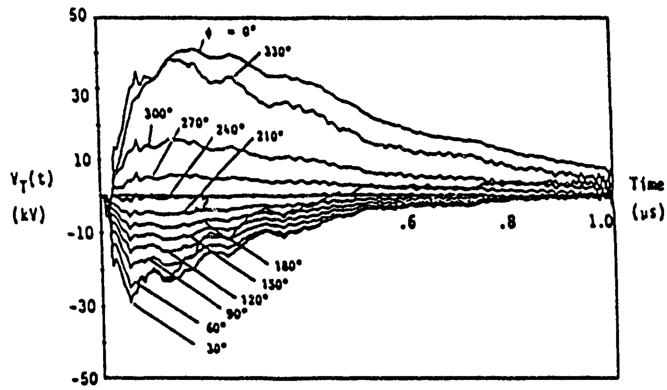

b. Loaded with the Transformer

Fig. 3.3.3-4. Open-circuit voltage (a) and loaded voltage (b) across transformer for line at position P (-1130, 0.0) km. Guy wire is absent.
Source: Document III-6.

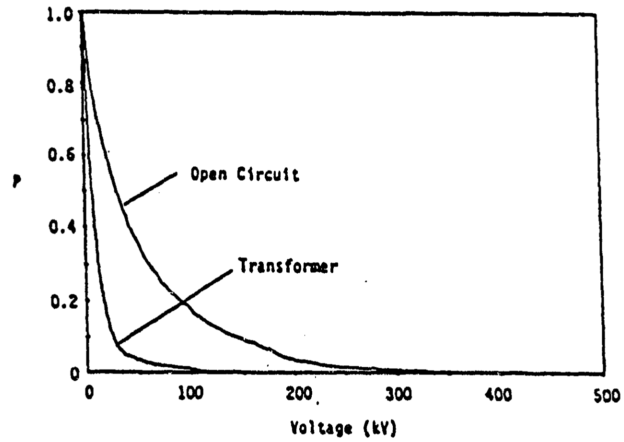

Fig. 3.3.3-5. Probability of the peak transformer voltage exceeding the abscissa value.
Source: Document III-6.

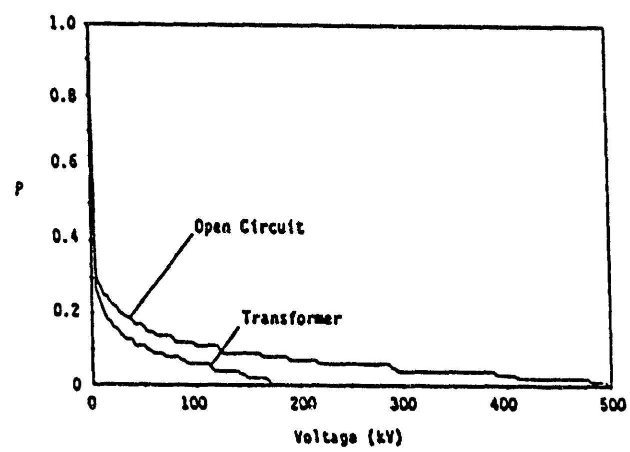

Fig. 3.3.3-6. Probability of the peak transformer voltage exceeding the abscissa value for line at position of maximum positive response.
Source: Document III-6.

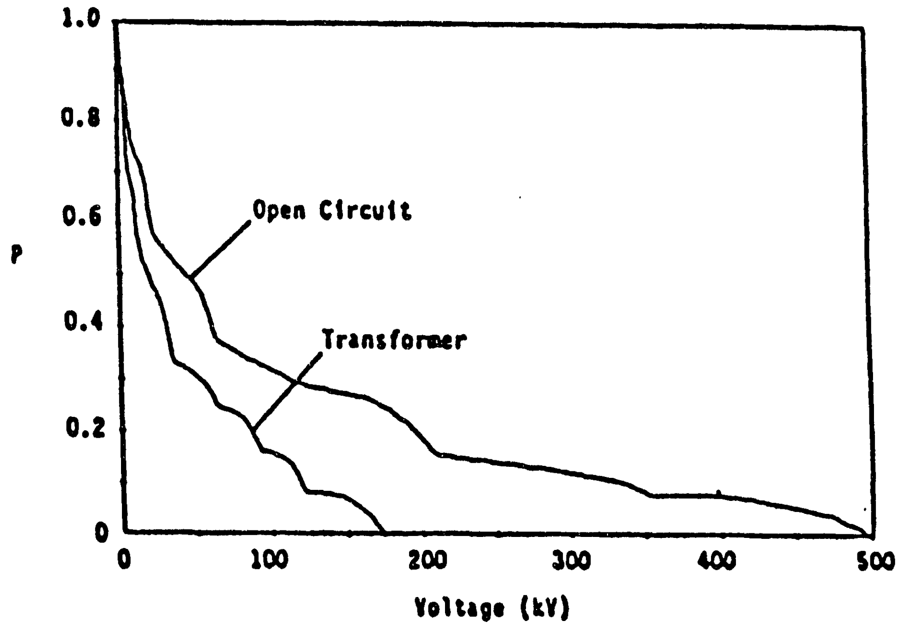

Fig. 3.3.3-7. Probability of the peak transformer voltage exceeding the abscissa value for line in a 500 km square region centered over the position of maximum line response. Source: Document III-6.

3.3.4 Apparatus Bushings

There is very little data on tests of power apparatus bushings. Document V-6 describes tests on a 115-kV, 550-kV BIL bushing; the results are shown in Table 3.3.4-1. There were no flashovers for the 10 x 150 ns waves (shown as a 30 x 350 ns wave due to the sloping of the wave by the bushing capacitance), but a failure occurred at 900 kV after 40 shots with the 100 x 500 ns wave. It was concluded that this was caused by a cumulative degradation of the core's insulation system.

With only these data, however, recommendations, conclusions, or guidelines are difficult to establish.

Table 3.3.4-1. Impulse testing on power-apparatus bushings.
Source: Document V-6.

SPEC. NO.	WAVESHAPE	CIFO +KV	CIFO -KV	FOW +KV	FOW -KV
1.6	1.2 × 50 μs	775[a]	641[a]	1130[b]	1120[b]
2.7	100 × 500 ns	---	---	---	900[c]
3.5	30 × 350 ns	---	>1099[d]	---	>1099[d]
3.5	1.2 × 50 μs	747[a]	694[e]	---	---

3.3.5 Reclosers

A simulated E_1 pulse test, described in Document V-5, was performed on two types of recloser-control units at the Defense Nuclear Agency (DNA) ARES facility at the Kirtland Air Force Base in New Mexico. For the test, two microprocessor-based control units and one electronic unit were exposed to approximately 60 shots with simulated E_1 fields up to 41 kV/m. One of the microprocessor units was found to be defective (a manufacturing defect existing prior to the tests), so its results were ignored. The other microprocessor unit showed no disruptive failures; the electronic unit tripped one time during setup of the equipment, but this effect could not be reproduced. Analysis of these data and others suggest that the probability of a misoperation from the assumed E_1 environment is small, provided proper grounding practices are followed [V-5].

3.4 Power Plants

The primary equipment in power plants (generators, large motors, transformers, etc.) will be largely unaffected by E_1 pulses. The large generators, for example, will have limited exposure to surges due to their unit system connections. Those supplied with generator breakers, as well as large motors, are subject to switching surges such as those shown on Fig. 3.4-1. A standard is being proposed for the impulse strength of rotating machines. This proposal is covered in Document V-4. For the line-to-ground insulation, the impulse strength is $1.25 \times \sqrt{2} \times (2V + 1)$ kV, where V is the rating of the motor in kV. To test the turn-to-turn strength, the curve of Fig. 3.4-2 is proposed. To protect against these switching surges, surge protection packages may be required at the machine terminals. These will protect against E_1 surges as well as the switching surges.

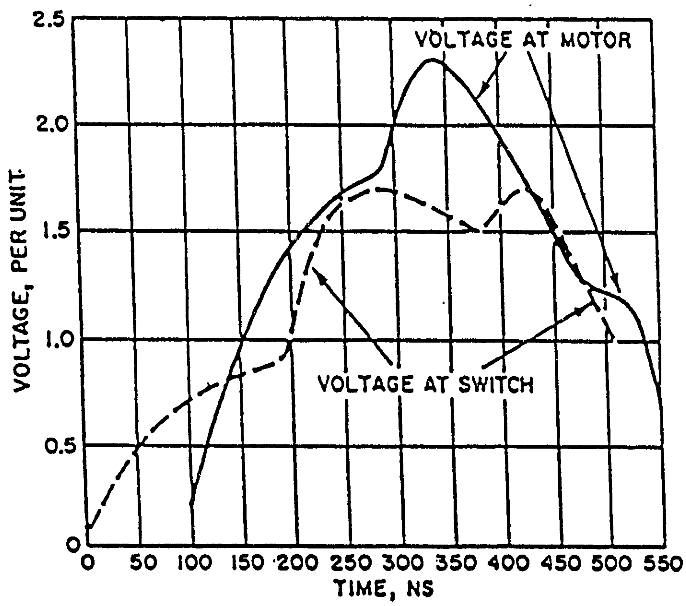

Fig. 3.4-1. Envelope of voltages following closure of switch.
Source: Document V-4.

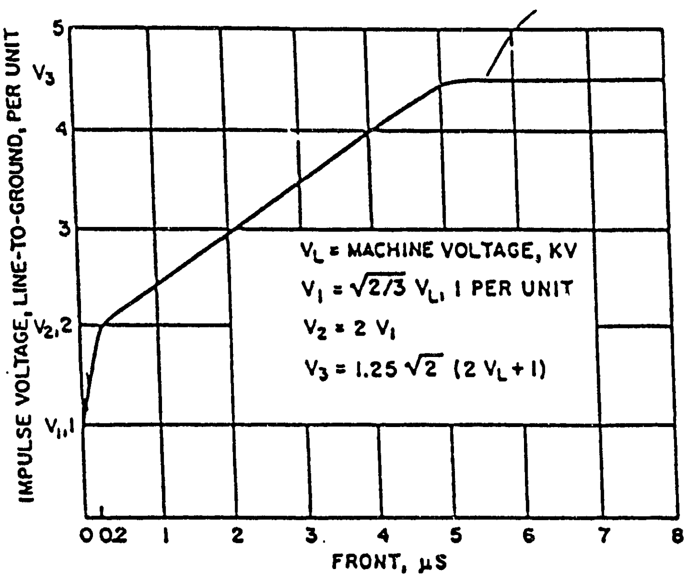

Fig. 3.4-2. Machine impulse voltage withstand envelope.
Source: Document V-4.

Whether surge protection packages are used on motors depends on the importance of the motor load and the exposure of the motors to lightning and switching surges. The protection practices vary from utility to utility. Most utilities use protection packages extensively in nuclear plants. For fossil plants however, some utilities use very little protection.

Smaller 480-volt motors without protection packages, in locations remote from the plant, and supplied by unshielded cable are subject to damage. Cooling tower fans, water treatment and demineralizing systems, fuel unloading and fuel transfer pumps, and cooling water treatment systems in fossil plants are in this category. Table 3.4-1 shows the results of a study that calculated the probable generation loss due to these types of failures. Note that these losses varied for various cable burial depths.

The shielding of fossil fuel plant buildings may be inadequate because of the many building openings. Perhaps only a 20 db attenuation exists [I-4]. Unshielded control circuits or those with the shields grounded at only one end could cause significant damage to the electronic equipment.

Nuclear plant buildings have better shielding than fossil plants: ≈ 40 db [1-4]. The safeguard instrumentation control cable is well shielded; only the general control cable is unshielded. Not as much control equipment damage should occur.

Combustion turbine plants also should not experience great damage because of their smaller size (shorter cables and metal buildings).

Table 3.4-1. Probabilities of generation loss based on 480-volt motor damage.
Source: Taken from Document I-7.

(2200 km Radius Area of Illumination)
(Motors Supplied by Unshielded Buried Cable)

Field Strength	Average Burial Depth		
	0.5 m	0.79 m	1.0 m
kV/m	Percent	Percent	Percent
25	0	0	0
39	1.8	0	0
50	4.4	1.6	0

Even without any control or equipment failures (or malfunctions), a number of generators or plants may shut down due to external causes. Loss of system load due to distribution system tripouts could cause generator overspeed or out-of-step conditions that will trip the generator units. Rapid restart procedures are desirable and should be developed. Small hydro plants have the greatest chance of short restart time because their gates and excitation can be controlled manually.

3.5 Protective Relaying

Ever since the first static or solid-state relay was introduced, relay designers and users have been concerned with their performance under the hostile transient environment of utility stations and substations. The users started installing shielded control cables in their substations, and the relay designers built various protection devices into their relay systems. The devices most frequently used are "soft limiters" such as Zener diodes and metal oxide varistors, "hard limiters" such as spark gaps, and various forms of filters. Figs. 3.5-1 and 3.5-2 show the use of Zeners to buffer relay outputs and input, respectively. "Surge packs" of capacitors are also commonly used. Figs. 3.5-3 and 3.5-4 show the induced voltages and protection schemes for pilot wire relays. Modern pilot wire relays are using fiber optics or audio tones for their communication channels.

After considerable analytical study and field tests, the IEEE Power Systems Relaying Committee established standard tests that supposedly duplicated the worst transient environment that a relay would see in a substation (at least for those relays properly installed in a properly designed substation). These tests are defined in ANSI/IEEE Standard C37.90.1 and IEEE Trial Use Standard C37.90.2. All relays and communication equipment associated with relaying (such as carrier and pilot wire) being designed and built in this country, are tested to these two standards.

C37.90.1 [X-2] defines two standard tests: the oscillatory surge withstand capability (SWC) test and the fast transient SWC test. The characteristics of these test waves are summarized in Table 3.5-1.

The oscillatory SWC wave is a wave having a frequency of between 1.0 and 1.5 MHz, a voltage crest of 2.5 to 3.0 kV, and an envelope decaying to 50% in not less than 6 μs.

The fast transient SWC wave is a unidirectional wave having a rise time, from 10 to 90%, of no more than 10 ns, a crest of 4 to 5 kV, and a time to half value of 150 ± 50 ns. Fig. 3.5-5 shows a time plot of the open-circuit voltage and of this test wave.

A third test, defined in IEEE C37.90.2 [XI-17], is an EM

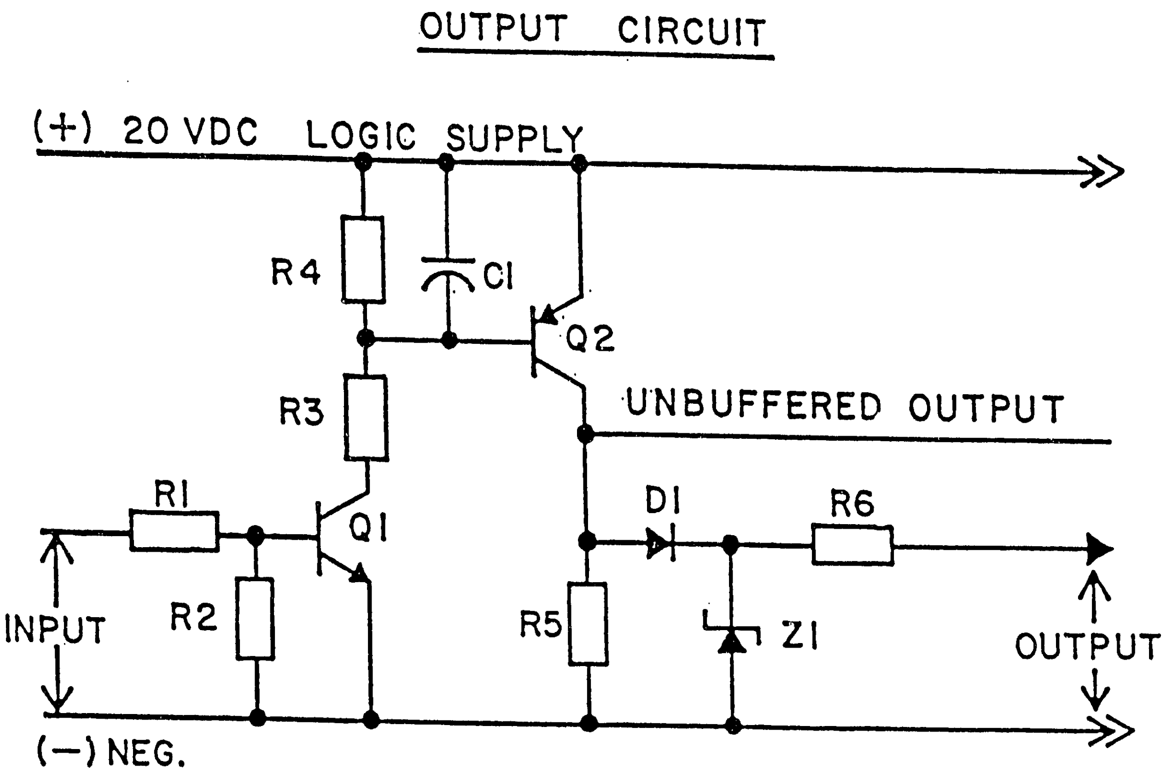

Fig. 3.5-1. Protection scheme for relay output circuits.
Source: Document VIII-6.

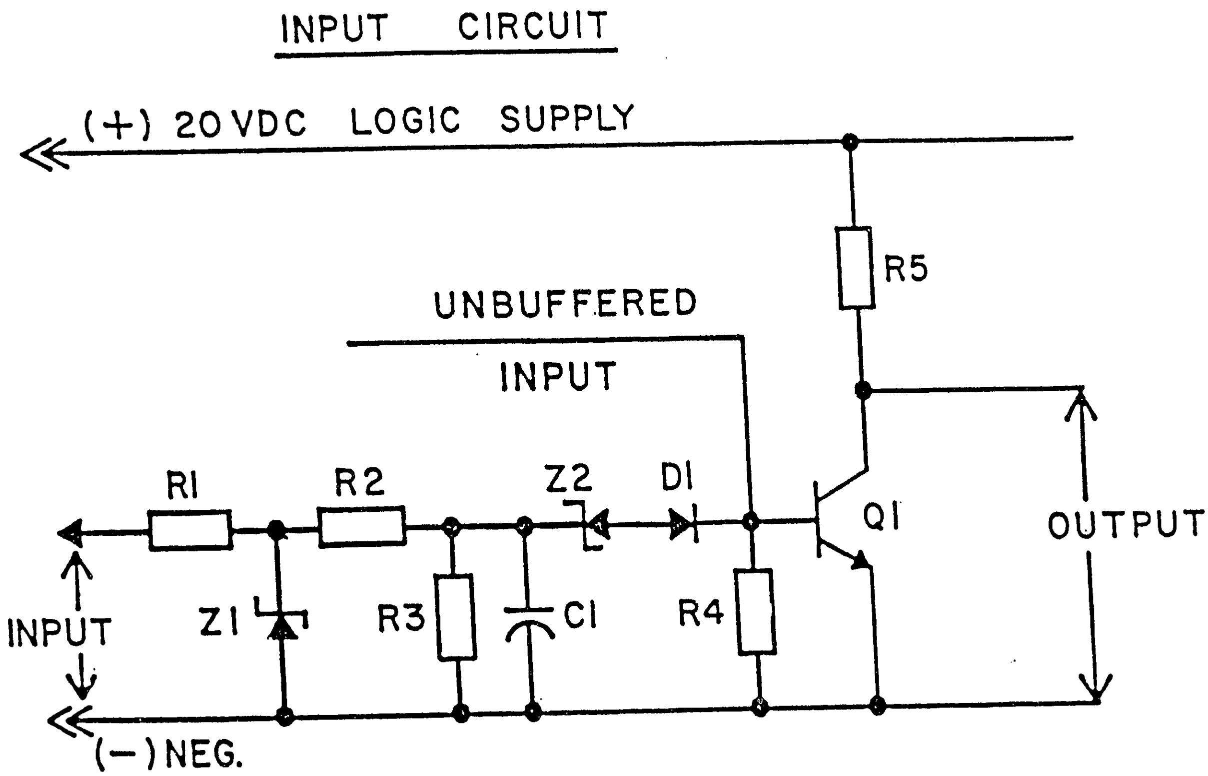

Fig. 3.5-2. Protection scheme for relay input circuits.
Source: Document VIII-6.

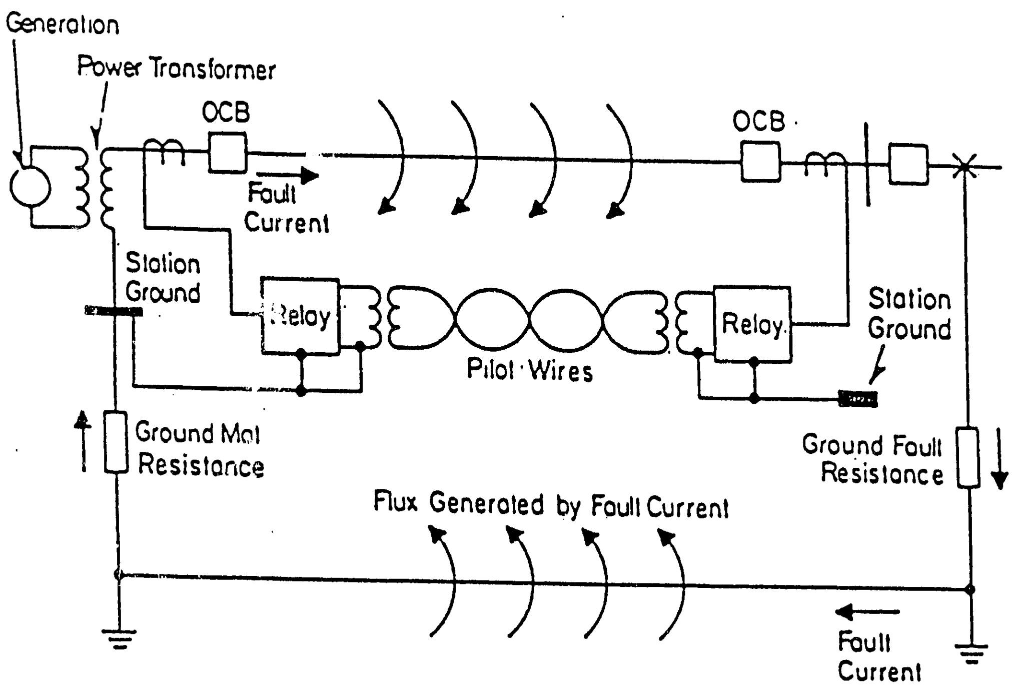

Fig. 3.5-3. Induced voltage along pilot wire by line fault.
Source: Document VIII-6.

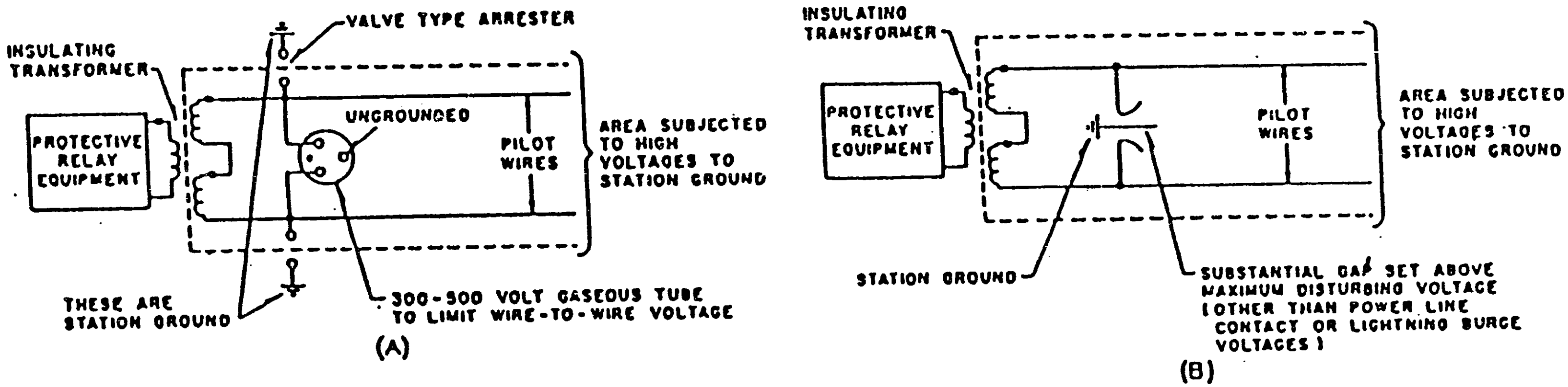

Fig. 3.5-4. Recommended protection schemes for pilot wire circuits.
Source: Document VIII-6.

Table 3.5-1. Characteristics of oscillatory and fast transient surge withstand capability tests.
Source: Taken from Document X-1.

Norm Waveshape	Oscillatory (Damped Cosine)	Fast Transient (Double Exponential)
Crest Value	2.5 kV - 3.0 kV	4 kV - 5 kV
Frequency	1.0 MHz - 1.5 MHz	NS*
Risetime (10 - 90%)	NS	10 ns
Decay (to 50%)	> 6 μs	150 ns + 50 ns
Crest Duration (above 90%)	NS	>50 ns
PRF	>50 Hz	> 50 Hz
Test Duration	2.0 s	2.0 s
Source Impedance	150 Ω - 200 Ω	< 80 Ω
Test Polarity	NS	Both
* - NS: not specified		

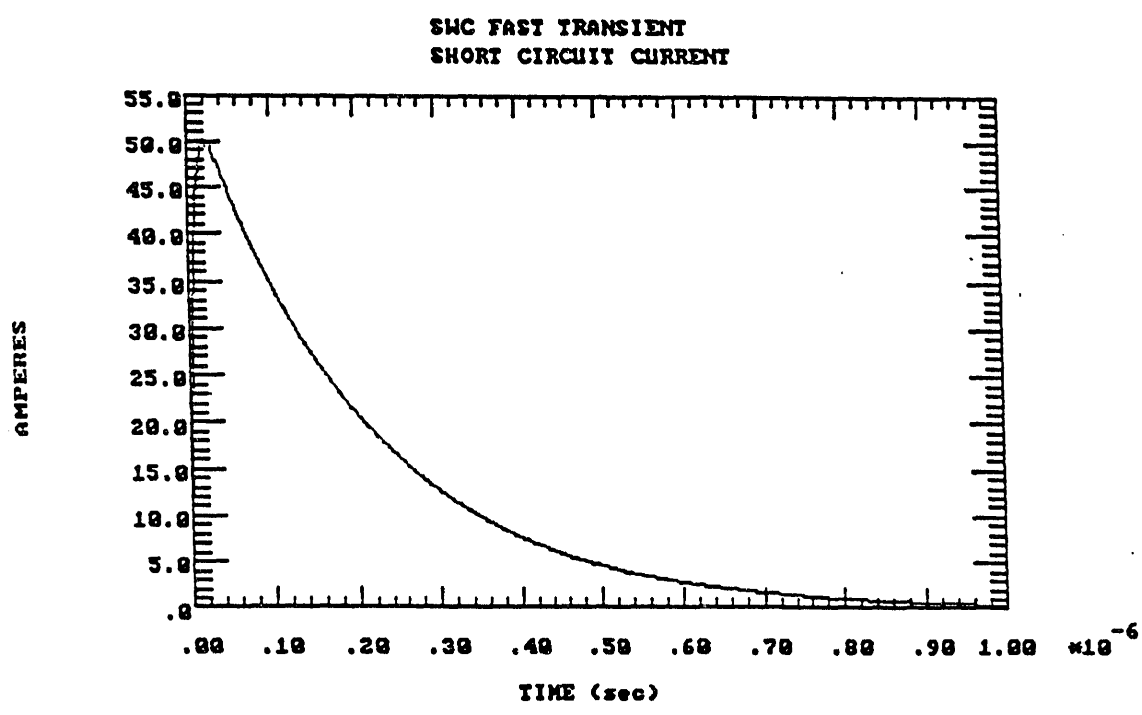

Fig. 3.5-5. Relay surge withstand capability fast transient test waveform specified by IEEE/ANSI C37.90.1-1989.
Source: Fig. 4.29a of Document X-2.

interference test established to evaluate the performance of static protective and control relays and their susceptibility to EM fields in the radio frequency domain, such as those generated by portable or mobile radio transceivers.

The test setup is shown in Fig. 3.5-6.* The relay under test is subjected to EM fields of 10 to 20 v/m. The frequency of the signal is varied over a range of 25 to 1000 MHz at a sweep rate of ≤ 0.005 octaves/s. For frequencies below 50 MHz, the signal is amplitude modulated at 90% with a 1000-Hz sine wave.

All digital equipment using clocked logic circuits shall also be subjected to EM radiation that is amplitude (pulse or square wave) modulated at a frequency close to 10 kHz but not in synchronism with the digital clock frequency. The 1000-Hz modulation test can be omitted when the 10-kHz modulation test is made.

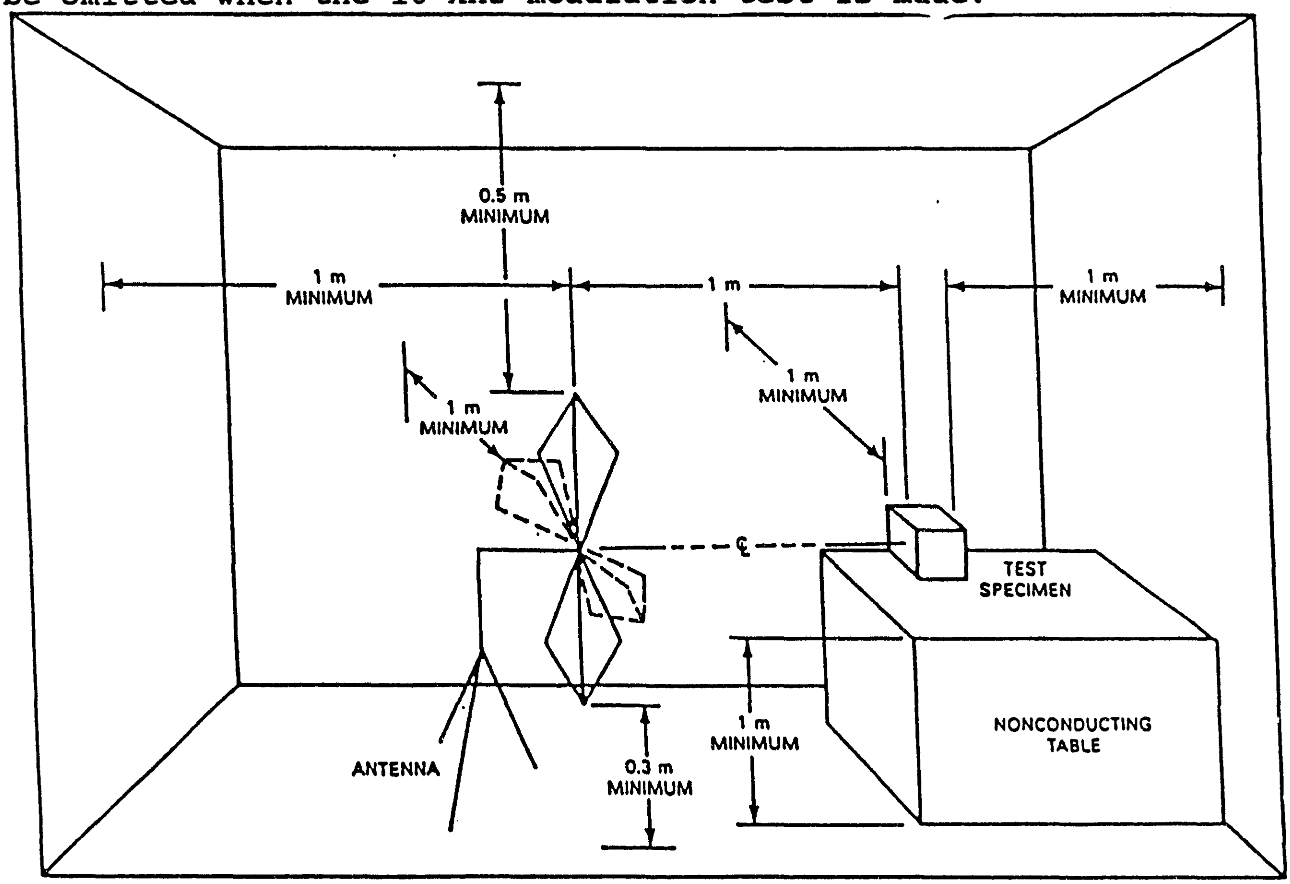

Fig. 3.5-6. Test setup for radiated susceptibility.
Source: Document XI-17.

* The EMC community has recently determined that conducting emission and suceptibility testing inside a resonant-cavity shield room is not a good practice. The FCC and most European standards now call for using open-air test sites (OATS) or anechoic chambers for these tests.

A test is successful when no erroneous output is present, no component failure occurs, and no change occurs in calibration exceeding normal tolerance.

The present 10 to 20 v/m level was selected based on a walkie talkie located no nearer than 1 m from the relay. A proposed revision by the IEEE Relay Committee would reduce this distance to 6 to 12 in., which could increase the field strength 4 to 8 times.

The International Electrotechnical Commission (IEC) has tests similar to the SWC ANSI tests. Their oscillatory test is identical except that they test at four frequencies (100 kHz, 1, 10, and 50 MHz) rather than the one (1 to 1.5 MHz) ANSI frequency.

Their "burst test" is similar to the ANSI fast transient test, except that their peak voltage is 2.0 kV (instead of the ANSI 4 to 5 kV); they use a 5 x 50 ns wave (instead of the 10 x 150 ns wave); their repetition rate is 2.5 Hz (instead of $\geq$ 50/s); and their test duration is 1 min (instead of 2 s).

Based on these tests, it is the opinion of the authors of Documents I-4 and VII-1 that electromechanical and static relays tested to the C37.90.1 "fast transient" surge withstand test would probably not be affected by the E_1 pulse. This assumes, of course, that the rest of the system (e.g., grounding and shielding of control wires) is properly designed and installed. (Note that this standard was produced around 1975, so equipment built before this time was not tested with this wave.)

Document VII-2 describes fast front impulse tests performed on a solid-state transformer differential relay. The impulses were applied with a square wave pulse generator (SPG). The pulses had either a 130 or 800 ns pulse width. The peak voltage with the SPG was limited to 8 kV, so a capacitor discharge pulser was also used to get surges up to 15 kV. The three wave shapes are shown in Fig. 3.5-7.

Pulses were applied to the various terminals of the relay. Table 3.5-2 gives a summary of the test results. There were a number of flashovers, but only one was classified as an upset or failure. (Note that an "upset" is a false trigger of the relay. A "failure" is any false operation of the relay, including a failure of the relay to respond.) The 12.3-kV pulse to the dc leads caused a fuse to blow for this failure. In no case was there permanent damage to the relay.

SPP protection packages (0.5 μF capacitors) were tested on the relay and the arcing caused by the 5-kV impulses was eliminated. They provided protection against arcing by impulses with magnitudes as high as 12 kV.

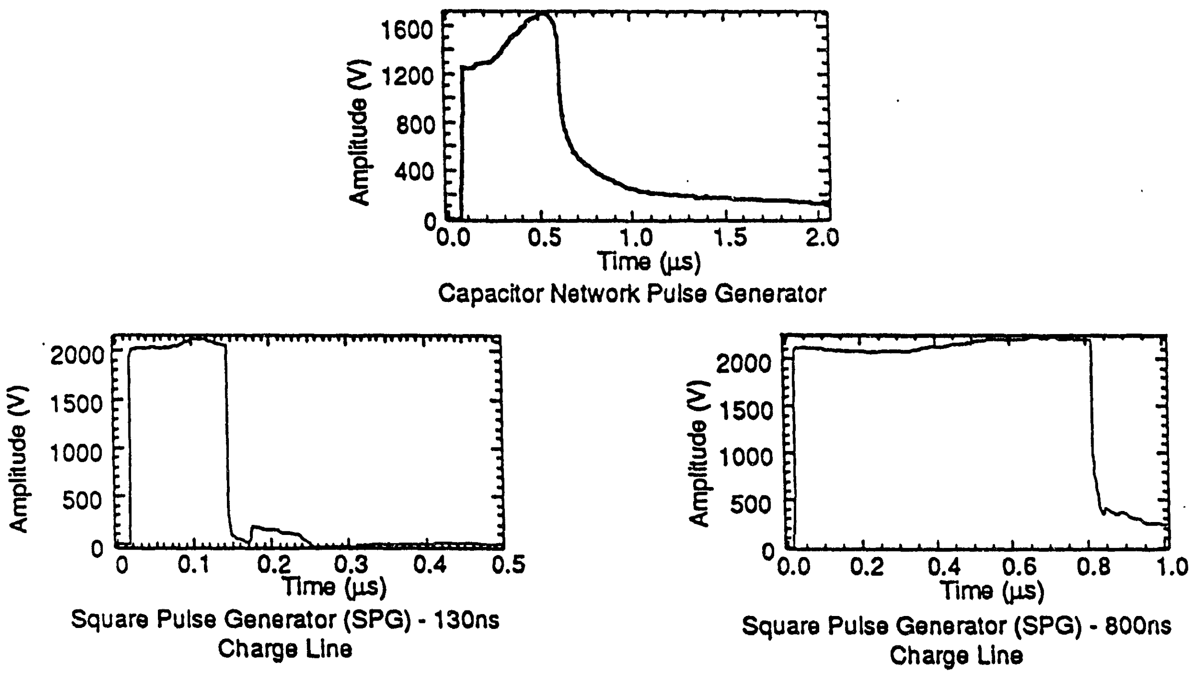

Fig. 3.5-7. Pulse generator waveforms into a 50-ohm load.
Source: Document X-2.

Table 3.5-2. Relay test summary.
Source: Document X-2.

CIRCUIT TYPE	PULSE INJECTION POINTS	PULSE GENERATOR	RELAY CONFIGURATION	FLASHOVER VOLTAGE	FLASHOVER LOCATION
AC	Term. 5 to Term 6	SPG 130ns	Current ratio matching plugs on 5A taps	6.5 kV	2.9A current tap
AC	Term. 5 to Term 6	SPG 130ns	Current ratio matching plugs on 2.9A taps	4.3 kV	8.7A current tap
AC	Term. 5 to Term 6	SPG 800ns	Current ratio matching plugs on 2.9A taps	4.0 kV	Instantaneous unit & differential current transformer
AC	Term. 5 to Term 6	SPG 800ns	Current ratio matching plugs on 2.9A taps	6.0 kV	8.7A current tap
AC	Term. 5 to Term 6	Capacitor	Current ratio matching plugs on 2.9A taps	2.3 kV	8.7A current tap
DC	Term. 2 to Term. 5 (Gnd)	Capacitor	Terminal 5 grounded	3.8 kV	Near relay contacts
DC	Term. 2 to Term. 5 (Gnd)	Capacitor	Terminal 5 grounded	8.0 kV	Near relay contacts & Instantaneous unit
DC	Term. 2 to Term. 10	SPG 130ns	Battery leads not grounded. No 25Ω resistor	4.7 kV	Telephone relay contacts
DC	Term. 2 to Term. 10	SPG 800ns	Battery leads not grounded. No 25Ω resistor	2.1 kV	Telephone relay contacts
DC	Term. 2 to Term. 10	Capacitor	Battery leads not grounded. No 25Ω resistor	2.5 kV	Telephone relay contacts
DC	Term. 1 to Term. 10 (Gnd)	Capacitor	Terminal 10 grounded	4.7 kV	Near base of relay contacts
DC	Term. 10 to Term. 1 (Gnd)	Capacitor	Terminal 1 grounded	4.8 kV	Instantaneous unit
DC	Term. 10 to Term. 1 (Gnd)	Capacitor	Terminal 1 grounded	12.3 kV*	Instantaneous unit.

* Susceptibility observed. DC circuit fuse blown due to current follow-through

Document X-2 describes a study that compared substation switching transients with E_1 induced transients. The objective of the study was to obtain an indication of the vulnerability of control and protection circuits to E_1 transients. Measurements were made in a 500-kV substation of E and H field strengths during various switching conditions. During these tests, current and voltage readings were also taken on the control wiring. Based on these measurements, models were generated to simulate the relay voltages that would occur because of the coupled voltages through the cts and vts, the control cable sheaths, and the other coupling sources. Using these models, the maximum relay control wire currents and voltages were calculated for:

- Switching a 500-kV disconnect switch with 2.0 per unit (pu) voltage across the open switch. This produces the worst (but relatively common) switching transient in the station. This condition is labeled *500 kV 2.0 PU ST* on the following tables.

- The E_1 transient seen at a point 500 km south of ground zero. This is the location of maximum E-field stress. The nominal field strength at this location is 39 kV/m, but for these calculations it was scaled up to 50 kV/m. The waveforms are shown on Figs. 3.5-8 and 3.5-9. This condition is labeled *short-range high altitude electromagnetic pulse* on the following tables.

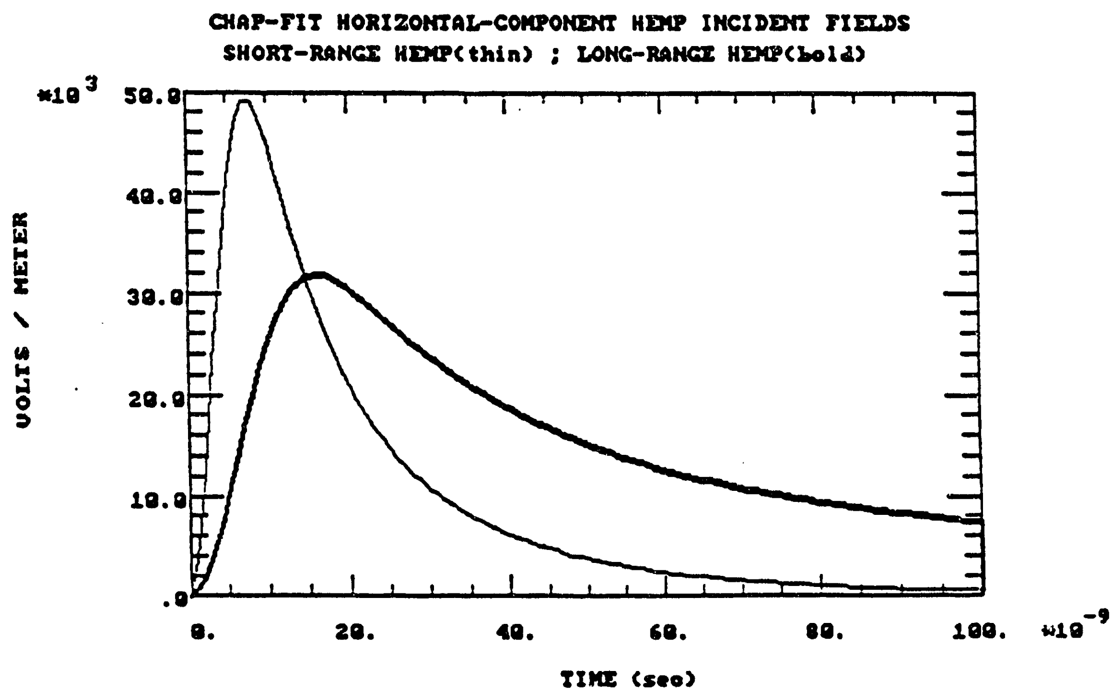

Fig. 3.5-8. Time domain waveforms for horizontal component of short-range (thin) and long-range (bold) high altitude electromagnetic pulse fields.
Source: Document X-2.

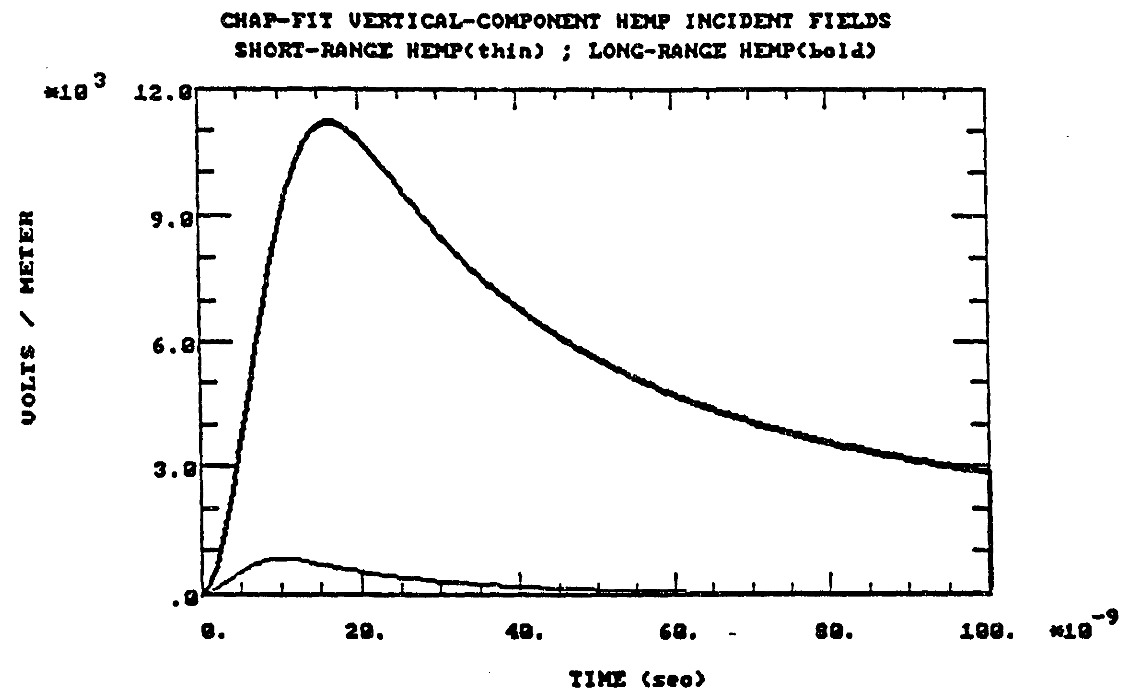

Fig. 3.5-9. Time domain waveforms for vertical component of short-range (thin) and long-range (bold) high altitude electromagnetic pulse fields.
Source: Document X-2.

- The E_1 transient seen at a point 1660 km north-northwest of ground zero. This produces the maximum induced current stress. The scaled up horizontal field is 32 kV/m and vertical field is 11.2 kV/m as shown on Figs. 3.5-8 and 3.5-9. This condition is labeled Long-Range HEMP on the following tables.

Table 3.5-3 shows the peak amplitudes, the wave rise times, the derivatives (max rate-of-rise) and action integrals (the energy in the wave) for the transient bus currents and voltages. Table 3.5-4 shows the same quantities for the electric and magnetic fields at ground level in the station. Table 3.5-5 shows the currents induced in the control cable shields.

During the tests on the transformer differential relay described above [VII-2], impedance measurements were made of all the relay input circuits. Using these impedances, calculations were made of the control wire voltages and currents for the above three assumed transient conditions. Table 3.5-6 shows these voltages and currents assuming a constant 150 ohm load, a terminating impedance equal to the relay's current transformer (CT) lead input impedance, and a terminating impedance equal to the relay's dc battery lead input impedance.

Table 3.5-3. Norms for transient bus currents and voltages.
Source: Document X-2.

	500 kV 2 PU ST		Long-Range HEMP		Short-Range HEMP	
	Bus Current	Bus Voltage	Bus Current	Bus Voltage	Bus Current	Bus Voltage
Zero-Peak Amplitude	3.63 kA	1.30 MV	0.575 kA	70.3 kV	0.538 kA	84.9 kV
Local Risetime	13 ns	10 ns	22 ns	9 ns	15 ns	9 ns
Peak Derivative	1.24E11 $\frac{A}{sec}$	4.08E13 $\frac{V}{sec}$	1.25E10 $\frac{A}{sec}$	5.05E12 $\frac{V}{sec}$	3.36E10 $\frac{A}{sec}$	7.94E12 $\frac{V}{sec}$
Action Integral	8.54 A^2sec	6.86E6 V^2sec	0.042 A^2sec	454 V^2sec	0.049 A^2sec	896 V^2sec

Table 3.5-4. Norms for incident electric and magnetic fields at ground.
Source: Document X-2.

	500 kV 2 PU ST		Long-Range HEMP		Short-Range HEMP	
	Electric Field	Magnetic Field	Electric Field	Magnetic Field	Electric Field	Magnetic Field
Zero-Peak Amplitude	11.9 $\frac{kV}{m}$	179 $\frac{A}{m}$	11.2 $\frac{kV}{m}$ (vert. compt.)	29.7 $\frac{A}{m}$ (horiz. compt.)	50.0 $\frac{kV}{m}$ (horiz. compt.)	130 $\frac{A}{m}$ (vert. compt.)
Local Risetime	10 ns	23 ns	6.6 ns	6.6 ns	3.4 ns	3.4 ns
Peak Derivative	6.42E11 $\frac{kV/m}{sec}$	4.26E9 $\frac{A/m}{sec}$	1.16E12 $\frac{kV/m}{sec}$	3.08E9 $\frac{A/m}{sec}$	1.08E13 $\frac{kV/m}{sec}$	2.87E10 $\frac{A/m}{sec}$
Action Integral	86.6 $\left(\frac{V}{m}\right)^2$sec	0.022 $\left(\frac{A}{m}\right)^2$sec	4.54 $\left(\frac{V}{m}\right)^2$sec	3.19E-5 $\left(\frac{A}{m}\right)^2$sec	27.7 $\left(\frac{V}{m}\right)^2$sec	1.94E-4 $\left(\frac{A}{m}\right)^2$sec

Table 3.5-5. Norms for induced shield currents.
Source: Document X-2.

	500 kV 2 PU ST	Long-Range HEMP	Short-Range HEMP
Zero-Peak Amplitude	65.2 A	41.2 A	81.8 A
Local Risetime	11.5 ns	7.1 ns	4.6 ns
Peak Derivative	3.64E9 $\frac{A}{sec}$	2.77E9 $\frac{A}{sec}$	1.31E10 $\frac{A}{sec}$
Action Integral	8.44E-4 A^2sec	1.69E-4 A^2sec	4.75E-4 A^2sec

Table 3.5-6. Zero-peak amplitudes for transient control-wire currents and voltages for 150 Ω, current transformer, and direct current battery impedances (summed for all coupling modes).
Source: Document X-2.

	500 kV 2 PU ST		Long-Range HEMP		Short-Range HEMP	
	Wire Current	Wire Voltage	Wire Current	Wire Voltage	Wire Current	Wire Voltage
150Ω Lead	20.8A	3.12kV	4.47 A	0.67 kV	6.14 A	0.92 kV
Measd CT Lead	24.3 A	4.89 kV	7.82 A	1.01 kV	12.7 A	1.43 kV
Measd DC Lead	16.6 A	4.05 kV	5.74 A	0.803 kV	8.56 A	1.16 kV

The above values are for shielded control wires. Since the battery leads are sometimes unshielded, Table 3.5-7 shows the voltages and currents for both shielded and unshielded wires.

When the values of Table 3.5-7 are compared with the Fast Transient SWC test voltage of Fig. 3.5-5, it appears that there is no problem except for the unshielded 2 pu switching transient case. All the other voltages are less than the 5-kV test voltage. This is not a fair comparison, however. The 5 kV is an open-circuit voltage, and the Table 3.5-7 values are loaded conditions. To correct this partially, coupled open-circuit voltages and short-circuit currents were calculated for the three transient conditions. These values are shown on Table 3.5-8. Note that now while the two HEMP cases for shielded wires are satisfactory, the voltages for the other cases exceed the 5-kV SWC test value.

Based on this data, there should be relay failures during normal substation switching. Since this is not the case, there must be some reasons why not. One reason is that most control wiring uses shielded cables. Also, surge capacitors are used on most relay terminals. As described previously, Document VII-2 showed their effect.

For battery circuits that do not use shielded cables, Table 3.5-7 shows voltages higher than the SWC test. As described in Document X-2 (see Table 3.5-2), dc fuses could blow occasionally if surge capacitors are not used. However, most modern relays *do* use capacitors on their power supply terminals. Also, redundant dc circuits, separately fused, are used to minimize the possibility of complete loss of power to the relays and/or circuit breaker trip circuits.

Finally, the open circuit voltages and short circuit currents do not necessarily present an accurate comparison. Document X-1, for example, determined the voltage, current, power, and energy developed across a representative 150 ohm load for various shielding and filter conditions for both the calculated coupled surges due to 2.0 per unit disconnect switching (shown in Table 3.5-9) and the surges from the SWC oscillatory and fast transient test waves (shown in Table 3.5-10). The values in parentheses on Table 3.5-9 are the ratios of the values of Table 3.5-9 to those of Table 3.5-10 for the similar conditions. A value less than 1.0 means the SWC test is more severe.

Table 3.5-9 shows, like Table 3.5-8, that without shielding or filters, the disconnect switching case is more severe than the SWC test. The table shows that with shielding, a filter capacitor of at least 0.05 μF is required. Actually, the values of Table 3.5-10 assume the lower limits of the SWC test voltages (for example, 4 kV for the fast transient test). Since the relay manufacturers actually use the highest value of test voltage, (for example 5 kV or even higher for the fast transient test), the voltages and

Table 3.5-7. Load currents and voltages for sum over all coupling modes.
Source: Document X-2.

0-PEAK	2 PU SWITCHING TRANSIENT			LONG RANGE HEMP			SHORT RANGE HEMP		
	150 Ω	CT LEAD	DC BATT	150 Ω	CT LEAD	DC BATT	150 Ω	CT LEAD	DC BATT
TOTAL, SHLD	20.8 A 3.12 kV	24.3 A 4.89 kV	15.9 A 4.05 kV	4.47 A 670 V	7.82 A 1.01 kV	5.74 A 803 V	6.14 A 921 V	12.7 A 1.43 kV	8.56 A 1.16 kV
TOTAL, UNSHLD	55.6 A 8.34 kV	64.0 A 11.4 kV	53.0 A 10.7 kV	18.3 A 2.75 kV	22.6 A 2.86 kV	20.9 A 2.62 kV	28.1 A 4.22 kV	38.6 A 4.09 kV	32.5 A 3.88 kV

Table 3.5-8. Open-circuit voltages and short-circuit currents for sum over all coupling modes.
Source: Document X-2.

0-PEAK	2 PU SWITCHING TRANSIENT		LONG RANGE HEMP		SHORT RANGE HEMP	
	OPEN CIRCUIT VOLTAGE	SHORT CIRCUIT CURRENT	OPEN CIRCUIT VOLTAGE	SHORT CIRCUIT CURRENT	OPEN CIRCUIT VOLTAGE	SHORT CIRCUIT CURRENT
TOTAL, SHIELD	7.27 kV	48.4 A	1.19 kV	11.8 A	4.79 kV	17.4 A
TOTAL, UNSHIELD	17.1 kV	130 A	5.54 kV	31.6 A	8.55 kV	58.2 A

Table 3.5-9. Effect of filter capacitance on load/filter stress levels for 2 per unit disconnect switching interference coupling to current transformer control cables (150-ohm load).
Source: Document X-1.

STRESS: / CABLE CONFIG.	LOAD / FILTER VOLTAGE (KV)	LOAD CURRENT (A)	LOAD PEAK POWER (W)	LOAD AVE. PWR PER PULSE (W)	LOAD PEAK ENERGY (mJ)	FILTER CURRENT (A)	FILTER PEAK POWER (W)	FILTER AVE. PWR PER PULSE (W)	FILTER PEAK ENERGY (mJ)
NO SHIELD, NO FILTER	7.38 (2.8)	49.2 (2.8)	363000 (8.0)	12400 (23.0)	124 (23.0)	—	—	—	—
SHIELD, NO FILTER	3.04 (1.2)	20.3 (1.2)	61700 (1.4)	1754 (3.3)	17 (3.2)	—	—	—	—
NO SHIELD, 0.01 µF FILTER	1.73 (2.8)	11.6 (2.8)	20000 (8.1)	1650 (10.7)	16.5 (10.7)	109	78600	19.8	15.1
SHIELD, 0.01 µF FILTER	0.617 (1.0)	4.12 (1.0)	2540 (1.0)	211 (1.4)	2.11 (1.4)	41.6	9260	2.96	1.92
NO SHIELD, 0.05 µF FILTER	0.551 (3.1)	3.67 (3.1)	2020 (9.5)	160 (4.1)	1.60 (4.1)	131	41600	7.71	7.59
SHIELD, 0.05 µF FILTER	0.156 (0.88)	1.04 (0.88)	162 (0.76)	14.6 (0.38)	0.146 (0.38)	44.1	3090	1.11	0.610
NO SHIELD, 0.5 µF FILTER	0.086 (4.3)	0.573 (4.2)	49.3 (18.1)	6.27 (3.2)	.063 (1.8)	131	6280	6.54	1.85
SHIELD, 0.5 µF FILTER	0.016 (0.80)	0.107 (0.79)	1.72 (0.63)	0.167 (0.09)	0.002 (0.06)	44.1	330	0.129	0.065

Note: Values in parentheses are ratios of Table 3.5-9 elements with corresponding elements of Table 3.5-10.

currents of Table 3.5-10 should be increased by 25% and the power levels by 1.23^2 or 55%. Note that if this were done, the 0.01 μF case of Table 3.5-9 would also be satisfactory. Actually, even the shielded unfiltered case of Table 3.5-9 would also be marginal.

It can be concluded, therefore, that provided the proper precautions are taken (shielded wires and surge capacitors), there will be no problem from these induced surges.

The preceding discussion has considered only induced surges. Table 3.5-4 showed that the HEMP electric field strengths at ground level were as high as 50 kV/m which is higher than the electromagnetic interference (EMI) test levels of C37.90.2. But Table 3.5-4 also shows that the 2.0 pu switching field strengths were also much higher (11.9 kV/m) than the C37.90.2 test levels. If the E_1 surges are a problem, then ordinary switching should be, also. Why is switching not a problem?

One modifying effect is that the Table 3.5-4 levels are measurements taken directly under the bus, whereas the relays are usually located some distance from the bus in the control house. Measurements reported in Document VII-4 show that while fields directly under a 500-kV bus during disconnect switching were 15.2 kV/m, those only 20 m away were 1.3 kV/m. Also, the control house and associated equipment shielding provides additional shielding. Finally, while the values of Table 3.5-4 are short pulse values, their energy levels are quite a bit lower than the continuous oscillating frequency of the C37.90.2 test. Perhaps these are the reasons that there have been so few cases of false relay operations due to switching.

For equipment located out in the switchyard, such as present data acquisition units (DAUs) and future relaying units, this can become a problem not only for E_1 pulses but also for disconnect switching transients. The IEEE/PES Power System Relaying Committee is also studying this problem with the goal of specifying guidelines for protection equipment in this environment.

3.6 Communication and Control Equipment

Systems containing small-signal electronic circuits are potentially susceptible to the E_1 transient. Communication equipment, computers, and microprocessor-controlled equipment use solid state components that can be damaged by E_1-induced transients on signal, ground, or power cables. Digital circuits used in computers and microprocessors can undergo a change of state due to single transient events such as a E_1 pulse; this may cause a data error or alter the software program. The induced effects of E_1 are the primary concern for upset (state change) and damage to sensitive elements such as detectors in communication receivers and integrated circuits in computers and microprocessors. The E_3 pulse may also damage components connected to 10--100-km-long lines, such

Table 3.5-10. Effect of filter capacitance on load/filter stress levels for surge withstand capability fast transient and oscillatory test levels (same for unshielded and shielded cables) (150-ohm load).

Source: Document X-1.

STRESS: / CABLE CONFIG.	LOAD / FILTER VOLTAGE (KV)	LOAD CURRENT (A)	LOAD PEAK POWER (W)	LOAD AVE. PWR PER PULSE (W)	LOAD PEAK ENERGY (mJ)	FILTER CURRENT (A)	FILTER PEAK POWER (W)	FILTER AVE. PWR PER PULSE (W)	FILTER PEAK ENERGY (mJ)
FAST SWC NO FILTER	2.61	17.4	45200	540	5.40	—	—	—	—
FAST SWC 0.01 µF FILTER	0.610	4.07	2480	154	1.54	48.5	10400	0.157	1.86
FAST SWC 0.05 µF FILTER	0.178	1.18	212	38.9	0.389	49.6	2760	0.01	0.794
FAST SWC 0.5 µF FILTER	0.020	0.135	2.73	1.96	0.035	49.9	274	4.95	0.102
OSCILL. SWC NO FILTER	1.250	8.33	10400	2160	21.6	—	—	—	—
OSCILL. SWC 0.01 µF FILTER	0.408	2.72	1110	106	1.06	17.6	4090	5.06	0.833
OSCILL. SWC 0.05 µF FILTER	0.102	0.677	68.8	7.30	0.073	17.1	1100	0.886	0.258
OSCILL. SWC 0.5 µF FILTER	0.010	0.069	0.721	0.167	0.0032	17.4	115	0.242	0.027

as power lines and telephone (or other communication) cables. To protect electronic equipment such as communication equipment and computers against the E_1 surge, it is necessary to provide an EM barrier around the equipment to exclude the E_1 fields and E_1-induced currents. The barrier consists of a shield and other devices that divert, interrupt, or suppress the effects of E_1 pulses. Although the barrier must exclude E_1, lightning, and other broadband interference sources, it must pass operating power and communication or data processing signals and allow for safe operation of the system through appropriate grounding. Fig. 3.6-1 illustrates some typical barriers that accommodate these requirements.

3.6.1 Building Shielding

The barrier that provides protection against transient sources may be installed at the equipment or at the building, or distributed between the building and equipment. For external sources such as lightning and E_1 pulses, the primary protection should be provided at the building level to minimize the overstress on interior components, which are typically designed for low-voltage applications. (In large structures, the barrier may be applied at the room housing the computing and control equipment, and for remote communication equipment the "building" may be a small transportable weather shelter; both of these are included when the term "building" is used.)

It has been shown that a closed, continuous metal shield only 1 mm thick almost completely excludes the E_1 transient from internal wiring (less than 3 mV in a 20 m diameter loop) [E.F. Vance, "Electromagnetic Interference Control" IEEE Transactions on Electromagnetic Compatibility, Vol. EMC-22, Nov. 1980, pp. 319-328]. This finding is important, because it illustrates that the penetration of the E_1 wave through metal is negligible. The protection effort should be applied to those parts of the barrier surface where the metal is discontinuous or absent entirely.

Most important are the power, signal, and ground wires that penetrate the shield. Wires entering the building from outside carry E_1- and lightning-induced currents into the building without attenuation even if the building is otherwise well shielded. Since such wiring is often connected to small-signal electronic circuits inside the building, it is important that barriers be installed to prevent these induced transients from entering the building on these wires. Barrier elements, such as filters, surge arresters, and isolation transformers, should be placed on signal and power conductors where they penetrate the shield, as illustrated in Fig. 3.6.1-1(c). Alternatively, signals may be transmitted through the shield on optical fibers or by other nonmetallic means.

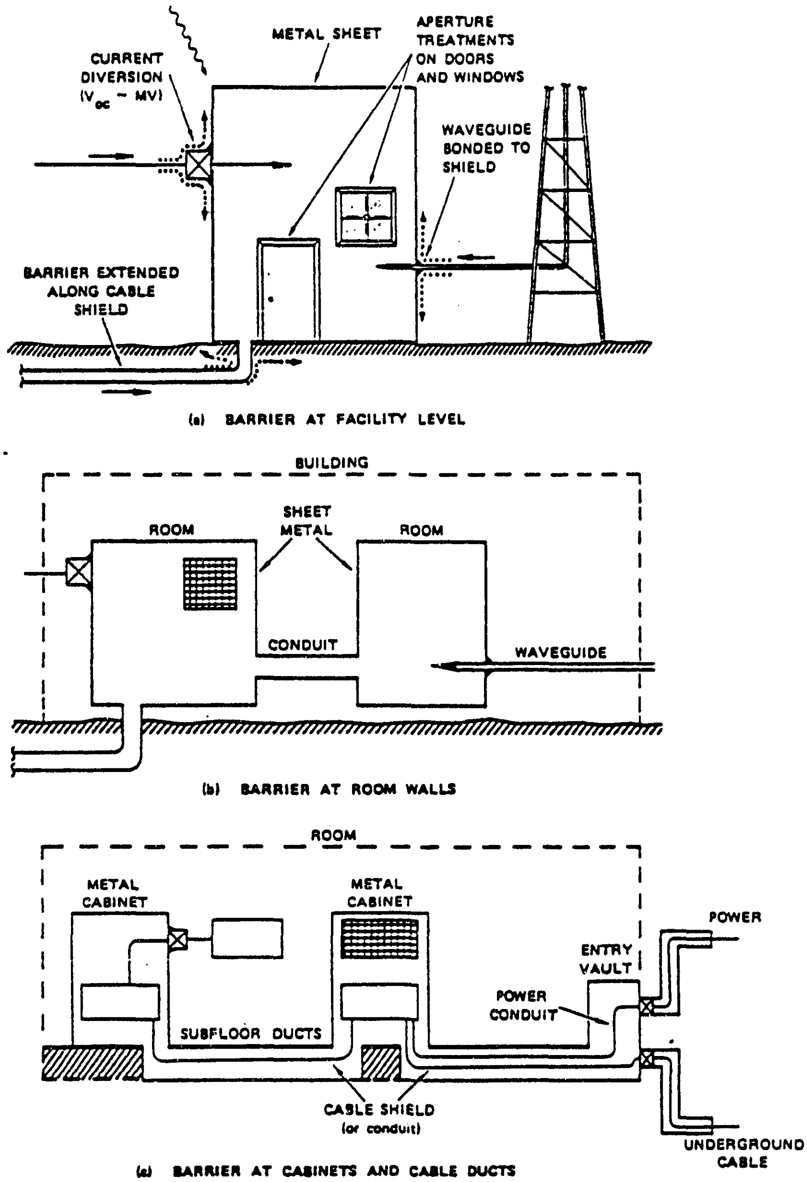

Fig. 3.6-1. Examples of first-level barriers.
Source: "Unification of Electromagnetic Specifications and Standards, Part I-Evaluation of Existing Practices", by E.F. Vance, W. Graf, and J.E. Nanevicz, DNA 5433F-1, SRI Project 8411, Contract DNA001-79-C-0206, 31 October 1980].

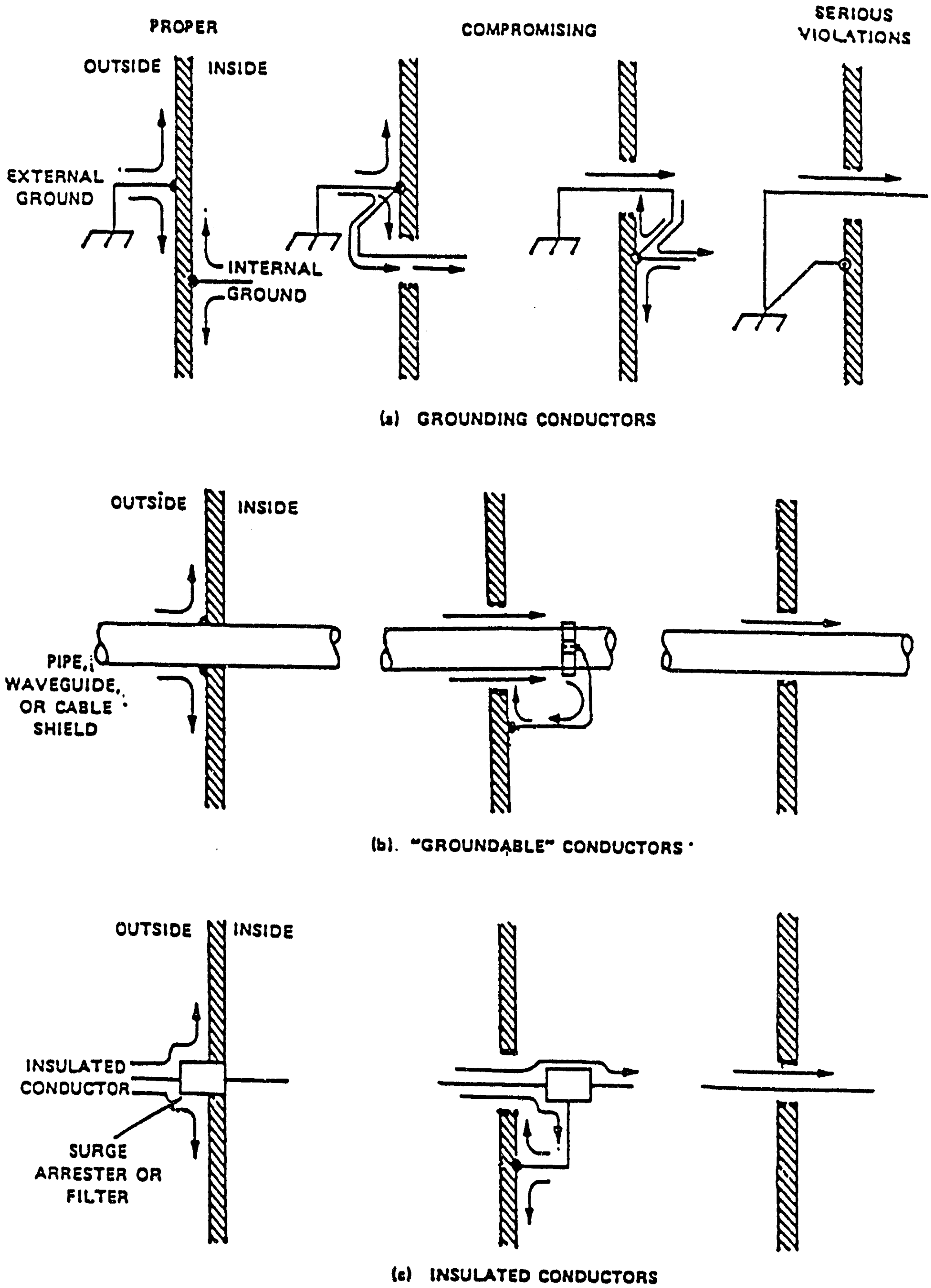

Fig. 3.6.1-1. Shielding integrity near interference-carrying external conductors.
Source: Document I-6.

Groundable conductors, such as cable shields, waveguides, grounding conductors, conduits, and pipes, should be bonded to the shield at the point of entry, as illustrated in Fig. 3.6.1-1(a) and (b). The preferred connection of the shield is a 360°-bond between the entering conductor and the building shield. Such a circumferential bond is necessary to preserve the integrity of a high-quality shield; it is less important for low-quality shields and partial shields (such as entry panels and ground planes). Nevertheless, it is important to divert as much of the externally induced E_1 current as possible to the shield or entry panel so that these transients remain outside the protected space.

Shield discontinuities and openings that do not have wires passing through them permit external fields to penetrate and interact with internal conductors, as illustrated in Fig. 3.6.1-2. As shown in the figure, the coupled currents and voltages are proportional to dE/dt and dB/dt, respectively, or in the frequency domain, $j\omega E$ and $j\omega B$, for apertures that are small compared to the shortest wavelength in the interference spectrum. The coupling to interior conductors is the strongest at the high-frequency end of the HEMP spectrum. Coupling through apertures can be reduced by closing, covering with metal mesh, or by using waveguides below cutoff.

Because aperture coupling depends on aperture excitation and decreases with separation between the aperture and the interior wiring, other control means are practical. It is possible to limit the excitation of apertures by preventing large E_1 and lightning currents from flowing over the shield. This is the principle of the single entry panel for all external conductors such as power and communication lines and the external grounding conductor (see Fig. 3.6.1-3).

Similarly, an economical way to control aperture coupling is to keep interior wiring away from openings such as windows, doors, and ventilators. A major improvement can be achieved by not routing the wiring directly over the aperture. Beyond that, if distance to the wiring is large compared to the biggest aperture dimension, the coupling varies as the inverse square of this distance.[K.S.H. Lee (Ed.) EMP Interaction: Principles, Techniques, and Reference Data, Washington, Hemisphere, 1986]. Hence, by keeping interior wiring away from apertures and by using a single entry panel to limit aperture excitation, it is possible to achieve a large measure of protection against transients on external lines with only moderate-quality shields. Thus, metal shelters for remote communication equipment may provide sufficient shielding if the single entry panel and wiring exclusion around large openings are used. These techniques are economical to apply and are effective against lightning and line transients as well as E_1 pulses.

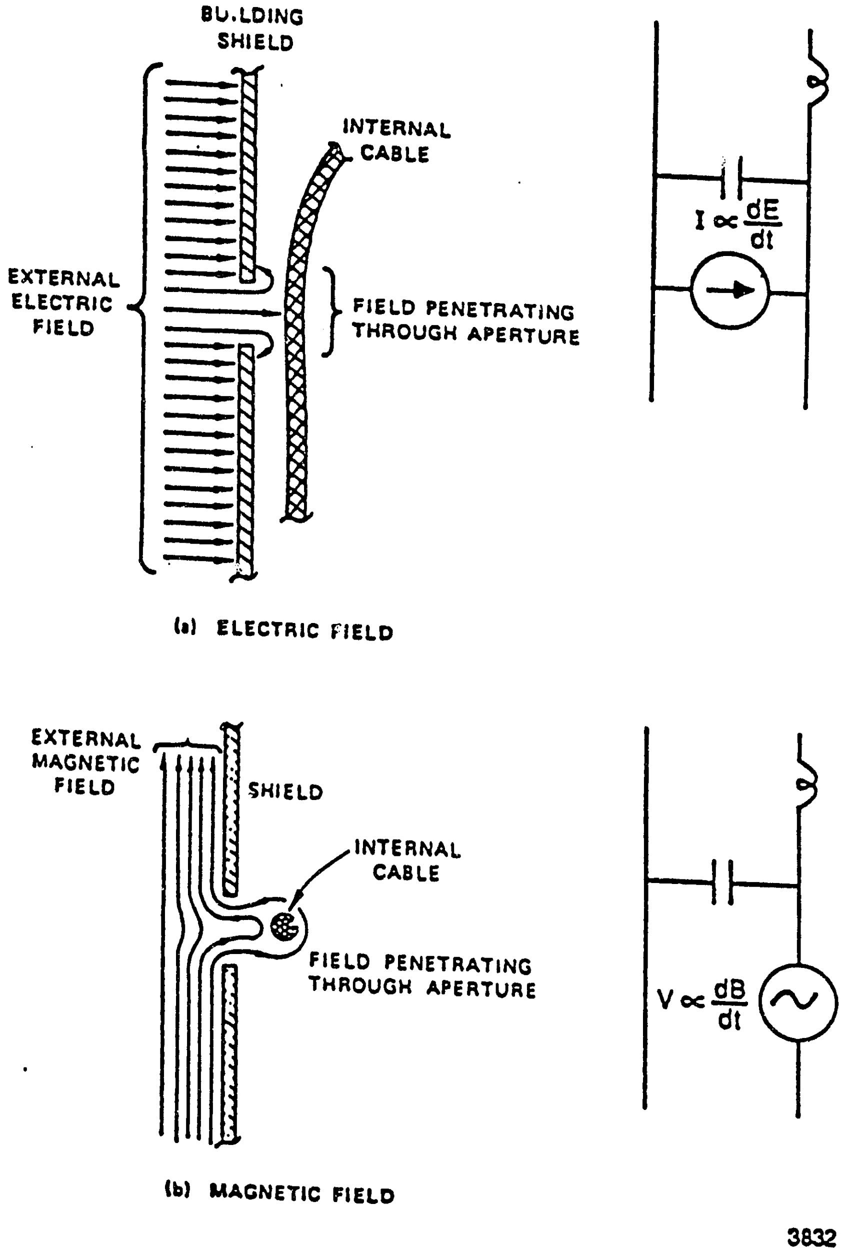

Fig. 3.6.1-2. Electromagnetic penetration of small apertures.
<u>Source</u>: Document VIII-2.

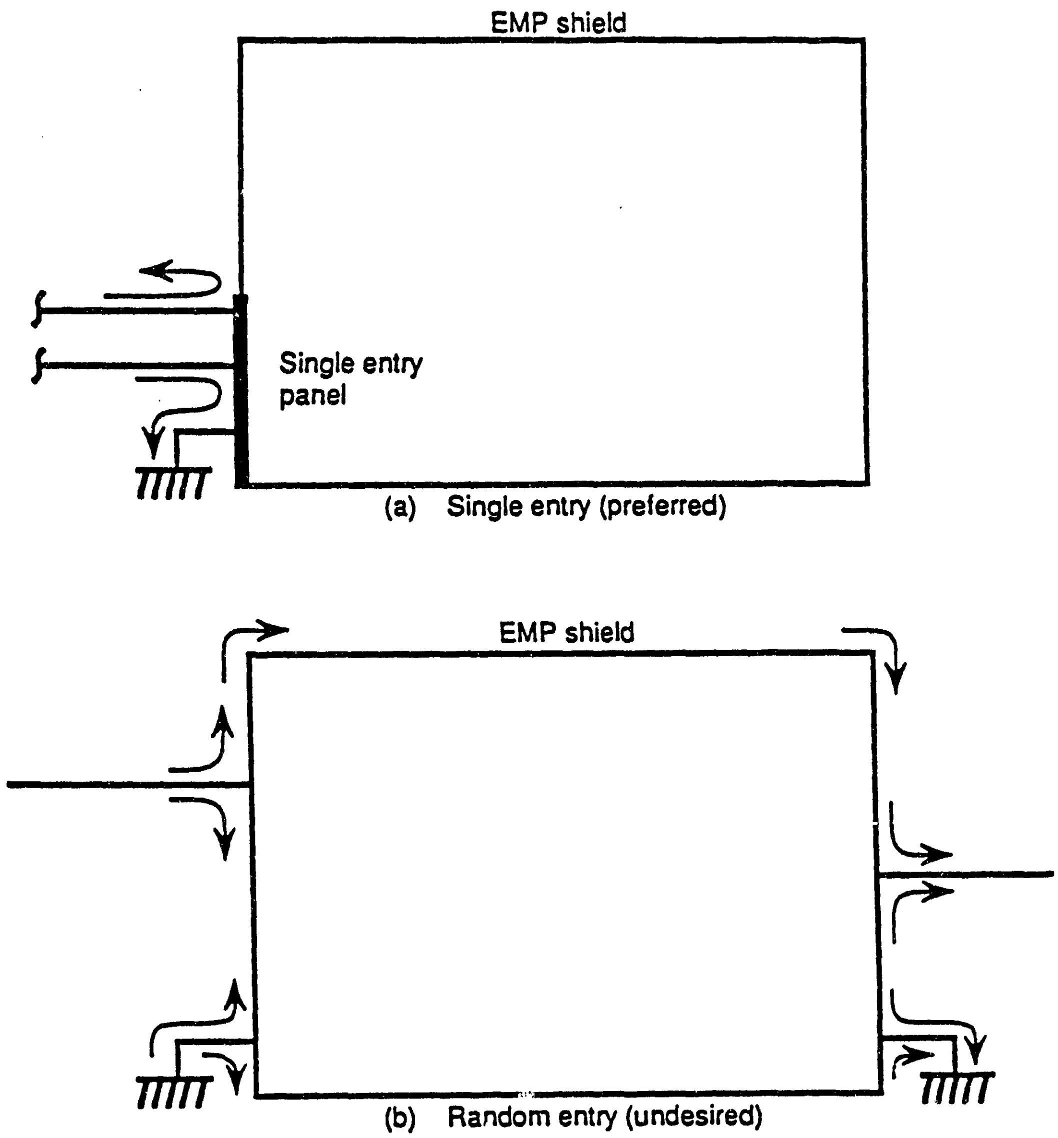

Fig. 3.6.1-3. Use of single entry panel to minimize external excitation of electromagnetic pulse shield.
Source: Document VIII-2.

It is recommended that large central computers be installed in moderate-quality (60 dB or better) shielded rooms with single entry panels and aperture controls. This will have peacetime benefits of increased reliability and greater tolerance for lightning and other transients. The protection for the central computing facilities and the communication equipment should also include an uninterruptible power system (UPS) and an independent gasoline- or diesel-powered emergency generator. As the operation of the power system becomes more dependent on the central computer system and reliable communications, the importance of protecting these from peacetime failures, as well as E_1 pulses, increases.

Normal utility control houses have more limited shielding effectiveness. Concrete block and tilt-up, precast concrete structures generally have low magnetic shielding effectiveness (approximately 20 dB) because of the relatively small amount of interconnected steel reinforcement in their construction. Poured-in-place buildings use an extensive network of interconnected rebars, resulting in greater magnetic shielding (ranging from 20 to 40 ds) than concrete block or precast concrete structures of comparable size. Even greater shielding effectiveness can be obtained by using solid metallic enclosures (50 to 80 dB).

To control aperture leaks, Document I-11 recommends that openings in the shielding be less than 0.2 x 0.2 m with an occasional maximum of 0.5 m. The total hole area should be ≤ 1% of the wall area. Wave traps (wave guides below cutoff) should be used for larger openings such as windows and doors. A table of required trap dimensions is given in Sect. 2.1.2.7 of Document I-11.

For some existing control houses, it may be practical to use zoned protection, such as shown on Fig. 3.6.1-4. Here the concrete building with its various apertures provided only 20 dB attenuation. By using a shielded cabinet, an additional 20 dB could be obtained. If further attenuation is required for a particular control device or element, it could have its own shield and, as shown, have a total attenuation of 60 dB from the outside environment. Note however that very high fields may exist in regions that have only 20 dB of shielding. The voltages induced by E_1 fields in these regions could cause arcing or other insulation failure.

Document VIII-6 describes such a two-zone installation. Ontario Hydro was installing a new control center located at a major 230-kV switching station. The control room and computer room would be located underneath three of the transmission lines. The computer manufacturer stated that the EM fields should be limited to 1 V/m and 0.1 A/m for satisfactory operation of the computer. The fields had to be

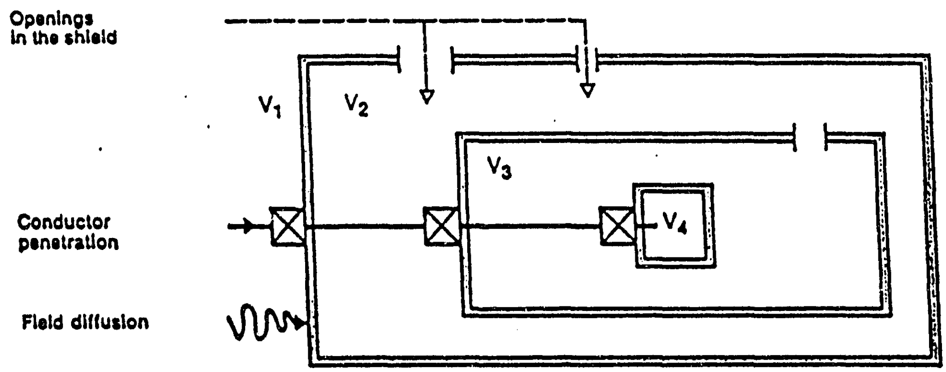

Volume	Attenuation	Total
V_1	0 dB	0 dB
V_2	20 dB	20 dB
V_3	20 dB	40 dB
V_4	20 dB	60 dB

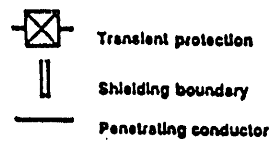

Fig. 3.6.1-4. Example of zoned protection.
Source: Document I-10.

limited to 16 V/m and 1 A/m for the display terminals in the control room. (Note: These limits are for only one vendor; other computer vendors should be consulted for their recommendations.)

Fig. 3.6.1-5(b) shows the bonding and shielding used for the control room and Fig. 3.6.1-5(c) shows the shielding used for the computer room. All standard practices for grounding, bonding, shielding and filtering of the building penetrations were also followed.

Table 3.6.1-1 shows the results of tests at various locations during various stages of construction. Lines C4R and C11R were switched with line disconnect switches and the field measurements were recorded. Fig. 3.6.1-6 shows the test locations. "1" and "2" are where the computer room is located; "3", "4", and "5" are where the control room is located; "6", "7", and "8" are outside the buildings. The various stages of the tests were

Stage 1: Before construction.

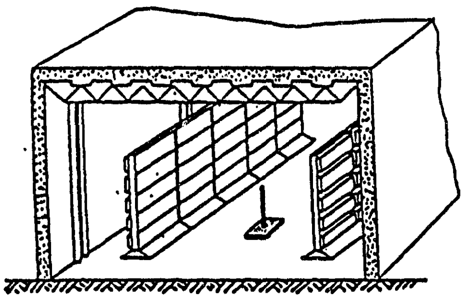

(A) CONVENTIONAL RELAY OR CONTROL BUILDING
5-15:1

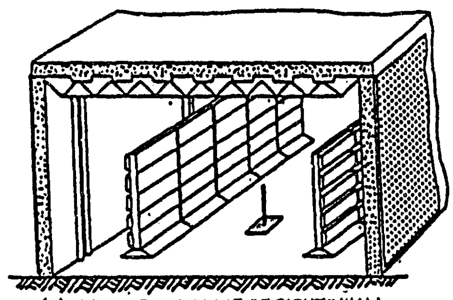

(B) BONDING AND "LINE OF SIGHT" WALL
CLADDING ADDED
15-30:1

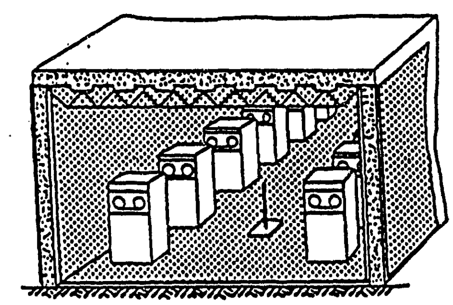

(C) INTERNAL SCREENED ROOM ADDED
400-1000:1

Fig. 3.6.1-5. Estimates of shielding by substation structures based on rod antenna measurements.
Source: Document VIII-6.

Table 3.6.1-1. Peak transient electric field amplitudes generated by line disconnects as a function of location and construction stage.
Source: Document VIII-6.

		E-Fields (V/M)							
		Location							
Line Switch	Stage	1	2	3	4	5	6	7	8
C4R	1	600			20	8			
	2	25	40	45	10	10		400	1000
	3	1	1	7	32			300	
	4	0.1							
C11R	1	150		370	90	20	200		
	2		70		40	15	380		
	3	1	1	4	30		400		
	4	0.1							

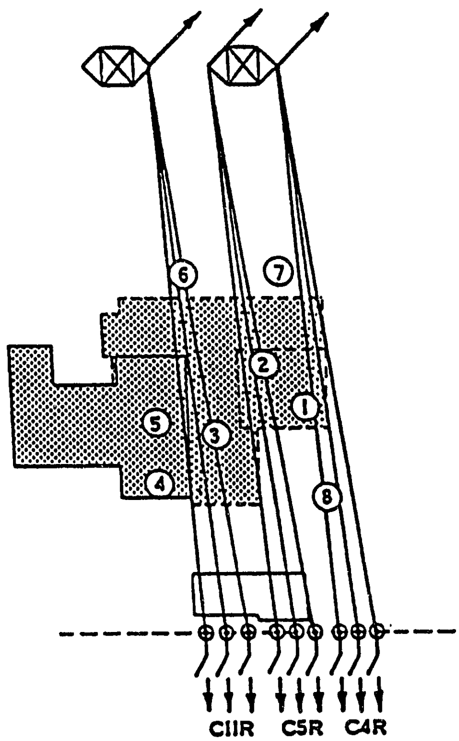

Fig. 3.6.1-6. Field measurement locations. The outline of the computer room encloses locations 1 and 2.
Source: Document VIII-6.

Stage 2: The new structure added with "line of sight" screening.

Stage 3: After computer room screening and installation of major services.

Stage 4: After computer is powered up and phased into a software development program.

Note that the fields in the computer room were reduced from 600 V/m to less than the computer manufacturer limits of 1 V/m and 0.1 A/m. The fields in the control room were only reduced to 32 V/m, which is twice the manufacturer's limit for the display terminals, but no problems have occurred.

A similar zoned approach was taken with the Electric Power Research Institute (EPRI) digital relaying terminals. Some of the relay cabinets used special EMI shielding and some did not. The yard DAUs all were shielded. It has been decided that the special shielding of the relay units was not needed, at least in the station environment where the demonstration units were installed. The yard DAUs, however, do require the shielding.

3.6.2 Building Penetrations

The building shield prevents the incident E_1 or other wave from inducing large transients directly on the interior wiring. However, large transients induced on exterior cables may propagate into the facility on power, signal, and grounding conductors unless barrier elements are installed on these where they penetrate the shield. Fig. 3.6.2-1 illustrates how these barrier elements are installed on power and signal cables with filters and surge arresters. Also illustrated in the figure is the way the shield is closed about groundable conductors such as cable shields, waveguides, conduits, and pipes with a 360° bond. Interior and exterior grounding conductors are attached to opposite sides of the shield so that neither penetrates the shield.

For shielded control houses or shielded cabinets inside the control house (see Fig. 3.6.1-4), the currents on the cable penetrations should be stripped off at their entry points and not on the equipment itself. All cable entry should be concentrated in one area. The entry panel, shown on Fig. 3.6.2-1, should be at least 2 x 2 m (or a complete wall of a small enclosure), and all shield wires and other earth connections should be made on the entry panel. The entry panel should be located at a distance at least twice its largest dimension from the nearest opening in the shield.

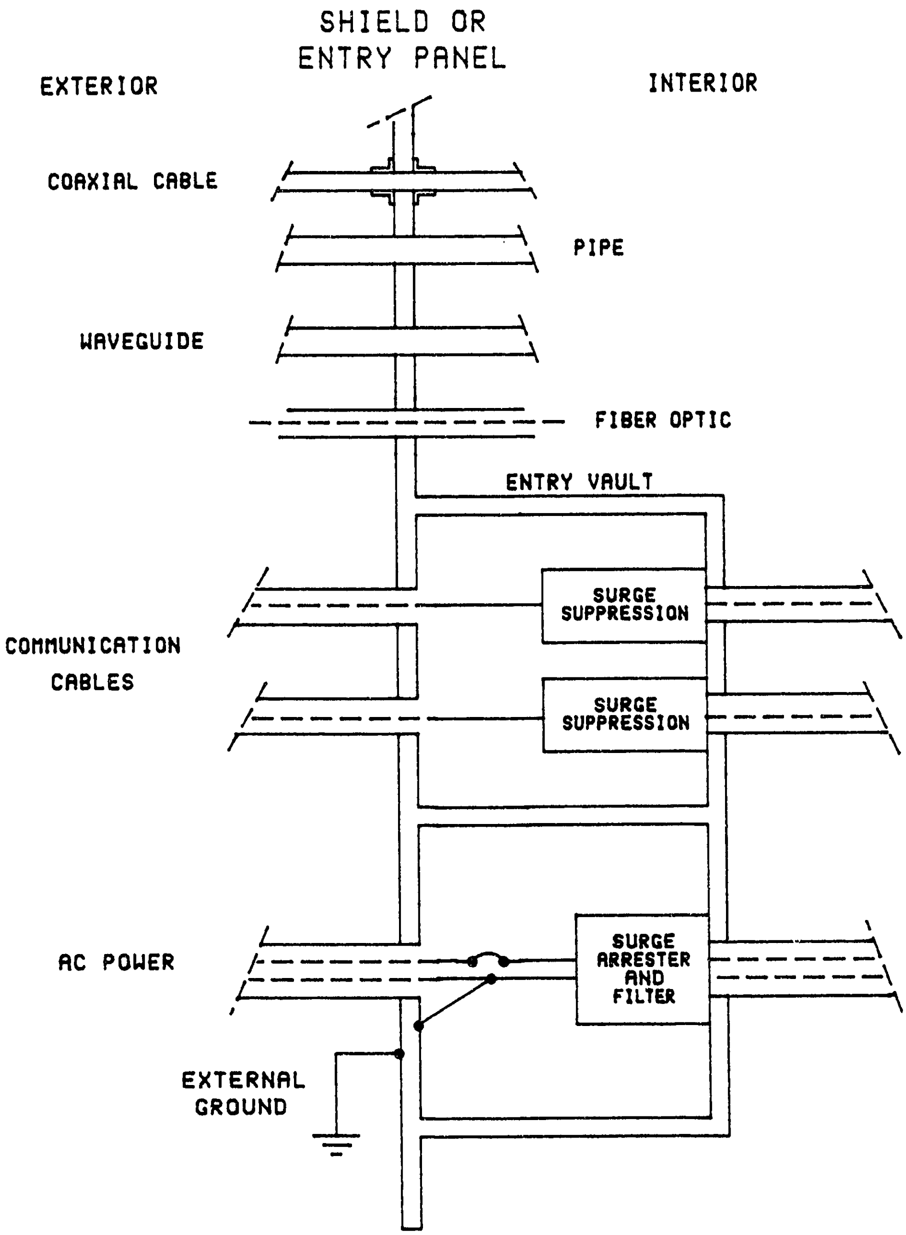

Fig. 3.6.2-1. Entry panel.
Source: Document I-6.

The power and telephone lines should be treated at their entry points with low-voltage surge protective devices, as illustrated in Fig. 3.6.2-1. The coaxial cable or waveguide antenna feeds should also be bonded to the shield with a feedthrough connector or waveguide flange that has contact around the entire periphery to the shield. Used in this way, a shielded room or cabinet can reduce the transient currents reaching the interior by a factor of more than 100.

For equipment installed in nonshielded enclosures, some improvement can be realized by installing a large sheet metal entry panel and ground plane, illustrated in Fig. 3.6.2-2 by the solid lines. The coaxial cable/waveguide, surge protectors, grounds, UPS, and communication equipment can be bonded to this partial shield in the same manner as discussed above for the shielded room or cabinet. The entry panel and ground plane, in turn, should be connected to the external earth electrode system (perhaps through the power grounding conductor). While this partial shield does not provide protection against the direct interaction of electro-magnetic fields with the interior wiring and equipment, it can prevent most of the external cable currents from propagating to the interior to the electronic equipment. A factor of ten reduction can be achieved in external cable currents, which tend to be the primary sources of interference. If the EM fields create a problem, shielded cables or ducts inside the enclosure may be required.

The power entrance conduit should be bonded to the entry panel and low-voltage surge protective devices should be installed in or adjacent to the main power disconnect with leads as short as possible. For added reliability, a UPS system for the computer and communication equipment could also be installed. When properly installed, the UPS can serve as the barrier to transients on the external power lines.

As shown on Figs. 3.6.1-1 and 3.6.2-2, the internal and external grounds to the entry panel should be kept separate. In this manner any transients induced on the exterior ground conductors flow onto the exterior of the shield. They can enter the interior only by diffusing through the metal shield, but only the low frequencies can diffuse through the shield wall without attenuation. If it is necessary to use a "pigtail" connection for these ground connections, the pigtail lead should be kept as short as possible.

No insulated grounding conductor (or any other conductor) should be allowed to penetrate the shield because all frequencies could then propagate through the shield unattenuated; transients induced on external conductors are carried directly into the interior. The technique of separating the exterior ground from the interior ground has

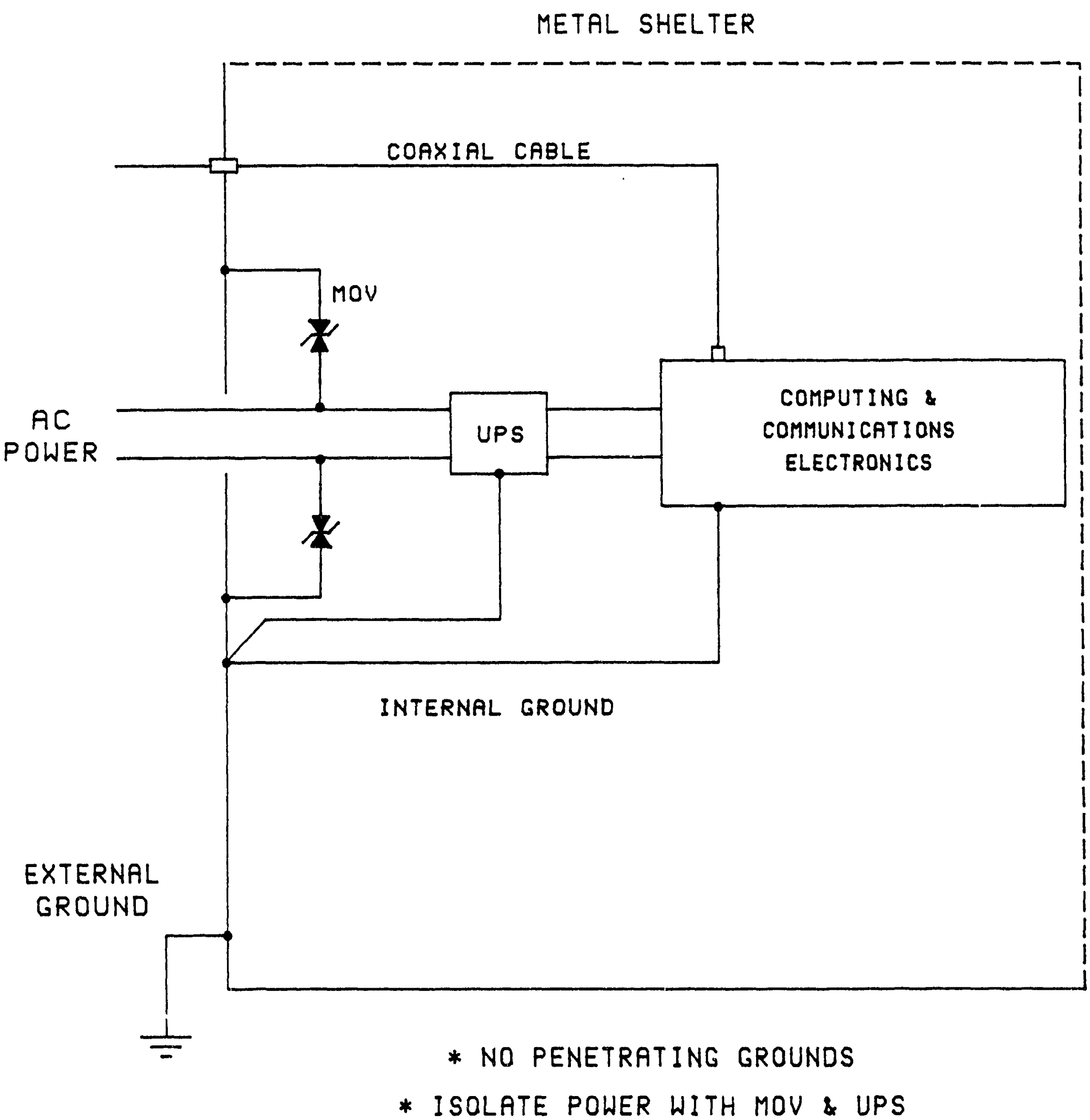

Fig. 3.6.2-2. Treatment of power and ground.
Source: Document I-6.

been demonstrated to provide noise reduction by a factor of more than 100 in controlled tests.

To eliminate these induced voltages altogether, fiber optic communication and control signal links should be used.

These grounding and shielding procedures are discussed in greater detail in Documents VIII-7 and -8 and Document XI-18.

For installations that do not have overall shields such as those discussed above, it may be possible to develop a closed shield from the equipment cases. This approach is more complicated than the overall shield, but it may be more economical for existing installations. In one approach, the equipment case or cabinet is treated as a shielded volume in much the same manner as the room or building shield; an entry panel is provided and all cables entering the cabinet are treated at this entry panel to prevent transients from being carried into the small-signal region. The procedures are identical to those used on building shields, but they are applied to each equipment case or cabinet individually.

In another approach, all equipment cases or cabinets are interconnected by shielded cables to form one large interconnected shielded volume. In this approach, the interconnecting cable shields are integral parts of the shield system. Fig. 3.6-1c illustrates a two-level shield system in which the cabinets and floor ducts form the outer level and the equipment cases and cable shields form the second level. External cable penetrations may enter through an entry vault, where they are treated in the same manner as they are in a shielded building. Because the interconnecting cable shields form a part of the transient barrier in this case, they must be closed on each other and with the equipment cases.

The quasistatic techniques of "grounding" cable shields with pigtails or of floating one end of the shield are not suitable for shielding against transients or other wideband sources. These quasistatic techniques were developed for controlling 60-Hz interference in instrument circuits (see XI-15). It is important to recognize that at 60 Hz, aperture coupling is negligible (because the frequency is so low) and the distinctions between shielding and grounding are blurred (because practical shields are transparent--less than a skin depth thick--at 60 Hz). For short transients, coupling to wires crossing apertures is important, and the distinction between shielding and grounding is sharp.

For transient interference from E_1 pulses, lightning, and power switching, the closed shield approach described above is applicable. Cable shields, conduits, and shielded ducts should be circumferentially bonded to the cases or cabinets that shield the terminal equipment. However, within the transient shield, any internal interference control techniques may be used, so long as they do not violate the transient shield. Thus if floating shields are required for 60-Hz suppression (or are required by the equipment manufacturer), they may be used inside the transient shield.

3.6.3 Protective Devices

No matter how good the building and penetration shielding, their protective ability is largely lost if a cable is led through without special protection at the point of entry or at the equipment itself. Fig. 3.6.2-1 showed examples of surge suppressors at the entry panel, whereas Figs. 3.5-1, 3.5-2, and 3.5-4 showed examples of devices on the equipment terminals.

The following devices could be used either at the entry panels or at the equipment terminals:

<u>Varistors</u>

- MOV
- SiC

<u>Semiconductors</u>

- Forward diodes (Si,Ge)
- Breakdown diodes (Si,Ge)
- Selenium-diode packages
- Diode thyristors (p-n-p-n)
- Triggered thyristors (silicon controlled rectifiers)

<u>Spark Gaps</u>

- Carbon blocks
- Ordinary gas tubes
- High-speed gaps
- Ordinary arresters
- Arresters using high-speed gaps

<u>Electromechanical Devices</u>

- Fuses
- Circuit breakers

<u>Filters</u>

- Lossy lines
- Ferrite chokes, beads
- Transformers

- Feed-through capacitors
- General RLC circuits

The uses of these devices can be summarized as follows:

<u>Varistors (MOV or SiC)</u> when used in surge arresters are rated 20 volts to hundreds of kilovolts. They are used when

- o Medium to large surge currents are expected.
- o Lines carrying ac or dc power require protection.
- o Nanosecond clamping of surges of either polarity is required.
- o Their capacitance (.001 μF) and leakage resistance are acceptable.
- o Size and cost matter.

The protective effect of even top quality overvoltage protectors is ruined if their connections are not as short as possible. The length of the connecting lead gives an additional voltage equal to L di/dt, which can be of the order of 1 kV/cm.

Fig. 3.6.3-1 from Document IX-3 illustrates the importance of keeping the arrester lead lengths as short as possible. It shows that just the metal oxide (MO) material turn-up for an arrester with a maximum continuous overvoltage value (MCOV) of 136 kV is approximately 1.3. The inductance of the block, the arrester stack, and the arrester leads add to this turn-up for the various values of T_{ri} (which is the time between the 30 and 90% points on the voltage wave). An inductance of 1 μhenry per meter of lead length is assumed.

A varistor with a lower clamping voltage than is necessary should not be selected because

- o In general, the lower the rating the greater the current and the smaller the volume of the varistor. Therefore, the energy limit for that volume may be exceeded. The discharge current rating should be checked before applying a specific rating.
- o The lower the rating, the lower the point of thermal runaway.

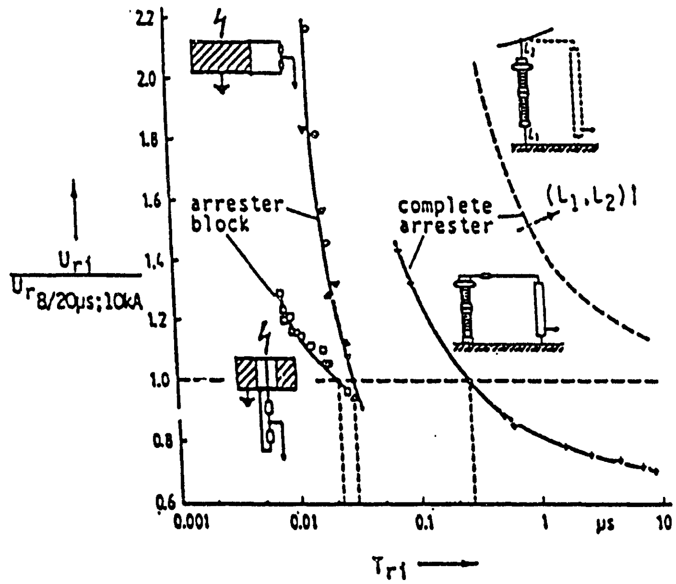

Fig. 3.6.3-1. Related voltage spike in the residual voltage waveshape of arrester blocks and a complete arrester (U_{MCOV} = 136 kV).
Source: Document IX-3.

- Repeated operation during momentary system overvoltages (or "swells") can cause failure.

Therefore the rating of the varistor should be kept as high as possible while still protecting the equipment.

Semiconductors (zener diodes) are rated 3 to 150 V. Some typical applications on electronic equipment are shown in Fig. 3.6.3-2. They are used when

- Low-level protection is needed.
- dc voltage extinction is required.
- Sub-nanosecond clamping is essential.
- High capacitance is acceptable.
- Low currents (<100 A) are expected.

Where the large inherent capacitance of zener diodes causes problems, diodes can be put in series with the zeners in a bridge circuit to negate this capacitance effect.

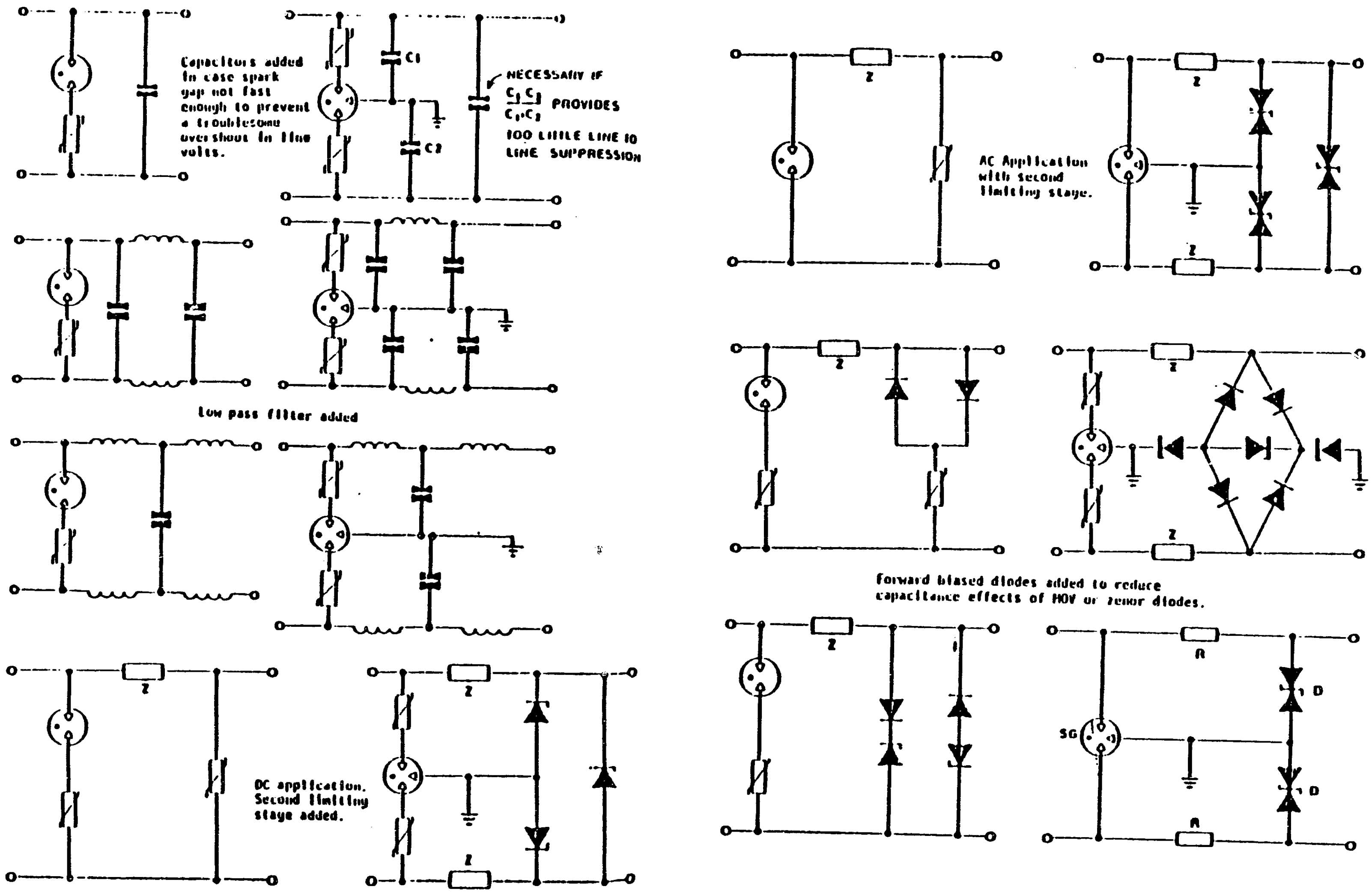

Fig. 3.6.3-2. Use of spark gaps, filters, varistors and zenor diodes to limit surges from electromagnetic pulses on electronic equipment.
Source: Document I-15.

Spark Gaps (both air gaps and gas tubes), shown on Fig. 3.6.3-3, are rated 60 V to 30 kV. They are used when:

- High surge currents in the kAs are expected.
- Minimum capacitance and maximum resistance are essential.
- Gap is guaranteed to reseal or fault current can be controlled by a series resistor.
- Energy passing the gap during turnon is acceptable.
- Protection levels of <60 volts are not required.

Air gaps and gas tubes are useful where the large inherent capacitance of MOVs and zener diodes cause problems. The gas tubes can also handle much greater surge currents. Their disadvantage is the volt-time turnup at fast fronts and their difficulty in extinguishing the power follow current.

Filters are almost essential for protecting electronic equipment. They should be installed, for example, between spark-gap arresters and the electronics to buffer the gap's non-linear shock excitation when the gap fires. Some typical filters are shown on Figs. 3.6.3-4 and 3.6.3-5.

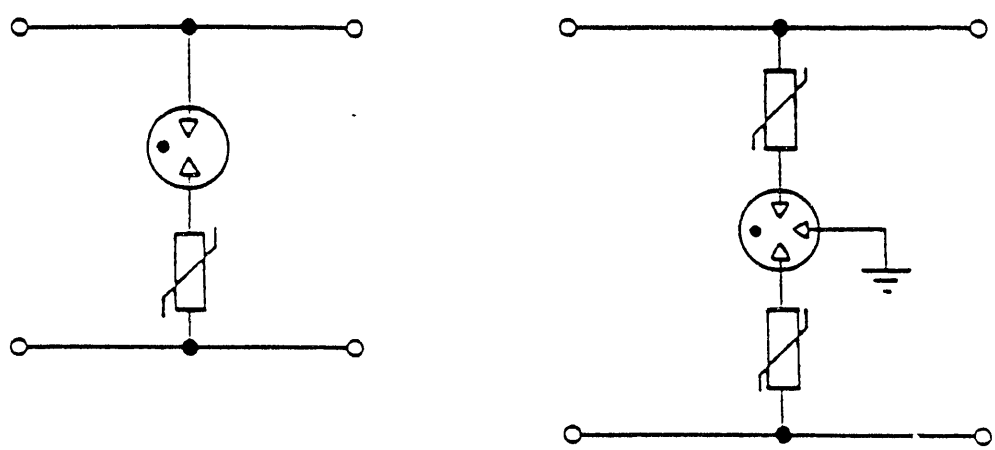

Fig. 3.6.3-3. Use of two- and three-electrode spark gaps with current limiting non-linear resistance.
Source: Document I-15.

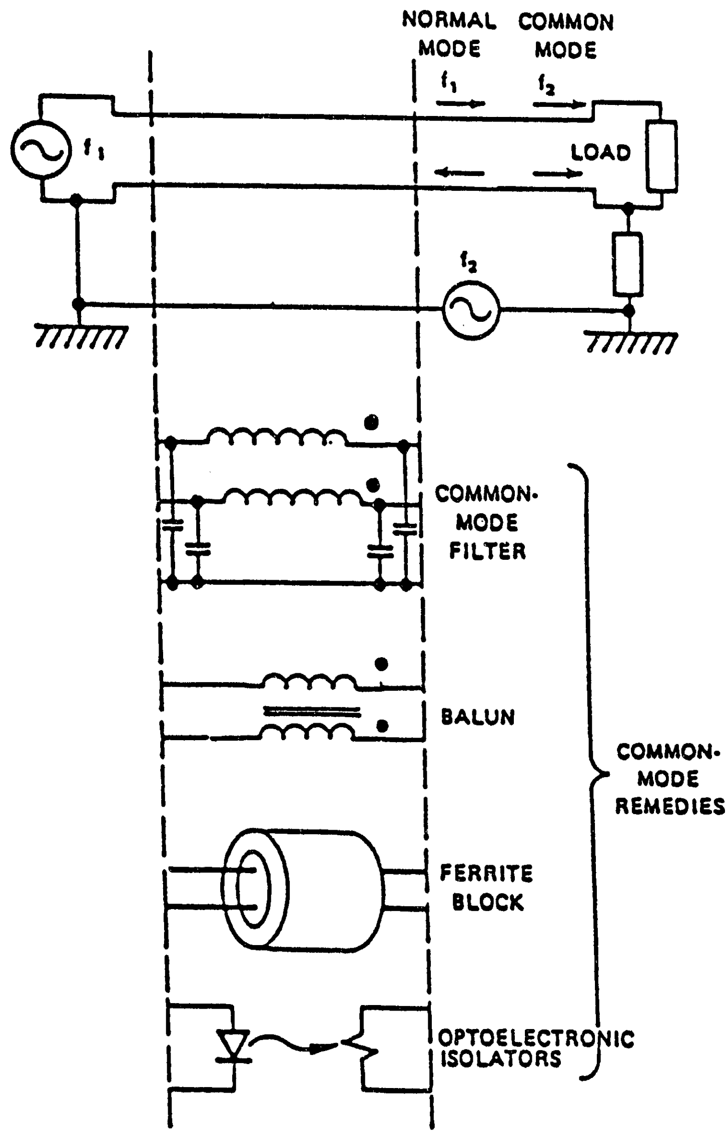

Fig. 3.6.3-4. Common-mode interference and some remedies.
Source: Document XI-16.

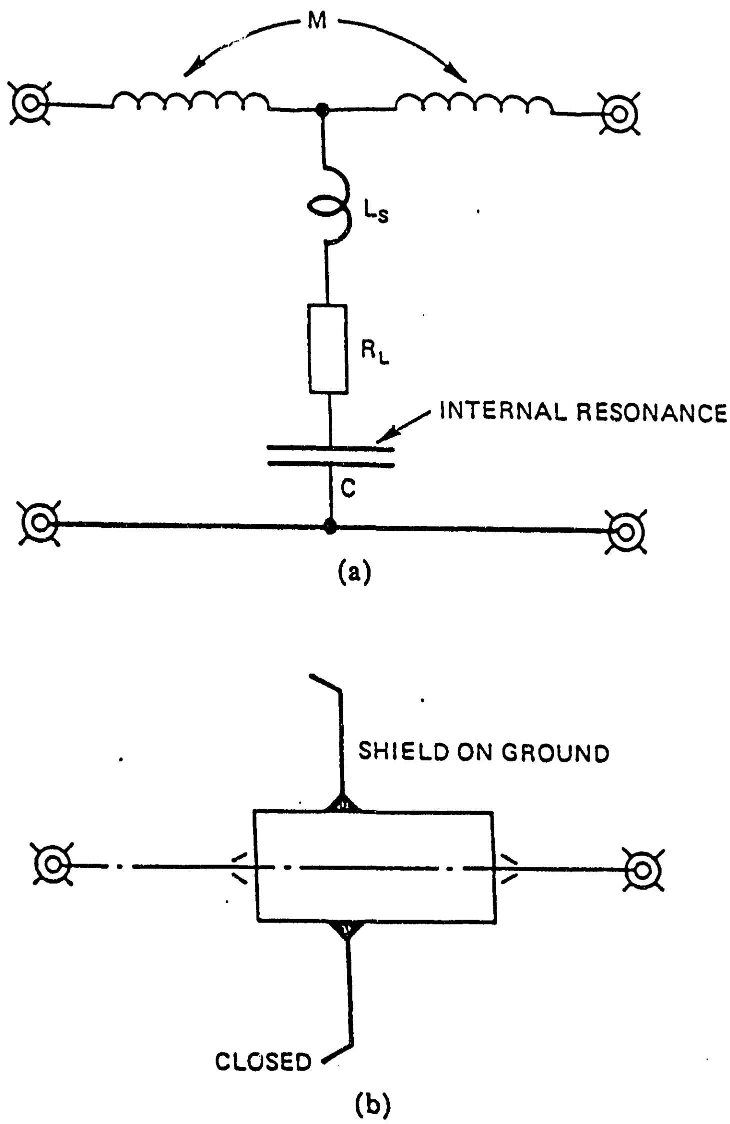

Fig. 3.6.3-5. Reasons for nonideality of real capacitors (a) equivalent circuit of shunting capacitor, not constructed as feed through. (b) feed-through configuration.
Source: Document XI-15.

Capacitor-input filters are recommended for power line penetrations because inductive-input filters usually cannot withstand the large open-circuit voltage on these lines. Capacitors also increase the rise time or front of the incoming wave, thereby reducing the overshoot of MOVs or spark gaps. They also absorb the spike passed by spark-gap arresters, making them a good buffer between the spark gaps and the electronic circuits. As mentioned in Sect. 3.5, practically all modern solid-state and microprocessor relays being built today contain capacitor filters (surge packs) on their terminals.

The following problems can arise in the design and use of filters:

- Iron or ferrite core inductors can lose much of their inductance by saturation. Also, because of their distributed capacitance, they can appear as a capacitance at the higher frequencies. A ferrite bead or block appears as an inductance of 20 to 50 ohms (45° phase angle) at 1 MHz and above but as negligible impedance at low frequencies.

- Figs. 3.6.3-5 and 3.6.3-6 show what to consider in the use of so-called capacitors ("so-called" because of the inherent internal and/or external inductance of their circuits). Fig. 3.6.3-5(b) shows that feed-through capacitors should be used to minimize the capacitive and inductive coupling between input and output leads. A_1 and A_2 of Fig. 3.6.3-6 show the effect when the internal inductance of some capacitors causes a series resonance and ultimately appears as an inductance at the higher frequencies.

  In the same figure, B shows the effect of the internal shield of some wound capacitors and C shows the effect of series resistance of tantalytic capacitors. Discoidal (disklike) feed-through capacitors (E) are better than tubular ceramic capacitors (D). By splitting the ceramic capacitors into two portions and providing a ferrite bead in the interconnection, the capacitors can be made better (F_1, F_2, and F_3) than even ideal capacitors.

- Resistance-inductance-capacitance (RLC) filters can be passive or active; the latter combine resistances, capacitances, and integrated operational amplifiers to effectively replace inductance-capacitance (LC) filters.

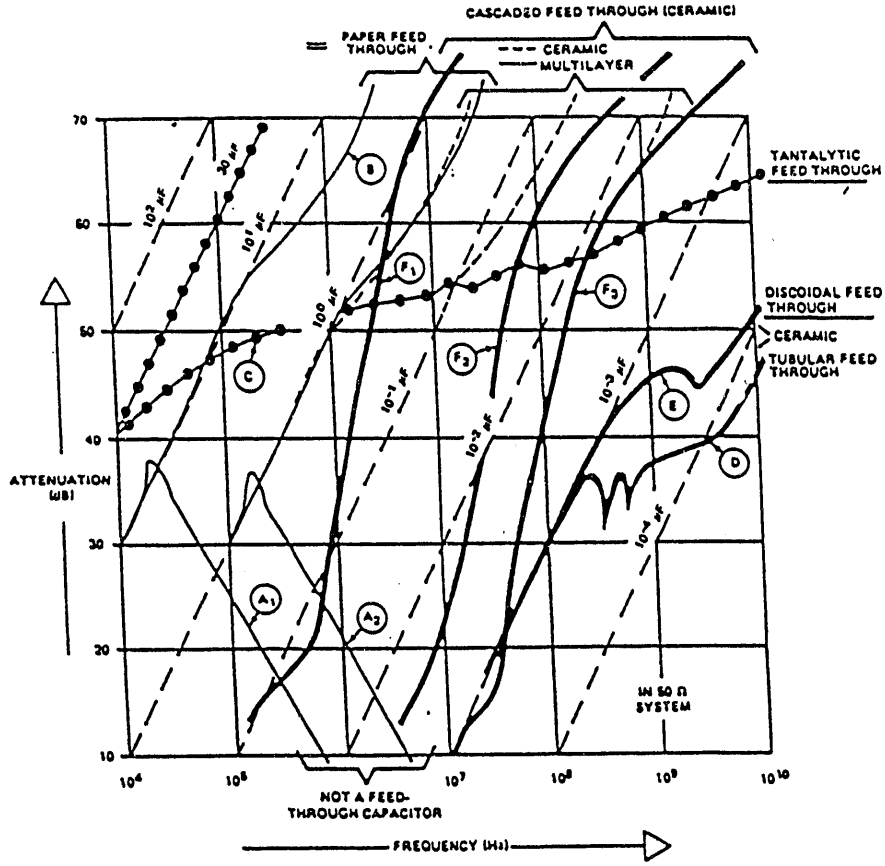

Fig. 3.6.3-6. Attenuation of so-called capacitors.
Source: Document XI-15.

- Isolation transformers (Fig. 3.6.3-7) are useful in suppressing low frequency common mode interference. For use at high frequencies, these transformers must have very low and (as noted in Document VIII-7) balanced inter-winding capacitance and no conductive path between the grounded terminals of either winding.

- Optoelectronic couplers (Fig. 3.6.3-8) are also used, but the most appropriate solution is to replace the entire signal transmission line with fiber optic cable.

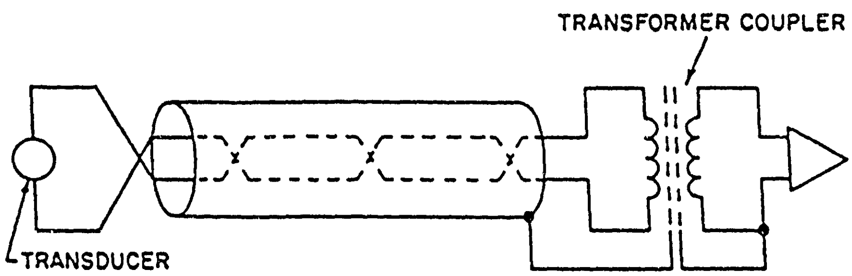

Fig. 3.6.3-7. Transformer-coupled input.
Source: Document XI-1.

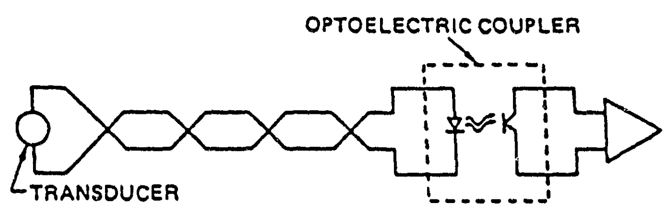

Fig. 3.6.3-8. Optoelectronic coupler circuit.
Source: Document XI-15.

Tests were run to determine the effectiveness of filters and voltage suppressors against E_1-induced transients. These tests are described in Document IX-2. Fig. 3.6.3-9 shows that E_1-type impulses (V_o) were applied to the primary of a 7200/250/125- volt, 25-kVA distribution transformer through a 400-ohm resistor. This primary voltage (V_a) produced a secondary voltage (V_s) that was impressed on the filter and/or transient surge suppressor. The output voltage (V_L) was measured across an 11-ohm resistor simulating the load. Three types of commercially available filters and two types of secondary class transient voltage suppressors (a 275-V MOV with a slow-front clamping voltage of 750 volts, and a 250-V back-to-back diode type with a slow-front clamping voltage of 652 V) were tested.

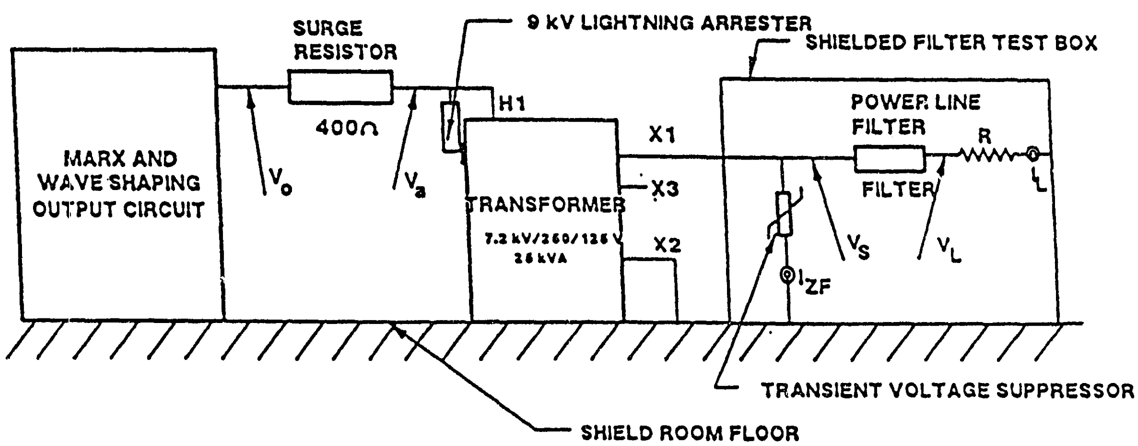

Fig. 3.6.3-9. Block diagram of the experimental setup to perform the filter tests.
Source: Document IX-2.

Table 3.6.3-1 gives the results of the tests. The filters provided from 38 to 54 dB of attenuation and the surge suppressors provided an additional 2 to 8 dB. The load voltages were limited to 75 to 204 volts with the various combinations of filters and suppressors. Note the effect of lead inductance in the various voltage drops.

During the tests one of the filters appears to have been damaged by the surges. This may have occurred during one of the tests without the voltage suppressor. It is recommended that surge suppressors always be used to protect the filters. The leads should be kept short to minimize the lead inductance. Since damage did occur during the tests, the authors recommend that further tests be run and on a larger number of filters.

Table 3.6.3-1. Performance summary of power line filter C with and without a transient voltage suppressor installed at the filter's input terminal.
Source: Document IX-2.

Shot	V_o (kV)	V_a (kV)	V_s (kV)	V_L (V)	I_L (A)	I_{ZP} (A)	Transient voltage suppressor	Filter	Attenuation (dB)
1252	1300	163	19.5	6000	-	-	None	None	N/A
1278	1350	161	6.4	75	-	230	Type 1	Yes	48
1280	1350	156	10.7	204	4.4	-	None	Yes	40
1281	1350	158	6.6	150	3.2	416	Type 2	Yes	42
1282	696	91.2	14.4	6100	420	-	None	None	N/A
1279	696	91.0	7.3	176	3.0	-	None	Yes	38
1284	788	100.8	8.0	4800	232	392	Type 1	None	10
1286	1300	-	11.1	5400	304	560	Type 1	None	11
1287	740	100.0	8.3	4600	208	400	Type 2	None	10
1289	1400	163	11.6	6000	304	580	Type 2	None	10

[a]Filter attenuation with and without a transient suppressor is defined here as 20 $\log_{10} (V_s/V_L)$. V_s is the voltage at the filter input without the filter in the circuit. V_L is the load voltage. For a peak load voltage of 204 V, attenuation = 20 $\log_{10}$ (19,500/204) = 39.6 dB.

Note 1: Figure 3 depicts the locations of voltage and current measurements (i.e., V_o, V_a, V_s, V_L, I_L and I_{ZP}).

Note 2: Type 1 transient suppressor = metal oxide varistor.
Type 2 transient suppressor = back-to-back diode.

3.7 Summary

The E_1 component of the high-altitude burst should cause relatively minor problems to utility systems provided proper design and operating procedures are followed. Specifically:

1. Transmission and subtransmission lines will probably be unaffected by E_1 surges because of their relatively high insulation levels. Under the single-burst scenario, distribution lines of 15 kV and below may encounter some flashovers. Unpublished studies suggest that dispersed, multiple bursts could increase the probability of a flashover to 100% at some point on every overhead distribution circuit. In either event, the use of surge arresters at every two or three poles may alleviate this problem.

2. Power cable systems (cables and potheads) should not present a problem provided surge arresters are properly applied directly on the potheads.

3. The turn-up in the protective levels of surge arresters for E_1 type surges is modest, at most 1.2 to 1.6 times the protective level for lightning type surges. Due to the steep fronts of E_1 waves however, the L di/dt of their down leads can be a problem. These lead lengths should be kept as short as possible.

4. Provided that surge arrester leads are kept short, power transformers will be relatively immune to E_1 surges.

5. It appears that there is little probability of distribution transformer failure, even without surge arresters.

6. While there is little data on bushings, it appears that there will be no problems.

7. Based on limited test data, the probability of a relay misoperation from the E_1 environment appears small.

8. The primary equipment in power plants (e.g., generators, large motors, transformers) will be largely unaffected by E_1 surges. Smaller 480-V motors that cannot afford the protection packages and that are located away from the plant and supplied by unshielded cable are subject to damage. Even without any control or equipment failures (or malfunctions), a number of generators or plants may shut down due to external causes. Loss of system load due to distribution system tripouts can cause generator overspeed or out-of-step conditions that could trip the generator units.

9. Relays and communication and control equipment tested to the C37.90.1 "fast transient" surge withstand test and supplied by

properly shielded, filtered, and grounded control cables would probably not be affected by the induced E_1 surges. If the standard were changed to require applying the test wave to individual terminals (rather than allowing the paralleling of like logical terminal groups), this equipment would be even more secure. The E and H E_1 *fields*, however, exceed the C37.90.2 test levels; but since the fields due to substation switching also exceed these levels and few problems have occurred, from these occurrences the E_1 field problem presently appears to be minimal. In the future, when relays and other electronic equipment are mounted in the switchyard, problems could occur. But disconnect switching could also cause problems to these installations. The Power Engineering Society Power System Relaying Committee is studying this problem.

10. A number of industry standards or guides, while not written specifically for E_1 surges, contain sections or requirements that, if followed, will reduce the probability of damage from this source. There is a need, however, for a separate standard emphasizing the control of transient interference in digital equipment installations. Note that complete adherence to these guides or standards may be too expensive for retrofitting existing facilities, but not necessarily too expensive for new installations.

Note that while proper protective practices and procedures are specified in standards and utility company guides, if they are disregarded in actual installations (e.g., allowing excessive surge arrester down leads, improper cable grounding and/or shielding) E_1-caused failures may occur.

4.0 E_3 WAVES

As mentioned in Sect. 2.0, the E_3-induced current wave is similar to the geomagnetically induced current (GIC) wave that accompanies the geomagnetic storm. The E_3 field has a greater intensity and time rate-of-change than the storm but a shorter duration, lasting a few hundred seconds compared with tens of minutes to hours for the storm. Their equivalent frequencies are both less than 1 Hz (in effect, dc currents). Despite their differences, there is sufficient similarity that their effects on the power system can be analyzed in similar ways.

Many papers and reports have been written on GICs and their effect on power systems (Documents II-1 through -13 and -20 & -21). Because of the similarities with the E_3 waves, these GIC effects will be explained in detail in the following discussion of how they are similar to or different from the E_3 effects.

4.1 Geomagnetically Induced Current Characteristics

Solar flares and other solar phenomena produce a rarified plasma of protons and electrons called the "solar wind". These solar wind particles interact with the earth's magnetic field to produce auroral currents that, in turn, produce fluctuations in the earth's magnetic field; fluctuations of sufficient intensity are termed "geomagnetic storms."

The magnetic field fluctuations induce electric potential gradients in the earth, which are termed earth-surface-potentials (ESPs). These ESPs are highest in areas of low earth conductivity (high resistance). Low conductivity occurs in regions of igneous rock geology. These areas in the United States are shown in Fig. 4.1-1.

While an ESP is caused by currents flowing through the earth, the power system provides a parallel path. As shown on Fig. 4.1-2, the difference in potential causes a current flow path similar to zero sequence currents through the grounded neutrals of wye-connected transformers or autotransformers. Since the ESP is expressed in volts/kilometer, the greatest potential difference exists for the longer transmission lines. Since the extra high voltage (EHV) lines are generally the longest and almost always have the lowest dc resistance, the largest GICs are known to occur on these highest voltage lines.

The magnetic field fluctuations usually take place over relatively long periods. Fig. 4.1-3 shows measurements taken in Quebec, Canada, during the severe magnetic storm of March 13, 1989, which caused a complete shutdown of the Hydro-Quebec system. Note that these measurements show the variations over approximately a 24-hour period. Fig. 4.1-4 shows the wave shape of the E-field over approximately a one-hour period.

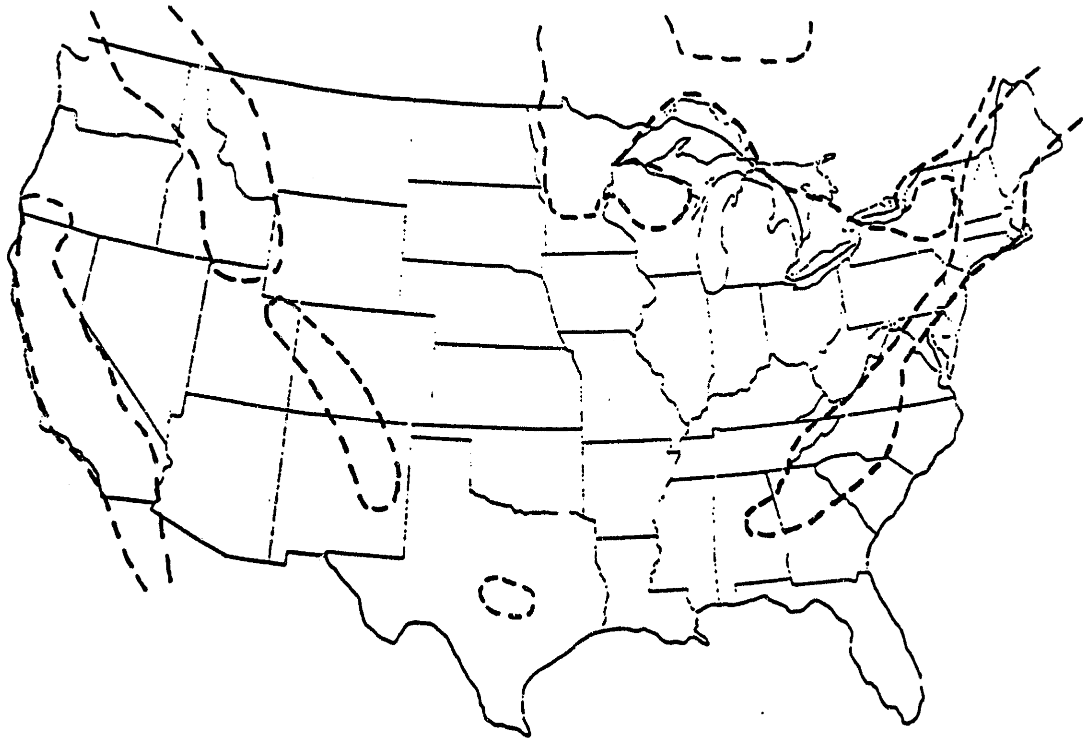

Fig. 4.1-1. General areas of igneous rock geology in the United States and Canada.
Source: Document II-1a.

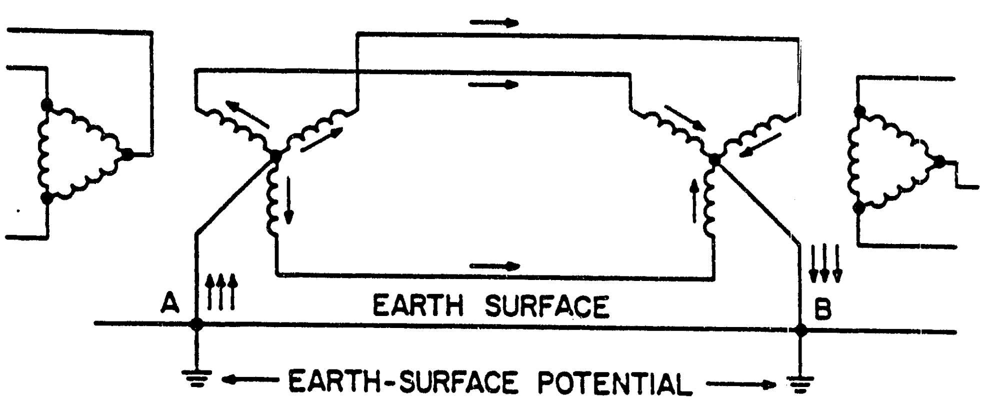

Fig. 4.1-2. Induced earth-surface-potential producing geomagnetically induced currents in power systems.
Source: Document II-1a.

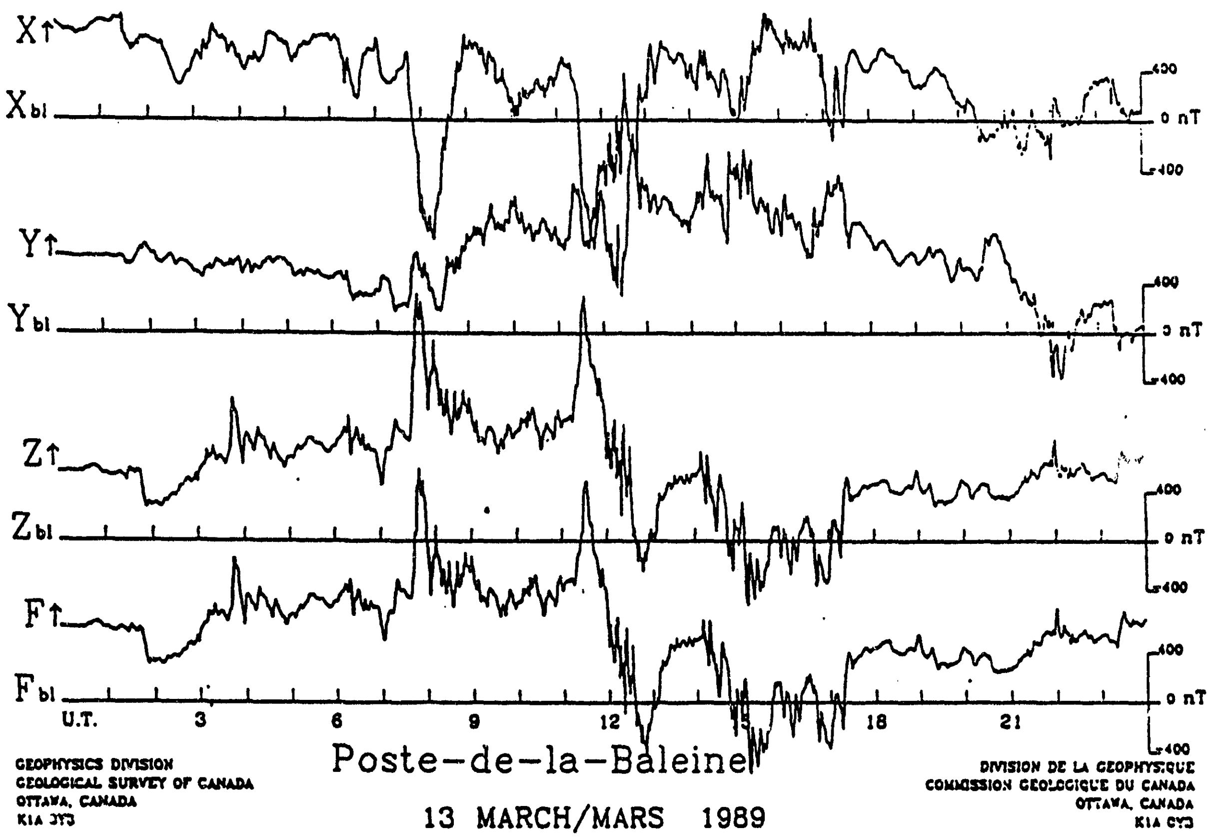

Fig. 4.1-3. Magnetogram from Poste-de-la-Baleine Magnetic Observatory, James Bay, Quebec, Canada.
<u>Source</u>: Document II-1a.

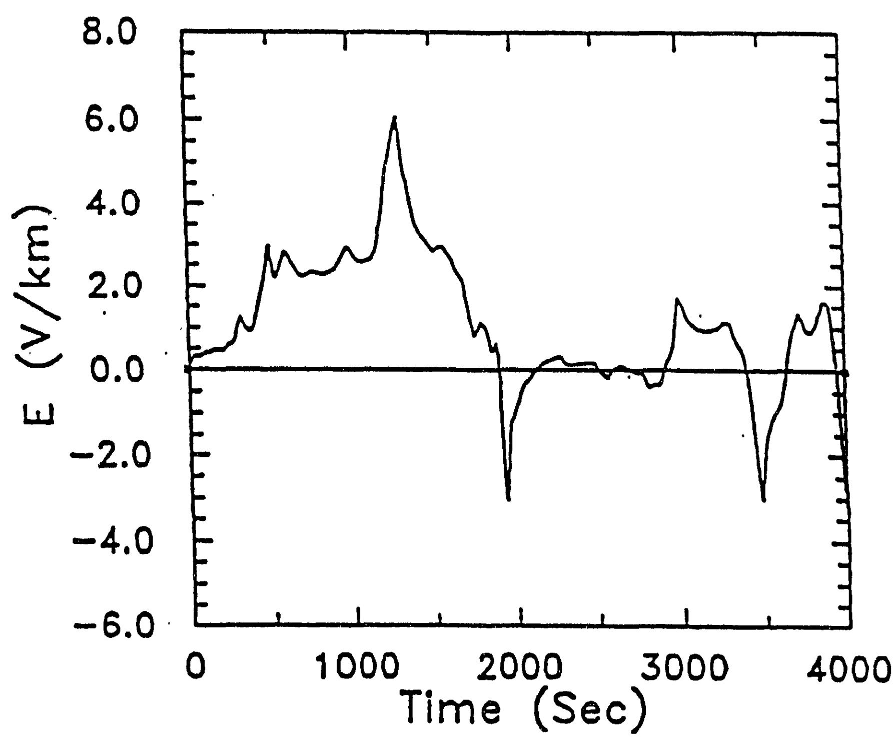

Fig. 4.1-4.Typical geomagnetic storm electric field.
Source: Document II-4.

4.2 Effect of Geomagnetically Induced Current on Power Systems

The quasi-dc current flowing in an electric power system can have serious effects. On March 13, 1989, GICs caused a complete blackout of the Quebec-Hydro system. This disturbance is discussed in detail in Document II-1b and other documents. The effects of GICs on various elements of the power system are discussed in the following:

4.2.1 Power Transformers

The flow of GIC currents has a biasing effect on the flux of power transformers and can cause partial saturation of the iron core. This is illustrated in Fig. 4.2.1-1. These currents affect transformers to different degrees depending on the winding connection, core configuration, and design details. For example, Fig. 4.1-2 shows that only wye-connected transformers or autotransformers provide a path for the GIC currents. Delta connected units therefore are not thought to be affected.

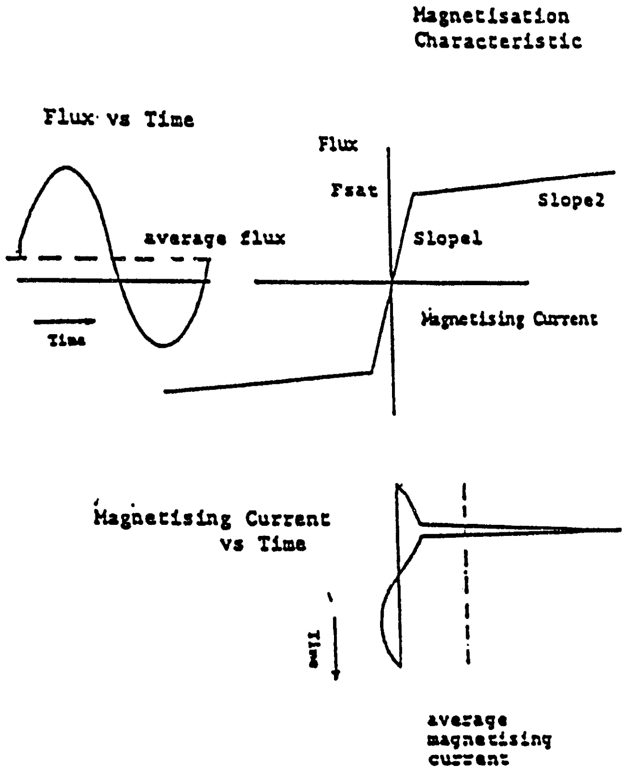

Fig. 4.2.1-1. Flux and magnetising current waveforms for a transformer in partial saturation.
Source: Document II-13.

Fig. 4.2.1-2 also shows that the currents are essentially equal in each phase; and, since they are quasi-dc, they appear as essentially zero-sequence quantities as far as the flux distribution is concerned. The core construction therefore determines the path for the flux in the units. Fig. 4.2.1-2 shows the flux paths for different types of core construction.

The single-phase shell or core form unit has equal areas of iron inside the winding and through the return path. Thus the reluctance for the flux caused by the dc currents is small and saturation can occur for relatively small values of dc. The 3-legged, 3-phase core form unit, however, has no return path for the dc flux. Its reluctance to this flux is therefore very high, and a large dc is required to cause saturation of the winding portion of the core and thus disturb the flux distribution in this area and cause overheating. Therefore, the GIC currents have little effect for these units compared with the single phase units.

The 5-legged, 3-phase core has .25 to .33 times the area of core in the return path as in the winding core area; while the return path will saturate, a larger value of dc is

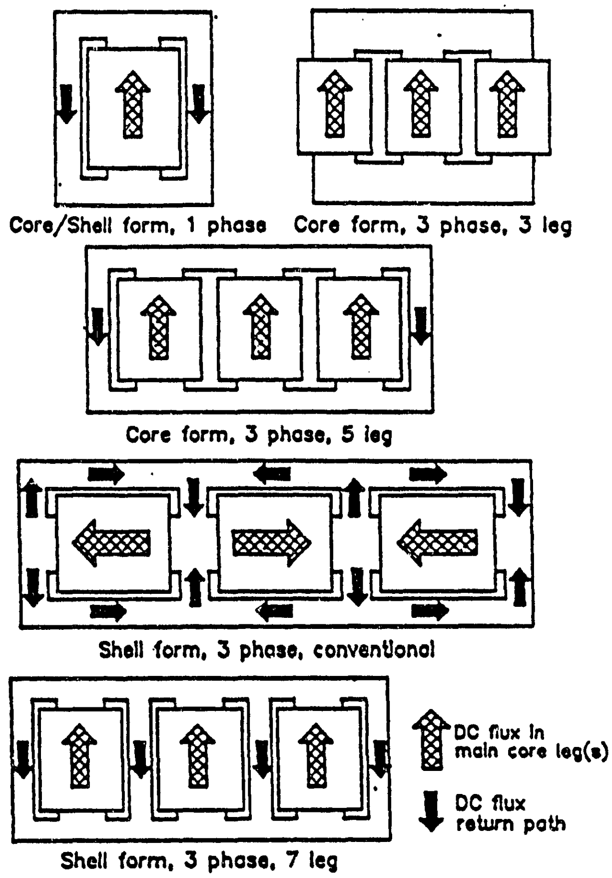

Fig. 4.2.1-2. Direct current flux path for several core arrangements.
<u>Source</u>: Document II-2c.

required to saturate the winding core area. So while it is more susceptible to GIC than the 3-legged, 3-phase core form unit, it is nowhere near as susceptible as the single-phase core or shell form units. Table 4.2.1-1 shows how the other units compare.

Another factor affecting the shell form units versus the core form units concerns the flux magnitude and direction in the winding space for normal versus saturated conditions. The flux paths in a core form unit are similar for both conditions. Therefore, since the designer has to design the conductor and circuit configurations for the normal load condition, the abnormal fluxes during saturation are not as damaging as with the shell form units. In these units the saturated flux patterns are quite a bit different from the load condition for which the unit had been designed. For example, core form units have to use continuously transposed conductors made up into a cable; no transpositions are used within the winding pancakes in the shell form units. Thus when the transformer is saturated, unanticipated circulating currents are produced in the shell units with consequential extra losses and temperature rise.

The consequences of transformer saturation are three-fold:

a) <u>Transformer Damage</u>

The abnormal flux distribution causes localized heating in parts of the windings, core, tank, leads, etc. This in turn can lead to gassing in the oil, insulation deterioration, and even failures. The seriousness of the occurrence depends on the duration of the overexcitation. The references give some idea how to determine the seriousness of the problem and the permissible duration of the saturation.

For example, the authors of Document II-7 describe a perhaps oversimplified method for estimating how long a transformer can withstand the GIC. First they calculate an equivalent exciting current

$$I_{eq} = I_{exc} + K \times I_{dc}$$

where I_{eq} is the equivalent ac root-mean-square (rms) magnetizing current,
I_{exc} is the rated rms magnetizing current,
I_{dc} is the GIC per phase,
$K = 2.8$.

Using this I_{eq} in Fig. 4.2.1-3, the authors determine an equivalent pu flux or excitation. They then use Fig. 4.2.1-4 to determine the allowable time.

Table 4.2.1-1
Relative sensitivity to geomagnetically induced current damage as measured by per unit core area available for direct current flux return.
Source: Document II-2c.

Core Configuration	Per Unit Core Area For DC Flux Return
Core or Shell Form; Single-Phase	1.00
Shell Form; 3-Phase, 7-Leg	0.67
Shell Form; 3-Phase, Conventional	0.50
Core Form; 3-Phase, 5-Leg	0.24-0.33
Core Form; 3-Phase, 3-Leg	0

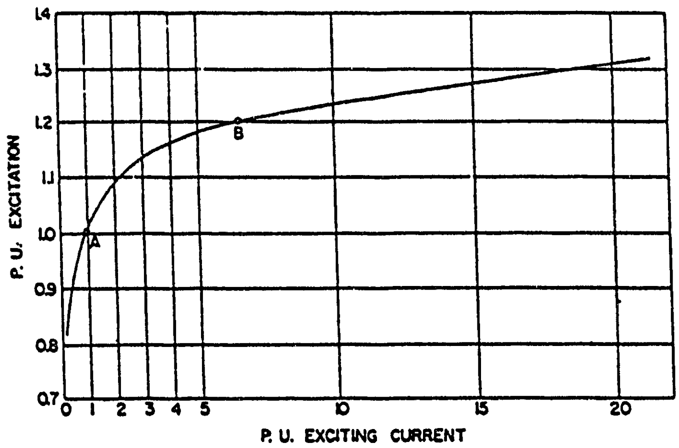

Fig. 4.2.1-3. Typical transformer alternating current saturation curve.
Source: Document II-7.

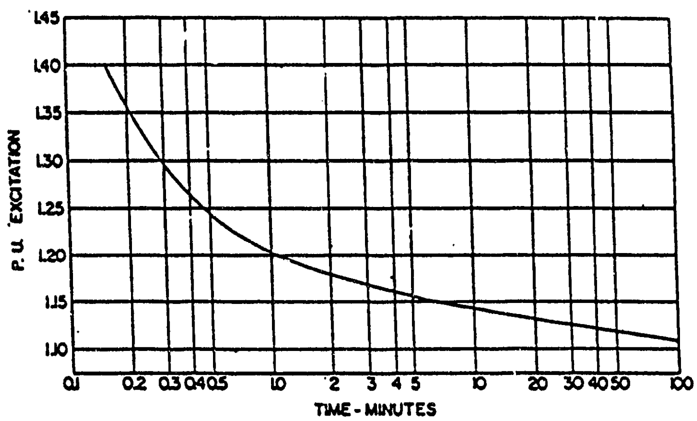

Fig. 4.2.1-4. Short time overexcitation limits of power transformers.
Source: Document II-7.

For example: With I_{exc} = 1.0 pu and I_{dc} = 2.0 pu, I_{eq} is equal to 6.6 pu. Fig. 4.2.1-3 gives 1.2 pu excitation and Fig. 4.2.1-4 shows that it can withstand this excitation for 1 minute.

As mentioned, this method seems a bit oversimplified as it does not consider the core type, design details, etc. Documents II-1, -2, -3, and -6 discuss these effects in more detail.

b) Increased System Vars

Under saturated conditions, the exciting current of the transformers become quite high. Fig. 4.2.1-5 shows the normal magnetizing current for a wye-delta stepup bank and Fig. 4.2.1-6 shows the current when 60 A of dc are inserted in the wye winding. Note that the peak current increased from approximately 165 A to almost 7000 A.

Since the transformer exciting current is in phase with the transformer flux which in turn lags the applied voltage by 90°, the increased magnetizing current due to saturation appears as lagging vars to the system. Multiplying the above equation for I_{eq} by $\sqrt{3}$ times system voltage gives the equivalent var drain on the system due to the saturated transformer. As discussed below, this var drain can cause low system voltage, unusual MW and Mvar swings, and problems with generator var limits and could cause system shutdowns.

c) Harmonics:

Fig. 4.2.1-6 is an idealized current for a saturated single-phase transformer. Fig. 4.2.1-7 shows the waves for the three exciting currents of a certain three-phase bank showing the effect of the coupling between the different phase windings. Note that in both cases, however, the currents are rich in even and odd harmonics. Fig. 4.2.1-8 shows the harmonic components for different values of GIC in the windings. Table 4.2.1-2 shows the pu harmonic currents for a GIC of 4.8% of rated load in a transformer.

These harmonics generated by the transformers can cause overloading of capacitor banks, possible misoperation of relays, sustained overvoltages on lines, higher secondary arc currents during single-pole switching, higher circuit breaker transient recovery voltages (TRVs), overload of harmonic filters on high voltage direct current (HVDC) terminals, and other effects discussed in the following section.

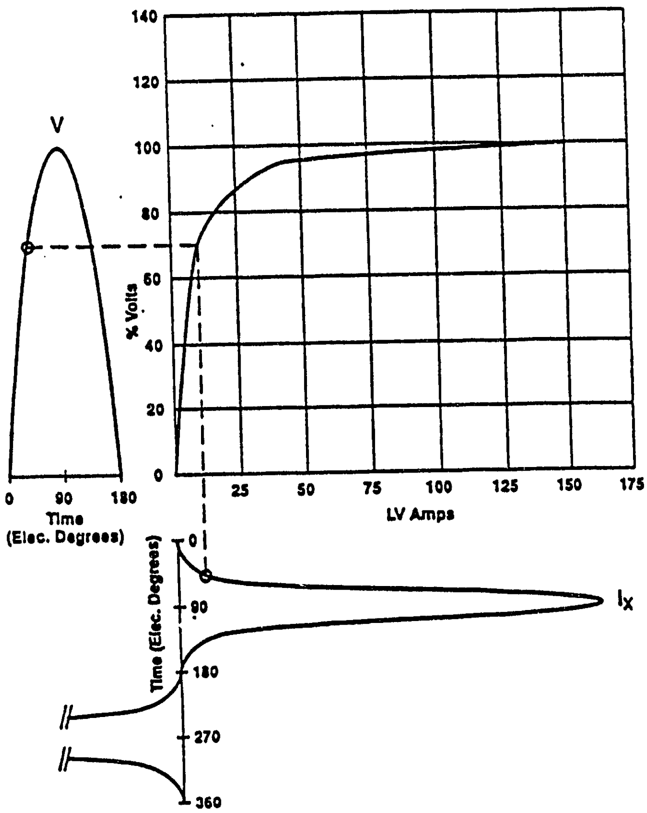

Fig. 4.2.1-5. Alternating current magnetization characteristic for Public Service Electric and Gas Salem generator stepup unit transformer.
Source: Document II-2c.

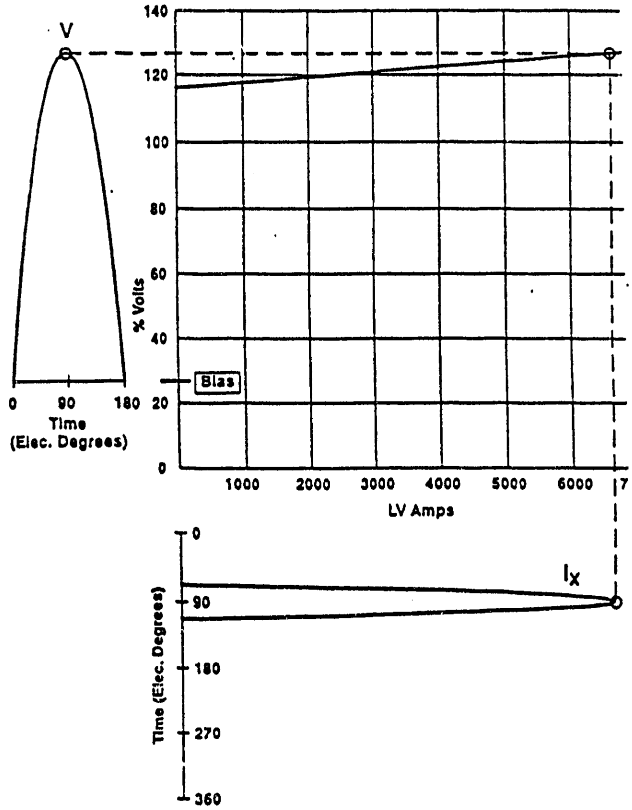

Fig. 4.2.1-6. Magnetization characteristic for Public Service Electric and Gas Salem generator stepup unit transformer with 60 A direct current in the high voltage winding.
Source: Document II-2c.

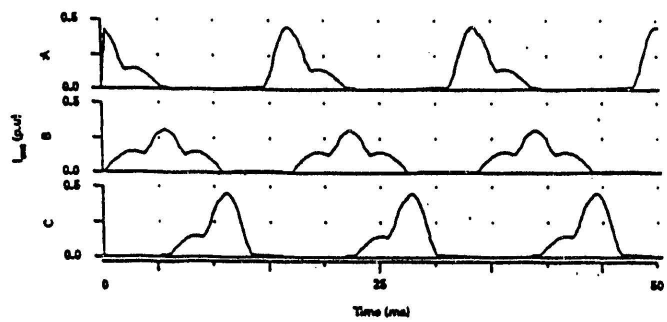

Fig. 4.2.1-7. Phase exciting-currents of 5-leg, core-form transformer with .1 per unit geomagnetically induced current.
Source: Document II-5.

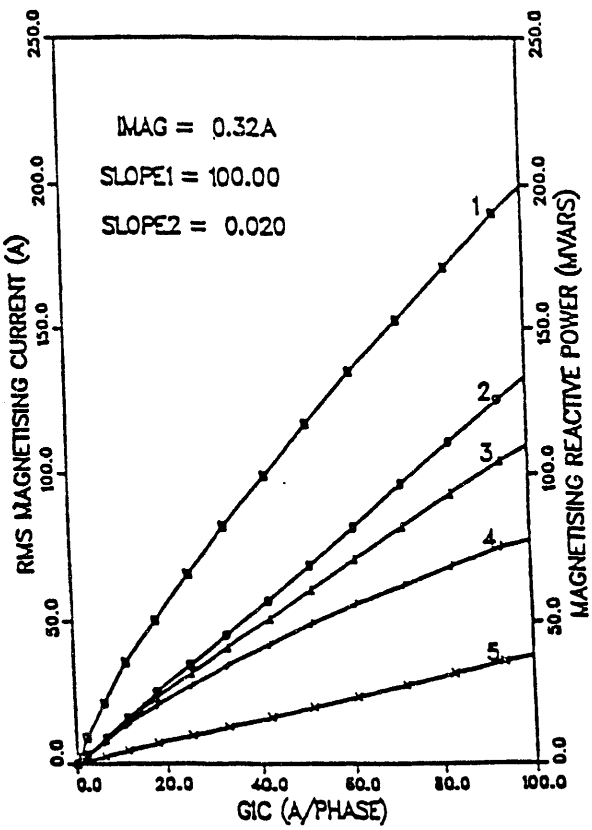

Fig. 4.2.1-8. Model calculations of the effects of geomagnetically induced current on transformer T4 at Williston showing the relation between: (1) total magnetising current, (2) 60-Hz harmonic current, (3) 120-Hz harmonic current, (4) 180-Hz harmonic current, (5) reactive power demand, and the magnitude of geomagnetically induced current.
Source: Document II-13.

Table 4.2.1-2
Per unit harmonic composition of magnetizing current for geomagnetically induced current equal to 4.8% of rated load current in the high voltage winding.
Source: Document II-2c.

Harmonic						
1st	2nd	3rd	4th	5th	6th	7th
.067	.062	.054	.044	.033	.019	.009

4.2.2 Instrument Transformers

The direct effect of GICs on voltage transformers (VTs) is minimal. There will be some increase in the harmonic contents of the secondary signal from VTs, but these will be the result of the primary voltage becoming distorted from power transformer saturation. The distortion from dc bias within the VTs will be negligible with respect to the fundamental. The capacitors in a capacitor voltage transformer (CVT) will block any effect of the dc on their output. The ferroresonance and transformer circuits in the secondary of the CVT will alter the harmonic content of the transformer primary signal (normally thought to be in the direction of suppressing the harmonics).

The GICs can cause saturation in the current transformers, resulting in errors in the secondary currents and additional harmonics impressed on the relays. Fig. 4.2.2-1 is an example of these errors. The extent of these errors depends on the burden and winding ratio used. Fig. 4.2.2-2 shows that using the full winding, the flux excursion in the ct is only from A_1 to A_2; the result is very little error. Using only the partial winding (the 100:1 tap) of this same ct, the flux excursion is now from D_1 to D_2 with a much greater error.

Normal interruption of the primary current with a GIC superimposed on the load current could result in a large trapped flux or remanence flux in the CT. Table 4.2.2-1 shows this remanence flux versus GIC for a representative CT. This remanence flux reduces the time to saturation of the CT, which can affect the relay performance.

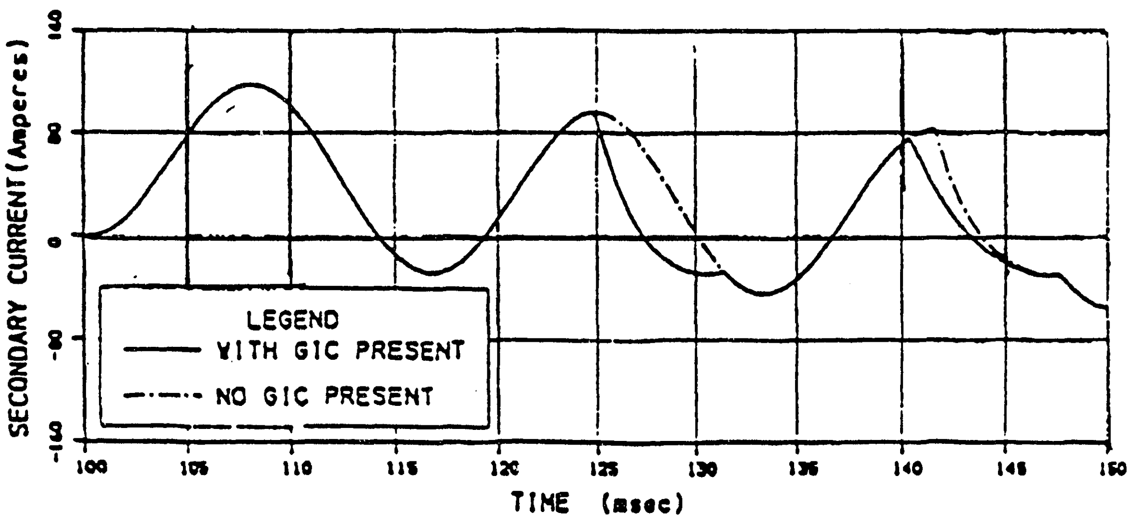

Fig. 4.2.2-1. Calculated current transformer secondary current with and without geomagnetically induced current.
Source: Document II-2b.

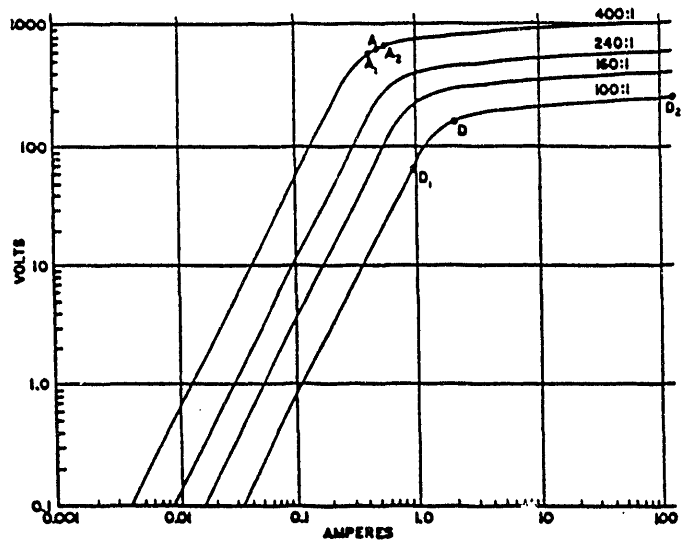

Fig. 4.2.2-2. Current transformer secondary saturation characteristic.
Source: Document II-1f.

Table 4.2.2-1
Percent current transformer remanent flux vs. geomagnetically induced current. Current transformer ratio 400:1. Standard burden 1.0 + j1.73 ohms.
Source: Document II-11.

GIC Primary Amps. Per Phase	Percent Remanent Flux
50	17.4
100	44.4
200	74.8
300	75.6
400	77.8

4.2.3 Protective Relaying

While the GIC currents themselves do not affect the power system relays, the saturation of the power and instrument transformers has a marked effect. For example, the harmonics generated by these devices appear as sequence quantities to the relays and other elements of the system. For example:

Positive Sequence	1, 4, 7, 10 -- harmonics
Negative Sequence	2, 5, 8, 11 -- harmonics
Zero Sequence	3, 6, 9, 12 -- harmonics

These can affect the protection of the various system elements.

a) Transformer Protection

The large increase in exciting current due to the GIC appears as an internal fault to the old CA-type differential relays and they could operate falsely. The newer HU-type harmonic restraint relays would be restrained by the harmonics generated by the saturated condition so that they would not trip falsely. There is some concern that these harmonics would prevent tripping on a transformer internal fault; but it is felt that should a fault occur, the harmonic components would be swamped out by the fault current. If this should become a problem, it has been suggested that the relay should base its percentage of harmonics on the through currents and not on the operating current.

Some method of detection of GICs and protection of transformers against them is desired. Protection against overheating could be accomplished by (a) Bucholz gas accumulation relay, (b) some means of overflux measurement, or (c) neutral current.

b) Capacitor Protection

Since a large amount of third harmonic currents could be generated by nearby saturated transformers, the simple neutral current capacitor bank unbalance protection schemes can trip falsely. Those schemes compensated by system voltage measurement will not trip. Only grounded capacitors are affected because they provide a path for the triple harmonics.

Capacitors *can fail* because of excessive harmonics. Protection against this condition is difficult, if not impossible.

The capacitor banks in static var generators (SVGs) and filter banks for SVGs and HVDC installations are also subject to these protection problems.

c) Line Protection

As mentioned above, the second and third harmonic currents appear as negative and zero sequence (I_2 and I_0) currents. Harmonic filters should therefore be used on I_2 and I_0 relays.

Unequal saturation of power transformers could cause ground relay tripping. The I_0 setting would have to be < 5% of load current, however.

Distance relays could reach further through transformers because of reduced leakage reactances.

Current differential systems could operate falsely because of unequal saturation of CTs.

Pilot systems could be affected by communication problems (see Sect. 4.2.4 below).

d) Generator Protection

Generator step-up transformers generate harmonics when subjected to GICs. These harmonics will flow both out on the system and back into the generator. Generator rotor heating due to harmonics is similar to heating due to negative sequence currents. This heating is proportional to the square root of the harmonic. (Example: 4% 7th harmonic equivalent to 10% I_2.) Older I_2 relays can trip falsely, but newer relays that contain bandpass filters will not. New relays to protect against generator overheating due to these harmonics may be needed.

4.2.4 Communications

In addition to causing GICs, geomagnetic storms cause atmospheric disturbances that can interfere with long-haul high frequency (HF) communications just at the time when these communications are required for GIC mitigation. Microwave systems are generally not affected since they are not subject to solar fading.

Some HF radio signals fade out, while others interfere from long distances. The disturbed ionosphere causes very high frequency (VHF) anomalies, such as long-distance bounces of the ionosphere. This could affect utility load control, sectionalizing, or distribution automation systems if such systems were employed.

Satellites are also affected by tumbling. If utilities use them for monitoring and control, they should be aware of potential problems.

Wire-based communications are affected, as are power lines. Induced voltages as high as 7 V/km can occur (from the effects of solar storms). Carbon blocks can arc over and fail, and 60 Hz power to repeaters can be affected.

Fiber optic cables are unaffected by geomagnetic storms, but repeater power supplies could be affected. Local power or fiber systems not requiring repeaters should be used.

Power line carriers can have a decrease in the S/N ratio due to low frequency and harmonic related noise.

4.2.5 Other System Effects

Section 4.2.1 discussed the increased var demand caused by the saturated transformers. This increased var demand can cause a severe decrease in system voltage. Table 4.2.5-1 shows the results of a study of var demand due to GIC in the Manitoba Hydro-Minnesota Power & Light-Northern States Power intertie (see Document II-10). The lower voltages shown caused increased generator var output--sometimes up to the generator limits--decreases in total system generation, decreases in total system load, changes in system losses, and reduced tie line transfer capabilities.

Table 4.2.5-1
Examples of estimated voltage droop due to geomagnetically induced current based on summer 1980 load flow.
Source: Document II-10.

			BUS VOLTAGE (PER UNIT)				
Location	kV	Company	No GIC	GIC CASE 1	GIC CASE 2	GIC CASE 3	GIC CASE 4
Dorsey	500	MHEB	.98	.92	.85	.93	.87
Forbes	500	MP&L	.92	.82	.80	.86	.81
Chisago	500	NSP	.95	.88	.86	.90	.85
Red Rock	345	NSP	1.00	.97	.95	.97	.93
A.S. King	345	NSP	1.00	.96	.95	.97	.92
Roblin	230	MHEB	.99	.78	.78	.92	.79
Shannon	230	MP&L	1.00	.94	.92	.96	.93
Blackberry	230	MP&L	1.02	.97	.95	.97	.95
Arrowhead	230	MP&L	1.00	.94	.91	.95	.91
Budoura	230	MP&L	1.05	.98	.89	.93	.95
Long Prarie	115	MP&L	1.01	.95	.86	.89	.92
Scott Co.	115	NSP	.96	.91	.89	.91	.85

Energizing a long line in the presence of GIC can result in sustained overvoltages that exceed the line and equipment ratings.

The secondary arc currents during single-pole switching exhibit a high harmonic content and as much as a ten-fold increase in magnitude, which reduces the probability of a successful reclosure.

Circuit breaker recovery voltages can be higher. During switching of an unloaded transformer or a reactor, no current zero may exist, which can result in current chopping.

High harmonic currents produced by the saturated transformers can overload the harmonic filters of HVDC terminals, and the distortion of the ac voltage may result in a loss of the dc terminal altogether.

The simultaneous presence of ac and dc in distribution fuses may affect their coordination, although the dc currents will probably be so small as to have little effect.

4.3 Geomagnetically Induced Current Mitigation Measures

To prevent the GIC from affecting the power system, various mitigation measures have been discussed. They include the following:

4.3.1 Polarizing Cells

These devices pass ac and block dc up to 1.8 V/cell. Above the 1.8 V the cell again passes dc. This low blocking voltage requires too many cells in series to make this a practical solution.

4.3.2 Linear Resistor

Resistors in the neutral of transformers have been considered but some studies (Document II-21) have shown that relatively high ohmic values, up to 500 Ω, are required for blocking. This high resistance produces a transformer neutral voltage and resistor losses that are too high for normal steady-state unbalance currents.

4.3.3 Nonlinear Resistor (MOV)

Too many units are required to handle the energy dissipation during line to ground (L-G) faults. Therefore the cost is too high for this application.

4.3.4 Active Direct Current Device

This device would measure the line and neutral GIC and insert a dc into a broken delta tertiary. An ac pass filter is required across the break in the delta for normal unbalanced currents. This scheme is more complex and costly than a neutral capacitor. Also, it could not be used at all locations since not all tertiaries can be broken. In addition, it does not block dc from a system; it merely nullifies the effect of the dc on one transformer.

4.3.5 Neutral Capacitors

The neutral capacitor is one of the most effective and economical devices. It has problems, however. For example, it can block neutral currents but not series winding currents in autotransformers. A system study showed that finding the correct neutrals to block was a problem. Also, the capacitor must be bypassed during faults. It can cause ferroresonance problems, so it requires a high-speed bypass device. Also, relay problems could be caused by the capacitor's affecting the apparent impedance to the fault. Transients due to shorting of the capacitor can influence the relay. The fault contribution from the far end of the line can also be affected.

Document II-2d describes a device installed in the neutral of a power transformer to block the quasi-dc GICs. The specifications for this device are that

- it offers low impedance to ac;
- it offers high impedance to dc;
- it allows 50 A ac continuous (a Minnesota Power requirement);
- it have maximum dc voltage of 4 kV (another Minnesota Power requirement);
- it carry 10 kA for 10 cycles; and
- it not overstress the transformer neutral insulation.

The device developed by the authors of Document II-2d is shown in Fig. 4.3.5-1.

<u>Capacitor module:</u>	four 300 kvar 7.2 kV capacitors ($61.4\ \mu F$--$43.2\ \Omega$ 60 Hz).
<u>Spark gap module:</u>	14 kV rms setting (16 kV minimum--24 kV maximum sparkover) Time ≈ 1 msec. Gap used instead of MOV because of high energy.

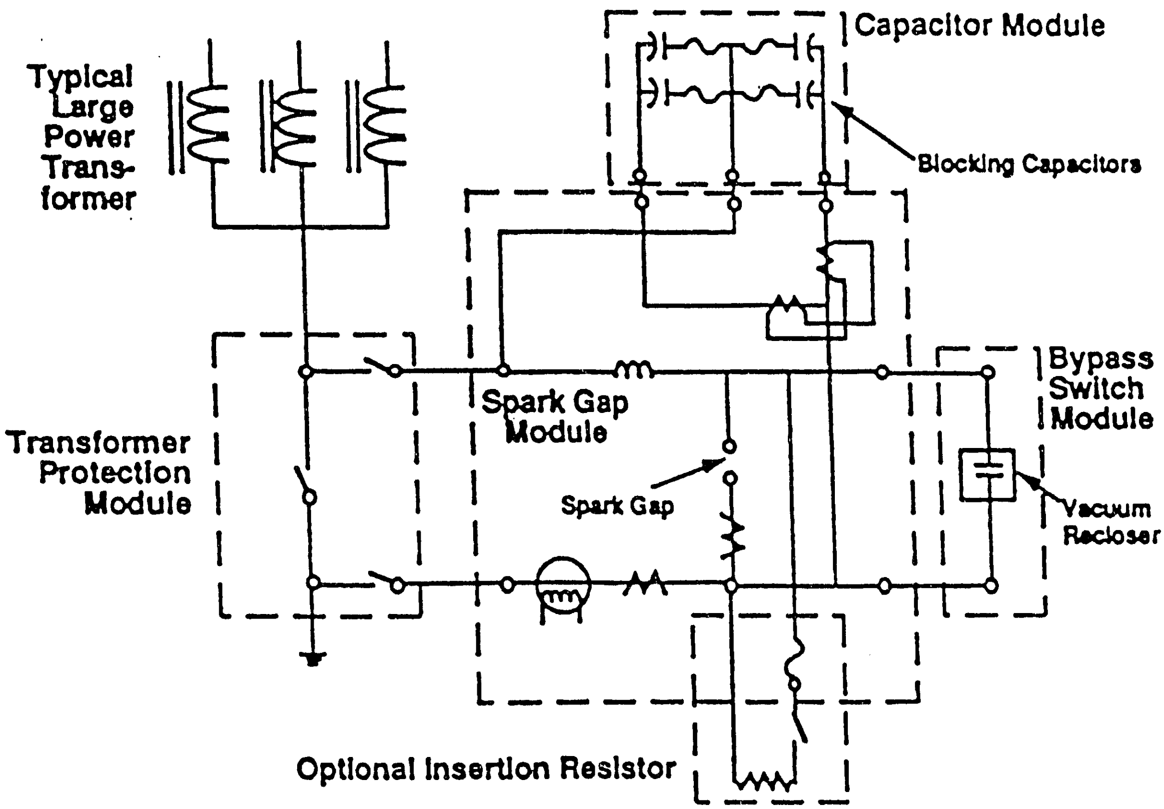

Fig. 4.3.5-1. Schematic for neutral blocking/bypass device.
Source: Document II-2d.

Bypass switch module:

Vacuum circuit breaker.
Normally closed but opened by supervisory control when GIC is predicted.

Transformer protection module:

Manual bypass for maintenance.

Insertion resistor module:

Optional. Maybe required when inserting capacitor to prevent overvoltages that trigger gap.

While the prototype of this device is not large relative to major power transformers, there still may be major space constraints in trying to use it as a retrofit in many existing substations. The estimated installed cost is in the neighborhood of 10% of the transformer's cost. Without dramatic proof of harmful effects to transformers from GIC, the industry will not embrace such cost increases.

4.3.6 Series Capacitors

The installation of series capacitors in the transmission lines overcomes the objection that the neutral capacitors do not block the currents in the series windings of the autotransformers. Series capacitors also improve the power transmission capabilities of the system in addition to their quasi-dc blocking ability. Unfortunately, their cost is prohibitive unless they are required for other than dc blocking reasons.

4.4 E_3 Characteristics

The wave shape of the E_3 pulse depends on the location of the observer or system with respect to the X-ray patch under the nuclear burst. The wave shape for a point just outside the X-ray patch has a high magnitude but a relatively short duration. For an observer directly under the patch, the wave has a lower magnitude but a longer duration. This wave is shown on Fig. 4.4-1. Note that this wave is normalized by a factor E_{max}, the value of which depends on many factors, including the burst yield and other parameters, the exact observer location, and the earth's conductivity.

Figs. 4.4-2, -3, and -4 show the results of a study, described in Document II-17, of the currents induced in three classes of representative transmission, subtransmission, and distribution lines for these waves. The values are given as I_c/E_0, so the values

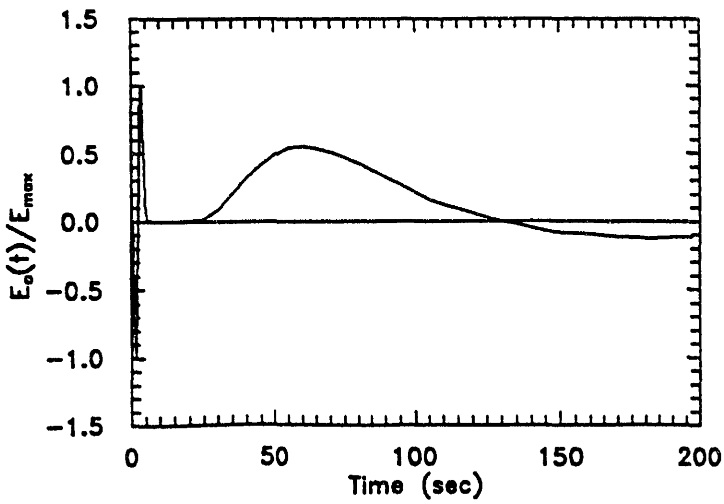

Fig. 4.4-1. Normalized composite magnetohydrodynamic electromagnetic pulse electric field.
Source: Document II-17.

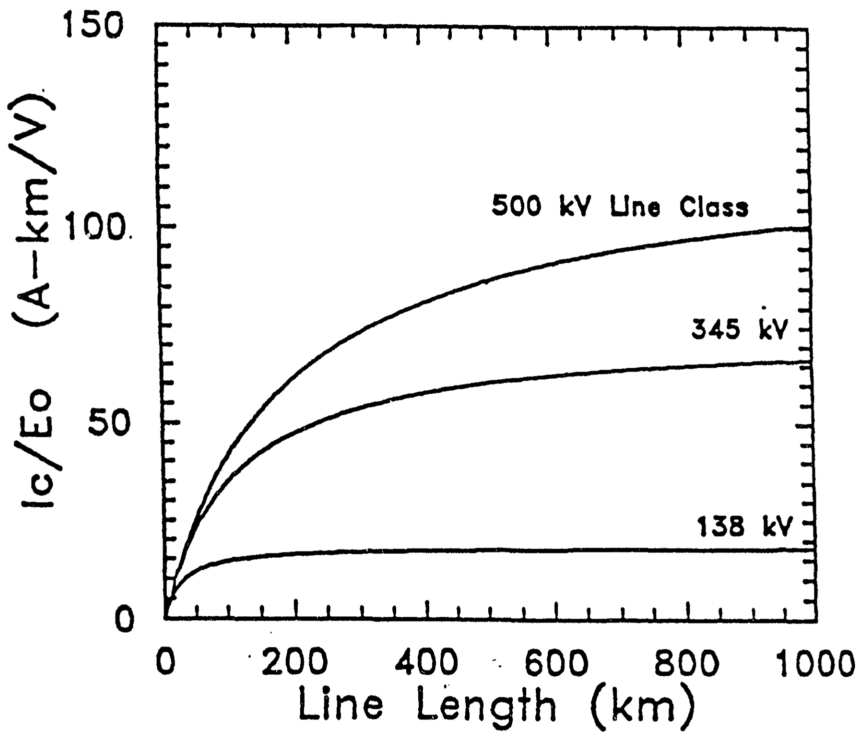

Fig. 4.4-2. Magnetohydrodynamic electromagnetic pulse-induced current for transmission lines (case 1).
Source: Document II-17.

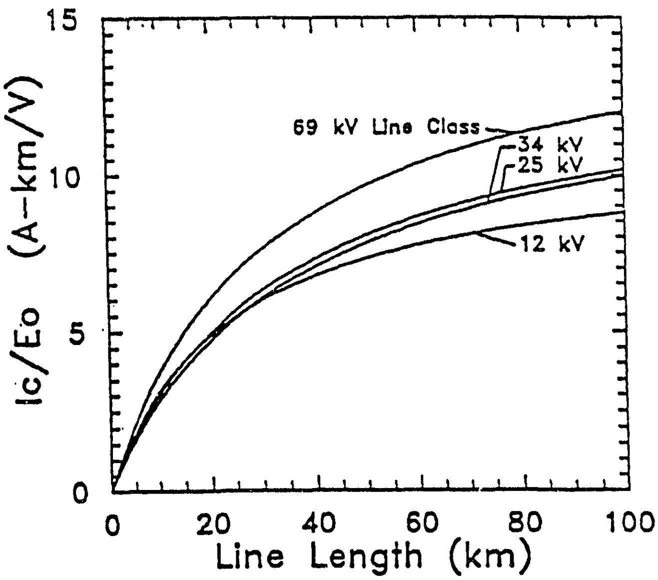

Fig. 4.4-3. Magnetohydrodynamic electromagnetic pulse-induced current for subtransmission and distribution lines (case 2 - substation grounding).
Source: Document II-17.

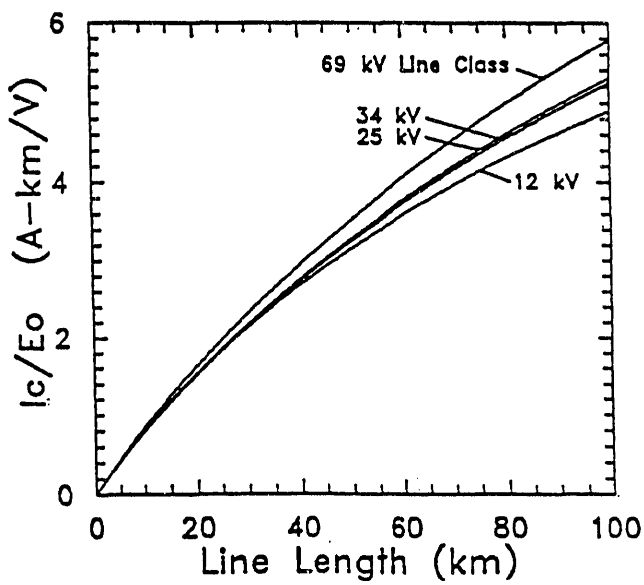

Fig. 4.4-4. Magnetohydrodynamic electromagnetic pulse-induced current for subtransmission and distribution lines (case 3 - stake grounding at one end and substation grounding at the other).
Source: Document II-17.

from these curves should be used to multiply the wave shape of Fig. 4.4-1. These values are for unshielded lines. Similar calculations were made for shielded lines. Note that overhead ground wires generally decrease the induced currents.

Fig. 4.4-5(a) shows another version (from Document II-4) of the wave shape of the MHD-EMP E-field. Fig. 4.4-5 (b) is the shape of a geomagnetic storm E-field wave from the same document. Note that this is the same wave shown on Fig. 4.1-4. Fig. 4.4-6 is the frequency spectra of both fields. While the relative magnitudes are not shown, the E_3 field can be larger (possibly approaching 10 times larger) than the geomagnetic disturbance (GMD) field (10 V/km for the March 13, 1989 disturbance) but much shorter in duration (tens to hundreds of seconds versus hours). The frequency spectra in Fig. 4.4-6 show that both are quasi-dc phenomena.

Most recorded waves from geomagnetic storms are of long duration, as shown in Fig. 4.4-5(b). Fig. 4.4-7 shows the measured E-field components from an October 28, 1991, storm. Fig. 4.4-8 shows a comparison of this waveform with that of Fig. 4.4-1. The similarity is striking. It should be noted that the October storm caused a

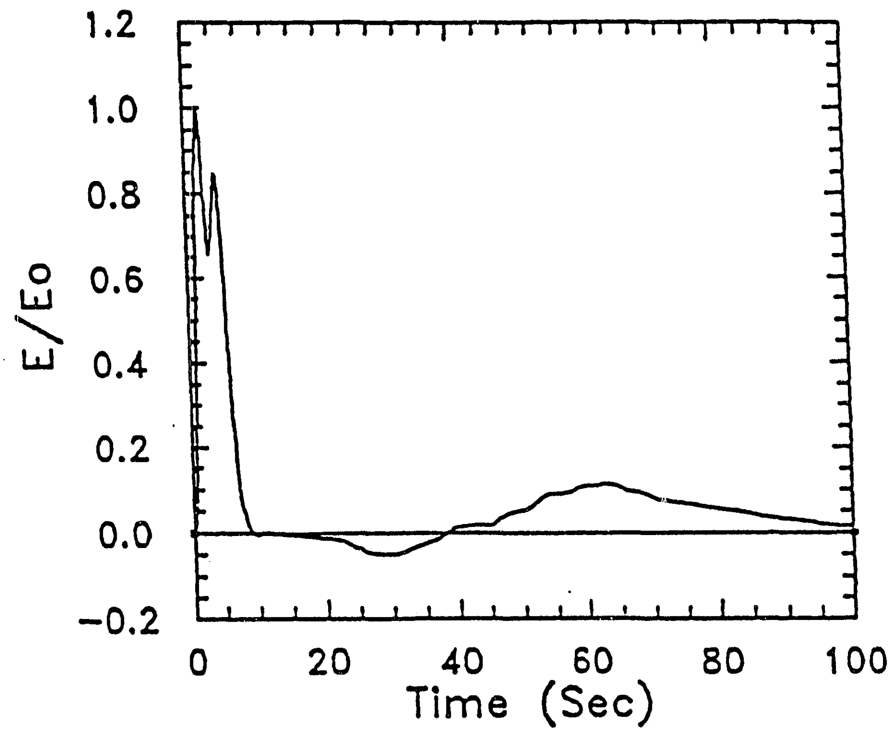

Fig. 4.4-5 (a). Normalized worst-case magnetohydrodynamic electromagnetic pulse electric field.
Source: Document II-4.

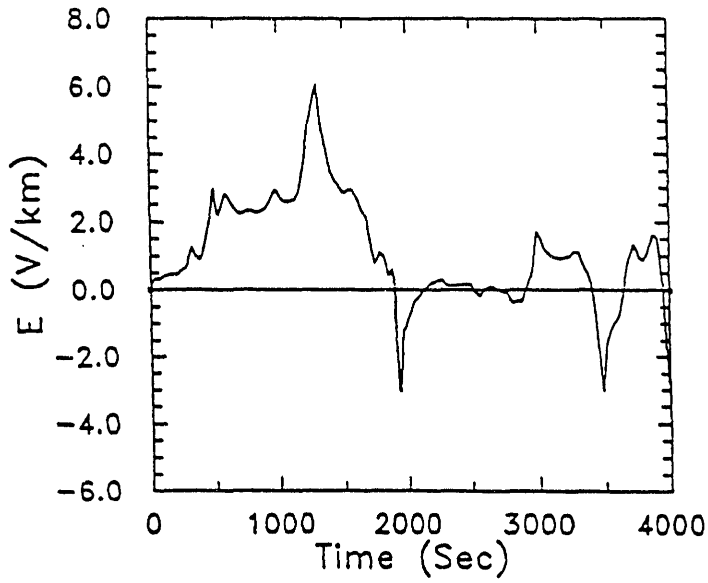

Fig. 4.4-5 (b). Typical geomagnetic storm electric field.
Source: Document II-4.

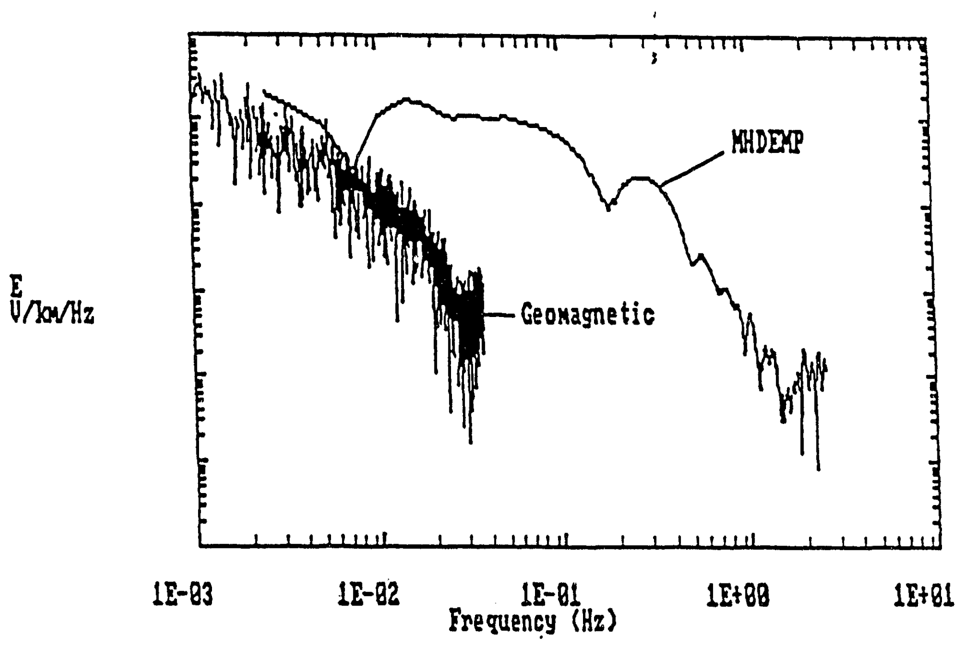

Fig. 4.4-6. Comparison of the spectra of the magnetohydrodynamic electromagnetic pulse field and the geomagnetic storm electric field.
Source: Document II-4.

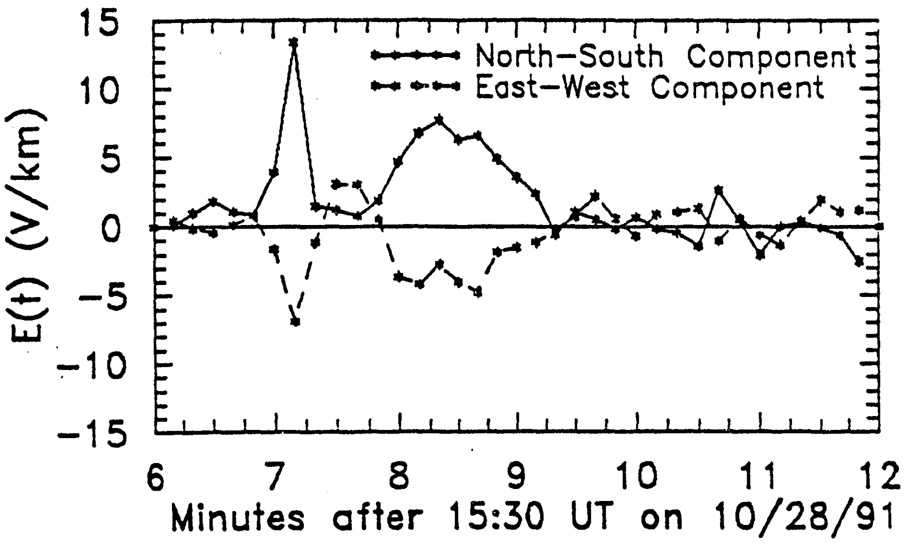

Fig. 4.4-7. Computed electric field components for October 28, 1991.
Source: Document II-17.

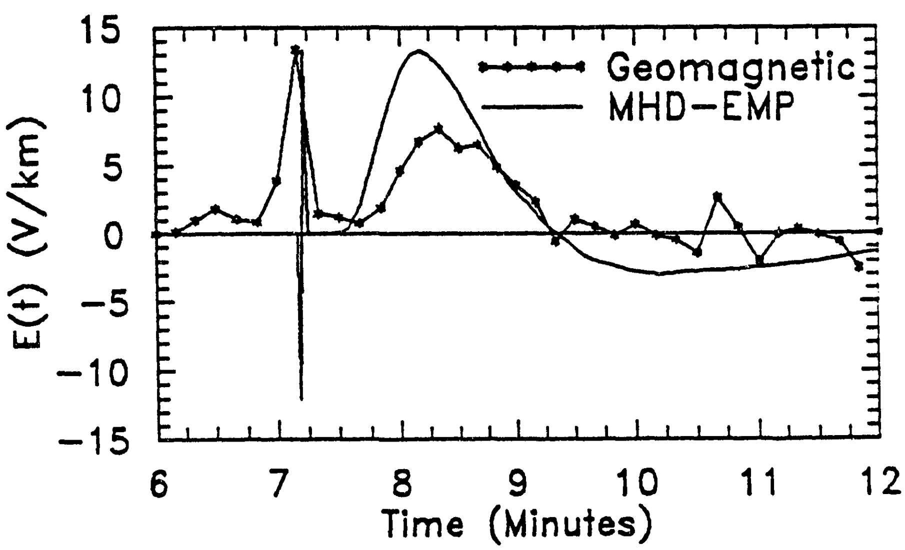

Fig. 4.4-8. Comparison of magnetohydrodynamic electromagnetic pulse with geomagnetic storm electric field waveforms.
Source: Document II-17.

number of power system problems. Therefore, we now have hard evidence of the ability of the E_3 MHD-EMP wave to cause significant system upset.

4.5 Effect of E_3 on Power Systems

While the E_3 magnitudes are larger than GIC, the difference in duration, as shown in Fig. 4.4-5, raised questions whether the power system would be affected by the two types of current to the same extent. For example, most of the serious consequences of the GIC are due to transformer saturation. Would the duration of the E_3 pulse be long enough to cause transformer saturation?

Fig 4.5-1 shows the results of a study in which a current of 100 A dc was injected into the neutral of a 600-MVA 500/230-kV bank of single phase transformers. The study showed that the time-to-saturation for the transformer was 20 s after current injection.

Fig. 4.5-2 shows the results of another study on a 1100 Mva 115/500 kva two-winding step-up transformer showing the effect of loading on saturation for a 20 V/km simulated E_3 wave. With the transformer operating at no load, it would take a 50 s wave to cause saturation; for a fully loaded transformer, however, a 5 s wave would cause saturation. A 60-V/km disturbance would drive the transformer into saturation in 3 s. If these results are representative, transmission systems could be affected by E_3 disturbances.

Table 4.5-1 shows the extent of the system upsets at Minnesota Power's Forbes substation caused by the October 28, 1991, geomagnetic storm. Fig. 4.5-3 shows a recording made by the Electric Power Research Institute's SUNBURST network on October 28. This figure shows the GIC in the neutral of an autotransformer in New Jersey. The sample period was every 5 s. It can be seen that this GIC matches almost perfectly with the predicted E_3 wave shape. The system impacts reported in Table 4.5-1 were almost certainly a result of the sudden and massive harmonic flow generated by widespread transformer saturation.

Document II-17 describes a parametric study on a Minnesota Power Company 500-kV transmission line terminated at each end with 1050-Mva 500/115-kV grounded wye-delta transformers. The wave shape of Fig. 4.5-4 was used as the energizing quantity. This curve was normalized to have a peak value of 1 V/km and then was varied according to Table 4.5-2 for the parametric study. Table 4.5-3 shows the range of other constants used as variables in this study.

Fig. 4.5-5 (a), (b) and (c) show the maximum magnetizing current for the "early time" waves. Because of the low current levels the transformer did not saturate for most of these conditions. Fig. 4.5-6 (a), (b) and (c) shows the maximum magnetizing current for the "late time" waves. Here the transformer does saturate, and

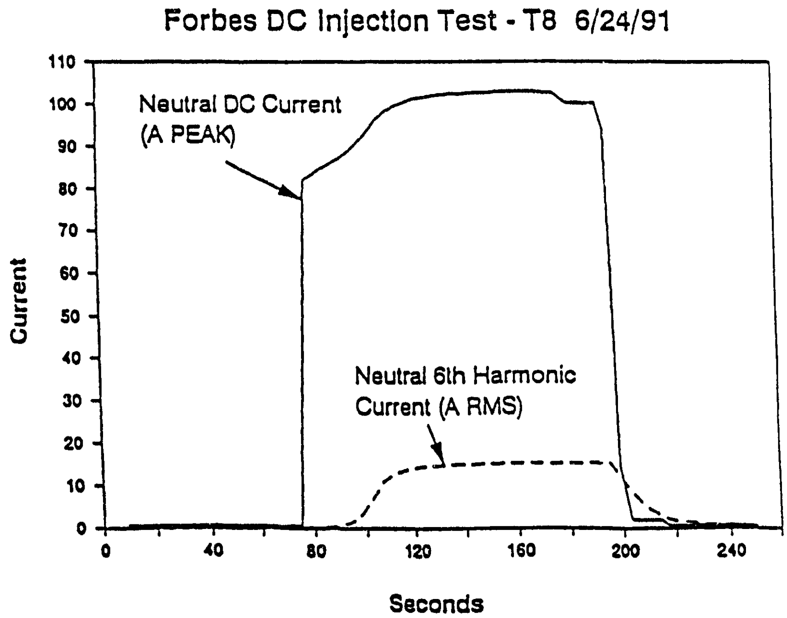

The time-to-saturation response of a transformer to DC current has been an issue of discussion. This test shows that the transformer went into saturation within 20 seconds of the application of DC current

Fig. 4.5-1. Forbes direct current injection test - T8, June 24, 1991.
Source: Document II-3d.

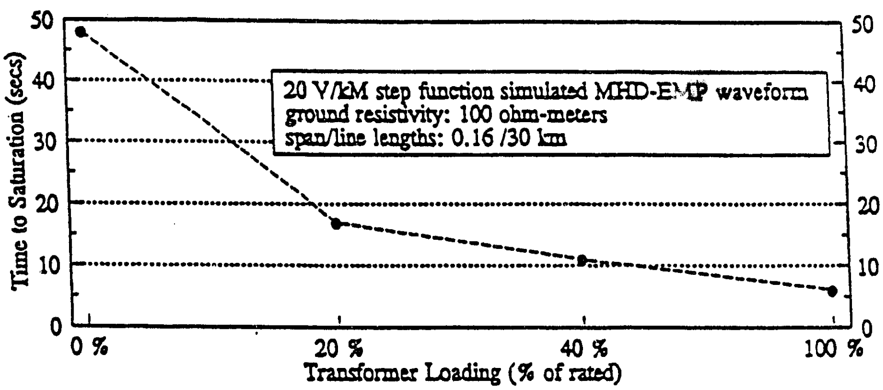

Source: P. R. Barnes et. al., MHD-EMP Interaction with Power Transmission and Distribution Systems, ORNL/Sub/90-SG828U/1 (to be published).

Fig. 4.5-2. Time to saturation as a function of transformer loading for a 1100 MVA 115/500 kV three-phase delta/grounded-wye connected power transformer consisting of 115/288 kV single phase transformers.
Source: Document II-18.

Table 4.5-1
System upsets caused by October 28 geomagnetic storms.
Source: Document II-20]

BPA	At 0737 PST October 28, 1991, shunt capacitors started tripping and continued to trip until 0739 PST at Chemwa, Keeler, Tillamook, Ross, Bandon, McMinnville, Alvey, Cosmopolis, and Long View Substations. Operators reported "strange" transformer noises at Keeler and Peal Substations. Also there was a report of transformer noise at Portland General Electric's Boardman Generation Plant.
SCE	At 0737 PST October 28, 1991, the 550 kV transmission system voltage dropped from 530-535 kV to 518-524 kV. It recovered within three minutes.
	At 0801 PST October 28, 1991, the 550 kV transmission system voltage again dropped from 530-535 kV to 522-526 kV. It recovered within three minutes.
	Also a fault recorder triggered an abnormal neutral current at the Serrano 230/550 kV substation which is located southeast of Los Angeles. Off line analysis indicated the neutral current magnitude was between 150 and 200 amperes and principally third harmonic current with 32% 6th harmonic current. Phase A current evaluation revealed strong 2nd and 4th harmonic currents, 1.7% and 1.0% respectively, of the banks rating.
NMPS	At 0838 MST October 28, 1991, the ac-dc-ac back-to-back tie at Blackwater went off line.
NEPSCo	At 1037 EST October 28, 1991, the New England Hydro Phase II dc tie with Hydro Quebec tripped.
PSE&G	At 2257 EST October 28, 1991, the Salem Unit was backed off to 80%.
APS	At 1050 EST October 28, 1991, Allegheny Power System SCADA armed the capacitor bank trip restraint and enabled the Meadowbrook transformer gas detector trip. No capacitor banks tripped in the minutes before the restraint was initiated.
	At 2259 EST October 28, 1991, The T4 transformers at Meadowbrook tripped on gas detection.
	At 2316 October, 1991, APS removed T2 at Meadowbrook per operating procedures.
WEPCo	Reported transformer growling at approximately 0930 CST October 28, 1991 at its Point Beach Power Plant.
VEPCo	At 1041 EST October 28, 1991, 230 kV - 100 MVAR capacitor bank at Chuckatuck tripped due to neutral unbalance.
	At 1041 EST October 28, 1991, 230 kV - 150 MVAR capacitor bank at Dooms tripped due to neutral unbalance.
	At 1102 EST October 28, 1991, 115 kV - 25 MVAR capacitor bank at Staunton tripped due to neutral unbalance.
PJM	At 0128 EST, October 29, 1991, PJM solar storm operating procedure was put in place.

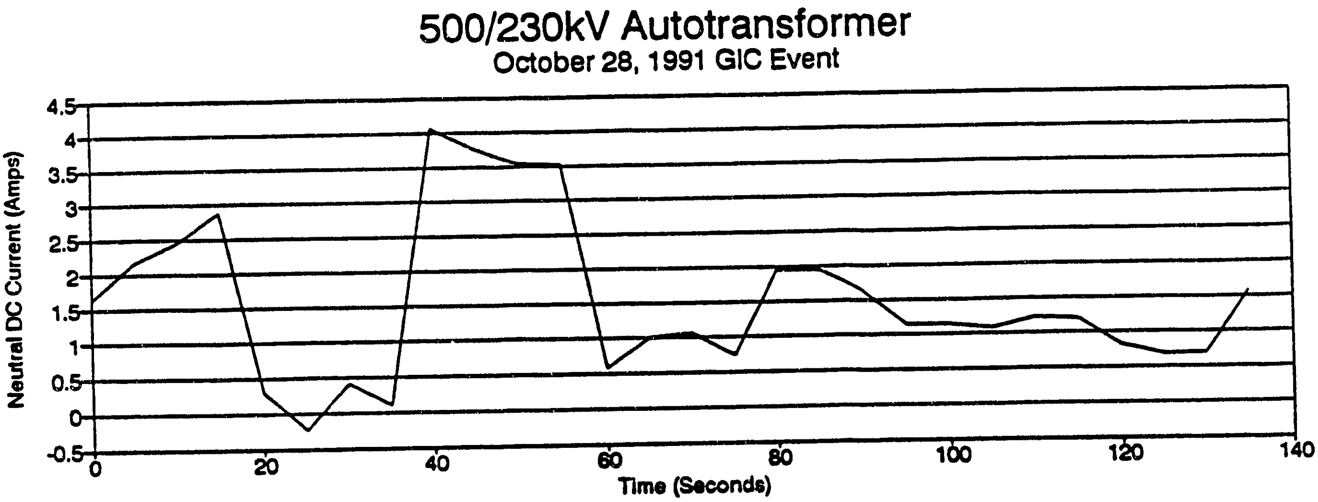

Fig. 4.5-3. Geomagnetically induced current in neutral of autotransformer.
Source: Document II-20.

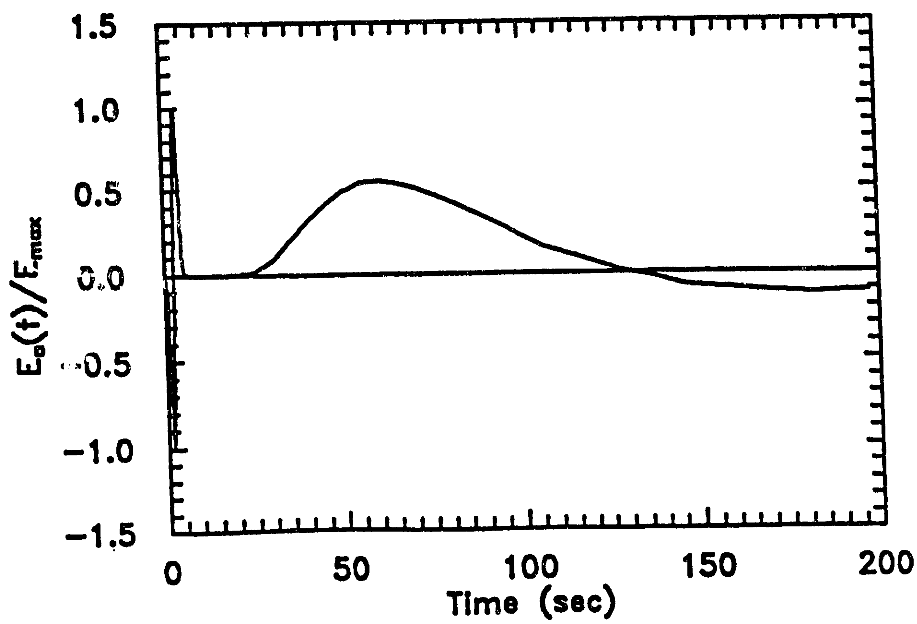

Fig. 4.5-4. Normalized composite magnetohydrodynamic electromagnetic pulse electric field.
Source: Document II-17.

Table 4.5-2
Peak magnetohydrodynamic electromagnetic pulse electric fields used in parametric study.
Source: Document II-17.

Early Time Waveform Amplitude (Volts/km)	Late Time Waveform Amplitude (Volts/km)
10	10
20	20
60	40
120	80
300	180
500	300

Table 4.5-3
Line and ground constants used in parametric study.
Source: Document II-17.

Soil Resistivity	100						Ω–m
Tower Footing Resistance	25	∞					Ω
Line Length	30	50	100	200	400	1000	km
Span Length	0.16	0.40					km

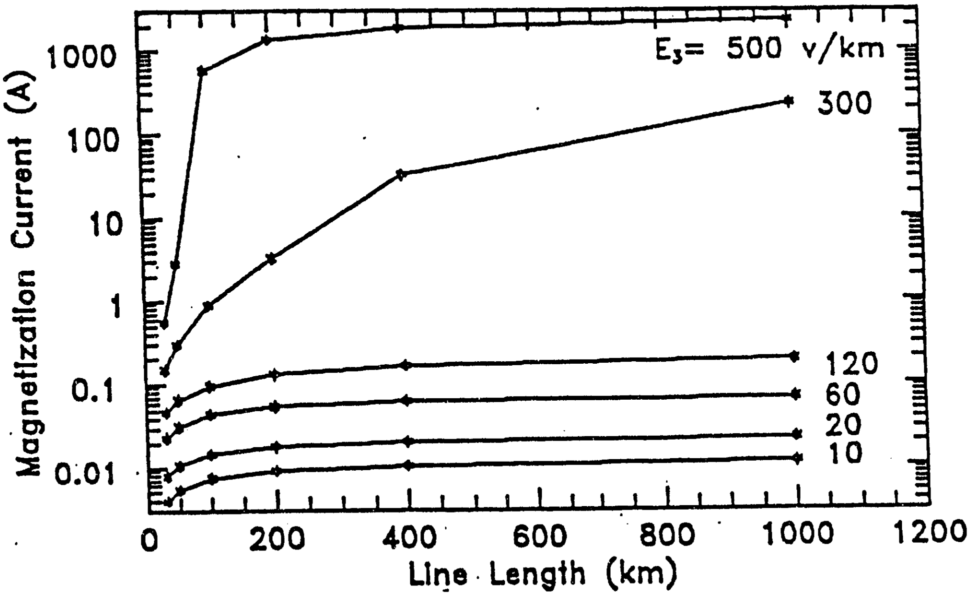

Fig. 4.5-5 (a). The maximum magnetization current for the early time magnetohydrodynamic electromagnetic pulse waveform and ρ= 100 Ω-m Shield wire connected to tower with span of 0.16 km.
Source: Document II-17.

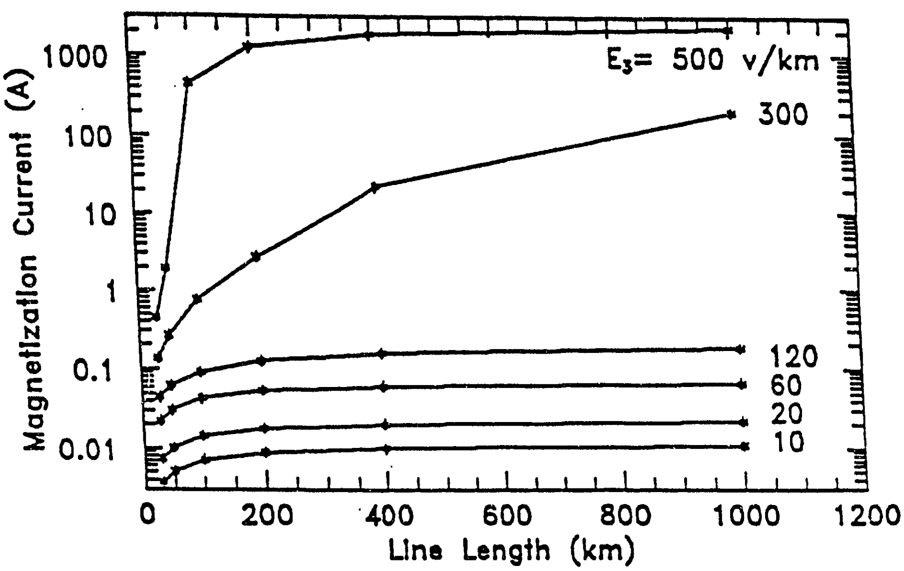

Fig. 4.5-5 (b). The maximum magnetization current for the early time magnetohydrodynamic electromagnetic pulse waveform and ρ= 100 Ω-m Shield wire connected to tower with span of 0.40 km.
Source: Document II-17.

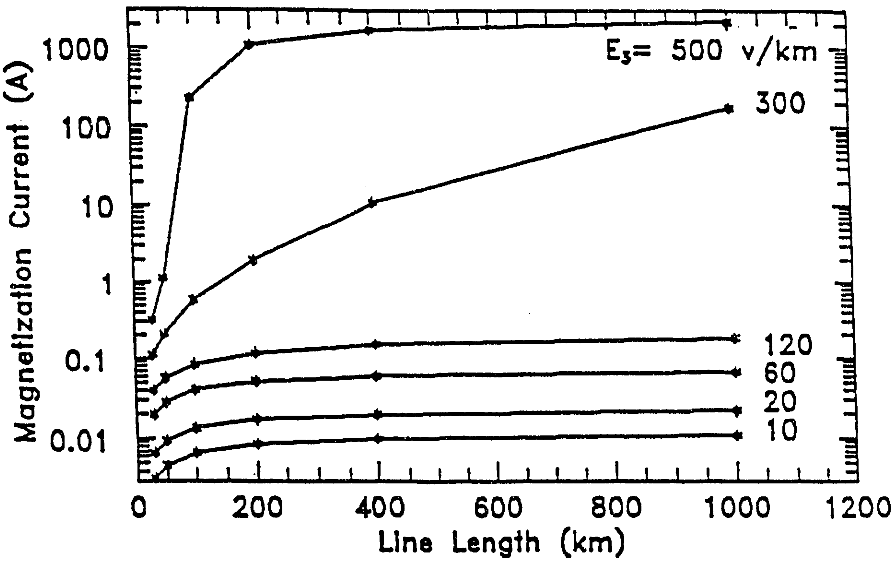

Fig. 4.5-5 (c). The maximum magnetization current for the early time magnetohydrodynamic electromagnetic pulse waveform and ρ= 100 Ω-m. Shield wire insulated from tower.
Source: Document II-17.

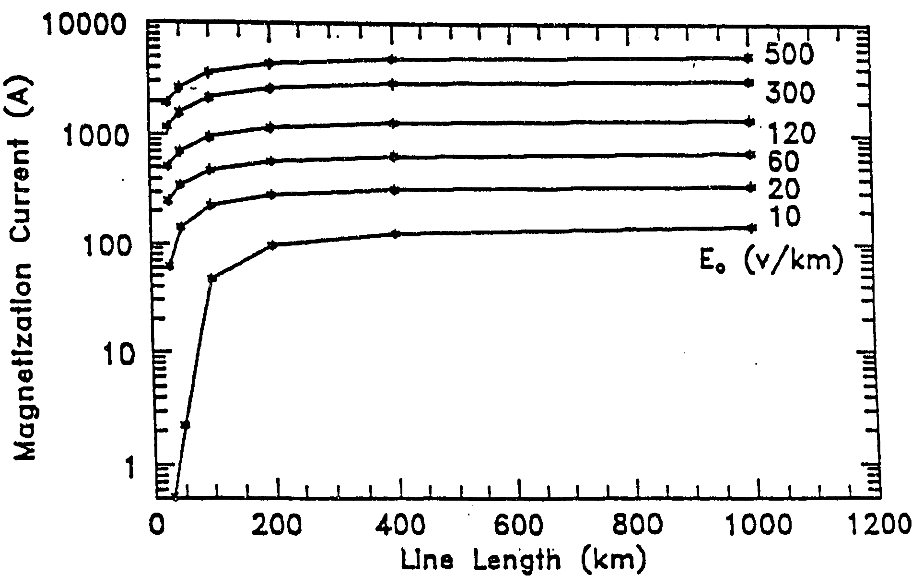

Fig. 4.5-6 (a). The maximum magnetization current for the late time magnetohydrodynamic electromagnetic pulse waveform and ρ= 100 Ω-m. Shield wire connected to tower with span of 0.16 km.
Source: Document II-17.

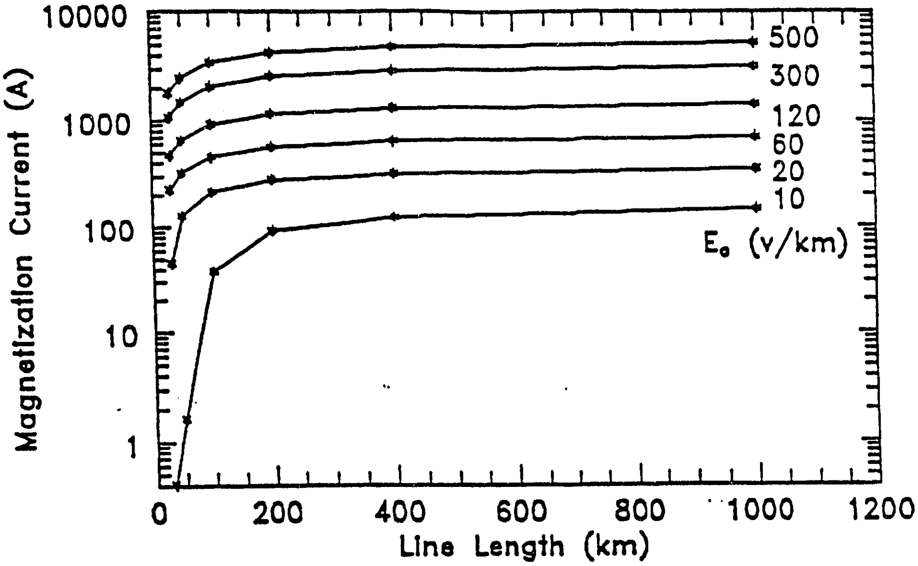

Fig. 4.5-6 (b). The maximum magnetization current for the late time magnetohydrodynamic electromagnetic pulse waveform and ρ= 100 Ω-m. Shield wire connected to tower with span of 0.40 km.
Source: Document II-17.

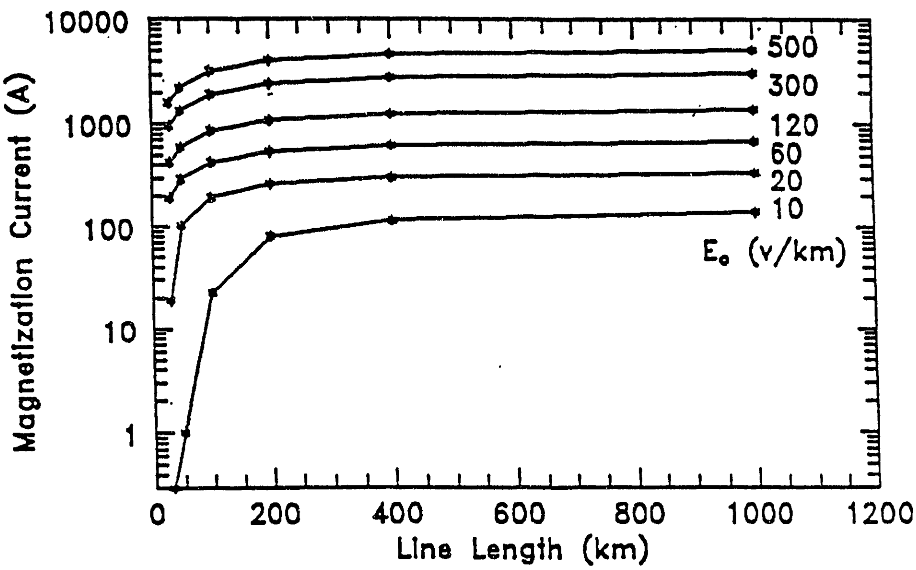

Fig. 4.5-6 (c). The maximum magnetization current for the late time magnetohydrodynamic electromagnetic pulse waveform and ρ= 100 Ω-m. Shield wire insulated from tower.
Source: Document II-17.

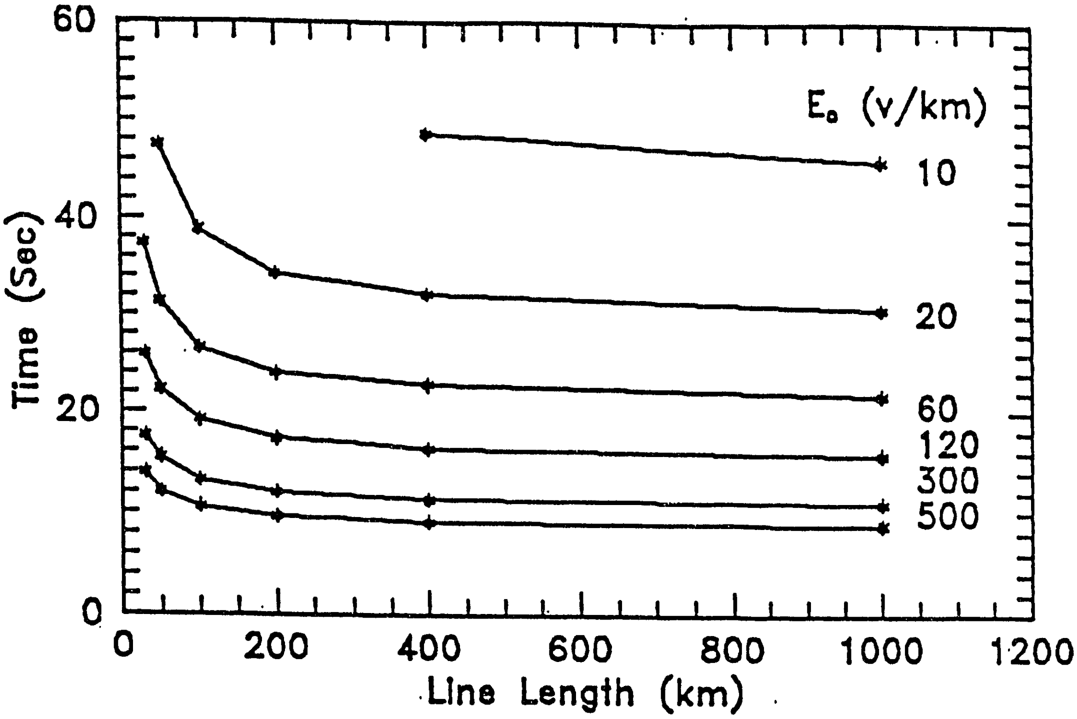

Fig. 4.5-7 (a). Time delay to transformer saturation for the late time magnetohydrodynamic electromagnetic pulse waveform and ρ= 100 Ω-m. Shield wire connected to tower with span of 0.16 km.
Source: Document II-17.

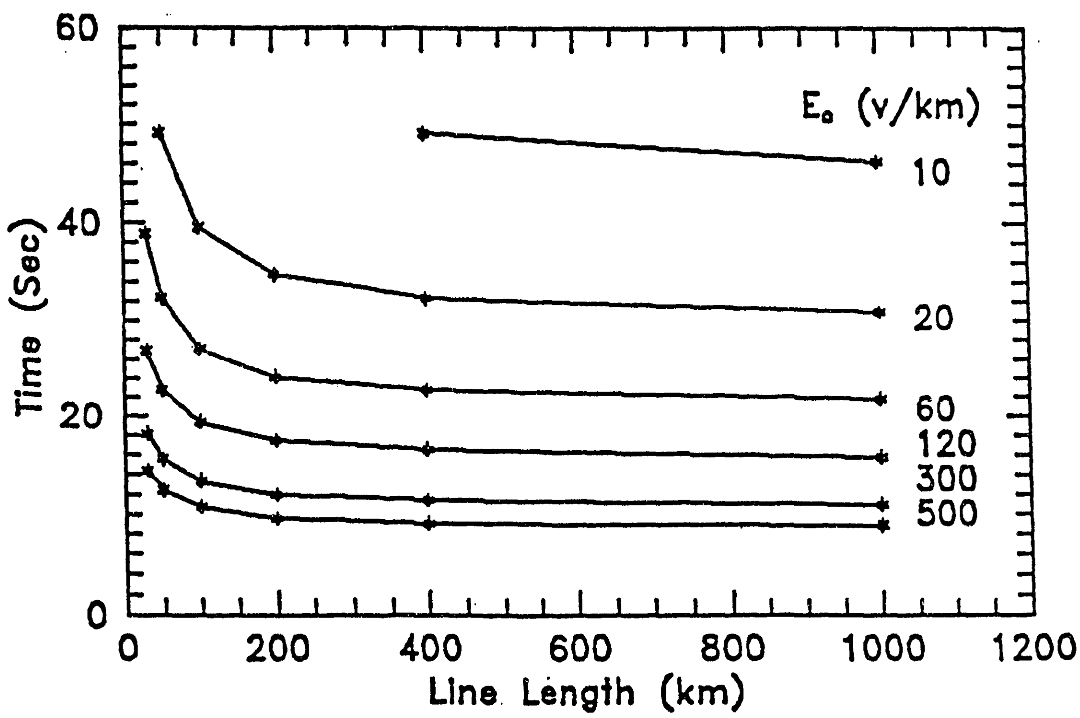

Fig. 4.5-7 (b). Time delay to transformer saturation for the late time magnetohydrodynamic electrmagnetic pulse waveform and ρ= 100 Ω-m. Shield wire connected to tower with span of 0.40 km.
<u>Source</u>: Document II-17.

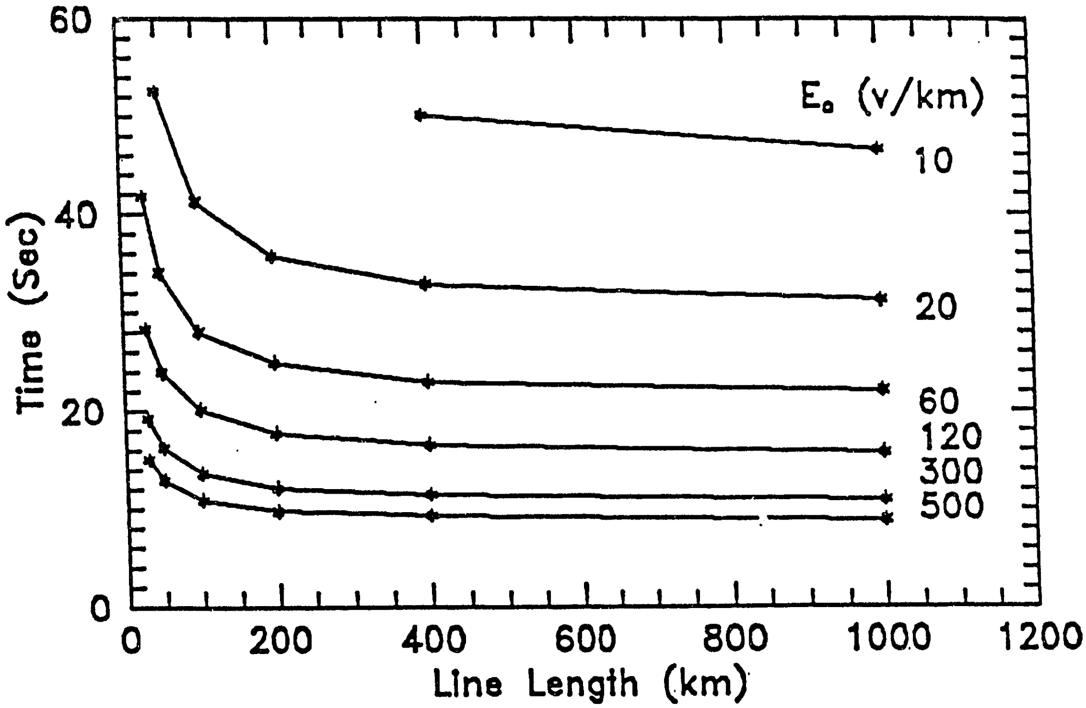

Fig. 4.5-7 (c). Time delay to transformer saturation for the late time magnetohydrodynamic electromagnetic pulse waveform and ρ= 100 Ω-m. Shield wire insulated from tower.
Source: Document II-17.

Figs. 4.5-7 (a), (b) and (c) show the times to saturate. These curves were for the transformer unloaded condition. Table 4.5-4 shows the effect of transformer loading for the 30 km, 20 V/km shielded case.

The authors of this study conclude that MHD-EMP environments on the order of 20 V/km can have a measurable effect on transformer operation in the form of core saturation, harmonic generation, and an increase in reactive power demand. Larger field strengths would increase the severity of these effects.

According to Document II-18, distribution transformers can saturate in less than a second for dc currents of approximately 5 A. The increased reactive load on distribution circuits can cause low system voltage. This and the harmonics produced by the saturated units could result in system wide outages.

It should be noted that the short duration of the saturation, if it should occur, would probably cause no permanent damage to the transformers from overheating. The increased vars and harmonics produced were demonstrated by the October 28th storm to cause the other GIC effects discussed in Sect. 4.2. Since this naturally occurring geomagnetic disturbance with a relatively low earth-surface potential (ESP) caused significant and widespread upset, it must be concluded that a stronger E_3 wave, occurring at the wrong time, could lead to a system shutdown. It must also be noted that these calculations were done for 100 ohm-meter earth which is representative of the whole United States. GIC phenomena are almost always discussed only for regions with earth resistivities greater than 1000 ohm-meters.

While the distribution transformers may not be damaged by the E_3 pulse, various electronic devices connected to the feeders could be damaged. During a GIC disturbance, for example, Wisconsin Electric Power reported a number of failures of TVs, VCRs and other electronic equipment. The cause of these failures was assumed to be either the harmonics produced by the saturated distribution transformers or the voltage surge produced when the transformers came out of saturation.

Note that the analysis of these effects involves an iterative process. For example the dc could cause a line trip-out, which in turn could redistribute the currents and cause another transformer to become saturated. Also note that the E_3 pulse occurs *after* the E_1 pulse so the effects of the latter should be considered first.

The E_1 wave is of short duration; therefore, multiple bursts can be considered separate events separated by a short time. The E_3 wave, however, is of a relatively long duration. The pulses from a multiple burst will be either additive or the effects cumulative and thus of increased severity.

Table 4.5-4
Saturation time constant for loaded transformer.
Source: Document II-17.

Waveform Type: 20 V/km Step Function
Shield Connected to Towers
Span Length: 0.16 km
Ground Resistivity: 100 Ω–m

Transformer Load	Saturation Time Constant (Sec)
0 %	48
20 %	17
40 %	11
100 %	6

4.6 E_3 System Study

A study was made to determine the effects of the quasi-dc currents flowing in the Arizona Public Service system when the system was subjected to several combinations of E_3 pulses. This study is described in Documents II-15 and II-16. Single bursts over Topeka, Kansas, and Salt Lake City, Utah, and a combination of these two were studied.

The first step in the study was to define the E_3 environment. The per-unit time function assumed is shown in Fig. 4.6-1. Note that this is the same wave assumed in Document II-15 (see Fig. 2-7 of I-4). The magnitude contour assumed (for the burst over Salt Lake City) is shown on Fig. 4.6-2. The assumed field direction contour is shown on Fig. 4.6-3. These three functions defined the exposure of the various elements of the APS system.

The next task was to define the power system exposed to the electric fields. Definition included:

- o the initial state of the system;
- o the location, resistance and winding connection of all the transformers and reactors;
- o the location and terminating resistance of all ground points;
- o the location of all series capacitors and similar dc blocking devices (the series capacitors had potential transformers shunting them so this location had to be represented);

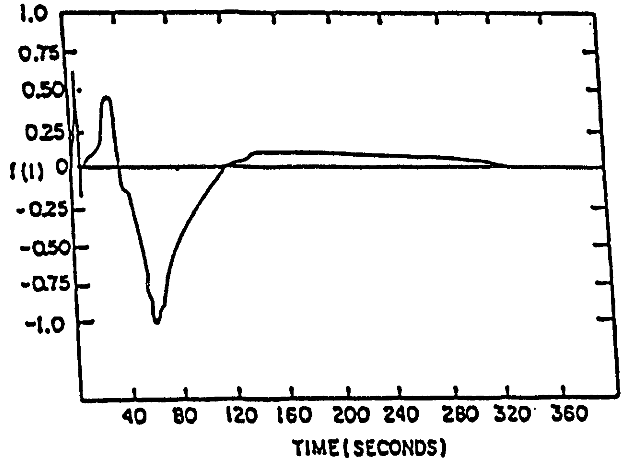

Example of MHD-EMD
f(t) function.

Fig. 4.6-1. Example of magnetohydrodynamic electromagnetic disturbance f(t) function.
Source: Document II-15.

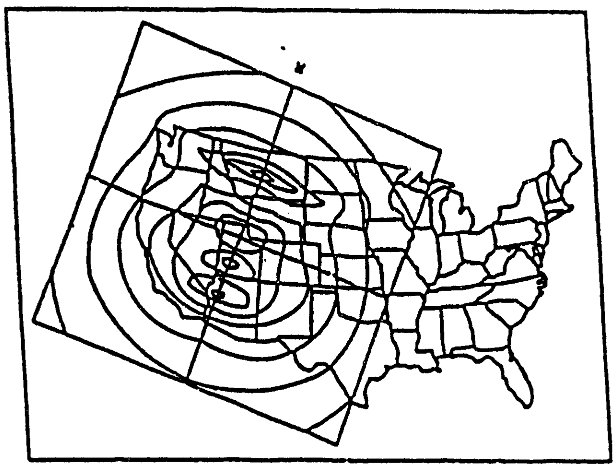

Example of MHD-EMP
c(x,y) function.

Fig. 4.6-2. Non-scaled magnitude contours of magnetohydrodynamic electromagnetic pulse.
Source: Document II-15.

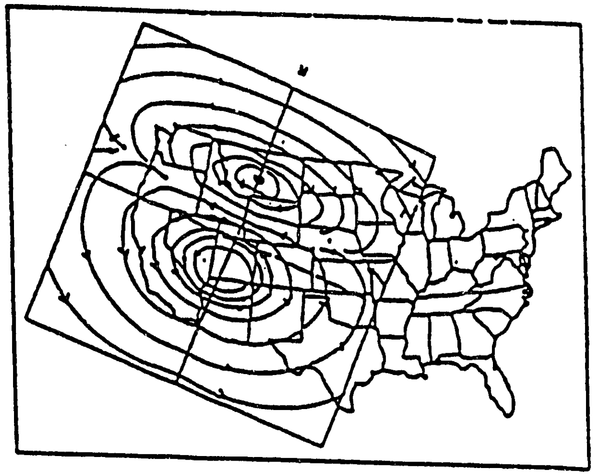

Example of MHD-EMP
e(x,y) function.

Fig. 4.6-3. Direction of magnetohydrodynamic electromagnetic pulse gradients.
Source: Document II-15.

- the spatial orientation and length of all applicable transmission, subtransmission and distribution circuits;
- the dc resistance per unit length of the various circuits; and
- the earth resistance of the area.

Using these data, the dc networks were represented. The distribution system was isolated from the subtransmission and transmission systems by delta transformer windings so that they could be studied separately.

Using these networks, the system was subjected to six conditions: a burst over Topeka with and without the series capacitors, a burst over Salt Lake City with and without the series capacitors, and a combined burst over both Topeka and Salt Lake City again with and without the series capacitors. The maximum quasi-dc currents recorded are shown on Table 4.6-1.

The column titled "Maximum Current" should be ignored, since it was measured through the system equivalents for the adjoining systems. It is the summation of all the currents flowing out of the system, which would actually be split between several circuits. The column "APS System Maximum Current" values are more pertinent. The distribution system was also studied, but the dc currents resulting from the bursts should cause no problem to the distribution transformers.

Table 4.6-1
Magnetohydrodynamic maximum direct current values.
<u>Source</u>: Document II-15.

SIMULATION	STATUS SERIES CAPACITORS	MAXIMUM CURRENT (Amperes/Phase)	MEDIAN CURRENT (Amperes/Phase)	MEAN CURRENT (Amperes/Phase)	APS SYSTEM MAXIMUM CURRENT (Amperes/Phase)
1a. TOPEKA	IN-SERVICE	39.1 WEST MESA	6.3	3.8	18.3 LEUPP
1b. TOPEKA	BY'PASSED	36.4 WEST MESA	1.8	5.6	25.0 SW MANUEL
2a. SALT LAKE	IN-SERVICE	323.0 KYRENE	9.8	33.8	180.0 PRECHCYN
2b. SALT LAKE	BY PASSED	436.0 ELDORADO	16.0	60.6	380.0 FOUR CORNERS
3a. Combined Event	IN-SERVICE	342.0 KYRENE	10.4	35.9	176.0 PRECHCYN
3b. Combined Event	BY-PASSED	440.0 ELDORADO	12.4	61.3	376.0 FOUR CORNERS

In the third step, the quasi-dc currents were assumed to cause varying degrees of saturation in the transformers. The effect of the resulting increase in var flow was calculated by system load flow and stability studies. These studies considered only the Salt Lake City burst with series capacitors in service, which was considered the worst single burst case with a realistic system configuration.

Figs. 4.6-4 and -5 show the voltage and phase angle response of the system from the stability run. The curves show large oscillations initially but demonstrate a high degree of damping. The transients are severe and suggest that the system is only marginally stable. However, the study assumed a step-function event. Since the actual dc function is a slow rising ramp function with the peak occurring only after several seconds, it is highly likely that the system damping would cause the system to be more stable than predicted in this discussion.

Tables 4.6-2 and -3 show the results of the load flow analysis; Table 4.6-2 is the area interchange before the E_3 event and Table 4.6-3 the area interchange during the event. Note the 60% increase in real power export and the massive increase in reactive power import. Not only the area interchange, but also the internal system bus voltages were affected. In the APS system, 54% of the busses fell below 0.9 pu, 41% below 0.8 pu, 18% below 0.7 pu, and 2% below 0.6 pu with most of the latter actually below 0.5 pu. Under these conditions, it is likely that relay operations will occur to break up the system.

An event of one-half the magnitude previously defined in Figs. 4.6-1, -2 and -3 was studied and found to be nowhere near as severe, with no bus voltage falling below 0.9 pu. An event of twice magnitude was found to quite severe (as expected) and in fact load-flow-solution convergence was difficult to obtain. If the

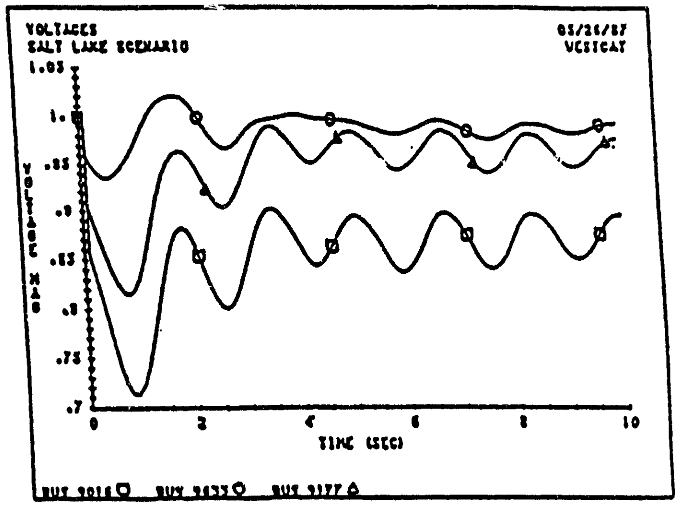

Fig. 4.6-4. Typical voltage responses.
Source: Document II-16.

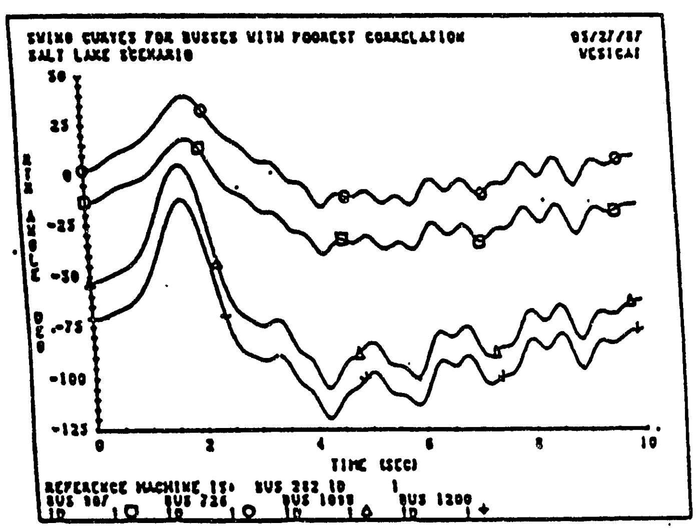

Fig. 4.6-5. Typical swing curves.
Source: Document II-16.

Table 4.6-2
Summary of area interchange without the presence of magnetohydrodynamic electromagnetic pulse.
Source: Document II-16.

FROM AREA	TO AREA	MW FLOW	MVAR FLOW
ARIZONA	IMPERIAL CALIFORNIA	65.15	0.00
	LOS ANGELES	902.43	30.34
	NEVADA	383.70	0.00
	PUB. SERVICE OF NEW MEX.	-403.38	7.06
	SAN DIEGO	394.56	0.00
	SOUTHERN CALIFORNIA	1701.21	29.37
	TEXAS - NEW MEXICO	205.66	0.00
	UTAH	-279.82	0.00
	WESTERN AREA POWER ADMIN.	-881.65	0.00
	TOTAL EXPORT	2087.73	66.76

Table 4.6-3
Summary of area interchange during a magnetohydrodynamic electromagnetic pulse event.
Source: Document II-16.

FROM AREA	TO AREA	MW FLOW	MVAR FLOW
ARIZONA	IMPERIAL CALIFORNIA	73.34	5.01
	LOS ANGELES	1299.25	-336.95
	NEVADA	359.49	-85.32
	PUB. SERVICE OF NEW MEX.	-338.76	-543.79
	SAN DIEGO	343.65	-622.04
	SOUTHERN CALIFORNIA	2015.01	-439.07
	TEXAS - NEW MEXICO	227.12	-69.82
	UTAH	74.21	-141.86
	WESTERN AREA POWER ADMIN.	-636.10	-469.21
	TOTAL EXPORT	3417.21	-2703.04

real E_3 environment is of this magnitude, stability could be a problem.

For the base case and twice the base case, the effect on the distribution system was negligible. The circuit lengths are so short that the small induced currents caused negligible effects on the transformers. This outcome confirms the results of the previous study (see Document II-15).

It should be noted that the study did not consider the possibility that the harmonics caused by the transformer saturation could trip some of the shunt capacitor banks on the system. In this regard, the study was not as pessimistic as it should have been, since the capacitor tripping would cause even lower system voltages.

4.7 E_3 Mitigation Measures

Circuit shielding and filters are used to prevent HEMPs from entering control and communication facilities. For the long E_3 pulses, the open circuit voltages are small and shields and filters are transparent. Transformers, fiber optics or capacitors must be used to interrupt the currents. Delta-wye transformers and separate grounds (as shown on Figs. 4.7-1 and 4.7-2) can be used to make sure remote ground currents go down into earth rather than up the facility ground.

Since the system effects of the E_3 pulses are of the same character as those from GIC, the various mitigation methods discussed in Sect. 4.3 have been considered for the E_3 pulses. The comments and opinions expressed in Sect. 4.3 are also appropriate here.

4.8 Summary

Contrary to the conclusions reached about E_1, since no universally practical mitigation solution exists, further work needs to be done on the E_3 problem. Since the effects of these waves are so similar to those of the GIC, mitigation solutions for one should be applicable to the other. This provides added emphasis for the solution to the problem. It must be noted, however, that only northern utilities located in GIC-prone areas are likely to pursue GIC mitigation. Major regions of the country will therefore remain susceptible to E_3 effects.

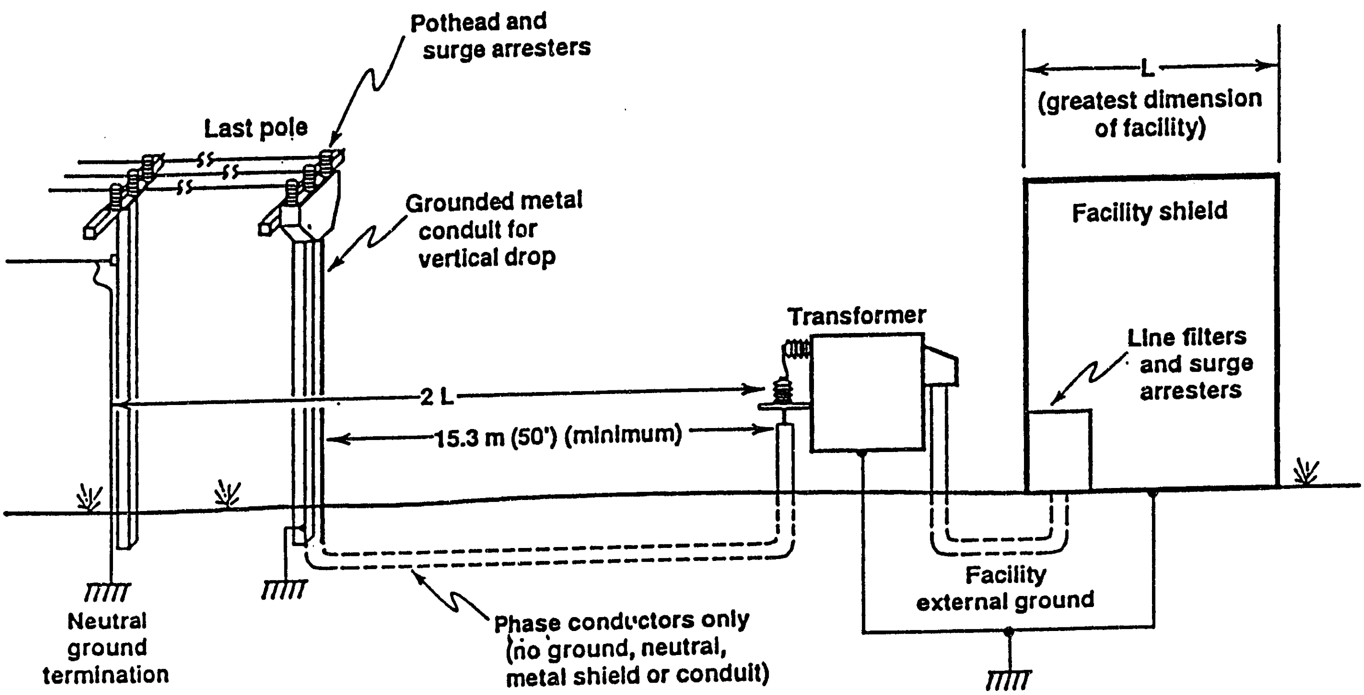

Fig. 4.7-1. Long-pulse treatment--overall arrangement of power service.
Source: Document I-6.

LONG-PULSE TREATMENT

Distribution transformer in configuration to serve as the long-pulse barrier

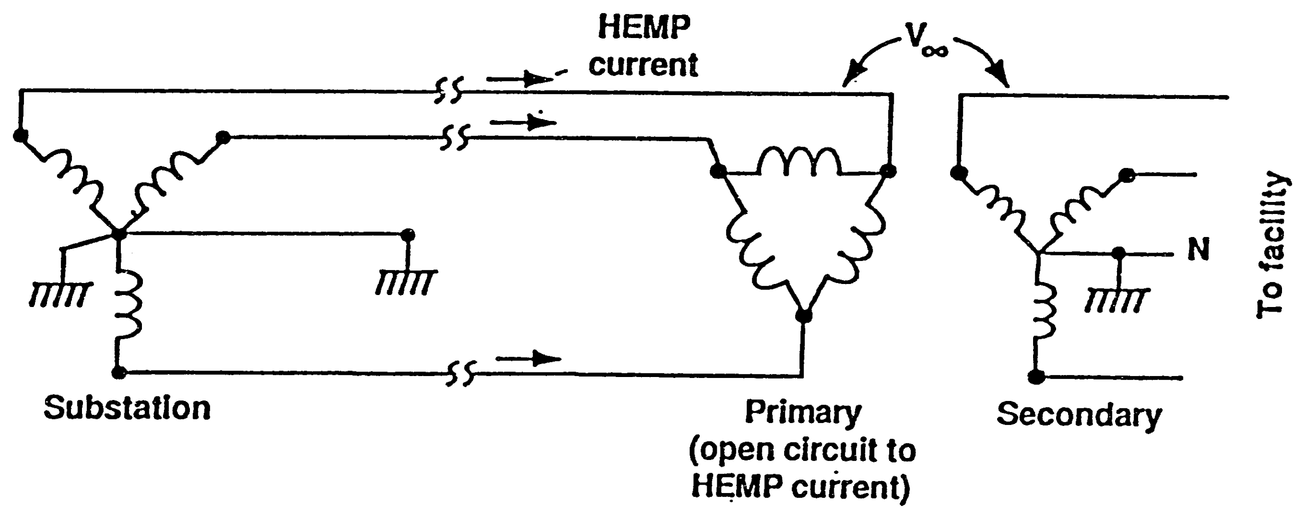

Fig. 4.7-2. Long-pulse treatment--distribution transformer in configuration to serve as the long-pulse barrier.
<u>Source</u>: Document I-6.

5.0 HIGH ALTITUDE ELECTROMAGNETIC PULSE MITIGATION MEASURES

While various means of protection against the effects of E_1 and E_3 waves have been mentioned in the preceding sections, for convenience they will be listed and discussed briefly in the following sections.

5.1 E_1 Surges

Since the characteristics of the E_1 surges are similar to those of certain lightning and switching impulses, the mitigation measures recommended for the latter apply also to the E_1 pulses.

For overhead lines, the transmission and subtransmission lines will be unaffected, but distribution lines of 15 kV and below may encounter flashovers. These flashovers could be eliminated or at least minimized by increasing the distribution voltage (and thus the line insulation) to some higher voltage, such as 34.5 kV. Another method would be to install surge arresters at every second or third pole. Perhaps an MOV built into the pole insulator could be used. All of these alternatives are costly, however, and it is doubtful that utilities could justify this expense.

The major protection for cables and T&D equipment is surge arresters applied directly on the equipment terminals. Due to the steep fronts of the E_1 waves, however, the L di/dt of the arrester down leads can be a problem. These lead lengths should be kept as short as possible.

The grounding system for the arrester leads and other equipment grounds should be designed to minimize the ground potential rise, the mutual couplings of the leads, and other interfering signals that might affect any sensitive electronic control equipment (such as recloser controls or tap changer controls) in the T&D apparatus.

Motor insulation can be damaged by the steep fronts as well as high magnitudes of the E_1 pulses. Surge protection packages--consisting of capacitors to slope off the fronts and surge arresters to limit the magnitudes--are used to protect important motors in power plants against lightning and switching surges. These packages would also protect against the E_1 surges.

Relay designers build various protection devices into their relay systems. The devices most frequently used are "soft limiters" such as Zener diodes and metal oxide varistors, "hard limiters" such as spark gaps, and various forms of filters. Surge capacitors of 0.01 μfarads or greater are also installed on all input and output circuits. Shielded cable should be used for the control wiring from the instrument transformers to the relay terminals. Fiber optics are also sometimes used for these circuits. These measures, if properly designed and installed, will provide protection against E_1 as well as other transient surges.

Communication and control equipment can be protected by establishing an EM barrier around the essential parts of the system. There are three elements to this barrier:

1) Building shield: This element consists of an essentially closed surface (shield) around the equipment. A closed, continuous metal shield is preferable, but coupling through shield openings can be reduced by covering the apertures with metal mesh or using waveguides below cutoff. A more economical method is to keep interior wiring away from these apertures.

   Where shielding of the complete building or control house is impractical, zoned protection (shielding individual rooms, cabinets or even individual control elements) can be used.

2) Penetration control: The grounding system inside the shield should be separate from the external grounds. Proper current diverting must be provided for power, signal, and ground wires that penetrate the shield.

   Where possible, external fuel, water, sewer, and other pipes should have insulated sections as close as possible to their entrance to the building.

   Groundable conductors, such as cable shields and waveguides, etc. should be bonded externally to the building shield at the point of entry. A 360° bond between the conductor shield and the entry panel should be used. Grounding pigtails should not be used; if they are, they should be kept as short as possible.

   Barrier elements--such as filters, surge arresters, antenna surge suppressors, or isolation transformers--should be used on the signal and power conductors where they penetrate the shield. A properly installed UPS can isolate transients on the external power lines. The use of fiber optics can isolate the communication and control signal lines.

3) Protective devices: The following devices are used to limit the E_1 surges either at the building barriers or the equipment terminals:

   - arresters or varistors,
   - semiconductor devices,
   - air or gas spark gaps,
   - filters (capacitors, LC combinations, etc.),
   - isolation transformers, and
   - optoelectronic couplers.

The connecting leads of these devices can produce an additional voltage equal to L di/dt; therefore, they should be kept as short as possible.

Further details of these barrier designs are discussed in Sect. 3.6.

5.2 E_3 Surges

The circuit shielding and filters discussed previously for the mitigation of E_1 pulses in control and communication facilities are relatively ineffective for the E_3 pulses. For these longer pulses, transformers, capacitors, or fiber optics must be used to interrupt the currents. Delta-wye transformers, for example, could be used on the power supply inputs to ensure that remote ground currents do not enter the facility.

For the protection of the *system* against E_3 surges, the following mitigation methods have been suggested. These are similar to the GIC mitigation methods proposed and are discussed in greater detail in Sect. 4.3. None of these is considered practical for general use for the reasons cited:

- Polarizing cells: Too many blocking cells are required, resulting in excessive costs.
- Linear resistors: Transformer neutral voltage (and thus insulation) and resistor losses are too high.
- Non-linear resistors: Too many units are required for fault energy dissipation, resulting in excessive costs.
- Active dc devices: This method requires a broken delta tertiary in the transformer (not usually available); it doesn't block E_3 from the system (just in neutral); and the scheme is more complex than a neutral capacitor.
- Neutral capacitors: This is probably the most effective and economical device. Its problems are that: (1) it can block neutral currents but not series winding currents in autotransformers; (2) a complex system study is required to find the correct neutrals to block; (3) it must be bypassed during faults; (4) it can cause ferroresonance problems and so requires a high speed bypass device; (5) relay problems could be caused by the capacitor and could affect the impedance to the fault and induced transients due to shorting of the capacitor influencing the relay; (6) the fault contribution from the far end of the line can be affected; and (7) it is expensive.
- Series capacitors: The installation of series capacitors in the transmission lines overcomes the objection that

the neutral capacitors do not block the currents in the series windings of the autotransformers. Series capacitors also improve the power transmission capabilities of the system in addition to their quasi-dc blocking ability. Unfortunately, their cost is prohibitive unless they are required for reasons other than dc blocking.

None of these methods is considered practical for general use as E_3 mitigation devices, but neither is any one considered practical for GIC mitigation. Joint investigations for new methods to solve both problems are therefore indicated.

6.0 STANDARDS

A number of American (ANSI) and International Electrotechnical Commission (IEC) standards, while not written specifically for HEMP, contain sections or requirements that if followed, will prevent damage from HEMP. Document XI-1 contains a listing of some of the standards that have at least a partial application to the EMP problem environment.

These standards can be divided into three categories: protective device standards, cable and shielding standards, and equipment withstand standards. The ANSI documents are summarized in the following section.

6.1 Protective Device Standards

Standard C62.1 [XI-5] describes the service conditions, classifications and voltage ratings, design tests with corresponding performance characteristics, conformance tests, and certification test procedures for station, intermediate, distribution, and secondary class gapped silicon-carbide surge arresters.

In this standard and other C62 standards, current and voltage impulse waves are designated as "1.2/50" where 1.2 is the front time and 50 is the time to half value of the tail. This is the currently approved method of designation. The older method used "*" instead of the solidus. Thus "1.2/50" was formerly called a "1.2*50" wave. Note that some of the documents referred to in this report still used the "*" designation.

The standard ratings available in the different classes of arresters are:

Secondary	175 and 650 V
Distribution	1 through 30 kV
Intermediate	3 through 120 kV
Station	3 through 684 kV

The following tests are applicable for determining the protective levels:

1. Front-of-wave sparkover: Ramp waves of various rates of rise are applied with the arrester sparkover occurring before the crest of the wave. The following rates of rise are specified:
   - o 10 kV/μs for ratings of 3 kV or less,
   - o (100/12) kV/μs for each kilovolt of arrester rating --for ratings 3 to 240 kV, and
   - o 2000 kV/μs for ratings above 240 kV.

The rates of rise of E_1 waves are higher than these values, so Document VIII-5 reports the following suggested additions to the standard:

- Add 1000-, 2000-, and 5000-A discharge voltage tests using a wave shape of 0.16/0.4 μs.
- For arresters having series or parallel gaps, add front-of-wave impulse sparkover tests using rates of rise of:
  - 500 kV/μs for arresters 3 kV and lower
  - (5000/12) kV/μs per each kilovolt of rating for arresters rated 3 through 48 kV, or
  - 20 MV/μs for arresters above 48 kV.

These additions are not felt to be practical for high voltage (above 34.5 kV) arresters (1) because of the low probability of the arrester's ever seeing these waves, (2) because the previous HEMP investigators have shown that the volt-time turn-up of the equipment is sufficient to compensate for the turn-up of the arrester characteristic, and (3) because it is the L di/dt of the arrester leads that is the important element for the SFSD waves. Also, it is not known whether existing laboratories are capable of making these tests.

For lower voltage arresters (34.5 kV and below), some additional tests should be made, especially for those units purchased for protection against E_1 surges. What tests should be made and what tests are practical for the existing laboratories are not known, but perhaps the previously suggested tests could be examined by the standard-setting bodies.

2. <u>1.2/50 Impulse sparkover:</u> This is the highest standard lightning impulse voltage greater than 3 μs duration which the arrester will pass without sparkover.

3. <u>Switching surge impulse sparkover:</u> Waves with fronts of (a) 30 to 60 μs, (b) 150 to 300 μs, and (c) 1000 to 2000 μs and long tails are applied to all arresters rated at 60 kV and above. The highest wave sparking over 30 μs or longer is considered the switching surge sparkover value.

4. <u>Discharge voltage:</u> 8/20 current waves having magnitudes of 1500, 3000, 5000, 10,000 and 20,000 A are passed through the arresters. The resulting voltages are noted.

Tables 6.1-1, -2, -3, and -4 from ANSI/IEEE C62.2-1987 (Document XI-6) give typical values for these tests for the four classes of gapped silicon-carbide arresters.

Table 6.1-1

Protective characteristics of gapped silicon-carbide station arresters.

Source: Document XI-6.

Voltage Rating of Arrester kV rms)	Impulse Sparkover Voltage: Front-of-Wave — Rate of Rise of Test Voltage (kV/µs)	Impulse Sparkover Voltage: Front-of-Wave — kV Crest (Range of Maxima)	Impulse Sparkover Voltage: 1.2/50-µs kV Crest (Range of Maxima)	Switching Surge Sparkover Voltage kV Crest (Range of Maxima)	Discharge Voltage for 8/20-µs Discharge Current Wave: kV Crest for 1500 A (Range of Maxima)	kV Crest for 3000 A (Range of Maxima)	kV Crest for 5000 A (Range of Maxima)	kV Crest for 10 000 A (Range of Maxima)	kV Crest for 20 000 A (Range of Maxima)	kV Crest for 40 000 A (Range of Maxima)
3	25	10–18	10–14	–	4.7–6	5.3–6.5	6–7	6.7–7.5	7.7–8.3	–9.2
6	50	19–28	16–23	–	9.3–11	10–12	11.9–13	13.4–14.3	15.3–16.3	–18.5
9	75	28.5–38	24–32	–	13.9–17	16–18	17.8–19	20–21.5	22.9–24.3	–28
12	100	36–48	32–41	–	18.5–22	21.3–24	23.5–25.5	26.7–28.5	30.1–32.1	–37
15	125	45–57	40–51	–	23.1–27.5	26.6–30	29.5–32	33.4–36	38.2–40	–46
21	175	63–76	54–68	–	32.3–38.5	37.2–42	41–45	46.8–50	53.4–55.5	–65
24	200	71–86	62–77	–	36.9–44	42.5–48	47–51	53.4–57	61–63.5	–74
30	250	89–103	77–93	–	46.1–55	53.1–60	59–64	66.9–72	76.3–79	–92.5
36	300	107–118	92–108	–	55.3–66	63.7–72	70.5–76	80–85	91.5–94.5	–111
39	325	115–125	100–114	–	60–71.5	69–78	76.5–82.5	86.5–92	99.1–102	–120
48	400	143–148	122–132	–	73.8–88	84.9–96	94–102	106–114	122–126	–148
60	500	170–190	141–165	136–153	95–109	110–120	118–130	132–143	150–158	–185
72	600	204–226	169–190	163–178	114–131	130–144	141–155	159–170	180–189	–222
90	750	254–275	210–235	203–215	142–163	162–180	176–194	199–213	225–237	–277
96	800	270–295	218–245	218–225	151–174	173–192	188–218	212–227	240–253	–296
108	900	304–325	245–270	245–250	170–196	194–216	212–245	238–256	270–284	–333
120	1000	338–360	272–300	272–275	188–218	216–240	235–272	265–285	300–319	–370
144	1200	400–430	326–346	325–326	226–262	260–288	282–311	318–342	360–379	–444
168	1400	460–525	380–404	380–381	263–305	303–336	329–362	371–399	420–442	–517
180	1500	490–565	400–430	400–410	281–327	324–360	353–388	397–427	450–495	–554
192	1600	520–600	427–460	426–435	300–348	346–384	376–414	424–455	480–505	–591
240	2000	620–735	535–577	533–545	374–436	432–480	470–518	530–570	605–630	–739
258	2000	760–790	575–620	573–585	402–438	465–474	505–515	569–575	650–666	–795
276	2000	805–840	615–664	612–630	429–468	496–507	540–570	609–615	690–714	–850
294	2000	875–885	653–675	653–675	458–472	528–532	576–595	653–653	735–758	–906
312	2000	924–935	690–750	693–710	485–530	562–574	611–620	688–693	780–805	874–961
372	2000	1078–1100	870–890	790–830	562–610	655–680	726–738	809–826	932–955	1136–1145
396	2000	1140–1176	925–950	840–885	599–672	697–726	734–785	861–880	990–1015	1109–1226
420	2000	1200–1250	980–1005	890–940	634–713	739–770	819–830	913–930	1050–1070	1176–1294
444	2000	1265–1320	1035–1055	940–990	670–753	781–814	866–876	965–977	1110–1130	1243–1358
468	2000	1326–1390	1090–1110	992–1045	707–794	823–860	913–930	1018–1040	1170–1200	1310–1441
492	2000	1385–1425	1160–1165	1045–1090	742–830	865–925	958–1000	1070–1115	1232–1290	1500–1515
540	2000	1515–1555	1274–1280	1145–1200	814–890	949–990	1052–1070	1173–1195	1350–1390	1646–1663
576	2000	1616–1665	1359–1380	1225–1285	868–950	1012–1060	1122–1150	1251–1285	1440–1480	1755–1780
612	2000	1700–1765	1440–1480	1300–1370	924–1010	1076–1130	1193–1220	1330–1360	1531–1580	1865–1885
648	2000	1790–1865	1525–1570	1380–1445	977–1070	1138–1190	1261–1290	1407–1440	1619–1670	1974–1996
684	2000	1880–1960	1610–1680	1455–1525	1031–1130	1153–1260	1331–1360	1489–1520	1709–1765	2063–2107

Table 6.1-2
Protective characteristics of gapped silicon-carbide intermediate valve arresters.
Source: Document XI-6.

Voltage Rating of Arrester (kV rms)	Impulse Sparkover Voltage: Front of Wave: Rate of Rise of Test Voltage (kV/μs)	Impulse Sparkover Voltage: Front of Wave: kV Crest (Range of Maxima)	Impulse Sparkover Voltage: 1.2/50-μs kV Crest (Range of Maxima)	Switching Surge Sparkover Voltage kV Crest (Range of Maxima)	Discharge Voltage for 8/20-μs Discharge Current Wave: kV Crest for 1500 A (Range of Maxima)	kV Crest for 3000 A (Range of Maxima)	kV Crest for 5000 A (Range of Maxima)	kV Crest for 10 000 A (Range of Maxima)	kV Crest for 20 000 A (Range of Maxima)
3	25	11–12	11–12	–	5.2–7.5	6–8	6.6–9	7.5–10	8.7–12
6	50	21–21	19–19	–	10.4–13.5	11.9–14	13.2–15.5	15–17.5	17.4–20
9	75	31–33	27.5–32	–	15.6–21	17.9–23	19.8–25	22.5–28	26.1–31
12	100	38–42	35.5–37	–	20.8–27	23.8–29	26.4–32	30–34	34.8–37.5
15	125	47–51	43.5–46.5	–	25.9–34	29.7–36.5	32.9–39.5	37.5–43	43.5–47.5
21	175	67–73	58–64	–	36.3–47.5	41.6–51	46.1–56	52.5–60	60.9–66
24	200	75–78	66–75	–	41.5–54	47.6–58	52.7–64	60–68	69.6–75
30	250	91–97	81–91	–	51.8–68	59.4–73	65.8–79	75–86	87–95
36	300	108–116	95–103	–	62.2–82	71.3–87	79–95	90–102	104–113
39	325	116–126	102–110	–	67.4–91	77.3–97	85.5–106	97.5–114	113–126
48	400	143–154	121–132	–	83–109	95–116	105–127	120–136	139–150
60	500	166–190	147–155	185–206	104–136	119–145	131–159	150–171	174–189
72	600	201–230	171–191	219–245	124–163	143–174	158–191	180–204	209–225
90	750	250–283	223–233	274–304	155–204	178–218	197–239	225–256	261–282
96	800	268–300	236–250	292–323	166–217	190–232	211–254	240–273	278–300
108	900	283–335	258–265	328–362	187–244	214–261	237–286	270–307	313–338
120	1000	299–370	276–295	351–400	207–272	238–290	263–319	300–338	348–380

Table 6.1-3

Protective characteristics of gapped silicon-carbide distribution arresters.

Source: Document XI-6.

Voltage Rating of Arrester (kV rms)	Impulse Sparkover Voltage: Front of Wave: Rate of Rise of Test Voltage (kV/μs)	Impulse Sparkover Voltage: Front of Wave: Without External Gap: kV Crest (Range of Maxima)	Impulse Sparkover Voltage: Front of Wave: With External Gap: kV Crest (Range of Maxima)	Impulse Sparkover Voltage: 1.2/50-μs: Without External Gap: kV Crest kV Crest (Range of Maxim)	Impulse Sparkover Voltage: 1.2/50-μs: With External Gap: kV Crest kV Crest (Range of Maxima)	Discharge Voltage for 8/20-μs Discharge Current Wave: kV Crest for 1500 A (Range of Maxima)	kV Crest for 3000 A (Range of Maxima)	kV Crest for 5000 A (Range of Maxima)	kV Crest for 10 000 A (Range of Maxima)	kV Crest for 20 000 A (Range of Maxima)
3	25	14–25	24–38	12–22	24–37	8–10	8.4–11.5	10–12.4	11.5–13.8	13.5–15.7
6	50	27–35	45–57	23–33	35–55	16–20	17–23	20–24	22.5–26	25–30
9	75	39–48	60–76	34–45	48–65	24–30	25–34	29–36.5	32.5–41	36–46
10	83.3	40–48	62–76	35–49	48–67	25–30	27.5–34	29.5–37	32.5–44	36–52
12	100	49–60	73–96	44–57	59–85	32–40	34–46	29.5–48	43–53	49–61.5
15	125	47–75	80–115	49–65	69–100	40–50	42–55	39–60	54–65.5	60–76
18	150	55–90	96–133	58–76	79–118	48–60	51–66	46–72	65–78	71–91
21	175	63–90	110–139	66–78	–123	56–70	59–75	68–80.5	73–90	82–103
27	225	79–102	–	75–98	–	70–80	76–86	82–94	90–105	99–121
30	250	86–114	–	81–100	–	76–89	84–97	91–105	100–116	111–134

Table 6.1-4

Protective characteristics of gapped silicon-carbide secondary arresters.

Source: Document XI-6.

Voltage Rating of Arrester (kV rms)	Impulse Sparkover Voltage: Front-of-Wave: Rate of Rise of Test Voltage (kV/μs)	Impulse Sparkover Voltage: Front-of-Wave: kV Crest (Range of Maxima)	Impulse Sparkover Voltage: 1.2/50-μs: kV Crest (Range of Maxima)	Discharge Voltage for 8/20-μs Discharge Current Wave: kV Crest for 1500 A (Range of Maxima)	Discharge Voltage for 8/20-μs Discharge Current Wave: kV Crest for 5000 A (Range of Maxima)
0.175	10	2.3–3.0	2.1–2.5	1.0–1.5	1.4–1.8
0.650	10	2.8–3.8	2.5–3.5	2.2–3.8	2.9–5.0

Standard C62.11 [XI-7] is similar to C62.1 except that it concerns metal-oxide arresters rather than silicon-carbide units, although some of the testing and characteristics are different, but in general the protective characteristics that apply are similar--perhaps with slightly different values. The characteristics of the 1983 vintage of Westinghouse station, intermediate, and riser pole distribution MOV arresters are shown in Tables 6.1-5, -6, and -7.

Note that impulse sparkover values are not given on these tables. MOV arresters usually have no gaps and are simply highly nonlinear resistors; thus "sparkover" is meaningless. The 0.5 μs discharge value is the closest thing to the front-of-wave characteristic of the SiC arrester. This is the protective level produced by a current wave that produces a voltage wave cresting in 0.5 μs.

Standard C62.31 [XI-8] covers the test criteria and procedures for gas-tube surge-protective devices. There are a number of different tests, but the impulse breakdown voltage test is the one that applies most to the protective characteristics for E_1 surges. The waveform specified for the test consists of rates of rise of 100 V/μs, 500 V/μs, 1 kV/μs, 5 kV/μs and--when the device is to be used to protect against E_1 surges--an additional test at 100 kV/μs (100 V/μs is typical for lightning transients on metallic shielded communication or signal lines; 500 V/μs for unshielded lines; and 5 kV/μs for ac power switching transients). The average and maximum values allowed for the tests are given in Table 6.1-8 from C62.61 [XI-10].

Standard C62.33 [XI-9] describes the design tests to be performed on varistors used on systems with dc to 420-Hz frequency and voltages ≤ 1000 V rms or 1200 V dc. It does not give any particular values, however. The only test parameter given is an 8/20 current wave, although the standard defines the term "voltage overshoot," which refers to the magnitude of the voltage above the 8/20 clamping voltage (see Fig. 6.1-1), obtained under conditions of steep front current impulses at high amplitudes. This seems to imply that manufacturers can test these E_1-type impulses and measure the overshoot voltage. The standard cautions that this voltage will include the lead L di/dt drop.

6.2 Cable and Shielding Standards

Two standards that cover practices, if followed, should minimize E_1 surges arriving at the substation equipment terminals. IEEE Standard 518, the *IEEE Guide for the Installation of Electrical Equipment to Minimize Electrical Noise Inputs to Controllers from External Sources* [XI-15], covers the protection of control circuits for computers and solid-state controllers against various types of noise, including E_1 surges.

While this standard covers both low-frequency and high-frequency noise, the major portion is devoted to low-frequency audio and

Table 6.1-5
Westinghouse type SMX station surge arrester characteristics.
Source: Westinghouse Catalog.

Arrester Rating Duty Cycle kV-RMS	Arrester Maximum Continuous Operating Voltage kV-RMS	Maximum .5 μsec Discharge Voltage kV Crest①	Maximum Switching Surge Protective Level kV-Crest①	Maximum Discharge Voltage With an 8 × 20 μsec Current Wave kV-Crest: 1.5 kA	3.0 kA	5.0 kA	10 kA	20 kA	40 kA
2.7	2.20	7.4	5.5	6.0	6.3	6.6	7.0	7.7	8.9
3.0	2.54	8.5	6.3	6.9	7.2	7.5	8.0	8.7	10.2
4.5	3.70	12.6	9.2	10.2	10.6	11.0	11.8	12.9	15.0
5.1	4.20	14.1	10.4	11.5	12.0	12.4	13.3	14.5	16.9
6.0	5.10	17.2	12.7	14.0	14.6	15.2	16.2	17.7	20.6
7.5	6.10	20.3	15.0	16.5	17.2	17.9	19.1	20.9	24.3
8.5	6.90	22.7	16.9	18.4	19.2	19.9	21.3	23.3	27.1
9.0	7.62	24.8	18.5	20.1	21.0	21.8	23.3	25.5	29.6
10	8.47	28.2	20.8	22.9	23.9	24.8	26.5	29.0	33.7
12	10.3	34.4	25.3	27.9	29.1	30.2	32.3	35.3	41.1
15	12.7	42.3	31.2	34.3	35.8	37.7	39.8	43.5	50.6
18	15.2	50.0	37	40.5	42.3	44.0	47.0	51.4	59.7
21	16.9	56.0	41.5	45.4	47.3	49.2	52.6	57.5	66.9
24	19.5	63.8	47.0	51.7	54.0	56.1	60.0	65.6	76.3
27	22.0	73.3	53.9	59.4	62.0	64.5	68.9	75.3	87.6
30	24.4	80.8	59.8	65.5	68.3	71.0	75.9	83.0	96.5
36	29.3	96.8	71.8	78.5	81.9	85.7	91.0	99.5	116
39	31.7	106	78.0	85.6	89.3	92.8	99.2	108	126
45	37.0	136	91.2	101	105	109	117	128	149
48	39.0	143	95.9	106	111	115	123	134	156
54	42	132	102	108	111	116	123	132	143
60	47	149	115	123	127	131	137	150	164
72	56	180	138	148	151	157	165	180	195
90	71	228	175	187	192	199	209	228	247
96	75	240	184	197	202	210	220	240	260
108	86	275	212	227	232	241	253	276	299
120	94	298	230	246	252	262	275	300	325
132	105	335	265	276	283	293	308	336	364
144	112	358	284	296	303	314	330	360	390
168	127	413	322	335	343	357	375	408	442
172	140	444	350	365	374	389	407	444	481
180	147	459	369	384	393	408	429	481	509
192	152	484	383	399	408	425	446	486	530
228	169	538	426	443	454	472	495	540	585
240	175	574	454	473	485	503	528	576	624
258	210	664	540	547	560	582	610	666	722
264	214	675	550	557	571	592	622	678	735
276	220	694	565	571	586	608	638	696	754
288	227	718	584	591	606	629	660	720	780
300	234	742	604	611	626	650	682	744	806
312	238	754	614	621	637	660	693	756	819
336	252	796	647	655	672	697	731	798	865
360	275	874	711	720	738	765	803	876	949
396	318	1029	808	807	838	865	912	968	1053
420	340	1100	862	860	894	923	973	1032	1120
444	350	1129	886	885	919	949	1000	1062	1160
588	470	1605	1175	1185	1245	1270	1335	1365	1555
612	(Refer to Westinghouse)								

Note ①: Equivalent front-of-wave producing a voltage wave cresting in .50 μsec. Protective level is maximum discharge voltage for a 10 kA impulse current wave on arresters through 360 kV, 15 kA for rating 396 – 444 kV and 20 kA for 588 kV rating.

Table 6.1-6
Westinghouse type IMX surge arrester characteristics.
Source: Westinghouse Catalog.

Rating kV-RMS	Maximum Continuous Operating Voltage	Maximum .5 µsec Discharge Voltage kV-Crest①	Maximum Switching Surge (500A) Protective Level kV-Crest②	Maximum Discharge Voltage with an 8 × 20 µsec Current Wave kV-Crest					
				1.5 kA	3.0 kA	5.0 kA	10 kA	20 kA	40 kA
3	2.8	10.0	7.4	8.0	8.4	8.8	9.4	10.3	11.8
4.5	3.7	13.0	9.6	10.4	10.9	11.4	12.2	13.4	15.3
6	5.1	17.6	13.0	14.1	14.8	15.4	16.5	18.1	20.7
7.5	5.6	19.5	14.4	15.6	16.4	17.1	18.3	20.1	23.0
9	7.6	26.0	19.2	20.8	21.9	22.8	24.4	26.8	30.6
10.5	8.4	29.3	21.8	23.6	24.8	25.9	27.7	30.4	34.7
12	9.2	32.5	24.0	26.0	27.3	28.5	30.5	33.5	38.3
15	11.3	39.0	28.8	31.2	32.8	34.2	36.6	40.2	45.9
18	15.1	52.0	38.4	41.5	43.8	45.6	48.8	53.6	61.2
21	16.5	58.5	43.2	46.7	49.2	51.3	54.9	60.3	68.9
24	18.4	65.0	48.0	51.9	54.7	57.0	61.0	67.0	76.5
27	22.0	78.0	57.6	62.3	65.6	68.4	73.2	80.4	91.8
30	23.8	84.5	62.4	67.5	71.1	74.1	79.3	87.1	99.5
33	25.6	91.0	67.2	72.7	75.6	79.8	85.4	93.8	107
36	28	97.5	72.0	77.9	82.1	85.5	91.5	101	115
39	31	111	81.6	88.2	93.0	96.9	104	114	130
42	33	117	86.4	93.4	98.5	103	110	121	138
45	37	130	96.0	104	109	114	122	134	153
48	39	137	101	109	115	120	128	141	161
51	40	143	106	114	120	125	134	147	168
54	42	150	111	119	126	131	140	154	176
60	47	163	120	130	137	143	153	168	191
72	57	202	149	161	170	177	189	208	237
75	59	208	154	166	175	182	195	214	245
84	66	234	173	187	197	205	220	241	275
90	70	247	183	197	208	217	232	255	291
96	75	267	197	213	224	234	250	275	314
102	80	286	212	228	241	251	268	295	337
108	86	299	216	239	252	262	281	308	352
120	94	325	240	259	274	285	305	335	383

① This is the equivalent fast-front current producing a voltage wave cresting in .5 µsec. The protective level is the maximum discharge voltage for a 10 kA impulse current.
② The switching surge protective level is the maximum discharge voltage produced by slow-front current waves of 500 amps.

Table 6.1-7
Performance characteristics: Type RMX riser pole arresters.
Source: Westinghouse Catalog.

Arrester Rating	MCOV KV RMS	.5 µSEC 10KA Max. IR KV	500A Switching Surge Max. KV	Discharge Voltage KV Crest 8 x 20 µSEC Current Waves KV					
				1.5 KA	3.0 KA	5.0 KA	10.0 KA	20.0 KA	40.0 KA
9	7.65	28.1	19.6	20.1	21.4	22.4	24.0	25.8	27.8
10	8.4	30.2	21.0	21.6	22.9	24.1	25.8	27.7	29.8
12	10.2	37.5	26.1	26.8	28.5	29.9	32.0	34.4	37.1
15	12.7	46.8	32.6	33.5	35.6	37.4	40.0	43.0	46.3
18	15.3	56.2	39.2	40.2	42.7	44.8	48.0	51.6	55.6
21	17	63.1	44.0	45.1	48.0	50.4	54.0	58.0	62.4
24	19.5	72.5	50.5	51.8	55.1	57.8	62.0	66.6	71.7
27	22	81.9	57.0	58.5	62.2	65.3	70.0	75.2	81.0

Table 6.1-8
Impulse breakdown in volts.
Source: Document XI-10.

Impulse Breakdown in Volts

Primary Use	Initial: 100 V/µs Rise Line-to-Ground: Minimum Value	Maximum Average	Maximum Value	Initial: 10 kV/µs Rise Line-to-Ground: Minimum Value	Maximum Average	Maximum Value	End of Life: 100 V/µs Rise Line-to-Ground: Maximum Value	End of Life: 10 kV/µs Rise Line-to-Ground: Maximum Value
A	300	600	750	300	1000	1200	900	1500
B	510	–	1200	510	–	1600	1500	2000
C	–	–	1000	–	–	–	1000	–

NOTE: Dash (–) indicates no criteria.

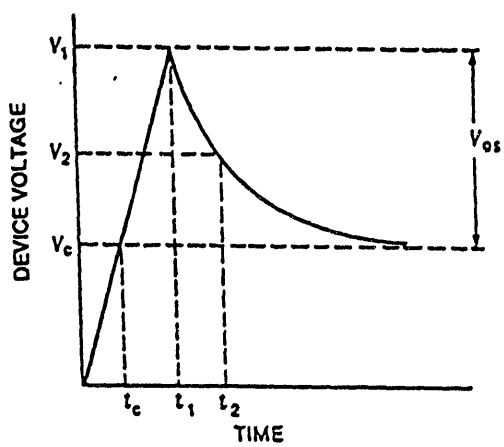

$$V_2 = \frac{V_1 + V_c}{2}$$

V_c = the device clamping voltage for an 8/20 µs current wave form
$V_{os} = V_1 - V_c$ = voltage overshoot
$t_2 - t_c$ = overshoot duration
t_c = the time for the device voltage to reach its clamping voltage
t_2 = the time for the device voltage to decay to 50% of its overshoot value
t_1 = the time for the device voltage to reach its peak value
$t_1 - t_c$ = response time

Fig. 6.1-1. Graph illustrating voltage overshoot, response time, and overshoot duration.
Source: Document XI-9.

power interference. Only a small section is devoted to high-frequency interferences such as EMP and lightning surges. The standard discusses various filters and buffers and what to watch out for in their design and use. Many of the comments and recommendations discussed in Sect. 3.6.2 of this report are covered, but in a very cursory manner. Similarly, the installation recommendations in #518 are very similar to those given in this report and in reports by other HEMP investigators, but again in a very cursory manner. There is a danger that the user of this standard will miss the high-frequency nuances and use only the low frequency recommendations and feel (falsely) that he/she has E_1 and lightning protection. There is a real need, therefore, for a separate standard on grounding and shielding cables for digital equipment and transient applications.

IEEE 525 [XI-16] is a general guide for installing cables in substations. It includes service conditions, performance data, sizing of the cables, coupling and sheath current calculations, fire protection, installation and handling, pulling stress calculations, acceptance tests, conduits and raceways, and trenches and direct burial. The shielding and grounding sections, however, more particularly pertain to the E_1 problem and again the recommendations in the standard are very similar to those given in this report and in reports by other EMP investigators.

Federal Information Processing Standards Publication 94 [XI-19], *Guideline on Electric Power for ADP Installations*, identifies and describes the electrical environment for safe, reliable operation of automatic data processing systems. The electrical environment in and immediately outside the computer rooms is considered. The guide describes the fundamentals that underline the power, grounding, and life-safety requirements and provides a guide and checklist for specifying and preparing automatic data processing sites, and evaluating their suitability. This document is concerned largely with high-frequency disturbances like E_1 surges, but like IEEE 518, it is not complete. Perhaps its material could be factored into the new standard recommended above.

ANSI/IEEE C57.13.3 [XI-4], *Guide for Grounding of Instrument Transformer Secondary Circuits and Cases*, does not specifically address E_1 surges; but its grounding recommendations affect the control circuit layout in the stations. It recommends that the secondary circuits of all current and voltage instrument transformers, irrespective of the number of transformer secondary windings connected to or in that circuit, should be connected to the station ground at only one point. The reasons for using one-point grounding are:

1) To prevent differences in potential (primarily at 60 Hz) in the circuit caused by differences in potential between different points of the ground mat. Differences could cause false operations of the relays.

2) To facilitate the temporary removal and reestablishment of the ground connection for testing purposes.

The cases of instrument transformers and connected equipment such as relays and instruments should also be bonded together and connected to a ground system in accordance with the recommendations of ANSI C1-1987.

IEEE #299 [XI-14] recommends uniform test procedures and estimation techniques to determine the relative effectiveness of room-size high-performance shielding enclosures. Procedures are provided to determine the effectiveness over the frequency ranges from 100 Hz to 20 MHz, from 300 to 1000 MHz, and from 1.7 to 12.4 gigahertz.

6.3 Equipment Withstand Standards

Insulation withstand standards for high voltage equipment such as transformers, circuit breakers, and disconnect switches do not cover the high rates of rise exhibited by E_1 surges, but the various EMP investigators have determined that there should be little difficulty with this equipment due to the relatively low magnitudes and/or protective characteristics of surge arresters.

Relays and control equipment, on the other hand, are low-voltage devices and could be damaged if not designed or protected adequately. Standards have been written to cover this area so that at least for modern devices, there should be no problem.

Standard C37.90.1 [XI-2], for example, defines the two types of surge tests that all modern relays and relay systems must be subjected to, to make them immune to damage and false operations due to various types of surges that may occur in substations. The two types of surges tests are

> Oscillatory SWC wave: This is a wave having a frequency of 1.0 to 1.5 MHz, a voltage crest of 2.5 to 3.0 kV and an envelope decaying to 50% in not less than 6 μseconds (Fig. 6.3-1).
>
> Fast transient SWC wave: This is a unidirectional wave having a rise time from 10 to 90% of no more than 10 ns, a crest of 4 to 5 kV, and a time to half value of 150 ± 50 ns (Fig. 6.3-2).

These test waves are to be applied to all terminals of the relay connected to the outside world. The test generator is coupled to each individual terminal or any like logical group of terminals (i.e. phase 1, phase 2, and phase 3 current circuits) in parallel.

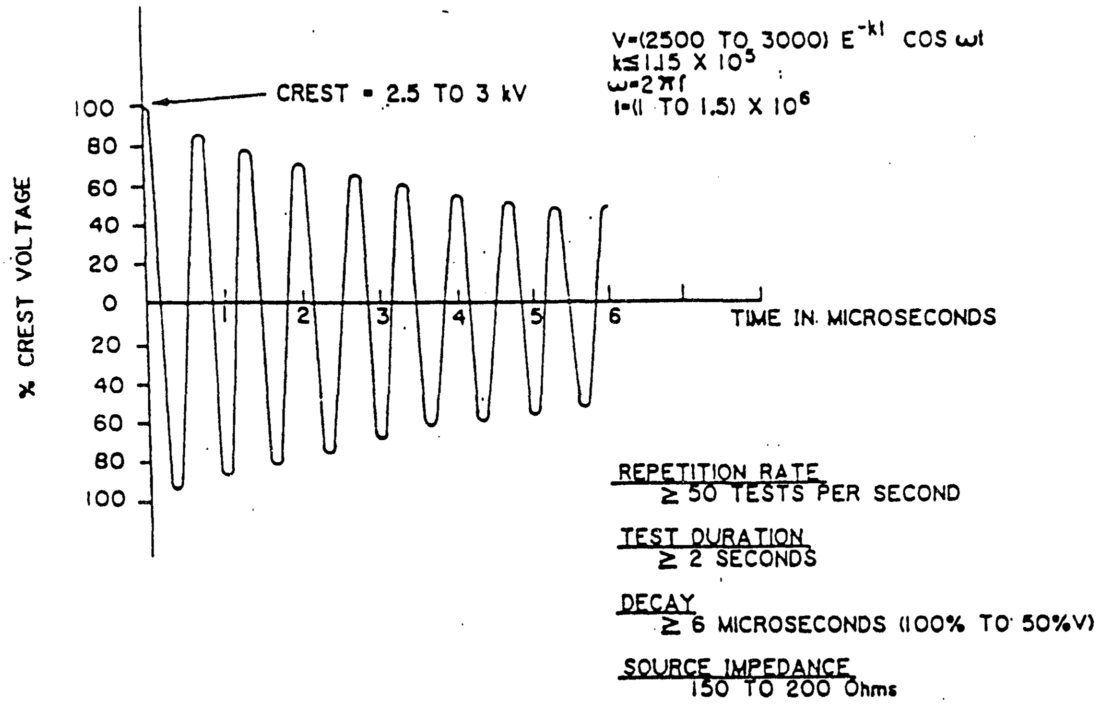

Fig. 6.3-1. Typical oscillatory surge withstand capability test wave (open circuit).
Source: Document XI-2.

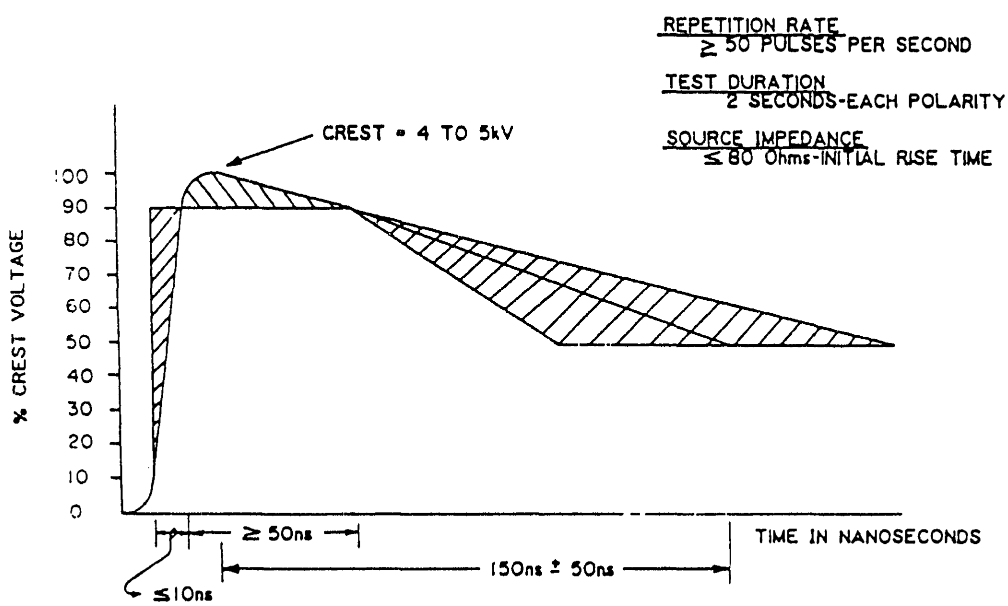

Fig. 6.3-2. Typical fast transient surge withstand capability test wave (open circuit).
Source: Document XI-2.

While specified for relay circuits, these tests are also specified in other equipment standards.

Standard C37.90.2 [XI-17] proposes a common reference and test procedure for evaluating the performance of static protective and control relays and their susceptibility to single-frequency EM fields in the radio frequency domain. While the standard was written to prevent operations due to fields generated by portable or mobile radio transceivers in the substation or control house, it would also seem applicable to fields generated by E_1 pulses. (Caution: see Footnote on p. 46.)

The test setup is shown on Fig. 3.5-6. The relay under test is subjected to EM fields of 10 to 20 V/m. The frequency of the signal is varied over a range of 25 to 1000 MHz at a sweep rate ≤0.005 octaves/s. For frequencies below 50 MHz, the signal shall be amplitude modulated at 90% with a 1000-Hz sine wave. The present 10 to 20 V/m level was selected based on a walkie talkie located no nearer than 1 m from the relay. A proposed revision by the IEEE Relay Committee would reduce this distance to 6 to 12 in. which could increase the field strength 4 to 8 times.

Digital equipment using clocked logic circuits shall also be subjected to EM radiation that is amplitude (pulse or square wave) modulated at a frequency close to 10 kHz but not in synchronism with the digital clock frequency. The 1000-Hz modulation test can be omitted when the 10-kHz modulation test is made.

IEC has tests similar to the ANSI/IEEE tests. Standard IEC 17A-(Sec)-339, "EMC for Secondary Systems for 72.5 kV and above" [XI-3], out for ballot in IEC, specifies three test requirements for input/output and power supply circuits for relays and other secondary equipment. While they specifically address gas insulated substations (GIS), these requirements should apply to all stations.

The first requirement is a 1.2/50 impulse test as described in Sects. E3.3 and E4 of IEC 255-4. The magnitude of the test voltage is 5 kV.

The second requirement is a high-frequency disturbance test described in Sect. E5 of IEC 255-4. The magnitude of this test wave is 2.5 kV (from Table 2 of the subject document). The waveform is a damped oscillatory wave decaying to one-half value in 3 to 6 cycles. Four frequencies should be used: 100 kHz, 1 MHz, 10 MHz, and 50 MHz. The duration should be 2 s and the repetition rate should be ≥50 applications per second.

The third requirement is a burst-shape voltage test as defined in IEC 801, Part 4. The test voltage should be 2.0 kV, as shown in Table 3 of the subject document. The characteristics for the test generator are shown in Sect. 6.1.1 of 801-4. The wave shape of the pulse is shown in Fig. 6.3-3. The rise time of the pulse is 5 ns ± 30%. The duration is 50 ns ± 30%. The repetition rate is 2.5 kHz ± 20%. The burst duration is 15 msec ± 20% with a burst period of 300 msec ± 20%.

6.4 Standards Modifications

As mentioned in the previous sections, most of the standards were written primarily for protection against lightning and switching surges and other common power system disturbances. Most of the requirements also apply to HEMP surges, but certain changes should be made to the existing standards and several new standards should be developed to cover the more extreme characteristics of these types of surges more completely. Some suggested modifications are as follows:

6.4.1 Protective Device Standards

The rates of rise of the applied test voltages and currents for lower voltage (34.5 kV and below) surge arresters should be increased. It has been suggested that a 0.16/0.4 μs wave shape be used for the 1000-, 2000-, and 5000-A discharge voltage test. For arresters having series or parallel gaps, the front-of-wave impulse sparkover tests should use rates of rise of 500 kV/μs for 3 kV and lower rated arresters and (5000/12) kV/μs per each kV of rating for ratings above 3 kV up to 34.5 kV. Whether or not these are practical and could be performed by existing laboratories should be determined by the appropriate standards bodies, in this instance the IEEE Surge Protective Devices Committee and the ANSI C62 Committee.

No E_1 type test waves and protective levels are specified in C62.33 [XI-9] or elsewhere for low-voltage surge protective devices used on ac systems of ≤1000 V rms or on dc systems of ≤1200 V. Magnitudes and waveforms appearing in secondary circuits are needed to classify the environment resulting from HEMP. The data from the unpublished study mentioned in Sect. 3.1 plus the calculated waves developed in the studies of Documents X-1 and X-2 might be used for this purpose. These data could be used by the appropriate standards bodies (again the IEEE Surge Protective Devices and ANSI C62 committees) to develop these new requirements.

6.4.2 Relay Standards

Standard C37.90.1 [XI-2] specifies that the SWC test waves can be applied either to individual terminals or to paralleled groups of like logical terminals. In the latter case, the energy in the test wave is split between the paralleled elements. This energy may be less than that produced by E_1, lightning, or switching surges in utility transmission substations. It is suggested that this standard be changed to

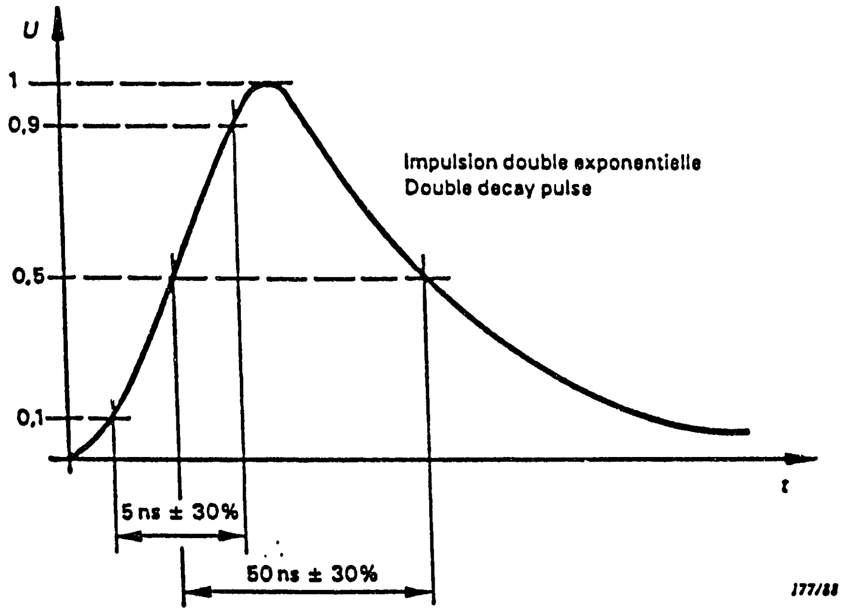

Fig. 6.3-3. Waveshape of a single pulse into a 50 Ω load.
Source: Document XI-3.

require testing each terminal separately. Based on the studies of Documents X-1 and X-2, this change would make the relay, communication, control, and other equipment tested to this standard more secure from these surges.

Standard C37.90.2 [XI-17] presently specifies an EMI test value of 10 to 20 V/m. While the IEEE Power System Relaying Committee (PSRC) is considering raising this value, the value they propose is still quite a bit lower than the fields calculated and measured in high voltage substations from E_1 pulses as well as from lightning and switching surges. Evidently the present test levels are satisfactory for existing installations inside control houses, since no major trouble has been reported. However, in the future, more and more equipment such as data control and acquisition units (DCAUs), will be installed out in the switchyard. Standard test values should be developed for this equipment and applied in non-resonant structures. An IEEE PSRC working group is studying this problem, and the study results from Documents X-1 and X-2 have been supplied to them.

6.4.3 Grounding and Shielding Standards

IEEE Standard 518 [XI-15] purports to cover grounding and shielding practices for all types of interference signals, including E_1 pulses. Its treatment of high-frequency signals, however, is cursory and easy to misinterpret. Considering the ever increasing use of electronic communication, control, and protection systems and digital processing equipment, such misinterpretation could be hazardous. A new standard or guide for protecting this type of equipment from high frequency transient interference, such as E_1, lightning, and switching surges, is recommended. This document could be developed jointly by groups from the Industrial Applications Society (who developed IEEE 518), the Power Engineering Society, and the Electromagnetic Compatibility Society. Some of the material from Federal Information Processing Standard 94 [XI-19] could be factored into the document.

6.4.4 E_3 Standards

Currently there are no standards specifically addressing the equipment capabilities or protective characteristics for E_3 type waves, including GIC. Until more is known about these capabilities or characteristics and practical mitigation measures are developed, standards or guides are not possible. It is hoped that joint studies between the GIC and HEMP communities will soon develop this data. At that time, new standards will be developed or existing standards will be modified accordingly.

7.0 CONCLUSIONS

The many studies, conducted or sponsored by ORNL and others, of the effects of high-altitude nuclear detonations have provided a fairly complete definition of the concerns to be considered by the electric utilities. Based on the results of these studies, published in the unclassified documents listed in Appendix A, the following conclusions have been reached.

If the proper protective practices and procedures specified in standards and utility company guides are followed, the E_1 component of the high-altitude burst should cause relatively minor problems to utility generation and transmission systems. Existing 15-kV-class overhead distribution designs may experience flashovers. The protective measures and equipment capabilities specified for the mitigation of other system transients should also mitigate the E_1 waves. If they are disregarded in actual installations (e.g., allowing excessive surge arrester down leads, improper cable grounding and/or shielding), E_1 failures can occur.

These conclusions are based on the assumed HEMP environments and the results of studies published in the available open literature listed in the Appendix. If the environment existing for an actual high-altitude nuclear detonation is more severe, then individual utilities or the utility systems as a whole could suffer more adverse effects. For example, if the more severe multiple burst scenario of the unpublished study mentioned in Sect. 3.1 should be realistic, then a major portion of the 12-kV and below overhead distribution circuits and the 220-volt residential secondaries could be lost.

The E_1 surges will have their greatest effect on electronic control, communication, and computing equipment. Therefore, proper shielding is extremely important for utility computer control facilities. Protection of utility communication equipment and facilities is not so critical because of the redundancy built into these systems. Most utilities have available various combinations of telephones, mobile radios, power line carriers, and microwaves as backup facilities should their primary system be disrupted by E_1 surges or other disturbances. Fiber optic systems are being used more and more by both telephone and utility companies. This represents a rather secure backup system. Amateur radio operators have also been used in past emergency conditions. They represent an additional communication source.

The relative E_1 hazards to the control and communication equipment will diminish in the future because of the increased use of optoelectronics. Optical voltage and current transducers are already available, although they are in limited use. Predictions are that optical computers will soon replace the present electronic equipment, especially in the larger sizes. With the sensing, computing, and communication all being done with optical systems, the effect of E_1 and other EM transients will become a minor problem in the control of power systems.

The E_3 component of the burst is another matter. Since no universally practical mitigation solution exists, further work needs to be done on this problem. Since the effects of these waves are so similar to those of GIC, as evidenced by the October 28, 1991, K8 geomagnetic storm, mitigation solutions for one will be applicable to the other. This provides added emphasis for solution to the problem.

The following are suggestions for further activities:

1. At any specific site the E_1 surge effects are generally no more harmful than those of lightning, faults, and switching. However, both the simultaneous imposition of these effects and more severe effects on low voltage systems suggest that the study and standards work in these areas should be followed and supported. For example, Sect. 6.4 describes some suggestions for new standards or modifications to existing standards. Briefly these are

    a) Increase the rates of rise of the applied test voltages and currents for lower voltage (34.5 kV and below) surge arresters.

    b) Develop E_1-type test waves and protective levels for low-voltage surge protective devices used on ac systems ≤1000 V rms or dc systems ≤1200 V.

    c) Modify C37.90.1 to require the application of the SWC test waves to each relay terminal separately.

    d) Inform the working group considering modifications to C37.90.2 and the new working group of the Power System Relaying Committee considering equipment installed in the switchyard (as opposed to equipment in the control house) of the magnitude and wave shape of the fields encountered because of lightning and switching surges as well as HEMP.

    e) A new standard or guide for the protection of electronic communication, control and protection, and digital processing equipment against high-frequency transient interference should be developed by a joint group from Power Engineering Society, Electromagnetic Compatability, and the Industrial Applications Society.

    f) When more is known about the effects, capabilities, and mitigation methods for GIC and E_3 surges, new standards should be developed or existing standards modified accordingly.

2. The effect of HEMP on distribution automation deserves further study. How will the E_1 surges affect the communication equipment and the meter packages? A momentary disruption will not hurt, but equipment damage might be a concern. Can equipment be designed to withstand these surges? What protective devices are available? Is the potential damage level sufficiently low that just maintaining an adequate supply of spares will be satisfactory?

   While the amount of distribution automation is very small at present, its use should increase. Equipment capabilities and mitigation methods should be developed now to avoid the expense of possible retrofitting later.

3. Since the E_3 effects are so similar to the effects of GIC, work on detection and mitigation devices or equipment for both should be coordinated and perhaps co-sponsored. For example:

   a) Practical mitigation measures for both GIC and E_3 surges should be developed.

   b) Equipment and protection standards for both surges will be required.

   c) While GIC has definitely damaged transformers, it is "conventionally" considered that the E_3 surges are of insufficient duration to cause damage. Further studies should validate or disprove this opinion. At the very least, the Salem transformer should be reconditioned and tested under a wide range of E_3 conditions.

   d) Existing studies claim that distribution systems are not damaged by E_3 pulses, but indications are that certain consumer electronic devices could be affected. This possibility should be examined.

   e) The impact of E_3 on system protection must be thoroughly examined. If any impacts on the reliability or security of system protection are found, concepts such as adaptive relaying need to be carefully explored. Some utilities in GIC-prone systems send system control and data acquisition signals to desensitize capacitor bank relays. Systems experiencing either GIC or E_3 effects would greatly benefit from a more automatic protective action.

   f) Any attempt to move to an automated adaptive solution may require a careful study of transducer responses under half-cycle saturation conditions. For example, the general response of capacitor voltage transformers may need to be well defined for their transforming of harmonic laden signals.

4. While equipment failures will probably be minimal, there will be system outages because of both the E_1 and E_3 waves. Proper restoration procedures should be developed and adopted for such a contingency.

5. Articles could be written in the various utility journals warning of the potential hazards of not adhering to proper design, installation, and operating procedures. These articles should also stress that while lines and substations may be relatively immune to HEMP and other system transients, communication facilities, including any telephone company facilities, also must be protected. More and more electronics and communication equipment will be used in the future. Utilities should design *now* for electromagnetic compatability against switching, lightning, and fault transients; then HEMP transients, should they ever occur, will be taken care of. If utilities do not design properly for protection now, they may be unable to correct the situation later.

These conclusions and recommendations suggest that if the E_1 and E_3 waves are no more severe than the peacetime stresses impinging on utility systems, then they will have little overall effect on utility operations. A question sometimes raised, however, is whether the toleration of these peacetime stresses depends on redundancy of equipment and quick repair of local failures. If so, EMP stresses, existing system-wide and affecting both the primary and back-up facilities, might cause system-wide outages with which utilities could not cope.

It has also been stated that while experience has taught system designers and operators how to handle peacetime stresses and outages, there has been no such experience with nuclear EMP disturbances. Document I-14 states that there were only 10 to 100 U.S. and Soviet nuclear EMP occurrences prior to the 1962 Nuclear Atmospheric Test Ban and that these involved little or no exposure (a few kV/m) to utility systems. In only one instance, the STARFISH burst in 1962, were any system effects noticed. In this case, 30 strings of series-connected street lights failed on the island of Oahu. So it is true that utility designers and operators have no experience in coping with nuclear EMP outages. However, if the values released in the open literature are accurate, then the results and conclusions reached by the authors of the reference documents and summarized in this report should provide a good indication of the impacts of HEMP on electric power systems.

ACKNOWLEDGEMENTS

The authors wish to express their appreciation to the following for their assistance in supplying many of the documents listed in the Appendix (and in fact authoring a number of them), adding unpublished information to the study, supplying comments during the study, and critiquing the final draft of the report: P. R. Barnes (Oak Ridge National Laboratory), A. R. Hileman (Consultant), J. L. Koepfinger (Duquesne Light Co.), S. L. Nilsson (EPRI), F. M. Tesche (Consultant), E. F. Vance (Consultant), D. R. Volzka (Wisconsin Electric Power Co.), and C. M. Wiggins (BDM Corp.).

APPENDIX A

REFERENCE DOCUMENTS

The following papers, reports, standards, and other documents were reviewed and a summary of one or more pages was prepared for each. They have been broken down into 11 classifications or categories:

I. GENERAL
II. MAGNETOHYDRODYNAMIC ELECTROMAGNETIC PULSE
III. OVERHEAD LINES
IV. CABLES
V. EQUIPMENT
VI. POWER PLANTS
VII. RELAYS
VIII. GROUNDING AND SHIELDING
IX. PROTECTION DEVICES
X. TESTING
XI. STANDARDS

Category I contains general documents covering many aspects of the problem, including the electromagnetic pulse phenomenon itself, the expected magnitudes of the generated fields, the induced voltages and currents, and the effect on the power system with and without the protective devices and practices.

Category II is similar to I except that these documents are primarily concerned with the magnetohydrodynamic electromagnetic pulse phenomena.

Categories III through VII cover the effect on the power system: the lines, cables, transmission and distribution equipment, equipment in the power plants, and relaying.

The documents in Categories VIII and IX discuss the mitigation methods--including the grounding and shielding--and the various protective devices.

Category X covers some of the testing that has been done.

Category XI documents the standards that might apply to the mitigation of the effects of the EMP fields.

Note that for each of these categories, certain basic documents have been listed. These may be considered to be primarily directed at the subject. A number of the documents, however, especially those listed under Category I, contain material pertaining to several categories. These documents are therefore also referred to at the end of each category listing.

I. GENERAL

1. "EMP Engineering & Design Principles" - Bell Laboratory Publication, Whippany, NJ, 1975.

2. "EMP Analysis" - Electric Research & Management Report

3. "Nuclear EMP" - L. C. Martin, Livermore Labs Report.

4. "Electromagnetic Pulse Effects On A Typical Electric Utility System" - D. R. Volzka, IEEE Transactions on Power Apparatus and Systems, Vol. 103, No. 8, pp. 2215-21, Aug. 1984.

5. "A Nominal Set of High-Altitude EMP Environments" - ORNL Report # ORNL/Sub-86-18417/1 - C.L. Longmire, R.M. Hamilton, and J.M. Hahn.

6. March 7,1991, Meeting at State College with presentations by P.R.Barnes, E.F.Vance and F.M.Tesche.

7. "Impacts of a Nominal Nuclear Electromagnetic Pulse on Electric Power Systems - Phase III Final Report" - ORNL Report # ORNL/Sub-83-43374/2 - V.J.Kruse, D.L.Nickel, J.J.Bonk, and E.R.Taylor.

8. "Nuclear Electromagnetic Pulse (EMP) and Electric Power Systems" - ORNL Report #6033. - P.R.Barnes, E.F.Vance and H.W.Askins,Jr.

9. "DOE EMP Review Meeting Program 11/2/1989 - Presentation Abstracts"

10. "Hardening of Telecommunication Networks against Electromagnetic Pulses" - M.W.Wik - Ericsson Review Magazine, Vol. 61, No. 1, 1983, pp. 59-68.

11. "Practical Methods for Electromagnetic Interference Control" - Ericcson Manual LZT 109123 Ue.

12. "Nuclear Electromagnetic Pulse (EMP) Protection Manual for Emergency Broadcast Radio Stations and Emergency Operations Centers" - R.I.Crutcher, M.E.Buchanan, D.C. Agouridis, D.B. Clark, and R.P. Gates II - ORNL Report.

13. "EMP Research on Electric Power Systems - Program Update" ORNL Report ORNL/M-1392 - P.R. Barnes

14. "Differences Between Lightning and Nuclear Electromagnetic Pulse Interactions" - E. F. Vance and M. A. Uman, IEEE Transactions on Electromagnetic Compatibility, Vol. 30, No. 1, pp. 54-62, Feb. 1988.

15. "EMP Pulse Protection" - D.A. Woodford - Prepared by Manitoba Hydro Transmission Planning Dept. for the Canadian Electric Association, June 1984.

Also see Documents [V-1], [V-6], [X-1], [X-2], and [XI-6].

II. MAGNETOHYDRODYNAMIC ELECTROMAGNETIC PULSE

1. "Effects of Solar-Geomagnetic Disturbances on Power Systems" - Special Panel Session Report at the 1989 PES Summer Power Meeting - PES Special Publication 90TH0291-5-PWR.

   a) "Geomagnetic Disturbance Causes and Power System Effects" - V.D. Albertson.

   b) "The Hydro-Quebec System Blackout of March 13, 1989" - D. Larose.

   c) "Transformer DC Excitation Field Tests and Results" - J.G. Kappenman.

   d) "Geomagnetic Effects on Power Transformers" - R.J. Ringlee and J.R. Stewart.

   e) "Investigation of Transformer Overheating Due to Solar Magnetic Disturbances" - P.R. Gattens, R.M. Waggel, R. Girgis, and R. Nevins.

   f) "GIC Effects on Relay and CT Performance" - J.G. Kappenman. D.L. Carlson, and G.A. Sweezy.

   g) "Measurement and Instrumentation for Disturbance Monitoring of Geomagnetic Storm Effects" - V.D. Albertson.

   h) "Real-Time Monitoring and Predicting of Geomagnetic Activity" - C.C. Balch.

   i) "Mitigation Techniques to Block GIC" - V.D. Albertson and J.G. Kappenman.

   j) "A Researchers Point of View" - F.S. Young.

2. "Geomagnetic Storm Cycle 22: Power System Problems on the Horizon" - Special Panel Session Report at the 1990 PES Summer Meeting - PES Special Publication 90TH0357-4-PWR.

a) "Solar Effects on Communications" - Working Group on Solar Effects of the IEEE Communications Committee.

b) "The Effects of Solar Magnetic Disturbances on Protective Relaying" - Working Group K11 of the Power System Relaying Committee.

c) "The Effect of GIC on Power Transformers" - W.J. McNutt.

d) "GIC Mitigation: A Neutral Blocking/Bypassing Device to Prevent the Flow of GIC in Power Systems" - J.G. Kappenman, S.R. Norr, G.A. Sweezy, D.L. Carlson, V.D. Albertson, J.E. Harder, and B.L. Damsky.

e) "Potential Economic Costs from Geomagnetic Storms" - P.R. Barnes, and J.W. Van Dyke.

f) "System Operation Guidelines During Magnetic Storms" - J.Z. Ponder.

g) "Effect of Geomagnetically-Induced Currents on Static Var Compensators" - E.V. Larsen and J.M. Cutler.

h) "Measuring GIC in Power Systems" - D.A. Fagnan, P.R. Gattens, and R.D. Johnson.

i) "GIC Measurement System in Japan" - I. Iyoda, S. Yanese, and H. Kuratani.

j) "An Integrated GIC Monitoring System" - W.E. Feero.

k) "The SUNBURST Network" - B.L. Damsky and W.E. Feero.

l) "Windsock: A Solar Wind Monitor Satellite for Geomagnetic Storm Alerts" - G. Heckman, and R.D. Zwicki.

3. "Geomagnetically-Induced-Current (GIC) Effects on Electric Power Systems" - Special Panel Session Report at the 1991 Power Engineering Society Transmission and Distribution Conference.

a) "Geomagnetic Storm Phenomena and Effects Overview" - V. Albertson.

b) "Summary of March 13, 1989 Geomagnetic Storm Effects" - G. Gucchi and J. Ponder.

c) "Transformer DC Injection Tests" - A. Dutil.

d) "Neutral Blocking/Grounding Device and DC Injection Tests" - J. Kappenman.

e) "GIC Mitigation Methods and Considerations" - E.R. Taylor and V. Albertson.

f) "GIC Prediction from Magnetometer Data" - T.A. Wakely.

g) "Comparisons Between Changes in the Geomagnetic Field and the Geomagnetically-Induced-Currents in a Power Transmission System" - R.L. Coles, K. Thomson, and G.J. van Beek.

h) "Sunburst: North American Geomagnetic Disturbances Effects Monitoring" - W.E. Feero and J. Porter.

i) "Windsock: Solar Wind Monitoring and GMD Alerting" - J. Kappenman.

4. "Electric Utility Industry Experience With Geomagnetic Disturbances" - ORNL Report # 6665 - P.R. Barnes, D.T. Rizy, B.W. McConnell, F.M. Tesche, and E.R. Taylor.

5. "Characteristics of Transformer Exciting Current During Geomagnetic Disturbances" - R.A. Walling and A.H. Khan <u>IEEE Transactions on Power Delivery</u>, Vol. 6, No.4, Oct. 1991, pp. 1707-14.

6. "Calculation Techniques and Results of Effects of GIC Currents as Applied to Two Large Power Transformers" - R.S. Girgis and C.D Ku - <u>IEEE Transactions on Power Delivery</u>, Vol. 7, No.2, April 1992, pp. 699-705.

7. "Solar Induced Currents in Power Systems: Cause and Effects" - V.G. Albertson, J.M. Thorson, R.E. Clayton, and S.C.Tripathy, <u>IEEE Transactions on Power Apparatus and Systems</u>, Vol. PAS 92, March/April 1973, pp. 471-77.

8. "The Effects of Geomagnetic Storms on Electric Power Systems" - V.G. Albertson, J.M. Thorson, and S.A. Miske, <u>IEEE Transactions on Power Apparatus and Systems</u>, Vol. PAS 93, July 1974, pp. 1031-44.

9. "Harmonics and Switching Transients in the Presence of GIC" - N. Mohan, J.G. Kappenman, and V.G. Albertson, <u>IEEE Transactions on Power Apparatus and Systems</u>, Vol. PAS 100, Feb. 1981, pp. 585-93.

10. "Load Flow Studies in the Presence of GIC" - V.G. Albertson, J.G. Kappenman, N. Mohan, and G.A. Skarbakka, IEEE Transactions on Power Apparatus and Systems, Vol. PAS 100, Feb. 1981, pp. 594-601.

11. "Current Transformer & Relay Performance in the Presence of GIC" - J.G. Kappenman, V.G. Albertson, and N. Mohan, IEEE Transactions on Power Apparatus and Systems, Vol. PAS 100, March 1981, pp. 1078-88.

12. "Effect of DC Excitation on Instrument Transformers" - J.D Aspnes, and R.P Merritt, IEEE Transactions on Power Apparatus and Systems, Vol. PAS 102, Nov. 1983, pp. 3706-12.

13. "Effects of Geomagnetically Induced Currents in the B.C. Hydro 500 kV System" - D.H. Boteler, R.M. Shier, T. Watanabe, R.E. Horita, IEEE Transactions on Power Delivery, Vol.4, No.1, Jan.1989, pp.818-23.

14. "A Methodology to Asses the Effects of Magneto-hydrodynamic Electromagnetic Pulse (MHD-EMP) on Power Systems" - J. R. Legro, N. C. Abi-Samra, J. C. Crouse, and F. M. Tesche, IEEE Transactions on Power Delivery, Vol. PWRD-1, No. 3, pp.203-210, July 1986.

15. "Simulation of Geomagnetic Currents Induced in a Power System by Magnetohydrodynamic Pulses" - G. B. Rackliffe, J. C. Crouse, J. R. Legro, and V. J. Kruse, IEEE Transactions on Power Delivery, Vol. PWRD-3, No. 1, pp. 392-97, Jan. 1988.

16. "Load Flow Studies in the Presence of Magnetohydrodynamic Electromagnetic Pulse" - V. J. Kruse, G. B. Rackliffe, and P. R. Barnes, IEEE Transactions on Power Delivery, Vol. 5, No. 2, pp. 1158-63, April 1990.

17. "MHD-EMP Interaction With Power Transmission and Distribution Systems" - ORNL Report # ORNL/Sub/90-SG828U/1 - F.M. Tesche, P.R. Barnes, and A.P. Meliopoulos.

18. "Results of an Experiment to Determine the Impact of Quasi-dc Currents on Three-Phase Distribution Transformer Installations" - ORNL-6670 (to be published)- B.W. McConnell, P.R. Barnes, and F.M. Tesche.

19. "Mitigation of Magnetohydrodynamic Electromagnetic Pulse (MHD-EMP) Effects from Commercial Electric Power Systems" - ORNL Report # ORNL-6709 - P.R. Barnes, F.M. Tesche, and E.F. Vance.

20. "Measured Effects of GMD on Power Systems (SUNBURST Status Report) - EPRI Project RP 3211-01" - R.L. Lesher, W.E. Feero, and J. Porter, Doble Conference Paper, April 8, 1992.

21. "Mitigation Of Geomagnetically Induced and DC Stray Currents" - J.W. Porter, (EPRI Project Manager), et al, EPRI Report El-3295, Project 1770-1, Final Report December 1983, prepared by Minnesota Power & Light Co., Duluth, MN.

22. "Study to Assess the Effects of Magnetohydrodynamic Electromagnetic Pulse on Electric Power Systems - Phase I - Final Report" - ORNL Report # ORNL/Sub/83/43374/1/V3 - J.R. Legro, N.C. Abi-Samra, and F.M. Tesche.

Also see References [I-6], [I-7], [I-13],and [VIII-5].

III. OVERHEAD LINES

1. "Coupling to Shielded Cables", E. F. Vance, (book), John Wiley & Sons, New York, 1978.

2. "The Steep-Front, Short-Duration Pulse Characteristics of Distribution Insulators with Wood" - S.Grzybowski, and P. B. Jacobs, IEEE Transactions on Power Delivery, Vol. 5, No. 3, pp. 1608-1616, July 1990.

3. "An Estimation of Lightning Insulation Level of Overhead Distribution Lines" - P. B. Jacobs, S. Grzybowski, and E. R. Ross, IEEE Transactions on Power Delivery, Vol. 6, No. 1, pp. 384-90, Jan. 1991.

4. "Impacts of a Nominal Nuclear Electromagnetic Pulse on Electric Power Systems: A Probablistic Approach" - V. J. Kruse, D. L. Nickel, E. R. Taylor, J. J. Bonk, P. R. Barnes, IEEE Transactions on Power Delivery, Vol. PWRD-6, No. 3, pp.1251-63, July 1991.

5. "Flashover Vulnerability of Transmission and Distribution Lines to High Altitude Electromagnetic Pulse (HEMP)" -V. J. Kruse, F. M. Tesche, T. K. Liu, and P. R. Barnes, IEEE Transactions on Power Delivery, Vol. 5, No. 2, pp. 1164-69, April 1990.

6. "The HEMP Response of an Overhead Power Distribution Line" - F. M. Tesche and P. R. Barnes, IEEE Transactions on Power Delivery, Vol. 4, No. 3, pp. 1937-44, July 1989.

7. "The Effects of Steep-Front, Short-Duration Impulses on Power Distribution Components" - D. B. Miller, A. E. Lux, S. Grzybowski, and P. R. Barnes, IEEE Transactions on Power Delivery, Vol. 5, No. 2, pp. 708-15, April 1990.

8. "The Steep-Front Short-Duration Impulse Strength of Power Distribution Lines" - P.R. Barnes - Draft Report

Also see Documents [I-1], [I-4], [I-5], [I-6], [I-7], [V-6], and [VIII-2].

IV. CABLES

1. "Effects of Voltage Impulses on Solid Dielectric Cable Life" - R.A. Hartlein, V.S. Harper and H.W.Ng, Proposed Paper for IEEE/PES.

Also see Documents [I-1], [I-5], [I-10], [III-1], [III-7], [VIII-2], and [XI-16].

V. EQUIPMENT

1. "Surge Arrester Protection and Very Fast Surges" - R. E. Clayton, I. S. Grant, D. E. Hedman, and D. D. Wilson, IEEE Transactions on Power Apparatus and Systems, Vol. 102, No. 8, pp. 2400-2412, Aug. 1983.

2. "Experimental Determination of the Effects of Steep-Front Short-Duration Surges on 25 kVA Pole-Mounted Distribution Transformers" - C. H. Eichler, J. R. Legro and P.R. Barnes, IEEE Transactions on Power Delivery, Vol. PWRD-4, No. 2, pp. 1103-09, April 1989.

3. "Steep Front Short Duration Low Voltage Impulse Performance of Distribution Transformers" - L. M. Burrage, E. F. Veverka, and B. W. McConnell, IEEE Transactions on Power Delivery, Vol. 2, No. 4, pp. 1152-56, Oct. 1987.

4. "Impulse Voltage Strength of AC Rotating Machines" - IEEE Working Group Progress Report, IEEE Transactions on Power Apparatus and Systems, Vol. PAS-100, No. 8, pp. 4041-47, August, 1981.

5. "HEMP Test and Analysis of Selected Recloser Control Units" - T. K. Liu, S. H. Sands, F. M. Tesche, and P. R. Barnes, Report # ORNL/Sub/88--02238/1.

6. "Impact of Steep-Front Short-Duration Impulse on Electric Power System Insulation - Phase II: Laboratory Evaluation of Selected Power System Components" - L. M. Burrage, E. F. Veverka, J. H. Shaw, and B. W. McConnell - Report # ORNL/Sub/85-28611/2.

Also see Documents [I-6], [I-7], [III-4], [III-6], [III-7], and [IX-1].

VI. POWER PLANTS

See Documents [I-4], [I-7], and [V-4].

VII. RELAYS

1. "Effects of EMP on Protective Relaying Systems" - Power System Relaying Committee Report.

2. "Steep Front Impulse Flashover Tests on a Solid-State Relay" - T. M. Salas, C. M. Wiggins, and P. R. Barnes, IEEE Transactions on Power Delivery, Vol. 5, No. 3, pp. 1281-87, July 1990.

3. "On the HEMP Environment for Protective Relays" - Thomas, Wiggins, Salas, & Barnes Draft, to be published in IEEE Transactions on Power Delivery.

4. "Switching Transient Fields in Substations" - C. M. Wiggins, and S. E. Wright, IEEE Transactions on Power Delivery, Vol. 6, pp. 591-600, April 1991.

5. "Some Expected EMI Effects Due to Switching of Electromechanical Relays" - E.B.Joffe - Paper 26 F3, pp.131-36.

See also Documents [I-4], [VIII-5], [X-1], [XI-3], and [XI-17].

VIII.GROUNDING AND SHIELDING

1. "EMI Practical Fixes" - Interference Control Technologies, Inc.

2. "EMP Engineering Practices Handbook - NATO" - NATO File No. 1460-3

3. "Recommendations for Electric Utilities" - P. R. Barnes - December 1989 - To be published by Livermore National Laboratory

4. "Grounding and Shielding Electronic Instrumentation" - Dr. T. P. Van Doren - Short Course Notes.

5. "Mitigation Measures for the Effects of the High-Altitude Electromagnetic Pulse in the Electric Power System - Task Report" -E. R. Taylor, Jr. - AST ABB Report 89-2160 to ORNL.

6. "Electromagnetic Shielding of a System Computer in a 230 kV Substation" - S. M. Harvey and W. J. Panke IEEE Transactions on Power Apparatus and Systems, Vol. PAS-95, No. 1, pp. 187-196, Jan/Feb 1976.

7. "Cable Grounding for the Control of EMI" - E. F. Vance, EMC Technology Magazine, Jan-March, 1983, pp. 54-58.

8. "Summary Report for Microwave Communication Installations for the Wisconsin Electric Power Co." - E. F. Vance.

See also Documents [I-1], [I-4], [I-5], [I-6], [I-10], [I-11], [I-12], [III-1], [XI-4], [XI-15], and [XI-16].

IX. PROTECTION DEVICES

1. "The Response of MOV and SiC Arresters to Steep-Front Longer Duration Current Pulses" - D. B. Miller, H. B. Fan, and P. R. Barnes, IEEE Transactions on Power Delivery, Vol. 6, No. 2, pp. 666-71, April, 1991.

2. "Steep-Front Short-Duration Voltage Surge Tests of Power Line Filters and Transient Voltage Suppressors" - P. R. Barnes and T. L. Hudson, IEEE Transactions on Power Delivery, Vol. 4, No. 2, pp. 1029-36, April 1989.

3. "Behavior of MO-Surge-Arrester Blocks to Fast Transients" W. Schmidt, J. Meppelink, B. Richter, K. Feser, L. Kehl, and D. Qiu, IEEE Transactions on Power Delivery, Vol. 4, No. 1, pp. 292-300, Jan. 1989.

4. "Lightning and NEMP Transient Protection with Metal Oxide Varistors" - F. D. Martzloff - 7/8/81 Report

5. "Selecting Varistor Clamping Voltage: Lower Is Not Better" - F. D. Martzloff and T. F. Leedy - Paper 27 F4, pp.137-42.

See also Documents [I-1], [I-5], [I-7]], [I-11], [I-12], [III-7], [V-6], [VIII-1], [VIII-2], [VIII-3], and [VIII-5].

X. TESTING

1. "Electromagnetic Transients in Substations - Vol. I: Project Summary and Recommendations " EPRI RP2674-1 Draft Final Report, Electric Power Research Institute, Palo Alto, CA 94304, February 1992 - C. M. Wiggins, F. S. Nickel, T. M. Salas, and D. E. Thomas.

2. "HEMP-Induced Transients in Electric Power Substations - Final Report" - ORNL Report ORNL/Sub-88-SC863 - C. M. Wiggins, D. E. Thomas, and T. M. Salas.

3. "Some Characteristic Signatures of Power Disturbances on AC Mains" - A. McEachem - Paper 25 F2, pp.125-30.

See also Documents [VII-4] and [XI-2].

XI. STANDARDS

1. "EMP Related Standards" - J. L. Koepfinger

2. "IEEE Guide for Surge Withstand Capability (SWC) Tests - ANSI/IEEE C37.90.1-1989" - IEEE Power Systems Relay Committee

3. "IEC 17A-(Sec)-339 EMC for Secondary Systems for 72.5 kV and above GIS"

4. "Guide for Grounding of Instrument Transformer Secondary Circuits and Cases - ANSI/IEEE C57.13.3-1983"

5. "IEEE Standard for Gapped Silicon-Carbide Surge Arresters for AC Power Circuits - ANSI/IEEE C62.1-1989"

6. "IEEE Guide for the Application of Gapped Silicon-Carbide Surge Arresters for Alternating Current Systems - ANSI/IEEE C62.2-1987"

7. "IEEE Standard for Metal-Oxide Surge Arresters for AC Power Circuits - ANSI/IEEE C62.11-1987"

8. "IEEE Standard Test Specifications for Gas-Tube Surge-Protective Devices - ANSI/IEEE C62.31-1987"

9. "IEEE Standard Test Specifications for Varistor Surge-Protective Devices - ANSI/IEEE C62.33-1989"

10. "American National Standard for Gas-Tube Surge-Arresters on Wire Line Telephone Circuits - ANSI C62.61-1985"

11. "IEEE Guide for Surge Voltages in Low-Voltage AC Power Circuits - ANSI/IEEE C62.41-1980"

12. "IEEE Guide for the Application of Gas Tube Arrester Low Voltage Surge-Protective Devices - ANSI/IEEE C62.42-1987"

13. "IEEE Guide on Surge Testing for Equipment Connected to Low-Voltage AC Power Circuits - ANSI/IEEE C62.45-1987"

14. "IEEE Recommended Practice for Measurement of Shielding Effectiveness of High-Performance Shielding Enclosures - IEEE Std. 299-1969 (Trial Use)"

15. "IEEE Guide for the Installation of Electrical Equipment to Minimize Electrical Noise Inputs to Controllers from External Sources - IEEE Std. 518-1982"

16. "IEEE Guide for the Design and Installation of Cable Systems in Substations ANSI/IEEE Std. 525-1987"

17. "IEEE Trial Use Standard Withstand Capability of Relay Systems to Radiated Electromagnetic Interference from Transceivers - ANSI/IEEE C37.90.2-1987" - IEEE Power Systems Relay Committee

18. "Guide on Shielding Practice of Low Voltage Cables" - In preparation as Draft #6 of IEEE P1143 by Subcommittee #9 of the IEEE/PES Insulated Conductors Committee.

19. "Guideline on Electric Power for ADP Installations" - Federal Information Processing Standards (FIPS) Publication #94.

Also see Documents [V-4], [VIII-5], [X-1], and [X-2].

INTERNAL DISTRIBUTION

1-10. P. R. Barnes
11. G. E. Courville
12. C. W. Curtis
13. P. S. Gillis
14. M. A. Kuliasha
15. B. W. McConnell
16. D. T. Rizy
17. R. B. Shelton
18. J. N. Stone
19. J. P. Stovall
20. ORNL Patent Office
21. Central Research Library
22. Document Reference Section
23-25. Laboratory Records
26. Laboratory Records-RC

EXTERNAL DISTRIBUTION

27. Ram Adapa, EPRI, P.O. Box 10412, Palo Alto, CA 94303.

28. R. B. Adler, Philadelphia Electric Co., 2301 Market Street N-31-1, Philadelphia, PA 19101.

29. A.J. Adoue, Louisiana Power & Light, 142 Delaronde, New Orleans, LA 70140.

30. V. D. Albertson, Dept. of Electrical Engineering, University Of Minnesota, 123 Church Street, S.W., Minneapolis, MN 55455.

31. L.H. Alesi, N.Y. State Electric & Gas, 4500 Vestal Pkwy, Binghamton, NY 13902.

32. R.W. Alexander, PP&L, N4, 2N. 9th Street, Allentown, PA 18101.

33. J.G Anderson, 1101 West Street, Pittsfield, MA 01201.

34. G. Applegren, Main Coordination Center, 1n301 Swift Road, P.O. Box 278, Lombard, Illinois 60148.

35. J.C. Appleyard, Wisconsin Power & Light, 500 Townline Rd., Rte 3, Beloit, WI 53511.

36. R.H. Arndt, RTE Corp., Components Div., 1045 Hickory Street, Pewaukee, WI 53072.

37. G. H. Baker, HQ DNA/RAEE, 6801 Telegraph Road, Alexandria, VA 22310-3398.

38. C.W. Barnett, Texas Utilities Electric, 400 N. Olive St. (LB81), Dallas, TX 75201.

39. G. D. Birney, Western Area Power Administration, P. O. Box 3402, Golden, CO 80401.

40. J. Bladow, Western Area Power Admin., Box 3402, A2110, Golden, CO 80401.

41. P. D. Blair, Energy and Materials Program, Congress of the United States, Office of Technology Assessment, Washington, DC 20510.

42. Ellery Block, SAIC, 6725 Odyssey, Huntsville, AL 35806-3301.

43. L. Bolduc, Hydro Quebec, 1800 Montee Ste Julie, Varennes, QC, Canada, J3X 1S1.

44. A. Bonner, McGraw Edison Co.,, Systems Engineering, P.O. Box 100, Franksville, WI 53126.

45. B. Bozoki, Ontario Hydro, 700 University Ave. (H10), Toronto, Ont., CANADA M5G1X6.

46. E. H. Brehm, Dipl.-Ing., ASEA Brown Boveri AG, Postfach 351, Abt. GK/NP 25, 6800 Mannheim 1, Germany.

47. Larry Bressler, Western Area Power Administration, P. O. Box 3402, Golden, CO 80401.

48. G.D. Breuer, General Electric Co., Transmission Systems, 1 River Road, Bldg. 2-605, Schenectady, NY 12345.

49. Bob Brewer, Office of Energy Management, U.S. Dept. of Energy, CE-141, 5G-023/FORS, 1000 Independence Ave., SW, Washington, DC 20585.

50. W. J. Budney, Distribution Systems, Public Service Electric & Gas Co., 80 Park Plaza, Newark, NJ 07101.

51. J.J. Burke, Power Technologies Inc., 1482 Erie Blvd., Schenectady, NY 12305.

52. R.O. Burnett, Georgia Power, P.O. Box 4545, 2/333, Atlanta, GA 30302.

53. A.A. Burzese, Tennessee Valley Authority, 1S 35B Signal Place, Chattanooga, TN 37402.

54. H. S. Cabayan, Lawrence Livermore National Laboratory, P.O. Box 5504, L-81, Livermore, CA 94550.

55. R. F. Campbell, Transmission & Electrical Projects, Tennessee Valley Authority, 3N 53A Missionary Ridge Place, Chattanooga, TN 37402-2801.

56. J.P. Castillo, R&D Associates, P.O. Box 9377, Albuquerque, NM 87119-9377.

57. C.H. Castro, Public Service Electric & Gas, P.O. Box 570, Code T19M, Newark, NJ 07101.

58. J. Chadwick, 902 Glamis Circle, Signal Mountain, TN 37377.

59. K.R. Chakravarthi, Southern Co. Services, P.O. Box 2625, Birmingham, AL 35202.

60. S.R. Chano, Hydro Quebec, 855 Ste. Catherine E., 20th Floor, Montreal, Quebec H2L 4P5, CANADA.

61. M. Charest, Hydro Quebec, 75 Dorchester West, Montreal, Quebec H2Z 1A4, CANADA.

62. Vern Chartier, Bonneville Power Admin., Division of Labs, Box 491 E1, Vancouver, WA 98666.

63. A. Chodorow, Mission Research Corp., 1720 Randolph Rd. SE, Albuquerque, NM 87106-4245.

64. D. J. Christofersen, Manager, Electrical Engineering Division, United Power Association, P. O. Box 800, Elk River, MN 55330-0800.

65. P. Chrzanowski, Evaluation & Planning Program, Lawrence Livermore National Lab, P.O. Box 808, L-81, Livermore, CA 94550.

66. R. F. Chu, Research Engineer, Philadelphia Electric Co., Research Division (S10-1), 2301 Market Street, Philadelphia, PA 19101.

67. D.M. Clark, Duke Power, Box 1010, Charlotte, NC 28201.

68. T. Clark, Phoenix Electric Corp., P.O. Box 53, Readville Station, Boston, MA 02137.

69. W.T. Clarke, Burns & McDonnell, P.O. Box 419173, Kansas City, MO 64141.

70. A. Clerici, Engineering Info. Tech, Sadelmi, Via Pergolesi 25, Milano, Italy 20124.

71. F.M. Cleveland, ECC, 1530 The Alameda, San Jose, CA 95126.

72. S. Cluts, Sargent & Lundy, Engineers, 55E Monroe, Chicago, IL 60603.

73. W.H. Cole, 788 Fairgate Dr., Hendersonville, NC 28739.

74. Lynn Coles, Principal Policy Advisor, SERI, 1617 Cole Boulevard, Golden, CO 80401.

75. O. R. Compton, Richmond Plaza, P. O. Box 26666, Richmond, Virginia 23261.

76. S.P. Conrad, Public Service Co. of N.M., Alvarado Square, Albuquerque, NM 87158.

77. T. B. Cook, 80 Castlewood Dr., Pleasanton, CA 94566.

78. G. H. Coplon, U.S. Department of Energy, Rm. 8F089, 1000 Independence Avenue, S.W., Washington, DC 20585.

79. W.T. Croker, 595 Rowland Rd., Stone Mountain, GA 30083.

80. G.A. Cucchi, Philadelphia Electric Co., 2301 Market Street, Philadelphia, PA 19101.

81. Dave Curtice, T/Systems, 480 San Antonio Road, Suite 200, Mountain View, CA 94040.

82. S. J. Dale, Manager Transmission Technology Institute, ABB Power T&D Company Inc., Centennial Campus, 1021 Main Campus Drive, Raleigh, NC.

83. B. Damsky, EPRI, P.O. Box 10412, Palo Alto, CA 94303.

84. A.N. Darlington, Tampa Electric, P.O. Box 111, Tampa, FL 33601.

85. G.A. Davidson, Stone & Webster Eng., P.O. Box 5406, Denver, CO 80217.

86. D.C. Dawson, Southern California Edison, P.O. Box 800, R295, Rosemead, CA 91770.

87. R.W. Dempsey, Potomac Electric Power, 1900 Pennsylvania Ave., NW, Washington, DC 20068.

88. F.A. Denbrook, 3457 Loren Rd., Jackson, MI 49203.

89. A.E. DiBiase, Ohio Edison, CAPCO Office, 48 First St. NE, Massillon, OH 44308.

90. C.C. Diemond, 4840SW Fairhaven Ln., Portland, OR 97221.

91. H. Disante, Kansas Gas & Electric, P.O. Box 208, Wichita, KS 67201.

92. J.J. Dougherty, 4766 Calle De Lucia, San Jose, CA 95124.

93. D.A. Douglass, Power Technologies, Inc., P.O. Box 1058, Schenectady, NY 12301.

94. P.R. Drum, Duke Power, P.O. Box 1010, WL02G, Charlotte, NC 28201.

95. Raymond Dunlop, Director of Research, New England Power Service Co., 25 Research Drive, Westborough, MA 01582.

96. L.L. Dvorak, Western Area Power Administration, P.O. Box 3402, Golden, CO 80401.

97. H. Elahi, General Electric Co., 1 River Road, Schenectady, NY 12345.

98. H. Elbadaly, Underground T&D Research Manager, Consolidated Edison Company, 4 Irving Place, New York, NY 10003.

99. F.J. Ellert, Ellert Consulting Group, Inc., 37 Via Maria Dr., Scotia, NY 12302.

100. J.T. Emery, Virginia Power, P.O. Box 26666, Richmond, VA 23261.

101. J.C. Engimann, Commonwealth Edison Co., 13195 First Ave., Maywood, IL 60153.

102. D. Fagnan, Philadelphia Electric Co., 2301 Market Street, Philadelphia, PA 19101.

103. G.V. Fantozzi, EBASCO Services, 1280 Wall Street West, Lyndhurst, NJ 07071.

104. E.C. Fennell, Florida Power & Light, P.O. Box 14000, Juno Beach, FL 33408.

105. G. Fenner, ABB, P.O. Box 341, Bloomington, IN 47402.

106. R.J. Fernandez, Pennsylvania Power & Light, 2 North 9th St., Allentown, PA 18101.

107. W. E. Ferro, Electric Research and Management, Inc., P.O. Box 165, State College, PA 16804.

108. L.H. Fink, Wisconsin Electric Power Co., 333 W. Everett St., A264, P.O. Box 2046, Milwaukee, WI 53201.

109. D.J. Finley, Illinois Power, 500 S. 27th. Street, Decatur, IL 62525.

110. W.G. Finney, 1212 Northwood Lane, Muscatine, IA 52761.

111. W.N. Fredenberg, Rochester Gas & Electric, 89 East Avenue, Rochester, NY 14649.

112. C.W. Fromen, Houston Lighting & Power, P.O. Box 1700, Houston, TX 77251.

113. Larry Fry, Teledyne Brown Engineering, MS-50, 300 Sparkman Dr., Huntsville, AL 35807-7007.

114. D. Fulton, Seattle City Light, 1015 Third Ave., RM 216, Seattle, WA 98104.

115. Hugh Gardner, 7466 Twin Brook Drive, Chattanooga, TN 37421.

116. R. Gates, EMP Program Manager, FEMA, RM 606, 500 C Street, S.W., Washington, DC 20472.

117. P. R. Gattens, Allegheny Power, 800 Cabin Hill Dr., Greensburg, PA 15601.

118. M. R. Gent, President, North American Electric Reliability Council, 101 College Road East, Princeton, New Jersey 08540-8060.

119. T. Gentile, Eastern Edison, P.O. Box 471, 110 Mulberry St., Brockton, MA 02402.

120. Bill Getson, E-Systems, Inc., ECI Division, MS-31, P.O. Box 12248, St. Petersburg, FL 33730.

121. D.A. Gillies, 65460 E. Sandy River Ln., Rhododendron, OR 97049.

122. E.J. Goodwin, Sverdrup Technology/TLMRC, 100 Research Drive, P.O. Box 220, Haslet, TX 76052.

123. M. Grady, University of Texas/Austin, Department of EE, Engineering Science Building, Austin, TX 78712.

124. M. Granger, Hydro-Quebec, Planning Systems Division, 855 East Ste-Catherine, 20 ieme etage, Montreal, Quebec, Canada, H2L 4PS.

125. I.S. Grant, Power Technologies Inc., P.O. Box 1058, Schenectady, NY 12301.

126. T. Grebe, Electrotek Concepts, Inc., 10305 Dutchtown Rd., Suite 103, Knoxville, TN 37932.

127. J. D. Gregory, Southern Company Services, Inc., P. O. Box 2625, Birmingham, AL 35202-2625.

128. S.E. Grier, Dayton Power & Light, P.O. Box 1247, Dayton, OH 45401.

129. I. Gyuk, Program Manager, U.S. Department of Energy, 1000 Independence Ave., S.W., Washington, DC 20585.

130. R.W. Haas, Cincinnati Gas & Electric, P.O. Box 960, Cincinnati, OH 45201.

131. J.G. Hanson, Western Power Administration, P.O. Box 3402, A2220, Golden, CO 80401.

132. J.E. Harder, Westinghouse Electric Corp., T&D Components Division, P.O. Box 341, Bloomington, IN 47402.

133. E.L. Harris, 46 Boonstra Drive, Wayne, NJ 07470.

134. R.E. Hart, Seattle City Light, 1015 3rd Ave., RM 216, Seattle, WA 98104.

135. D.R. Hemming, L.A. Dept. of Water & Power, 1630 N. Main St., Bldg 7, Los Angeles, CA 90051.

136. W.S.C. Henry, 5273 Villa Majorca Ct., Sarasota, FL 34235.

137. C.F. Henville, B.C. Hydro, 970 Burrard St., Vancouver, BC, CANADA V6Z1Y3.

138. M.H. Hesse, RPI, Electric Power Engineering Sec 5008, Troy, NY 12181.

139. Wayne Hilson, Manager, Transmission and Electrical Systems Department, Tennessee Valley Authority, Missionary Ridge, 3 North 41, 1101 Market Street, Chattanooga, TN 37402-2801.

140. J.W. Hipke, Pudget Sound Power And Light Co., P.O. Box 97034/OBC 14-N, Bellevue, WA 98009.

141. J.W. Hohn, Indianapolis Power & Light, 25 Monument Circle, Indianapolis, IN 46206.

142. F. J. Hormozi, City of Los Angeles DWP, P.O. Box 111, Room 732 GOB, Los Angeles, CA 90051.

143. J.D. Huddleston, Georgia Power, P.O. Box 4545 (14/270), Atlanta, GA 30302.

144. H. Huynh, Hydro Quebec, 855 Ste.-Catherine Est, 20th Floor, Montreal, Quebec H2L 4P5, CANADA.

145. F. Iliceto, Universita Di Roma, Dipartimento Di Energia Elet, Via Audossiana 18, 00184 Roma, ITALY.

146. J.W. Ingleson, New York Power Pool, 3890 Carman Rd., Schenectady, NY 12303.

147. Helen M. Ingram, Director, Udall Center for Studies in Public Policy, The University of Arizonia, 803/811 East First Street, Tucson, AZ 85719.

148. W. Janischewski, Bendix Guidance Systems Div., Route 46, Mail Stop 2/17b, Teterboro, NJ 07608.

149. J. Kappenman, Minnesota Power, 30 W. Superior St., Duluth, Minnesota 55802.

150. G.G. Karady, Arizona State University, Electrical & Computer Engr. Dept., College of Engineering and Applied Science, Tempe, AZ 85287.

151. T.L. Kaschalk, Detroit Edison, 2000 2nd Ave., A-328 WSC, Detroit, MI 48226.

152. S. Kashyap, Defense Research Establishment — Ottawa, Electronics Division, 3701 Carling Ave., Ottawa, Ontario K1A0Z4, Canada.

153. D.C. Keezer, 22049 Los Alamos Lane, Cottonwood, CA 96022.

154. A.J.F. Keri, American Electric Power, Elec. Research Section, 1 Riverside Plaza, Columbus, OH 43215.

155. A.H. Khan, General Electric Company, Bldg. 5, Rm 320, 1 River Road, Schenectady, NY 12345.

156. A.E. Kilgour, Burns & McDonnell, 4600 E. 64th Street, Kansas City, MO 64141.

157. K. W. Klein, Energetics, Inc., 501 School Street, Washington, DC 20024.

158. Kurt Klunder, Office of Energy Management, U.S. Dept. of Energy, CE-14, 5E-036/FORS, 1000 Independence Ave., SW, Washington, DC 20585.

159. J. L. Koepfinger, Director, Systems Studies and Research, Duquesne Light Company, One Oxford Center, 301 Grant Street (19-5), Pittsburgh, PA 15279.

160. N. Kolcio, American Electric Power Service, EE, 1 Riverside Plaza, Columbus, OH 43215.

161. J.S. Komisarek, Wisconsin Public Service, P.O. Box 19002, Green Bay, WI 54307.

162. B. Korbutiak, Alberta Power, Ltd., 10035 195th St., Edmondton, Alberta T5J 2V6, Canada.

163. P.C.S. Krisnayya, Hydro Quebec, Montee Ste. Julie 1800, Varennes, Quebec J0L 2P0, CANADA.

164. V.J. Kruse, EPRI, 600 E. Las Colinas Blvd. Suite 1550, Irving, TX 75039.

165. J. Kulsetås, Division Manager/Research Director, Norwegian Electric Power Research Institute, Division of High Voltage Technology, N-7034 Trondheim, Norway.

166. H.T. Lam, South Carolina Public Service Authority, P.O. Box 1272, Moncks Corner, SC 29461.

167. J. Lapp, McGraw Edison Co., 11131 Adams Road, Franksville, WI 53126.

168. E. Larsen, General Electric, ESDS Bldg. 2, Rm 642, One River Road, Schenectady, NY 12345.

169. J.R. Latham, Public Service Co. of Oklahoma, P.O. Box 201, Tulsa, OK 74102.

170. Major Robert Launstein, Defense Nuclear Agency, DNA/RAEE, 6801 Telegraph Rd., Alexandria, VA 22310.

171. R.D. Lee, PP&L, 1005 Brookside Road, Allentown, PA 18106.

172. M. Lefrancois, B.C. Hydro, 970 Burrard St., Vancouver, B.C., CANADA V6Z1Y3.

173. J. Lemay, Hydro Quebec, 855 Ste.-Catherine E., 20th Floor, Montreal, Quebec H2L 4P5, CANADA.

174. R. C. Liimatainen, Committee on Science, Space and Technology, 374 Rayburn House Office Bldg., Rm. B., Washington, DC 20515.

175. K.E. Lindsey, P.O. Box 877, 760 North Georgia Avenue, Azusa, CA 91702.

176. Y.L. Liu, 1700 Terrace View #D, Blacksburg, VA 24060.

177. J. Lloyd, CEHND-ED-SY, U.S. Army, Engineering Division Huntsville, P.O. Box 1600, Huntsville, AL 35807.

178. W.F. Long, Professor, University of Wisconsin/Madison, Department of Engineering, 432 N. Lake Street, Madison, WI 53706.

179. C. L. Longmire, Mission Research Corporation, P.O. Drawer 719, Santa Barbara, CA 93102.

180. Calvin D. MacCracken, President, Calmac Manufacturing Corp., 101 West Sheffield Avenue, Englewood, NJ 07631.

181. A.A. Mahmound, Professor of EE, Dean of School of Engineering and Technology, Indiana-Purdue University, 2101 Coliseum E., Fort Wayne, IN 46805.

182. J.H. Mallory, Southern California Edison, P.O. Box 800, Rosemead, CA 91770.

183. G. Manchur, Ontario Hydro, 800 Kipling Ave., Toronto, Ont. CANADA M8Z5S4.

184. W.J. Marsh, Jr., Mississippi Power, P.O. Box 4079, Gulfport, MS 39501.

185. P.S. Maruvada, Hydro Quebec, 1800 Montee St. Julie, Vareness, Quebec J0L 2P0, CANADA.

186. David Mayhall, Lawrence Livermore National Laboratory, P.O. Box 808, L-156, Livermore, CA 94550.

187. T.J. McCarthy, Engineer, LA City Water Dept., 111N Hope Street, Rm. 760, Los Angeles, CA 90012.

188. T.J. McDermott, New York Power Authority, 123 Main Street, White Plains, NY 10601.

189. M.J. McDonald, Union Electric, 1901 Chouteau St. Code 450, St. Louis, MO 63166.

190. M. McGranaghan, Electrotek Concepts, 10305 Dutchtown Road, Suite 103, Knoxville, TN 37932.

191. A. P. Meliopoulos, Georgia Tech, School of Electrical Engineering, Atlanta, GA 30332.

192. D.J. Melvold, Los Angeles Dept. of Water & Power, Room 732, P.O. Box 111, Los Angeles, CA 90051.

193. S. R. Mendoza, Salt River Project, P.O. Box 52025, Phoenix, AZ 85072-2025.

194. D. Merewether, Electro-Magnetic Applications, Inc., P.O. Box 8482, Albuquerque, NM 87198-8482.

195. N. V. Mesland, Tot Keuring Van Elektrotechnische, Materialen, 6800 ET Arnhem, P.O. Box 9035, The Netherlands.

196. S. Mikhail, Consolidated Edison Co. of NY, 4 Irving Place, New York, NY 10003.

197. M. Morishita, Tokyo Electric Power Co., 1901 L. Street, NW, Suite 720, Washington, DC 20036.

198. G.P. Moskos, Boston Edison, 800 Boylston St., Boston, MA 02199.

199. C.J. Mozina, Centerior Service, P.O: Box 94661, Cleveland, OH 44101.

200. K.K. Mustaphi, Northern States Power, 1518 Chestnut Ave., No., Minneapolis, MN 55403.

201. B.D. Nelson, Wisconsin Power & Light, 222 W. Washington Ave., Madison, WI 53703.

202. J.L. Nicholls, The Ohio Brass Co., F.B. Black Research Center, 8711 Wadsworth Road, Wadsworth, OH 44281.

203. D. L. Nickel, Manager, ABB Power Systems, Inc., 777 Penn Center Blvd., Pittsburgh, PA 15235-5927.

204. G.B. Niles, Baltimore Gas & Electric, 1024 G&E Bldg, P.O. Box 1475, Baltimore, MD 21203.

205. S. Nilsson, Program Manager, Electric Power Research Institute, Electrical Systems Division, 3412 Hillview Avenue, P.O. Box 10412, Palo Alto, CA 94303.

206. D. Nordell, Northern States Power Co. MN, General Office, 414 Nicollett Mall, Minneapolis, MN 55401.

207. A. Okun, EUA Services, 750 W. Center St., W. Bridgewater, MA 02379.

208. R.P. Onate, Arizona Public Service, P.O. Box 53999, Phoenix, AZ 85072.

209. R.G. Oswald, Nebraska Public Power Dist., 1414-15th Street, Box 499, Columbus, NE 68601.

210. R.D. Owen, Cooper Power Systems, T.A. Edicson Center, P.O. Box 1900, Franksville, WI 53126.

211. J. Panek, General Electric Company, Bldg. 5-310A, 1 River Road, Schenectady, NY 12345.

212. B. M. Pasternack, American Electric Power Service Corp., 1 Riverside Plaza, P.O. Box 16631, Columbus, OH 43216-6631.

213. R.C. Pastore, United Illuminating, P.O. Box 1564, New Haven, CT 06506.

214. R.L. Patterson, 1971 Catalina Avenue, Jackson, MI 49201.

215. A.H. Pattman, Jr., Public Service of Indiana, 1000 E. Main St., Plainfield, IN 46168.

216. R.C. Peters, T&D, Sega Inc., P.O. Box 23158, 15238 Broadmoor, Overland Park, KS 66223.

217. K.J. Peterson, LA Department of Water and Power, Room 931, 111 N. Hope Street, Los Angeles, CA 90051.

218. R.D. Pettigrew, Beckwith Electric, P.O. Box 1239, Largo, FL 34294.

219. F.G. Picciano, New York State Electric & Gas Co., 4500 Vestal Parkway E., Binghamton, NY 13902.

220. T.A. Pinkham, Lapp Utility Group, Gilbert Str., LeRoy, NY 14482.

221. R.J. Piwko, General Electric Co., Bldg. 2-618, 1 River Road, Schenectady, NY 12345.

222. C.K. Poarch, 117 Woodbury Avenue, Stamford, CT 06907.

223. J.C. Poffenberger, Consulting Engineer, Preformed Line Products Co., 2172 Demington Drive, Cleveland Heights, OH 44106.

224. J. Z. Ponder, PJM Interconnection, 955 Jefferson Ave., Norristown, PA 19426.

225. J. W. Porter, Electric Power Research Institute, Suite 100, 1019 Nineteenth St. N.W., Washington, DC 20036.

226. J.M. Postforoosh, Puget Sound Power & Light, P.O. Box 97034 (OBC-14N), Bellevue, WA 98009.

227. F.S. Prabhakara, Power Technologies, Inc., P.O. Box 1058, Schenectady, NY 12301.

228. J.L. Price, Virginia Power Co., 2400 Grayland Avenue, Chester, VA 23831.

229. P.D. Quinn, South Carolina Public Service Authority, 1 Riverwood Drive, Moncks Corner, SC 29461.

230. M. Rabinowitz, Electric Power Research Institute, 3412 Hillview Avenue, P.O. Box 10412, Palo Alto, CA 94303.

231. W. Radasky, Metatech Corporation, P.O. Box 1450, Goleta, CA 93116-1450.

232. F.A. Rankin, Southwestern Electric Power, P.O. Box 21106, Shreveport, LA 71006.

233. J. J. Ray, Division of Syst. Planning, BPA, P.O. Box 3621, Portland, OR 97208.

234. R. Rebbapragada, Burns and Roe Enterprises, 800 Kinderkamack Road, Oradell, NJ 07649.

235. T. W. Reddoch, Electrotek Concepts, Inc., 10305 Dutchtown Rd., Suite 103, Knoxville, TN 37932.

236. J.R. Redmon, PSE&G, 80 Park Plaza, M/C13A, Newark, NY 07101.

237. J. Reeve, 1650 Panama #101, Brossard, Quebec J4W 2W4, CANADA.

238. W.E. Reid, Qual-Tech Engineers, Inc., 110 Fort Couch Road, Pittsburgh, PA 15241.

239. D.W. Reisinger, PG&E, 77 Beale St., Rm. H1413, San Francisco, CA 94106.

240. J. R. Rempel, Physicist, Defense Intelligence Agency, Washington, DC 20340-6761.

241. R.L. Retallack, American Electric Power Service, 1 Riverside Plaza, Columbus, OH 43216.

242. F.A.M. Rizk, Hydro Quebec Res. Inst., 1800 Montee Ste-Julie, Varennes, Quebec J0L 2P0, CANADA.

243. R. Rocamora, McGraw Edison, P.O. Box 1224, Greenwood, SC 29646.

244. Dietrich J. Roesler, U.S. Department of Energy, CE-141, 1000 Independence Avenue SW, Washington, DC 20585.

245. W.J. Ros, General Electric Company, Building 2-507, 1 River Road, Schenectady, NY 12345.

246. F. Rosa, Division of System Intg., Nuclear Regulatory Commission, MS P1030, Washington, DC 20555.

247. E.T. Sage, Baltimore Gas & Electric, P.O. Box 1474 (RM 1020A), Baltimore, MD 21203.

248. D.E. Sanford, Northeast Utilities, P.O. Box 270, Hartford, CT 06141.

249. J. E. Scalf, Florida Power & Light Company, P. O. Box 14000, 700 Universe Blvd., Juno Beach, FL 33408.

250. G. Scott, Hydro Quebec, Place Dupuis, 20th Floor, 855 Ste-Catherine E., Montreal, Quebec H2L 4P5, CANADA.

251. W. J. Scott, Hq DNA/RAEE, 6801 Telegraph Road, Alexandria, VA 22310-3398.

252. Joe Sefcik, Nuclear Design, Lawrence Livermore National Lab, P.O. Box 808, L-22, Livermore, CA 94550.

253. M. Sforzini, Enel-Centro Di Ricerca Elettr, Via A Volta a, Cologno Monzese, Milano, ITALY.

254. D.F. Shankle, 4731 W. Barlind Drive, Pittsburgh, PA 15227.

255. C. H. Shih, Manager, Electrical Research, American Electric Power Service Corp., 1 Riverside Plaza, Columbus, OH 43215.

256. B.R. Shperling, New York Power Authority, 123 Main Street, White Plain, NY 10601.

257. Jacqueline B. Shrago, Director, Office of Technology Transfer, Vanderbilt University, 405 Kirkland Hall, Nashville, TN 37240.

258. J.P. Skliutas, General Electric Company, Bldg. 2-507, 1 River Road, Schenectady, NY 12345.

259. M. L. Sloan, Austin Research Associate, 1101 Capital of Texas Highway S., Building B, Suite 210, Austin, TX 78746.

260. G.W. Smith, Oglethorpe Power, 2100 E. Exchange Place, Tucker, GA 30360.

261. H.S. Smith, Southern Company Service, P.O. Box 2625, Birmingham, AL 35202.

262. F. Soudi, Pacific Gas & Electric, 123 Mission, Rm H1813, San Francisco, CA 94568.

263. G.E. Stemler, Bonneville Power Administration, P.O. Box 491, ELI, Vancouver, WA 98666.

264. K.A. Stephan, Kansas Gas & Electric, Box 208, Wichita, KS 67201.

265. J.R. Stewart, Power Technologies Inc., P.O. Box 1058, Schenectady, NY 12301.

266. Dr. Robert L. Sullivan, Dean of Engineering, Florida Institute of Technology, 150 West University Boulevard, Melbourne, FL 32901.

267. P. Sullivan, Philadelphia Electric Co., 2301 Market Street (S10-1), Philadelphia, PA 19101.

268. F.Y. Tajaddodi, Anaheim Public Utilities, 13741 E. Bannon Dr., Cerritos, CA 90701.

269. E. R. Taylor, ABB Power Systems, Inc. , 777 Penn Center Blvd., Pittsburgh, PA 15235-5927.

270. R. L. Taylor, Director - Power Supply, Florida Power & Light Co., 9250 W. Flagler, Miami, FL 33102.

271. R.P. Taylor, Louisiana Power & Light, 142 Delaronde, New Orleans, LA 70114.

272. F. M. Tesche, Consulting Scientist, 6921 Spanky Branch Dr., Dallas, TX 75248.

273. M. V. Thaden, Potomac Electric Power Co., 1900 Pennsylvania Ave., NW, Rm. 311, Washington, DC 20068.

274. James L. Thompson, 501 Barrington Road, Signal Mountain, TN 37377.

275. K. Thompson, Ontario Hydro, 700 University Avenue, Toronto, Ontario M5G 1X6.

276. J. Towle, 3906 Bagley Ave. N., Suite 100, Seattle, WA 98103.

277. W.E. Triplett, Pacific Power and Light, 9120 SW Pioneer Ct., Suite B, Wisonville, OR 97070.

278. D.A. Tziouvaras, Pacific Gas & Electric, 123 Mission St., RM H1847, San Francisco, CA 94106.

279. E. F. Vance, 6885 HWY 1187, Fort Worth, TX 76140.

280. V. Varneckas, Consolidated Edison, 4 Irving Place, RM 1506S, New York, NY 10003.

281. S.S. Venkata, Professor, EE Department, FT-10, Univ. of Washington, Seattle, WA 98195.

282. J.J. Vithayathil, 3814 NE 136th Place, Portland, OR 97230.

283. D. R. Volzka, Senior Project Engineer, Wisconsin Electric Power Company, 333 West Everett Street, Milwaukee, WI 53201.

284. C. L. Wagner, 4933 Simmons Dr., Export, PA 15632.

285. T.A. Wakely, Philadelphia Electric Co., 2301 Market Street, N3-1, Philadelphia, PA 19101.

286. R. Walling, General Electric Company, Building 2, Rm 507, One River Road, Schenectady, NY 12345.

287. D.J. Ward, Virginia Power Co., 2400 Grayland Avenue, 2nd Floor, Richmond, VA 23220.

288. B.J. Ware, American Electric Power Service, 1 Riverside Plaza, Columbus, OH 43216.

289. W.P. Waudby, Consumers Power, 212 W. Michigan Ave., Jackson, MI 49201.

290. T.L. Weaver, Western Area Power Administration, P.O. Box 3402, Golden, CO 80401.

291. R. C. Webb, Defense Nuclear Agency, RAEE, 6801 Telegraph Road, Alexandria, VA 22310.

292. R.M. Westfall, Florida Power Corp., P.O. Box 14042, SP28, St. Petersburg, FL 33733.

293. A.C. Westrom, Kearney-National Inc., P.O. Box 49167, Atlanta, GA 30329.

294. H.B. White, P.O. Box 939, Hudson, Quebec J0P 1H0, CANADA.

295. E. P. Wigner, Consultant, 8 Ober Road, Princeton, NJ 08540.

296. M. W. Wik, Forsvarets Materielverk, Stockholm, S-11588, Sweden.

297. D.D. Wilson, Power Technologies Inc., P.O. Box 1058, Schenectady, NY 12301.

298. P.B. Winston, Georgia Power, 107 Technology Pkwy, Norcross, GA 30092.

299. D. Woodford, Suite 400, 1619 Pembina Ave., Winnipeg, Manitoba, R-3T-2G5, Canada.

300. F. S. Young, Director, Electrical Systems Division, Electric Power Research Institute, P.O. Box 10412, Palo Alto, CA 94303 .

301. J.A. Zipp, Consumers Power, 212 W. Michigan Ave., Jackson, MI 49201.

302. R. W. Zwickl, Space Environment Laboratory, Mail Stop R/E/SE, Boulder, CO 80303.

303. Office of Assistant Manager for Energy, Research and Development, DOE-ORO, P.O. Box 2001.

304-305. OSTI, U.S. Department of Energy, P.O. Box 62, Oak Ridge, TN 37831.

DATE
FILMED
3/22/93